**Department of Mechanical Engineering**

# Optimum and Robust Design of Fibre-Reinforced Hybrid Composites with Manufacture Related Uncertainties

**Mehdi Kalantari**

**This thesis is presented for the Degree of**

**Doctor of Philosophy (PhD)**

**of**

**Curtin University**

**August 2018**

## Declaration

To the best of my knowledge and belief, this thesis contains no material previously published by any other person except where due acknowledgement has been made. This thesis contains no material, which has been accepted for the award of any degree or diploma in any university.

Full Name: Mehdi Kalantari

Signature: Kalantari

Date: 19/5/2017

## Abstract

Hybrid composite laminates which take advantage of more than one type of reinforcement are widely used in different applications requiring high strength and low weight. In this research, different methods are presented for the design and optimization of laminated hybrid composites when design variables are not deterministic due to manufacture related uncertainties. Since flexural properties are more affected by fibre hybridization, this research has focused on the design and optimization of laminated hybrid composites under flexural load. The flexural behaviour of specimens made of carbon and glass fibre reinforced-epoxy hybrid composite under three-point bending were predicted by utilising classical lamination theory (CLT) with an appropriate failure model being employed to determine the flexural load carrying capacity. The analytical models were validated by comparing with existing experimental data. The effect of hybridization in fibre-reinforced composites was investigated with some rules for designing optimum stacking configurations being proposed. Since variations in design parameters due to uncontrollable variables in the manufacturing process usually degrade the performance of highly optimized materials, methods for designing optimal hybrid composites which are still robust to these variations are presented in this research. Three sources of uncertainties, namely, fibre misalignment, lamina thickness variation and the presence of matrix voids were incorporated into the model. The conflicting objectives for optimization were to minimize the cost and weight of the composite subject to the constraint of a minimum specified flexural strength. A hybrid multi-objective optimization evolutionary algorithm (MOEA) was introduced through modification of an elitist non-dominated sorting genetic algorithm (NSGA-II) and combining it with the fractional factorial design method, then the performance of the hybrid algorithm was improved by combining it with a simple genetic algorithm (GA) as an anti-optimizer. The algorithms were employed to solve the optimization problems. Pareto optimal and robust solutions were found for different levels of minimum flexural strength and the significance of each uncertainty source on the optimal cost and weight of the optimal designs were investigated by conducting

analysis of variance (ANOVA) tests. Different scenarios have been considered to illustrate the applicability of the obtained solutions in decision making processes. The results indicated that, in general, all three uncertainties affected the cost and weight of the optimal designs with the effect of voids being more critical for void contents of greater than 2%.

## Acknowledgements

I would like to thank many individuals as the accomplishment of this work would not have been possible without their kind technical and emotional support. In particular, I would like to acknowledge the following people:

To my supervisor, Dr Ian J. Davies, thank you for all that you have done over the past five years, from my PhD application until its completion, and the advice and support beyond my academic life. Especially, I appreciate your opinions and control on the quality of the work, together with the opportunities I had under your supervision.

To my co-supervisor, Dr Chensong Dong, I appreciate your attention, support and advice during my research. I was fortunate to have you in my supervisory panel. Life and work were given perspective using your technical advice, guidance, and made more authentic by passing the technical challenges that you raised.

I would like to express my gratitude to Australian government and Curtin University for their financial support via the Australia Postgraduate Award (APA) scholarship and Curtin University Postgraduate Scholarship (CUPS).

My acknowledgements would be incomplete without thanking the biggest source of my strength, my family. Special thanks go to my wife, Sahel, who was very patient and kindly supportive during my studies and also great thanks to my parents for their endless support and love during my life.

There are many others who deserve my gratitude. I sincerely apologise to those whose names are not mentioned here but played a role in my achievements so far. The blessings of my late parents.

## List of Publications Included as Part of the Thesis

1. Chensong Dong, Mehdi Kalantari, Ian J. Davies. Robustness for unidirectional carbon/glass fibre reinforced hybrid epoxy composites under flexural loading, Composite Structures, Volume 128, 15 September 2015, Pages 354-362, ISSN 0263-8223, http://dx.doi.org/10.1016/j.compstruct.2015.03.059

2. Mehdi Kalantari, Chensong Dong, Ian J. Davies. Numerical investigation of the hybridisation mechanism in fibre reinforced hybrid composites subjected to flexural load, Composites Part B: Engineering, Volume 102, 1 October 2016, Pages 100-111, http://dx.doi.org/10.1016/j.compositesb.2016.07.012

3. Mehdi Kalantari, Chensong Dong, Ian J. Davies. Multi-objective analysis for optimal and robust design of unidirectional glass/carbon fibre reinforced hybrid epoxy composites under flexural loading, Composites Part B: Engineering, Volume 84, January 2016, Pages 130-139, http://dx.doi.org/10.1016/j.compositesb.2015.08.050

4. Mehdi Kalantari, Chensong Dong, Ian J. Davies. Multi-objective robust optimisation of unidirectional carbon/glass fibre reinforced hybrid composites under flexural loading, Composite Structures, Volume 138, 15 March 2016, Pages 264-275, http://dx.doi.org/10.1016/j.compstruct.2015.11.034

5. Mehdi Kalantari, Chensong Dong, Ian J. Davies. Effect of matrix voids, fibre misalignment and thickness variation on multi-objective robust optimization of carbon/glass fibre-reinforced hybrid composites under flexural loading, Composites Part B: Engineering, Volume 123, 15 August 2017, Pages 136-147, http://dx.doi.org/10.1016/j.compositesb.2017.05.022

6. Mehdi Kalantari, Chensong Dong, Ian J. Davies. Multi-objective robust optimization of multi-directional carbon/glass fibre-reinforced hybrid composites with manufacture related uncertainties under flexural loading. Composite Structures, Volume 182, 15 December 2017, Pages 132-142, http://dx.doi.org/10.1016/j.compstruct.2017.09.019

## Statement of Contribution of Others

Chapter Three of this thesis is co-authored by Chensong Dong, Mehdi Kalantari and Ian J. Davies and has been previously published in Composite Structures, Volume 128, 15 September 2015, Pages 354-362, http://dx.doi.org/10.1016/j.compstruct.2015.03.059

Chapter Four of this thesis is co-authored by Mehdi Kalantari, Chensong Dong and Ian J. Davies and has been previously published in Composites Part B: Engineering, Volume 102, 1 October 2016, Pages 100-111, http://dx.doi.org/10.1016/j.compositesb.2016.07.012

Chapter Five of this thesis is co-authored by Mehdi Kalantari, Chensong Dong and Ian J. Davies and has been previously published in Composites Part B: Engineering, Volume 84, January 2016, Pages 130-139, http://dx.doi.org/10.1016/j.compositesb.2015.08.050

Chapter Six of this thesis is co-authored by Mehdi Kalantari, Chensong Dong and Ian J. Davies and has been previously published in Composite Structures, Volume 138, 15 March 2016, Pages 264-275, http://dx.doi.org/10.1016/j.compstruct.2015.11.034

Chapter Seven of this thesis is co-authored by Mehdi Kalantari, Chensong Dong and Ian J. Davies and has been previously published in Composite Structures, Volume 182, 15 December 2017, Pages 132-142, http://dx.doi.org/10.1016/j.compstruct.2017.09.019

Chapter Eight of this thesis is co-authored by Mehdi Kalantari, Chensong Dong and Ian J. Davies and has been previously published in Composites Part B: Engineering, Volume 123, 15 August 2017, Pages 136-147, http://dx.doi.org/10.1016/j.compositesb.2017.05.022

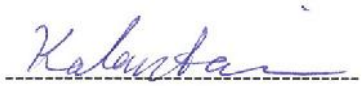

*Signature*

## Table of Contents

## List of Figures

## List of Tables

# 1

# Introduction

Composite materials, made from two or more constituent phases with different properties, have been widely used in industry as a successful replacement for metal components. Amongst the different types of composite materials available, fibre-reinforced polymers, also known as fibre reinforced plastics (FRP), are the most common due to their ability in achieving tailored properties and have found widespread use in aerospace, automotive, marine and civil applications. The fibres in FRP composites can be made in various forms such as short fibre, chopped fibre, long fibre or woven. The most commonly used fibres in FRPs are carbon, glass, basalt and aramid with the matrix usually being epoxy, polyester thermosetting plastic or vinylester.

In order to achieve particular properties in different directions, layers of fibrous composite (lamina) can be bonded together into an assembly known as a composite laminate. The stacking configuration of laminas plays a great influence on the mechanical properties of composite laminates. Figure 1-1 shows an example of an aerospace grade carbon-fibre/epoxy laminate.

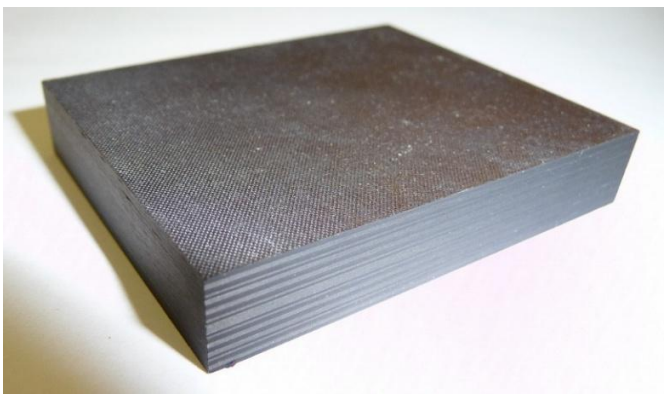

**Figure 1-1: Example of an aerospace grade carbon-fibre/epoxy laminate [1].**

When two or more types of fibre are used as reinforcing elements within a common matrix, the resulting material is known as a *hybrid* composite. Based on how the fibres are configured, different types of hybrid composites are available. The most common fibre configurations include layer-by-layer (interlayer or laminated), yarn-by-yarn (intralayer) and fibre-by-fibre (intayarn) as visualized in Figure 1-2 [2].

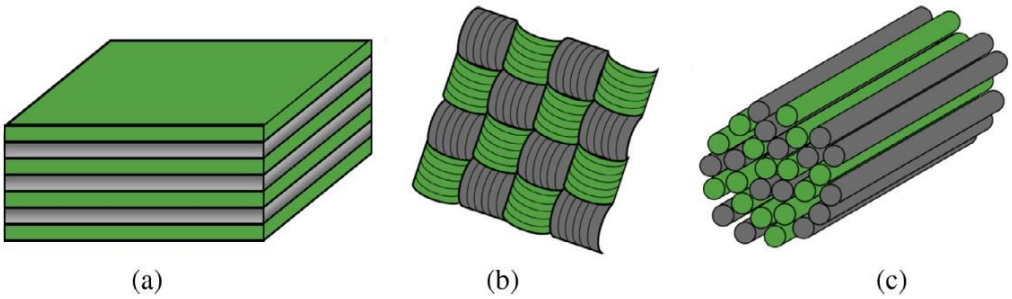


**Figure 1-2: Main types of fibre configuration in hybrid composites: (a) layer-by-layer (interlayer or laminated), (b) yarn-by-yarn (intralayer) and (c) fibre-by-fibre (intrayarn)**

In general, the purpose of hybridizing different fibres into a hybrid composite is to take advantages of both fibres and/or diminish their disadvantages. So far, several combinations of fibre types have been used to create hybrid composites. Carbon and glass fibre-reinforced epoxy laminates are good example of hybrid FRP composites that benefit from the properties of carbon and glass. Carbon fibres generally possess high strength and stiffness but relatively low strain-to-failure. Carbon fibre-reinforced epoxy composites are used in many applications that require a combination of high strength and low density; however, the low strain-to-failure and high material cost of carbon fibres limit the application of such composites, particularly when flexural strength is a design concern. In contrast to carbon fibres, most of the glass fibres possess a higher strain-to-failure and density and a relatively lower stiffness and lower price. Therefore, through the hybridization of carbon and glass fibres it may be possible to design a hybrid composite with higher strength and lower cost.

Since hybrid composites are the mixture of different materials, most of their properties can be determined using the rule of mixtures (RoM) which is simply the weighted average of the constituent properties. However, several researchers have

shown that not all the properties of hybrid composites follow the RoM. In the present research, the deviation of a hybrid composite property from the RoM is defined as the *hybrid effect*. This hybrid effect can be positive (which implies an improvement of the property through hybridization) or else it can be negative (which means that the property has been degraded by hybridization). The configuration of fibres in a hybrid composite plays an important role in the hybrid effect and thus the properties of the final product.

Finding the optimum stacking configuration of composite laminates with the hope of improving their mechanical properties has been a major area of interest within the field of composite materials. Since there are several parameters involved in the design of composite laminates, the design process of such materials is more complex when compared to traditional materials (*e.g.*, steel, cast iron and aluminium and alloys) with usually an optimization problem being required in order to find the best design(s). The main parameters determining the strength of composite laminate materials are:

- Material type of fibre and matrix in each lamina
- Thickness and number of lamina
- Fibre volume fraction of each lamina (the percentage of fibre volume in the entire volume of material)
- Fibre angle orientation
- Stacking configuration of laminas within the laminate

In the case of hybrid composites, the existence of a hybrid effect makes the optimization problem even more complicated and the stacking configuration of laminas becomes more influential.

Optimization problems deal with either minimization or maximization of one or more objective functions subjected to constraints. In all engineering disciplines, optimization methods are used as a powerful tool to improve the performance of products. In most real applications, in addition to the performance, the weight and/or cost of final products are of main concern which implies the existence of multiple objectives. In this situation, multi-objective optimization methods which

simultaneously optimize more than one objective need to be employed. Unlike single-objective optimization problems, the result of a multi-objective optimization will not be unique but instead a set of optimal solutions known as a Pareto optimal set. Pareto optimal sets give a better understanding of the problem and potential solutions to designer and the final decision about the optimal design could be made based on a higher level of information, *e.g.*, the preference of objectives and manufacturing limitations.

Although optimization methods aim to find the exact value of the design variables at which the performance (and/or other objectives) would be maximized, realistically, the design variables are not deterministic and have variations due to the manufacturing process and machinery limitations. Consequently, the exact values determined by the designer could rarely be achieved in manufacturing. Thus, the properties of the product will be different from what is expected. This difference is not always negligible, particularly for highly optimized designs which are very sensitive to any variations. Figure 1-2 presents the hypothetical behaviour of a material (performance) with respect to one of the design variables. Traditional optimization problems normally consider deterministic values for the design variables and other inputs and thus look for some point such as point A with the best performance; however, as can be seen at this point, a slight variation in the design variable will cause significant degradation in the performance. In contrast to this, point B which has theoretically a lower performance, exhibits a better performance when variations occur. For this particular case, the optimal design associated with point B is said to be more *robust* than point A. The problem of determining the most robust and optimal design is known as robust design optimization (RDO). RDO is an emerging area that tries to minimize the effect of uncertainties on the performance of products by incorporating uncertainties within the optimization problem. Several methods have been developed for modelling RDO. These methods are mainly classified as probabilistic and non-probabilistic. In probabilistic approaches, uncertain inputs are considered as random variables with a predefined probability distribution whereas non-probabilistic approaches do not require information about the probability distribution at an early stage of design.

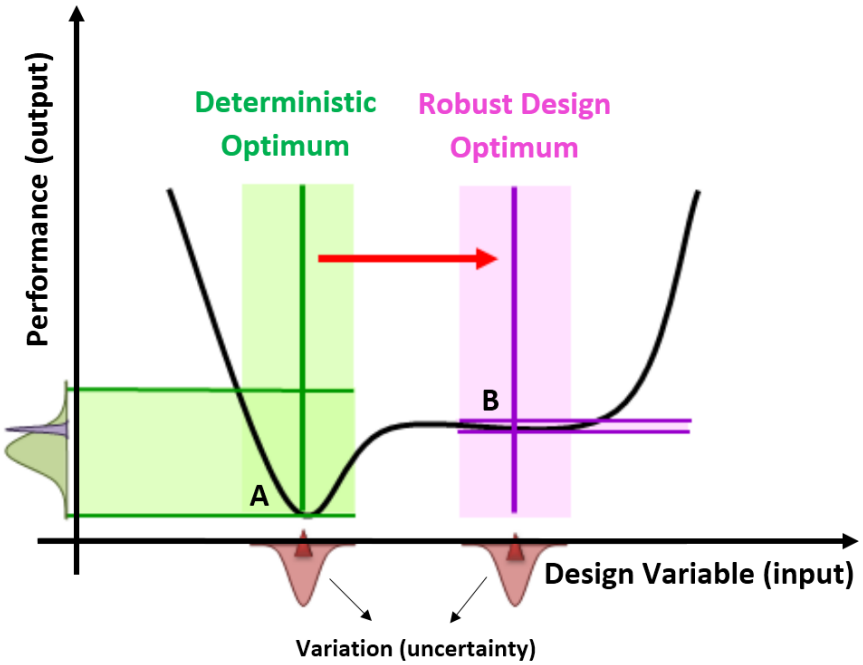


**Figure 1-3: Difference between deterministic and robust optimum.**

Several sources of uncertainty have been identified in the design and manufacture of composite materials. The most common manufacture related sources of uncertainty in laminated composites include the presence of resin rich regions, fibre misalignment and waviness and the presence of defects such as voids. Despite improvements in manufacturing tools and methods, variations of input variables may not be negligible and the consideration of uncertainties in the design of high performance laminate composite materials appears inevitable.

## 1.1. Project Aims and Significance

Minimizing the cost of products without degrading their performance has been one of the greatest challenges in the field of material design. Among all factors affecting the total cost of a product, material cost is the key cost driver in most industries. Other factors such as labour and equipment costs are not under the control of the designer. Therefore, minimization of material cost is one of the main objectives of optimization problems for real applications.

In most applications, the weight of the material is also a major concern. Weight affects the efficiency of machines and products in such a way that heavier materials result in less economical products. This is the reason why aerospace and automotive companies are always endeavouring to achieve materials with a higher specific strength (strength per unit density) even if the total product cost goes up.

Therefore, in most applications light materials with low price are in high demand. However, in general, most of the high strength and light materials are expensive whereas cheap materials are relatively heavier or else have inferior properties. For example, the tensile strength of high strength T700S carbon fibre is 40% higher than that of E glass fibre while it is 15 times more expensive. Thus, cost and weight are two conflicting objectives.

As mentioned above, through the design of hybrid composites it may be possible to take advantage of both fibre types. However, the behaviour of laminated hybrid composites cannot be easily predicted due to the presence of different materials and uncertainties in the properties and emergence of a hybrid effect. Therefore, the optimization problem become complicated with efficient methods and algorithms being required to accurately determine the optimum value of design variables (*e.g.*, stacking configuration and fibre volume fraction). Since, to date, there has been no reliable study on the robust optimization of hybrid composites, this study aims to contribute to this growing area of research by providing new insights into the hybridization mechanism. The present research also aimed to fill a gap in the literature by investigating the effect of manufacture related uncertainties on the optimal design of hybrid composites. The project goals can be summarized as follows:

1. Analysis of uncertainties and robustness assessment of carbon and glass fibre-reinforced epoxy hybrid composites under flexural load.
2. Investigate the mechanisms of hybridisation in fibre reinforced hybrid composites when subjected to flexural load.
3. Develop an efficient algorithm for solving RDO problems for unidirectional and multi-directional laminated hybrid composites.
4. Investigate the effect of different sources of uncertainties on the optimal and robust design of carbon and glass fibre-reinforced epoxy hybrid composites.

## 1.2. Research Method

In the present study, carbon and glass fibre-reinforced epoxy hybrid composites under three-point bending load have been studied. The material properties of the fibres were chosen to be the same as those used in previous experimental research so that the results could be compared and validated. Each lamina in the hybrid composite could be either pure carbon or glass fibre-reinforced epoxy.

First, the apparent flexural strength of the specimen was calculated. For this purpose, the strength components of carbon fibre and glass fibre epoxy laminas were estimated based on their failure modes. Classical lamination theory (CLT) was utilized to determine the stress distribution through the laminate thickness with an appropriate failure theory being employed to estimate the maximum allowable load. Having the maximum allowable load, the apparent flexural strength was determined based on static equilibrium prior to failure. In order to ensure the accuracy of results, a finite element method (FEM) was developed in ANSYS APDL to simulate the same conditions and compare the results with those from CLT.

In order to investigate the hybrid mechanism, the stress distribution in each lamina for different stacking sequences was determined and the flexural strength was estimated. By comparing the results, the reason behind the emergence of a hybrid effect could be explained.

A multi-objective robust optimization problem for minimizing material cost and weight subject to minimum required flexural strength was formulated. Uncertainties were incorporated into the optimization problem by considering uncertain but bounded variables and calculating the flexural strength of the specimen based on the worst case (*i.e.*, the worst combination) of uncertain variables. In the case of unidirectional hybrid composites, a modified version of the NSGA-II algorithm was combined with a fractional factorial design method to determine the robust Pareto optimal solutions more efficiently. For the case of multi-directional hybrid composites a large amount of computation resources was needed. To overcome this problem, an anti-optimization problem was defined and solved by the aid of a genetic algorithm (GA) as an internal loop within the NSGA-II in order to find the worst case

with less computational effort. All of these numerical calculations were carried out through programing in MATLAB.

## 1.3. Thesis Structure

This thesis is composed of nine chapters. A comprehensive literature review is presented in Chapter 2; in addition to this, in the Introduction section of the main chapters (Chapters 3 to Chapter 8), a comprehensive overview and literature review on the main subject of the chapter is presented.

In Chapter 3, robustness of unidirectional S-2 glass and T700S carbon fibre reinforced epoxy hybrid composites under flexural loading when the glass fibres are place at the compressive side is investigated. By the aid of classical lamination theory (CLT) and a regression model robustness indices are developed for both flexural strength and specific flexural strength. The main focus of this chapter is to identify robustness and the influence of parameter variation on the flexural properties.

The cost and density of hybrid composites is formulated in Chapter 4 with comprehensive analysis of different objectives in optimization of unidirectional hybrid composite under flexural load being presented. The robust index that is introduced in Chapter 3 is considered as one of the objective functions. The problem is converted to single-objective optimization with several scenarios for the preference of the objectives being examined.

In Chapter 5, the mechanism of hybridization when carbon and glass fibre laminas are used to form a hybrid composite is investigated. The chapter illustrates the variation in stress distribution through the laminas when two fibre types are hybridized with the reasons behind the emergence of hybrid effect being detected. Results are validated by finite element analysis (FEM) and the failure theories are compared. At the end of this chapter, general rules for achieving a positive hybrid effect are presented.

In Chapter 6, an efficient algorithm is proposed for solving the problem of multi-objective robust optimization of unidirectional hybrid composites. The algorithm is

applied to T700S carbon and E glass hybrid composites. Weight and cost are chosen as objectives and minimum required flexural strength is considered as a constraint.

Chapter 7 is concerned with the multi-objective robust optimization of multi-directional hybrid composites. Since this problem requires significant computational effort, a methodology is proposed for solving such problems more efficiently by combining optimization and anti-optimization.

Chapter 8 focuses on the effect of manufacture related uncertainties on the optimal results of hybrid composites and the contribution of each source of uncertainty in degrading the performance of the material.

The conclusions and future work recommendations are presented in Chapter 9.

## 1.4. References

[1] Wikipedia. Composite laminates. 2016 [cited 2017]; Available from: https://en.wikipedia.org/wiki/Composite_laminates.

[2] Swolfs, Y., L. Gorbatikh, and I. Verpoest, Fibre hybridisation in polymer composites: A review. Composites Part A: Applied Science and Manufacturing, 2014. 67: p. 181-200.

# 2

# Literature Review

## 2.1. Optimization of Composite Laminates

A large and growing body of literature has investigated the problem of design and optimization of laminated composite materials. Different classifications have been suggested for literature in this area such those based on:

- Optimization method (*e.g.*, analytical, enumeration and heuristic)
- Objective function (*e.g.*, buckling load, natural frequency, flexural stiffness and weight)
- Composite type (*e.g.*, constant stiffness, variable stiffness, unidirectional, multi-directional)

Most of the research in the field of optimization of composite laminates aims to achieve the optimum stacking configuration. Several optimization methods have successfully been applied to optimization problems of composite materials. These methods can mainly be classified into analytical (gradient-based), direct search and hybrid methods. Analytical methods such as the Quasi-Newton method [1-3], steepest descent [4, 5], method of feasible direction [6, 7] and approximation schemes [8-10] are based on the gradient of the objective and constraint functions and require significant computational efforts, however, they are known for their fast convergence rate. In contrast to this, direct search methods do not require the derivative of functions and approach the optimum solution by calculating the value of the objective and constraint functions. Since the calculation of derivatives is almost impossible in composite materials, direct search methods are more practical in this field with several methods such as the simplex method [11, 12], simulated annealing [13, 14], genetic algorithm [15-17], particle swarm optimization [18, 19]

and ant colony optimization [20] being developed and applied to composite laminates. Amongst all direct search methods the genetic algorithm (GA) is the most popular optimization method for composite laminates [17].

There are also exists other methods which have been developed specifically for the optimization of composite laminates, *e.g.*, layerwise optimization method [21] and discrete material optimization [22]. Some researchers have combined two or more optimization methods to take advantages of them. Such methods are known as hybrid methods. For example, GA was combined with the local optimization search algorithm to improve the convergence rate [23, 24].

A comprehensive review of the research in the area of composite laminate optimization can be found in the literature [25-28].

## 2.2. Hybrid Effect

Several researchers have studied the effect of hybridization on the properties of laminated hybrid composites [29-49]. Early examples of research into the hybrid effect include the study done by Hayashi [29] in 1972 who reported a 40% improvement in the failure strain of carbon and glass fibre hybrid compared to pure carbon fibre composites. Some researchers [33, 50] at that time did not believe the hybrid effect reported by Hayashi; however, Phillips [31] also reported the existence of a positive hybrid effect for glass and carbon hybrid composites under impact and fatigue load. The belief in the existence of a surprising improvement in failure strain of low elongation fibres when hybridized by high elongation fibres gradually increased when more experimental results showed the positive hybrid effect and more theories were developed to explain the reason behind the hybrid effect [32, 51-53]. So far, three different theories have been developed to describe the existence of the hybrid effect: (i) residual stress, (ii) failure development, and (iii) dynamic stress concentration. Although most of the theories have been applied to unidirectional hybrid composites, they can be extended to multi-directional composites by considering the failure of fibres in the loading direction [54]. Residual stress theories attribute the hybrid effect to differences in the coefficient of thermal

expansion (CTE) of low and high elongation fibres. According to this theory, the difference in thermal contraction of fibres during the curing process results in residual shrinkage stress in both fibre types. However, later researchers [30, 32, 36] showed that the effect of thermal residual stress is not the main reason of the hybrid effect and other important factor(s) should exist. The second theory for the reason of the hybrid effect, *i.e.*, failure development hypothesis, relates the hybrid effect to the changes in the way failure develops within the fibres due to differences in the stiffness and size of the fibres. This can interfere with the failure progress of the fibres and hinder the final failure of the material [55-57]. The third theory, *i.e.*, dynamic stress concentration, which was first pointed out by Hedgepeth [58] and extended to hybrid composites by Xing [59] relates the hybrid effect to the temporary dynamic stress concentration due to stress wave travelling along fibres during fibre rupture.

It is well known that the configuration of laminas, *i.e.*, stacking configuration, plays an important role in the performance of composite laminates. It also affects the sign and magnitude of the hybrid effect in hybrid composites, *i.e*, by placing low elongation and high elongation fibres in a proper order and direction, the maximum positive hybrid effect can be achieved for a specific property.

## 2.3. Tensile Properties of Hybrid Composites

Several researchers [29-31, 33, 34, 50, 60, 61] reported that the longitudinal tensile modulus of hybrid composites follows the RoM. There are a few studies reporting deviation from the RoM such as an experimental study done by Ren *et al*. [62] who reported a higher tensile modulus, however, the deviations in all of these studies are either due to uncertainties in material properties and geometries or an incorrect use of RoM [63, 64] and thus are not considered evidence of a hybrid effect. The fibre volume fractions are to be used as a composition parameter in RoM.

Although the hybrid effect is not expected to occur in the longitudinal modulus, it can exist in the transverse direction in special cases such as that reported by Taketa [65] for carbon fibre-reinforced polypropylene hybridized with woven self-reinforced polypropylene due to the high Poisson's ratio of the self-reinforced polypropylene.

Unlike tensile modulus, the hybrid effect exists in the tensile and failure strain of hybrid composites. As previously mentioned, the deviation of failure strain in hybrid composites from the RoM was the first known hybrid effect in composites [29] and now the hybrid effect in tensile strength is well established in the literature [30-32, 34, 36, 66-70] with the typical range of the hybrid effect being between 10% and 50% [54].

## 2.4. Flexural Properties of Hybrid Composites

The hybrid effect in the flexural properties of a laminated hybrid composite material is highly dependent on the stacking configuration of the laminas. Stacking configuration, *i.e.*, material type, volume fraction and orientation of the fibres in each lamina changes not only the stress distribution within the laminate but also the modulus of the material and thus makes interpretation of the hybrid effect even more complicated in flexural loading.

In 2001, Davies and Hamada [40] set up a series of experiments to evaluate the flexural properties of carbon and silicon carbide fibre hybrid composites. They studied specimens with different span-to-depth ratios under three point bending and reported a positive hybrid effect for the flexural strength when carbon fibres at the compressive side were replaced by silicon carbide fibres. Pandya *et al.* [47] carried out experiments on in-plane mechanical properties of carbon and glass fibre-reinforced epoxy composites and showed by placing glass fabric laminas in the exterior of the hybrid composite the tensile strength and ultimate tensile strain are improved. Dong *et al.* [44, 71] measured the flexural strength and stiffness of unidirectional carbon and glass fibre-rinforced epoxy hybrids and found that the flexural properties of the hybrid composite could be enhanced by placing glass fibre lamina at the compressive side. Similarly, Giancaspro *et al.* [43] conducted experiments and studied the effect of the following variables on the flexural performance of E-glass and carbon fibre hybrid composites:

- Type of carbon fabric
- Number of carbon laminas in hybrid composites

- Location of carbon laminas in hybrid composite

They found out that the strength of E-glass composite laminates can be improved by placing two or three carbon laminas on the tension side whilst placing carbon laminas in both the tension and compression faces does not provide a significant improvement in flexural capacity.

With regards to carbon and glass fibre hybrid composites, experimental data shows that the partial substitution of carbon fibres by glass fibres at the compressive side of flexural specimens increases the overall flexural strength (positive hybrid effect) [44]. However, placing glass fibers in the tensile side resultes in a negative hybrid effect [71].

Since the compressive strength, *i.e.*, strain to failure, is much lower in compression than in tension for carbon fibres [40], then the positive hybrid effect shown in flexural strength experiments can only be explained by the higher compressive strain to failure of the glass fibres. In order to achieve a higher flexural strength, it is required that the glass fibres be located in the compression zone of the hybrid composite.

As an example, the tensile and compressive strength of some pure glass fibre and carbon fibre reinforced epoxy composites are listed in Table 2-1 to show the relatively higher compressive strength of E-glass fibre reinforced plastic (FRP) composites.

**Table 2-1 Tensile and compressive strength of glass and carbon FRP composites [72].**

| Material | Tensile Strength (MPa) | Compressive Strength (MPa) |
|---|---|---|
| E-glass unidirectional FRP | 930.27 | 721.79 |
| Carbon T-300 unidirectional FRP | 1270.7 | 153.7 |
| Carbon T-700 unidirectional FRP | 1235.7 | 136.1 |

Carbon/glass fibre composites are being used in several industries with numerous applications including aircraft components, spacecraft, cars, sport equipment, building structures and musical instruments.

## 2.5. Fatigue Life of Hybrid Composites

Although fatigue resistance of hybrid composites is a key parameter in many applications such as aerospace, few studies are available in this area. Wu *et al.* [73] studied the fatigue behaviour of various FRP composites and carbon/glass and carbon/basalt hybrid composites under tensile load and showed that the fatigue resistance of basalt fibre composites is improved when it is hybridized by carbon fibres, however, this improvement was not observed in carbon/glass hybrid composites. Other experimental studies also reported the existence of a hybrid effect in fatigue resistance for different hybrid composites including carbon-high-performance polyethylene/epoxy [37], XAS-carbon/E-glass [74] and carbon/aramid [75].

## 2.6. Impact Resistance of Hybrid Composites

Extensive research has investigated the effect of hybridization on impact resistance of hybrid composites. This research shows, in general, that the behaviour of hybrid composites subject to impact loads is closely linked to layup, *i.e.*, stacking configuration of laminas [76-80].

Jang *et al.* [76] investigated the response of hybrid composites to low-velocity impact loading and suggested placing higher elongation fibres on the impact side for enhancement of impact resistance. However, other studies [77, 80] reported higher impact resistance when low elongation fibres are placed on the impact surface. This contradiction seems to be related to different damage mechanisms caused by different material types and interfaces. Understanding the damage mechanism in hybrid composites subject to impact load is one of the greatest challenges but it is essential in optimization problems.

A review of literature in the area of the hybrid effect has recently been done by Swolfs *et al.* [54].

## 2.7. Optimization of Hybrid Composites

Using different fibre types in a hybrid composite affects both the cost and weight of the material. Cost and weight have been of continuing concern in the design and manufacture of composite products. There is a relatively large body of literature related to the optimization of hybrid composites with regards to minimum weight and cost [81-88]. In order to simultaneously minimize the material cost and weight, a multi-objective optimization problem needs to be defined and solved. A detailed description concerning the methods of solving multi-objective opitmization problems has been published by Deb [89]. Most of the research in the area of optimization of hybrid compoites has avoided the complexity of multi-objective optimization and been restricted to the convertion of multi-objective problems to a single-objective form by utilizing preference-based classical methods such as wieghted sum method (WSM) [83, 86, 87, 90-94]. For example, Kaufmann *et al.* [94] used WSM and proposed a methodology for the optimization of cost and weight of aircraft components. Similarly, Hemmatian *et al*. [86, 87] investigated the problem of minimization of weight and cost of carbon and glass fibre hybrid composites by using WSM through a gravitional search algorithm and elitist ant system. Walker *et el.* [91] studied the problem of maximization of axial and torsional buckling loads for laminated cylindrical shells with the ply angle being considered as the only design variable. They investigated the effect of weighting factors in WSM and compared the results of single-objective and multi-objective designs.

There are several methods available for solving multi-objective optimization problems by targeting the Pareto optimal set without using the preference of the objectives at an early stage of the design – these include multi-objective evolutionary algorithms (MOEA), *e.g.*, strength Pareto evolutionary algorithm (SPEA-II) [93], Pareto archived evolutionary strategies (PAES) [96] and non-dominated sorting genetic algorithm (NSGA-II) [97]. So far, however, there has been little attention to MOEA in the field of composite materials such as the research carried out by Lakshmi

and Rao [98] who employed a new hybridized version of NSGA-II to minimize the weight and cost of laminated hybrid composite cylindrical shells. In another study which set out to optimize a helicopter composite blade, Visweswaraiah *et al*. [99] proposed an evolutionary non-dominated sorting hybrid algorithm (NSHA).

## 2.8. Uncertainties and Robust Design of Hybrid Composites

A review of the literature indicates that most of the research in the area of optimization of composite materials neglected uncertainties in design variables and used deterministic values of all input parameters (*e.g.*, material properties) with a factor of safety and/or load factor being applied to increase reliability of the design. However, several studies reported that the inclusion of uncertainties has a considerable effect on the performance of composite materials [100-102]. A number of methods have been proposed for the analysis of uncertainties and robustness assessment. Reviews of these methods can be found in the literature [103-105]. Robust design was first introduced by Taguchi [106] in 1987 to improve the quality and reduce the number of rejected products. Robust design methods have been developed after Taguchi and are used in many fields of engineering. Walker and Hamilton [107] proposed a procedure for the optimization of symmetrically laminated composites with manufacturing uncertaintiy in the ply angle. Manan and Cooper [108] developed a probabilistic method to design composite wings of aircraft when material properties, fibre direction angle and ply thickness are uncertain variables. They compared the results from the probabilistic method with Monte Carlo simulations and found good agreement. They also defined a reliability criterion to indicate the probability of failure. In another study, Antonio and Hoffbauer [109] presented an approach that simultaneously considers reliability and robustness of angle-ply composites. More recently, Lee *et al.* [110] investigated the importance of laminate stacking sequence on the robustness of a composite panel. They concluded that the survivability of the composite panel can be increased by considering uncertainties in the design stage.

From the above discussion it can be seen that, whilst significant research has already investigated the problem of design and optimization of laminated composite

materials, there is still the need for research in the area of robust design of hybrid composites. Despite several experimental studies with regard to different aspects of hybrid composites, very little is known about the reason behind the emergence of the hybrid effect and it is not clear what factors affect the performance of hybrid composites. Therefore, the studies presented thus far have not incorporated both the hybrid effect and uncertainties, simultaneously.

In the present research, the hybridization mechanism in fibre reinforced hybrid composite subjected to flexural load is studied to elucidate the hybrid effect with the hope of filling the gap in this area. Then, by considering the hybrid effect, the problem of robust optimization design has been investigated more accurately.

## 2.9. References


[1] Waddoups ME, McCullers LA, Olsen FO, Ashton JE. Structural synthesis of anisotropic plates. in AIAA/ASME 11th Struct., Struct. Dyn. and Math Conf., Denver, Colorado. 1970.

[2] Davidon WC. Variable metric method for minimization. SIAM Journal on Optimization. 1991;1:1-17.

[3] Kim C, Lee DY. Design optimization of a curved actuator with piezoelectric fibers. International Journal of Modern Physics B. 2003;17:1971-1975.

[4] Moh J, Hwu C. Optimization for buckling of composite sandwich plates. AIAA journal. 1997;35:863-868.

[5] Nocedal J, Wright SJ. Sequential quadratic programming. 2006: Springer.

[6] Saravanos D, Chamis C. An integrated methodology for optimizing the passive damping of composite structures. Polymer composites. 1990;11:328-336.

[7] Topal U, Uzman U. Maximization of buckling load of laminated composite plates with central circular holes using MFD method. Structural and Multidisciplinary Optimization. 2008;35:131-139.

[8] Svanberg K. The method of moving asymptotes—a new method for structural optimization. International journal for numerical methods in engineering. 1987;24:359-373.

[9] Bendsøe MP, Olhoff N, Taylor JE. A variational formulation for multicriteria structural optimization. Journal of Structural Mechanics. 1983;11:523-544.

[10] Bruyneel M, Fleury C. Composite structures optimization using sequential convex programming. Advances in Engineering Software. 2002;33:697-711.

[11] Tsau LR, Chang YH, Tsao FL. The design of optimal stacking sequence for laminated FRP plates with inplane loading. Computers & structures. 1995;55:565-580.

[12] Han L, Neumann M. Effect of dimensionality on the Nelder–Mead simplex method. Optimization Methods and Software. 2006;21:1-16.

[13] Romeijn HE, Zabinsky ZB, Graesser DL, Neogi S. New reflection generator for simulated annealing in mixed-integer/continuous global optimization. Journal of Optimization Theory and Applications. 1999;101:403-427.

[14] Erdal O, Sonmez FO. Optimum design of composite laminates for maximum buckling load capacity using simulated annealing. Composite Structures. 2005;71:45-52.

[15] Callahan KJ, Weeks GE. Optimum design of composite laminates using genetic algorithms. Composites Engineering. 1992;2:149-160.

[16] Kalantari M, Nami MR, Kadivar MH. Optimization of composite sandwich panel against impact using genetic algorithm. International Journal of Impact Engineering. 2010;37:599-604.

[17] Venkataraman S, Haftka RT. Optimization of composite panels-a review. in Proceedings-American Society For Composites. 1999.

[18] Kathiravan R, Ganguli R. Strength design of composite beam using gradient and particle swarm optimization. Composite Structures. 2007;81:471-479.

[19] Suresh S, Sujit P, Rao A. Particle swarm optimization approach for multi-objective composite box-beam design. Composite Structures. 2007;81:598-605.

[20] Aymerich F, Serra M. Optimization of laminate stacking sequence for maximum buckling load using the ant colony optimization (ACO) metaheuristic. Composites Part A: Applied Science and Manufacturing. 2008;39:262-272.

[21] Kere P, Lyly M, Koski J. Using multicriterion optimization for strength design of composite laminates. Composite Structures. 2003;62:329-333.

[22] Lund E, Stegmann J. On structural optimization of composite shell structures using a discrete constitutive parametrization. Wind Energy. 2005;8:109-124.

[23] Kogiso N, Watson LT, Gürdal Z, Haftka RT. Genetic algorithms with local improvement for composite laminate design. Structural and Multidisciplinary Optimization. 1994;7:207-218.

[24] Lin CC, YJ Lee. Stacking sequence optimization of laminated composite structures using genetic algorithm with local improvement. Composite Structures. 2004;63:339-345.

[25] Awad ZK, Aravinthan T, Zhuge Y, Gonzalez F. A review of optimization techniques used in the design of fibre composite structures for civil engineering applications. Materials & Design. 2012;33: 534-544.

[26] Ghiasi H, Fayazbakhsh K, Pasini D, Lessard L. Optimum stacking sequence design of composite materials Part II: Variable stiffness design. Composite Structures. 2010;93:1-13.

[27] Ghiasi H, Pasini D, Lessard L. Optimum stacking sequence design of composite materials Part I: Constant stiffness design. Composite Structures. 2009;90:1-11.

[28] Sonmez FO. Optimum design of composite structures: A literature survey (1969-2009). Journal of Reinforced Plastics and Composites. 2016;36:3-39.

[29] Hayashi T. On the improvement of mechanical properties of composites by hybrid composition. in Proc 8th intl reinforced plastics conference. 1972.

[30] Bunsell A, Harris B. Hybrid carbon and glass fibre composites. Composites, 1974;5:157-164.

[31] Phillips L. The hybrid effect—does it exist? Composites. 1976;7:7-8.

[32] Zweben C. Tensile strength of hybrid composites. in 18th Structural Dynamics and Materials Conference. 1977.

[33] Marom G, Fischer S, Tuler FR, Wagner HD. Hybrid effects in composites: conditions for positive or negative effects versus rule-of-mixtures behaviour. Journal of Materials Science. 1978;13:1419-1426.

[34] Kretsis G. A review of the tensile, compressive, flexural and shear properties of hybrid fibre-reinforced plastics. Composites. 1987;18:13-23.

[35] Summerscales J, Short D. Carbon fibre and glass fibre hybrid reinforced plastics. Composites. 1978;9:157-166.

[36] Manders P, Bader M. The strength of hybrid glass/carbon fibre composites. Journal of Materials Science. 1981;16:2233-2245.

[37] Peijs A, De Kok J. Hybrid composites based on polyethylene and carbon fibres. Part 6: Tensile and fatigue behaviour. Composites. 1993;24:19-32.

[38] Fu SY, Lauke B, Mäder E, Yue CY, Hu X. Tensile properties of short-glass-fiber- and short-carbon-fiber-reinforced polypropylene composites. Composites Part A: Applied Science and Manufacturing. 2000;31:1117-1125.

[39] Kim HS, Hong SI, Kim SJ. On the rule of mixtures for predicting the mechanical properties of composites with homogeneously distributed soft and hard particles. Journal of Materials Processing Technology. 2001;112:109-113.

[40] Davies IJ, Hamada H. Flexural properties of a hybrid polymer matrix composite containing carbon and silicon carbide fibres. Advanced Composite Materials. 2001;10:77-96.

[41] Sudarisman, Davies IJ. The effects of processing parameters on the flexural properties of unidirectional carbon fibre-reinforced polymer (CFRP) composites. Mater Sci Eng: A. 2008;498:65-8.

[42] Jarukumjorn K, Suppakarn N. Effect of glass fiber hybridization on properties of sisal fiber–polypropylene composites. Composites Part B: Engineering. 2009;40:623-627.

[43] Giancaspro JW, Papakonstantinou CG, Balaguru PN. Flexural response of inorganic hybrid composites with E-Glass and Carbon fibers. Journal of Engineering Materials and Technology. 2010;132:021005-1-8.

[44] Dong C, Ranaweera-Jayawardena HA, Davies IJ. Flexural properties of hybrid composites reinforced by S-2 glass and T700S carbon fibres. Composites Part B: Engineering. 2012;43:573-81.

[45] Banerjee S, Sankar BV. Mechanical properties of hybrid composites using finite element method based micromechanics. Composites Part B: Engineering. 2014;58:318-327.

[46] Subagia IA, Kim Y, Tijing LD, Kim CS, Shon HK. Effect of stacking sequence on the flexural properties of hybrid composites reinforced with carbon and basalt fibers. Composites Part B: Engineering. 2014;58:251-258.

[47] Pandya KS, Veerraju C, Naik NK. Hybrid composites made of carbon and glass woven fabrics under quasi-static loading. Materials & Design. 2011;32:4094-4099.

[48] Dong C, Davies IJ. Flexural and tensile moduli of unidirectional hybrid epoxy composites reinforced by S-2 glass and T700S carbon fibres. Materials & Design. 2014;54:893-899.

[49] Dong C, Davies IJ. Flexural and tensile strengths of unidirectional hybrid epoxy composites reinforced by S-2 glass and T700S carbon fibres. Materials & Design. 2014;54:955-966.

[50] Harris B, Bunsell AR. Impact properties of glass fibre/carbon fibre hybrid composites. Composites. 1975;6:197-201.

[51] Fukuda H, Chou TW. Stress concentrations in a hybrid composite sheet. Journal of Applied Mechanics. 1983;50:845-848.

[52] Harlow DG. Statistical properties of hybrid composites. I. recursion analysis. Proceedings of the Royal Society of London. A. Mathematical and Physical Sciences. 1983;389:67-100.

[53] Zeng QD, Fan FQ, Zhang YY. A random critical-core theory of microdamage in interply hybrid composites: I—First failure and hybrid effect. Composites Science and Technology. 1993;49:341-348.

[54] Swolfs Y, Gorbatikh L, Verpoest I. Fibre hybridisation in polymer composites: A review. Composites Part A: Applied Science and Manufacturing. 2014;67:181-200.

[55] Swolfs Y, Gorbatikh L, Verpoest I. Stress concentrations in hybrid unidirectional fibre-reinforced composites with random fibre packings. Composites Science and Technology. 2013;85:10-16.

[56] Curtin WA. Dimensionality and size effects on the strength of fiber-reinforced composites. Composites Science and Technology. 2000;60:543-551.

[57] Wisnom MR, Khan B, Hallett SR. Size effects in unnotched tensile strength of unidirectional and quasi-isotropic carbon/epoxy composites. Composite Structures. 2008;84:21-28.

[58] Hedgepeth JM, Van Dyke P. Local stress concentrations in imperfect filamentary composite materials. Journal of Composite Materials. 1967;1:294-309.

[59] Xing JI, Hsiao GC, Chou TW. A Dynamic Explanation of The Hybrid Effect. Journal of Composite Materials. 1981;15:443-461.

[60] Zhang Y, Li Y, Ma H, Yu T. Tensile and interfacial properties of unidirectional flax/glass fiber reinforced hybrid composites. Composites Science and Technology. 2013;88:172-177.

[61] Qiu Y, Schwartz P. Micromechanical behavior of Kevlar-149/S-glass hybrid seven-fiber microcomposites. II: Stochastic modeling of stress-rupture of hybrid composites. Composites Science and Technology. 1993;47:303-315.

[62] Ren P, Zhang Z, Xie L, Ren F, Jin Y, Di Y, Fang C. Hybrid effect on mechanical properties of M40-T300 carbon fiber reinforced Bisphenol A Dicyanate ester composites. Polymer Composites. 2010;31:2129-2137.

[63] Phillips MG. Composition parameters for hybrid composite materials. Composites. 1981;12:113-116.

[64] Phillips MG. Author's reply. Composites. 1982;13:18-20.

[65] Taketa I. Analysis of failure mechanisms and hybrid effects in carbon fibre reinforced thermoplastic composites (Analyse van faalmechanismen en hybride effecten in koolstofvezelversterkte thermoplastische composieten). 2011.

[66] Aveston J, Sillwood JM, Synergistic fibre strengthening in hybrid composites. Journal of Materials Science. 1976;11:1877-1883.

[67] Peijs AA, Catsman P, Govaert LE, Lemstra PJ. Hybrid composites based on polyethylene and carbon fibres Part 2: influence of composition and adhesion level of polyethylene fibres on mechanical properties. Composites. 1990;21:513-521.

[68] You YJ, Park YH, Kim HY, Park JS. Hybrid effect on tensile properties of FRP rods with various material compositions. Composite Structures. 2007;80:117-122.

[69] Taketa I, Ustarroz J, Gorbatikh L, Lomov SV, Verpoest I. Interply hybrid composites with carbon fiber reinforced polypropylene and self-reinforced polypropylene. Composites Part A: Applied Science and Manufacturing. 2010;41:927-932.

[70] Aveston J, Kelly A. Tensile First Cracking Strain and Strength of Hybrid Composites and Laminates. Philosophical Transactions of the Royal Society of London. Series A, Mathematical and Physical Sciences. 1980;294:519-534.

[71] Dong C, Davies IJ. Effect of stacking sequence on the flexural properties of carbon and glass fibre-reinforced hybrid composites. Advanced Composites and Hybrid Materials. 2018;1-1-11.

[72] Reddy CV, Babu PR, Ramnarayanan R, Das D. Mechanical Characterization Of Unidirectional Carbon And Glass/Epoxy Reinforced Composites For High Strength Applications. Proceedings of Materials Today 2017.

[73] Wu Z, Wang X, Iwashita K, Sasaki T, Hamaguchi Y. Tensile fatigue behaviour of FRP and hybrid FRP sheets. Composites Part B: Engineering. 2010;41:396-402.

[74] Dickson RF, Fernando G, Adam T, Reiter H, Harris B. Fatigue behaviour of hybrid composites. Journal of materials science. 1989;24:227-233.

[75] Fernando G, Dickson RF, Adam T, Reiter H, Harris B. Fatigue behaviour of hybrid composites. Journal of materials science. 1988;23:3732-3743.

[76] Jang BZ, Chen LC, Wang CZ, Lin HT, Zee RH. Impact resistance and energy absorption mechanisms in hybrid composites. Composites science and technology. 1989;34:305-335.

[77] Park R, Jang J. Impact behavior of aramid fiber/glass fiber hybrid composite: Evaluation of four-layer hybrid composites. Journal of materials science. 2001;36:2359-2367.

[78] Onal L, Adanur S. Effect of Stacking Sequence on the Mechanical Properties of Glass–Carbon Hybrid Composites before and after Impact. Journal of Industrial Textiles. 2002;31:255-271.

[79] Sevkat E, Liaw B, Delale F, Raju BB. Drop-weight impact of plain-woven hybrid glass–graphite/toughened epoxy composites. Composites Part A: Applied Science and Manufacturing. 2009;40:1090-1110.

[80] Sayer M, Bektaş NB, Sayman O. An experimental investigation on the impact behavior of hybrid composite plates. Composite Structures. 2010;92:1256-1262.

[81] Adali S, Verijenko V. Optimum stacking sequence design of symmetric hybrid laminates undergoing free vibrations. Composite Structures. 2001;54:131-138.

[82] Oh, J.H. and Y.G. Kim, Optimum bolted joints for hybrid composite materials. Composite structures. 1997;38:329-341.

[83] Walker M, Reiss T, Adali S. A procedure to select the best material combinations and optimally design hybrid composite plates for minimum weight and cost. Engineering Optimization. 1997;29:65-83.

[84] Abachizadeh M, Tahani M. An ant colony optimization approach to multi-objective optimal design of symmetric hybrid laminates for maximum fundamental frequency and minimum cost. Structural and Multidisciplinary Optimization. 2009;37:367-376.

[85] António CC. A hierarchical genetic algorithm with age structure for multimodal optimal design of hybrid composites. Structural and Multidisciplinary Optimization. 2006;31:280-294.

[86] Hemmatian H, Fereidoon A, Assareh E. Optimization of hybrid laminated composites using the multi-objective gravitational search algorithm (MOGSA). Engineering Optimization. 2014;46:1169-1182.

[87] Hemmatian H, Fereidoon A, Sadollah A, Bahreininejad A. Optimization of laminate stacking sequence for minimizing weight and cost using elitist ant system optimization. Advances in engineering Software. 2013;57:8-18.

[88] Sandeep G, Chakraborty D, Dutta A. Multi-objective optimization of hybrid laminates subjected to transverse impact. Composite Structures. 2006;73:360-369.

[89] Deb K. Multi-objective optimization using evolutionary algorithms: John Wiley & Sons; 2001.

[90] Adali S, Walker M, Verijenko VE. Multiobjective optimization of laminated plates for maximum prebuckling, buckling and postbuckling strength using continuous and discrete ply angles. Composite Structures. 1996;35:117-130.

[91] Walker M, Reiss T, Adali S. Multiobjective design of laminated cylindrical shells for maximum torsional and axial buckling loads. Computers & structures. 1997;62:237-242.

[92] Walker M, Smith RE. A technique for the multiobjective optimisation of laminated composite structures using genetic algorithms and finite element analysis. Composite structures. 2003;62:123-128.

[93] Almeida F, Awruch A. Design optimization of composite laminated structures using genetic algorithms and finite element analysis. Composite structures. 2009;88:443-454.

[94] Kaufmann M, Zenkert D, Wennhage P. Integrated cost/weight optimization of aircraft structures. Structural and Multidisciplinary Optimization. 2010;41:325-334.

[95] Zitzler E, Laumanns M, Thiele L. SPEA2: Improving the strength Pareto evolutionary algorithm. 2001, Tik-report.

[96] Knowles J, Corne D. The pareto archived evolution strategy: A new baseline algorithm for pareto multiobjective optimisation. in Evolutionary Computation, 1999. CEC 99. Proceedings of the 1999 Congress on. 1999. IEEE.

[97] Deb K, Pratap A, Agarwal S, Meyarivan TA. A fast and elitist multiobjective genetic algorithm: NSGA-II. IEEE transactions on evolutionary computation. 2002;6:182-97.

[98] Lakshmi K, Rao ARM. Multi-objective optimal design of laminated composite skirt using hybrid NSGA. Meccanica. 2013;48:1431-1450.

[99] Visweswaraiah SB, Ghiasi H, Pasini D, Lessard L. Multi-objective optimization of a composite rotor blade cross-section. Composite Structures. 2013;96:75-81.

[100] Adali S, Lene F, Duvaut G, Chiaruttini V. Optimization of laminated composites subject to uncertain buckling loads. Composite Structures. 2003;62:261-269.

[101] Miki M, Murotsu Y, Tanaka T, Shao S. Reliability-based optimization of fibrous laminated composites. Reliability Engineering & System Safety. 1997;56:285-290.

[102] Lee D, Morillo C, Oller S, Bugeda G, Oñate E. Robust design optimisation of advance hybrid (fiber–metal) composite structures. Composite Structures. 2013;99:181-192.

[103] Helton JC, Johnson JD, Sallaberry CJ, Storlie CB. Survey of sampling-based methods for uncertainty and sensitivity analysis. Reliability Engineering & System Safety. 2006;91:1175-1209.

[104] Huang B, Du X. Analytical robustness assessment for robust design. Structural and Multidisciplinary Optimization. 2007;34:123-37.

[105] Allen JK, Seepersad C, Choi H, Mistree F. Robust design for multiscale and multidisciplinary applications. Journal of Mechanical Design. 2006;128:832-843.

[106] Taguchi G. Performance analysis design. International Journal of Production Research. 1978;16:521-530.

[107] Walker M, Hamilton R. A technique for optimally designing fibre-reinforced laminated plates with manufacturing uncertainties for maximum buckling strength. Engineering Optimization. 2005;37:135-144.

[108] Manan A, Cooper J. Design of composite wings including uncertainties: a probabilistic approach. Journal of Aircraft. 2009;46:601-607.

[109] António CC, Hoffbauer LN. An approach for reliability-based robust design optimisation of angle-ply composites. Composite Structures. 2009;90:53-59.

[110] Lee MC, Mikulik Z, Kelly DW, Thomson RS, Degenhardt R. Robust design–a concept for imperfection insensitive composite structures. Composite Structures. 2010;92:1469-1477.

# 3

# Robustness for Unidirectional Carbon/Glass Fibre Reinforced Hybrid Epoxy Composites under Flexural Loading[1]

## 3.1. Introduction

Hybrid composites reinforced by more than one type of fibres are of great research interest because they provide a convenient way to achieving tailored material properties. Although carbon fibres are well known for high strength, they have low strain-to-failure because of their high stiffness. Compared to carbon fibres, glass fibres have much higher strain-to-failure due to their lower modulus. From this point, it is possible to increase the strain-to-failure by substitution of carbon fibres for glass fibres.

When considering the mechanical properties of hybrids, a general rule of mixtures (RoM) approach may be utilized which quantifies a material property with respect to the volume concentration of its constituents. Many researchers have however noted the existence of hybrid effects in which the material property as predicted by the RoM differs to that observed in reality. A positive or negative hybrid effect is defined as the positive or negative deviation of a certain mechanical property from the RoM behaviour, respectively [1].

Dong *et al.* [2-5] studied the flexural properties of unidirectional carbon/glass fibre reinforced hybrid epoxy composites using both experiments and finite element

[1] This Chapter has been published in Composite Structures, Vol 128, 2015, Pages 354-362

analysis (FEA). It is shown partial substitution of carbon fibres for glass fibres on the compressive side results in improved flexural strength, *i.e.* positive hybrid effect. Dong *et al.* [6-8] further investigated optimal design of hybrid composites. It is concluded that in order to achieve positive hybrid effects, the fibre volume fraction of the glass/epoxy section needs to be higher than that of the carbon/epoxy section [6, 7].

In addition to unidirectional composites, a recent study [9] on the hybrid composites made of carbon and glass woven fabrics showed that both the tensile and compressive strengths showed positive hybrid effects. For short fibre composites, Miwa and Horiba [10] found that the tensile strength of the hybrid composite could be estimated by the additive rule of hybrid mixtures, using the tensile strengths of both composites.

Traditional design of composites is based on a deterministic approach, and a large factor of safety is needed for incorporating the variability of data. A new alternative approach is probabilistic design [11-15], which allows the estimation of reliability and inclusion of stochastic variability [16].

Variability in the performance of composite materials arises mainly from the variability in constituent properties, fibre distribution, structural geometry, loading conditions and also manufacturing process [17]. Fertig *et al.* [18] shows that microstructural variations, especially volume fraction variations, lead to significant stress variations in composites. Spurgeon [19] shows the variation in fibre volume fraction can be as high as ±1%. Shaw [14] shows a 1.3% standard deviation for fibre volume fraction. Another important source of manufacturing related variation is ply thickness. According to Chamis [12], the coefficient of variation (CoV) can be as high as 5%.

Antonio and Hoffbauer [20] studied the uncertainty propagation on structural response of composites using three different approaches: a first-order local method, a Global Sensitivity Analysis supported by a variance-based method and an extension of local variance to estimate the global variance over all domain of inputs. The

uncertainty quantification and stochastic modelling approaches in FRP composites were reviewed by Sriramula and Chryssanthopoulos [21].

In this study, the robustness of unidirectional S-2 glass and T700S carbon fibre reinforced epoxy hybrid composites under flexural loading is investigated. The objective is developing an approach to the robust design of hybrid composites.

## 3.2. Flexural Properties Modelling

### 3.2.1. Material Properties

The hybrid composites being investigated in this study are made by embedding two types of fibres, T700S carbon and S-2 glass, into one common matrix, epoxy. The typical material properties of the fibres and matrix are shown in Table 3-1. The lamina properties, including the longitudinal modulus $E_{11}$, the transverse moduli $E_{22}$ and $E_{33}$, and the shear moduli $G_{12}$, $G_{13}$ and $G_{23}$, are derived from the constituent properties using Hashin's model [22], and the lamina stiffness matrices are derived.

**Table 3-1: Typical properties of fibres and resin**

| Material | Tensile modulus (GPa) | Tensile strength (MPa) | Density (kg/m$^3$) |
|---|---|---|---|
| Carbon fibres (T700S) | 230 | 4900 | 1800 |
| S-2 glass fibres | 86.9 | 4890 | 2460 |
| Epoxy | 3.1 | 69.6 | 1090 |

### 3.2.2. Flexural Strength

With reference to our previous studies [2-8], the stacking configuration for the hybrid composites is achieved by partially substituting carbon/epoxy laminas on the compressive side of a full carbon/epoxy composite laminate for glass/epoxy laminas. A hybrid composite specimen under the three point bending is schematically shown in Figure 3-1. The stress distribution can be conveniently obtained using the Classic

Lamination Theory (CLT) [23]. The CLT is chosen for the computation efficiency because a large amount of computation is needed. The details can be found in our previous studies [6-8]. Only a brief description is given here for completeness.

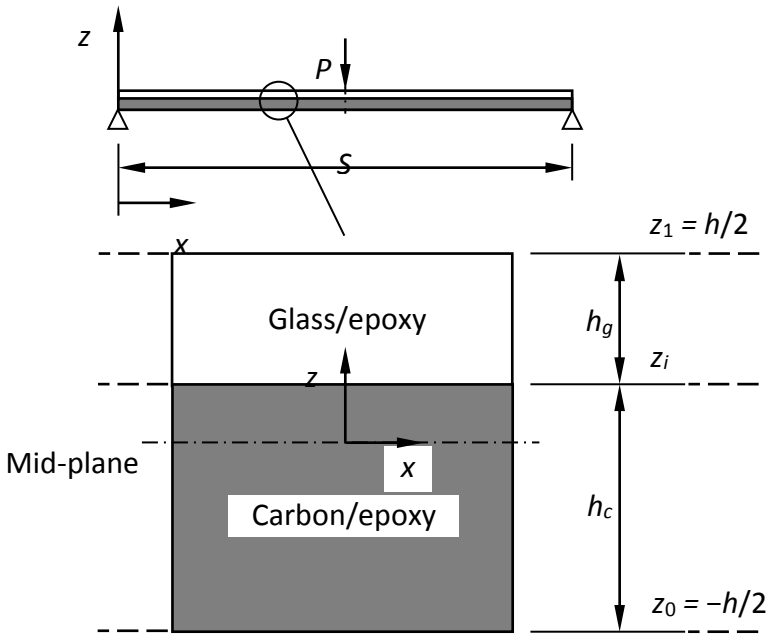


**Figure 3-1: A hybrid composite specimen under the three point bending**

For the purpose of quantitatively characterising the degree of hybridisation, hybrid ratio is introduced, which is the relative percentage of glass fibres with respect to all fibres, *i.e.*

$$r_h = \frac{h_g V_{fg}}{h_g V_{fg} + h_c V_{fc}} \tag{3-1}$$

According to the CLT, the strains in a laminate can be written in the form

$$\boldsymbol{\varepsilon} = \boldsymbol{\varepsilon}^0 + z\boldsymbol{\kappa} \tag{3-2}$$

For a test specimen under the three-point bending, the laminate consecutive equations are

$$\begin{Bmatrix} \mathbf{0} \\ \mathbf{M} \end{Bmatrix} = \begin{bmatrix} \mathbf{A} & \mathbf{B} \\ \mathbf{B} & \mathbf{D} \end{bmatrix} \begin{Bmatrix} \boldsymbol{\varepsilon}^{\mathbf{0}} \\ \boldsymbol{\kappa} \end{Bmatrix} \tag{3-3}$$

where, $\mathbf{M} = \begin{bmatrix} M_{xx} & 0 & 0 \end{bmatrix}^T$.

The mid-plane strain and curvature are computed as

$$\boldsymbol{\varepsilon}^{\mathbf{0}} = \mathbf{B}_{\mathbf{1}}\mathbf{M} \tag{3-4}$$

$$\boldsymbol{\kappa} = \mathbf{D}_{\mathbf{1}}\mathbf{M} \tag{3-5}$$

where,

$$\mathbf{B}_{\mathbf{1}} = -\mathbf{A}^{-1}\mathbf{B}\left(\mathbf{D} - \mathbf{B}\mathbf{A}^{-1}\mathbf{B}\right)^{-1}$$

$$\mathbf{D}_{\mathbf{1}} = \left(\mathbf{D} - \mathbf{B}\mathbf{A}^{-1}\mathbf{B}\right)^{-1}.$$

The strains at the upper and lower surfaces of the glass/epoxy section are

$$\begin{aligned} \boldsymbol{\varepsilon}_{\mathbf{g}}^{\mathbf{upper}} &= \boldsymbol{\varepsilon}^{\mathbf{0}} + \frac{h}{2}\boldsymbol{\kappa} \\ \boldsymbol{\varepsilon}_{\mathbf{g}}^{\mathbf{lower}} &= \boldsymbol{\varepsilon}^{\mathbf{0}} + z_i\boldsymbol{\kappa} \end{aligned} \tag{3-6}$$

Likewise, the strains at the upper and lower surfaces of the carbon/epoxy section are

$$\boldsymbol{\varepsilon}_{\mathbf{c}}^{\mathbf{upper}} = \boldsymbol{\varepsilon}^{\mathbf{0}} + z_i \boldsymbol{\kappa}$$
$$\boldsymbol{\varepsilon}_{\mathbf{c}}^{\mathbf{lower}} = \boldsymbol{\varepsilon}^{\mathbf{0}} - \frac{h}{2}\boldsymbol{\kappa} \tag{3-7}$$

where the *z* coordinate at the interface is

$$z_i = \frac{\left[(1-r_h)V_{fg} - r_h V_{fc}\right]h}{2\left[(1-r_h)V_{fg} + r_h V_{fc}\right]} \tag{3-8}$$

The stresses are

$$\boldsymbol{\sigma}_{\mathbf{g}} = \mathbf{Q}_{\mathbf{g}}\boldsymbol{\varepsilon}_{\mathbf{g}}$$
$$\boldsymbol{\sigma}_{\mathbf{c}} = \mathbf{Q}_{\mathbf{c}}\boldsymbol{\varepsilon}_{\mathbf{c}} \tag{3-9}$$

The stresses at both surfaces of each section are examined, and the applied load *P* is increased until one of the stresses reaches the strength. The maximum load is then used for calculating the flexural strength

$$S_F = \frac{3P_{\max}S}{2bh^2} \tag{3-10}$$

It should be noted that Equation (3-10) gives an apparent flexural strength based on the assumption of linear stress distribution along the thickness. When $V_{fc}$ = 50% and

$V_{fg}$ = 70%, the stress distribution for a [$0_G$/$0_{7C}$] hybrid composite laminate under the three point bending is shown in Figure 3-2, in which the normalised stress is given by $2bh^2\sigma/3PS$. It is clear that the stress distribution along the thickness is nonlinear. Thus, Equation (3-10) gives a measure of the maximum load which a specimen can withstand given the span and depth, i.e. apparent flexural strength.

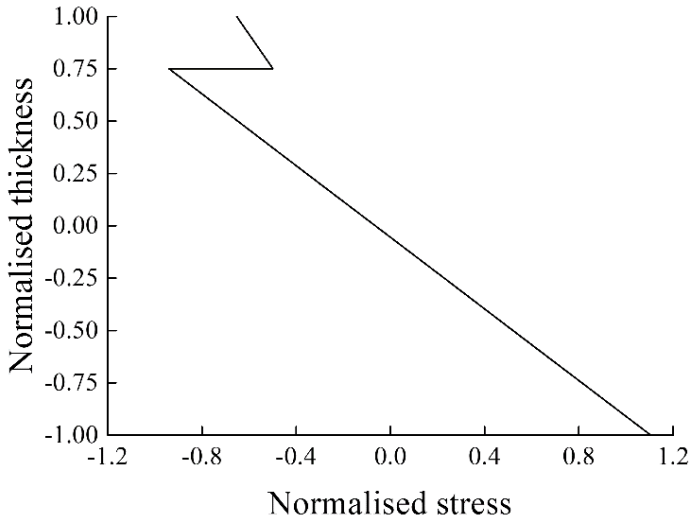


**Figure 3-2: Typical stress distribution under the three point bending**

The flexural strength of the hybrid composites using the rule of mixtures is given by

$$S_{FRoM} = S_{Fc}(1-r_h) + S_{Fg}r_h \tag{3-11}$$

The hybrid effect is given by

$$e_h = \frac{S_F}{S_{FRoM}} - 1 \tag{3-12}$$

### 3.2.3. Density

The density of carbon/glass fibre reinforced hybrid composites is given by

$$\rho_c = \rho_m + \frac{V_{fc}V_{fg}}{r_h V_{fc} + (1-r_h)V_{fg}}(\rho_{fc} - \rho_m) + \frac{r_h V_{fc}V_{fg}}{r_h V_{fc} + (1-r_h)V_{fg}}(\rho_{fg} - \rho_{fc}) \quad (3\text{-}13)$$

It is shown when $r_h$ = 0, which is for the full carbon composites, Equation (3-13) becomes

$$\rho_c = \rho_{fc}V_{fc} + \rho_m(1-V_{fc}) \quad (3\text{-}14)$$

Likewise, when $r_h$ = 1, which is for the full glass composites, Equation (3-13) becomes

$$\rho_c = \rho_{fg}V_{fg} + \rho_m(1-V_{fg}) \quad (3\text{-}15)$$

When $V_{fc} = V_{fg} = V_f$, Equation (3-13) is simplified to

$$\rho_c = \rho_{fc}(1-r_h)V_f + \rho_{fg}r_h V_f + \rho_m(1-V_f) \quad (3\text{-}16)$$

*i.e.* the density is in linear relationship with the hybrid ratio.

### 3.2.4. Specific Flexural Strength

The specific flexural strength is the ratio of the flexural strength and density, *i.e.*

$$SS_F = \frac{S_F}{\rho_c} \tag{3-17}$$

## 3.3. Robustness Evaluation

### 3.3.1. Variation Propagation

From the literature review it is shown that both the lamina thickness and fibre volume fraction can vary due to processing [24, 25]. If the lamina thickness increases, the corresponding fibre volume fraction will decrease. In this study, for simplicity, it is assumed variations only exist in the lamina thickness and the variations in the fibre volume fraction can be converted to the equivalent variations in the lamina thickness, which can have a CoV as high as 5%.

The variation in the hybrid ratio is related to the variations in the lamina thicknesses as given by

$$\sigma_{r_h}^2 = \left(\frac{\partial r_h}{\partial h_c}\right)^2 \sigma_{h_c}^2 + \left(\frac{\partial r_h}{\partial h_g}\right)^2 \sigma_{h_g}^2 \tag{3-18}$$

Where

$$\frac{\partial r_h}{\partial h_c} = -\frac{h_g V_{fc} V_{fg}}{\left(h_g V_{fg} + h_c V_{fc}\right)^2}$$
$$\frac{\partial r_h}{\partial h_g} = \frac{h_c V_{fc} V_{fg}}{\left(h_g V_{fg} + h_c V_{fc}\right)^2}$$

Equation (3-18) can be rewritten to

$$c_{vr_h}^2 = (1-r_h)^2\left(c_{vh_c}^2 + c_{vh_g}^2\right) \tag{3-19}$$

Equation (3-19) shows the variations in the thicknesses and fibre volume fractions can be represented by the variation in the hybrid ratio.

### 3.3.2. Regression Model

Using the CLT based approach, the flexural strengths at various hybrid ratios can be calculated, and the hybrid effects can be obtained using Eqns. 11 and 12. When the fibre volume fractions for both carbon/epoxy and glass/epoxy sections are 50%, the flexural strength and hybrid effect vs. hybrid ratio is shown in Figure 3-3.

It is seen from Figure 3-3 that a critical hybrid ratio exists around 0.25 at which the hybrid effect vs. hybrid ratio can be divided into two sections. The hybrid effect can be given by the following function by incorporating two boundary values, *i.e.*

$$e_h = \begin{cases} \dfrac{e_{hc}}{r_{hc}} r_h + a r_h\left(r_h - r_{hc}\right) & 0 \le r_h \le r_{hc} \\ e_{hc} - \dfrac{e_{hc}}{1-r_{hc}}\left(r_h - r_{hc}\right) + b_1\left(r_h - r_{hc}\right)\left(r_h - 1\right) & \\ + b_2\left(r_h - r_{hc}\right)\left(r_h - 1\right)^2 + b_3\left(r_h - r_{hc}\right)\left(r_h - 1\right)^3 & r_{hc} \le r_h \le 1 \end{cases} \tag{3-20}$$

where $a$, $b_1$, $b_2$, and $b_3$ are constants.

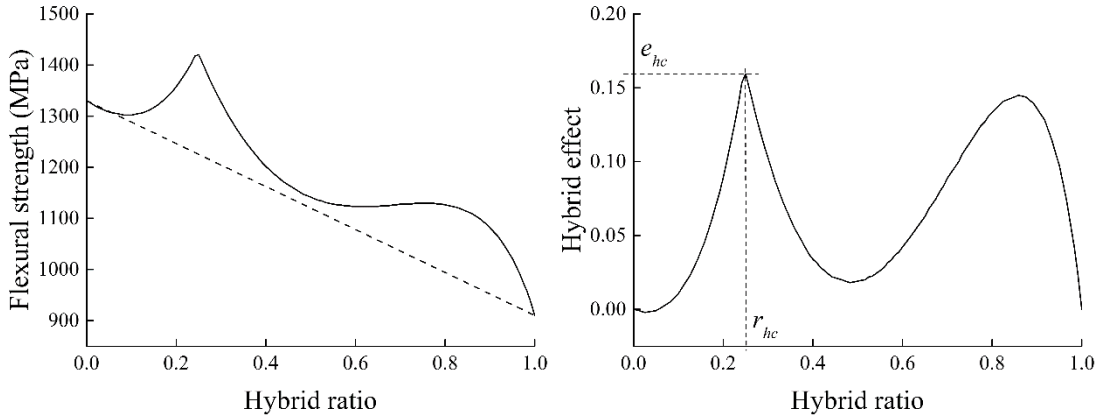


**Figure 3-3: Flexural strength and hybrid effect vs. hybrid ratio**

An examination of the strength data when the fibre volume fractions for both the carbon/epoxy and glass/epoxy sections are varied between 30% and 70% reveals that the critical hybrid ratio is strongly dependent on the compressive strength difference between the two sections. Figure 3-4 shows the critical hybrid ratio decreases with increasing compressive strength ratio. A regression model can be fitted to the data as given by

$$r_{hc} = -0.216 + 0.53\left(\frac{S_{Cg}}{S_{Cc}}\right)^{0.367} \tag{3-21}$$

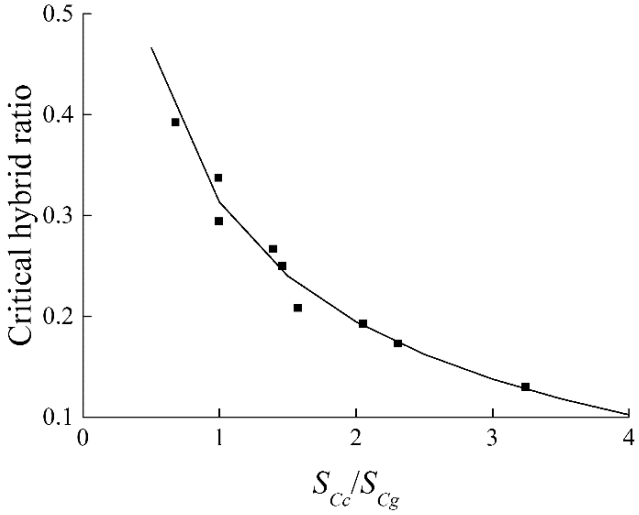


**Figure 3-4: Critical hybrid ratio vs. compressive strength ratio**

The corresponding hybrid effect at the critical hybrid ratio is found to be dependent on the critical hybrid ratio, as shown in Figure 3-5, from which it is seen that the hybrid effect at the critical hybrid ratio increases with the hybrid ratio. A regression model can be fitted to the data as given by

$$e_{hc} = 1.265 - 0.641 r_{hc}^{-0.386} \tag{3-22}$$

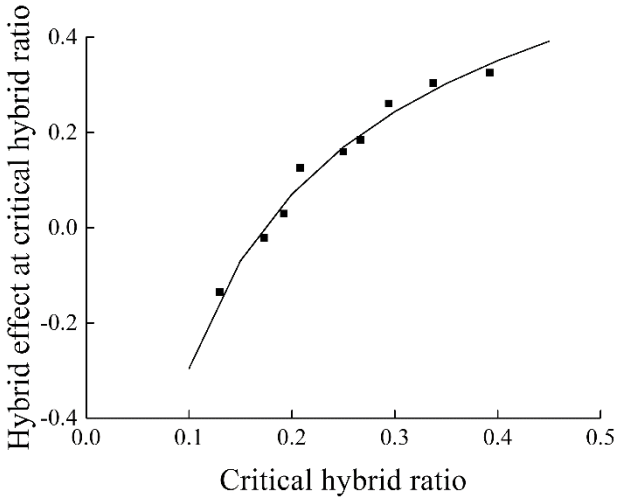


**Figure 3-5: Hybrid effect at critical hybrid ratio vs. critical hybrid ratio**

The constants $a$, $b_1$, $b_2$, and $b_3$ in Equation (3-20) are found to be dependent on the compressive strength ratio and the elastic modulus ratio, and the regression formulas are derived using multiple linear regression as given by

$$a = 2.3\frac{S_{Cc}}{S_{Cg}} + 0.2\left(\frac{S_{Cc}}{S_{Cg}}\right)^2 \tag{3-23}$$

$$b_1 = 0.867 - 8\frac{S_{Cg}}{S_{Cc}}\left(1 - 1.036\frac{E_g}{E_c}\right) \tag{3-24}$$

$$b_2 = 1.65 - 26.9\frac{S_{Cg}}{S_{Cc}}\left(1 - 1.022\frac{E_g}{E_c}\right) \tag{3-25}$$

$$b_3 = 7.83 - 31.1\frac{S_{Cg}}{S_{Cc}}\left(1 - 0.878\frac{E_g}{E_c}\right) \tag{3-26}$$

The $R^2$ of the developed regression model is 96.2%. Thus, a good fit is achieved. As an example, when the fibre volume fractions for both the carbon/epoxy and glass/epoxy sections are 50%, the hybrid effects from the CLT and regression model are shown in Figure 3-6, from which good agreement is found.

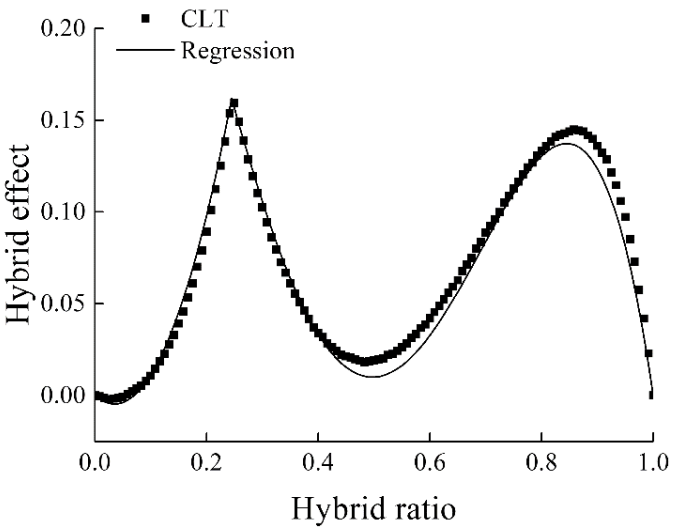


**Figure 3-6: Hybrid effect vs. hybrid ratio for both carbon/epoxy and glass/epoxy fibre volume fractions being 50%**

With the aid of the regression formulas, the change in the hybrid effect due to input variations can be conveniently evaluated by the first derivative of hybrid effect with respect to hybrid ratio, as given by

$$\frac{de_h}{dr_h}=\begin{cases}\dfrac{e_{hc}}{r_{hc}}-ar_{hc}+2ar_h & 0\le r_h\le r_{hc}\\ -\dfrac{e_{hc}}{1-r_{hc}}+b_1\left(2r_h-r_{hc}-1\right) & \\ +b_2\left(r_h-1\right)^2+2b_2\left(r_h-r_{hc}\right)\left(r_h-1\right) & r_{hc}\le r_h\le 1\\ +b_3\left(r_h-1\right)^3+3b_3\left(r_h-r_{hc}\right)\left(r_h-1\right)^2 & \end{cases} \tag{3-27}$$

When the fibre volume fractions for both the carbon/epoxy and glass/epoxy sections are 50%, the first derivative of hybrid effect is shown in Figure 3-7.

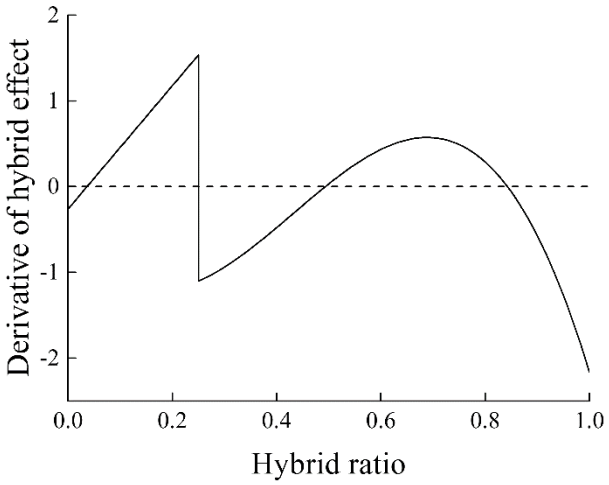


**Figure 3-7: Derivative of hybrid effect vs. hybrid ratio for both carbon/epoxy and glass/epoxy fibre volume fractions being 50%**

### 3.3.3. Robust Index

It is seen from Figure 3-7 that a large range exists for the first derivative of hybrid effect as this is a tangent value which can approach infinity. In order to limit the range, the arctangent is found for the absolute value of the derivative and divided by $\pi/2$, the resulting value is defined as robust index, *i.e.*

$$RI_{e_h} = \frac{2}{\pi}\tan^{-1}\left|\frac{de_h}{dr_h}\right| \tag{3-28}$$

A robust index close to zero means the laminate design is more stable or robust.

It should be noted that Equation (3-28) gives a robust index based on the hybrid effect, which is only valid when the strengths of full carbon/epoxy and full glass/epoxy composites are comparable. If the strengths are significantly different, the first derivative of flexural strength of the hybrid composites needs to be derived. From Eqns. 11 and 12, the flexural strength is given by

$$S_F = (1+e_h)\left[S_{Fc} + (S_{Fg} - S_{Fc})r_h\right] \tag{3-29}$$

In order to make the magnitude of the flexural strength comparable with the hybrid ratio, the flexural strength is normalised using a reference value, *i.e.*

$$\underline{S}_F = \frac{(1+e_h)\left[S_{Fc} + (S_{Fg} - S_{Fc})r_h\right]}{S_{Fref}} \tag{3-30}$$

The first derivative of normalised flexural strength with respect to the hybrid ratio is

$$\frac{d\underline{S}_F}{dr_h} = \frac{1}{S_{Fref}}\left\{\left[S_{Fc} + (S_{Fg} - S_{Fc})r_h\right]\frac{de_h}{dr_h} + (1+e_h)(S_{Fg} - S_{Fc})\right\} \tag{3-31}$$

Similar to Equation (3-28), the robust index for the normalised flexural strength is defined as

$$RI_{\underline{S}_F} = \frac{2}{\pi}\tan^{-1}\left|\frac{d\underline{S}_F}{dr_h}\right| \tag{3-32}$$

If the specific flexural strength is of the interest, the robust index can be derived in a similar way. The normalised specific flexural strength is given by

$$\underline{SS}_F = \frac{S_F\rho_{cref}}{S_{Fref}\rho_c} = \frac{\rho_{cref}\underline{S}_F}{\rho_c} \tag{3-33}$$

The first derivative of normalised specific flexural strength with respect to the hybrid ratio is

$$\frac{d\underline{SS}_F}{dr_h} = \frac{\rho_{ref}}{\rho_c^2}\left(\frac{d\underline{S}_F}{dr_h}\rho_c - \frac{d\rho_c}{dr_h}\underline{S}_F\right) \tag{3-34}$$

Where

$$\frac{d\rho_c}{dr_h} = \frac{V_{fc}V_{fg}\left[-V_{fc}\left(\rho_{fc}-\rho_m\right)+V_{fg}\left(\rho_{fg}-\rho_m\right)\right]}{\left(r_hV_{fc}+\left(1-r_h\right)V_{fg}\right)^2} \tag{3-35}$$

The robust index for the normalised specific flexural strength is given by

$$RI_{\underline{SS}_F} = \frac{2}{\pi}\tan^{-1}\left|\frac{d\underline{SS}_F}{dr_h}\right| \tag{3-36}$$

## 3.4. Results and Discussion

### 3.4.1. Robust Indices and Strengths

When the fibre volume fraction for the carbon/epoxy section is 50%, the robust indices for the normalised flexural strength and specific flexural strength are shown in Figure 3-8, in which the fibre volume fraction for the glass/epoxy section varies from 30% to 70%. It is seen the robust index reaches the maximum at the critical hybrid ratio, *i.e.* the design with the maximum hybrid effect is the least robust one. For flexural strength, in most cases, the most robust design occurs when the hybrid

ratio is around 0.6 or 0.8. Similar trend is found for specific flexural strength. However, as the fibre volume fraction for the glass/epoxy section increases, the most robust region is narrowed down to where the hybrid ratio is around 0.8.

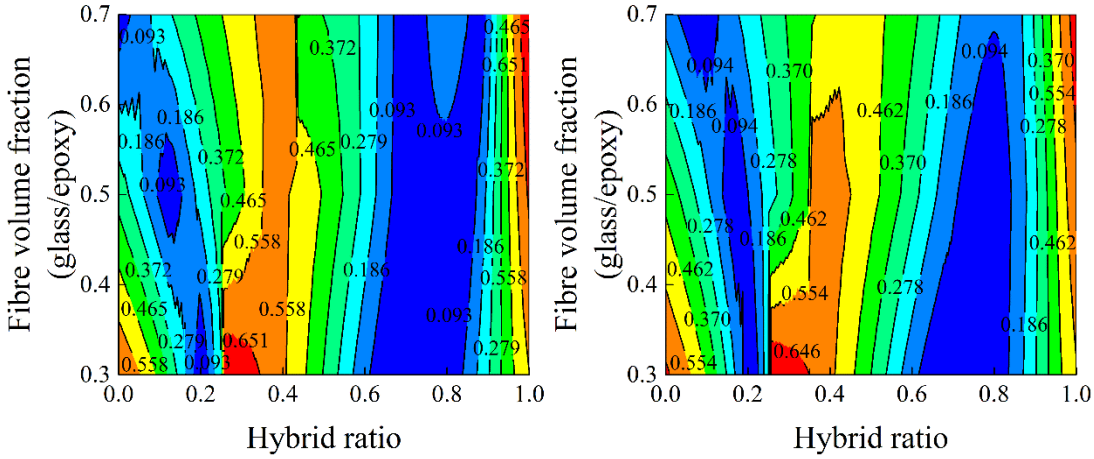


**Figure 3-8: Left: robust index for normalised flexural strength; right: robust index for normalised specific flexural strength (the fibre volume fraction for carbon/epoxy section is 50%)**

When the fibre volume fraction for the carbon/epoxy section is 50%, the normalised flexural strengths and specific flexural strengths are shown in Figure 3-9, in which the fibre volume fraction for the glass/epoxy section varies from 30% to 70%. It is shown that both the maximum flexural strength and maximum specific flexural strength occur when the fibre volume fraction for the glass/epoxy is 65%-70% and the hybrid ratio is ~0.4. This is consistent with our previous studies [6, 7] that in order to achieve positive hybrid effects, the fibre volume fraction of the glass/epoxy section needs to be higher than that of the carbon/epoxy section.

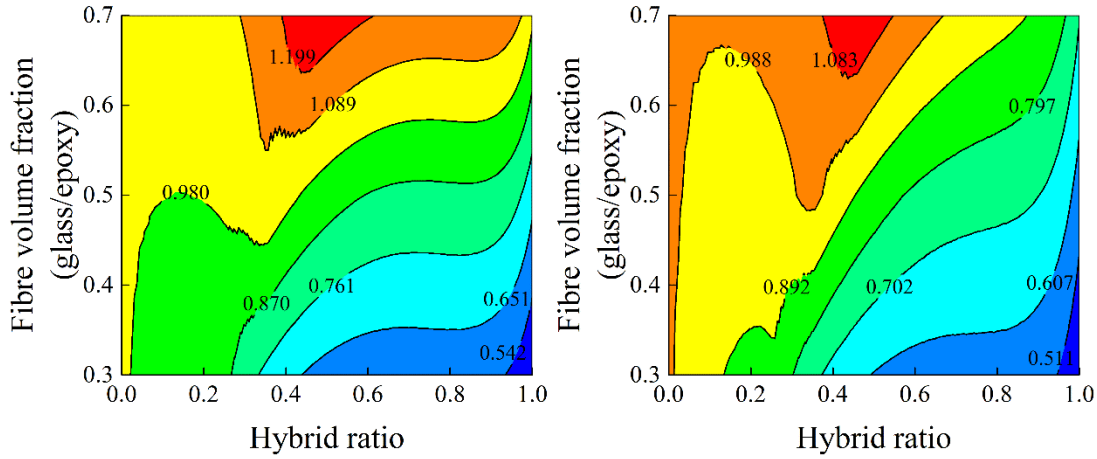


**Figure 3-9: Left: normalised flexural strength; right: normalised specific flexural strength (the fibre volume fraction for carbon/epoxy section is 50%)**

### 3.4.2. Robust Strength

It is seen that the flexural strength and robust index are two conflicting criteria. In order to obtain a unified design criterion, the normalised flexural strength and robust index are combined into the normalised robust flexural strength, which is defined to be

$$\underline{RS}_F = \frac{\underline{S}_F}{1 + RI_{\underline{S}_F}} \tag{3-37}$$

Likewise, the normalised robust specific flexural strength is given by

$$\underline{RSS}_F = \frac{\underline{SS}_F}{1 + RI_{\underline{SS}_F}} \tag{3-38}$$

When the fibre volume fraction for the carbon/epoxy section is 50%, the normalised robust flexural strength and specific flexural strength are shown in Figure 3-10, in which the fibre volume fraction for the glass/epoxy section varies from 30% to 70%.

It is shown that the optimum for the robust flexural strength occurs when the fibre volume fraction for the glass/epoxy is 65%-70% and the hybrid ratio is 0.7-0.9. The optimum for the robust specific flexural strength occurs when the fibre volume fraction for the glass/epoxy is 50%-70% and the hybrid ratio is ~0.1. The low hybrid ratio is due to the lower density of carbon fibres. These can serve as a design guideline for robust hybrid composites.

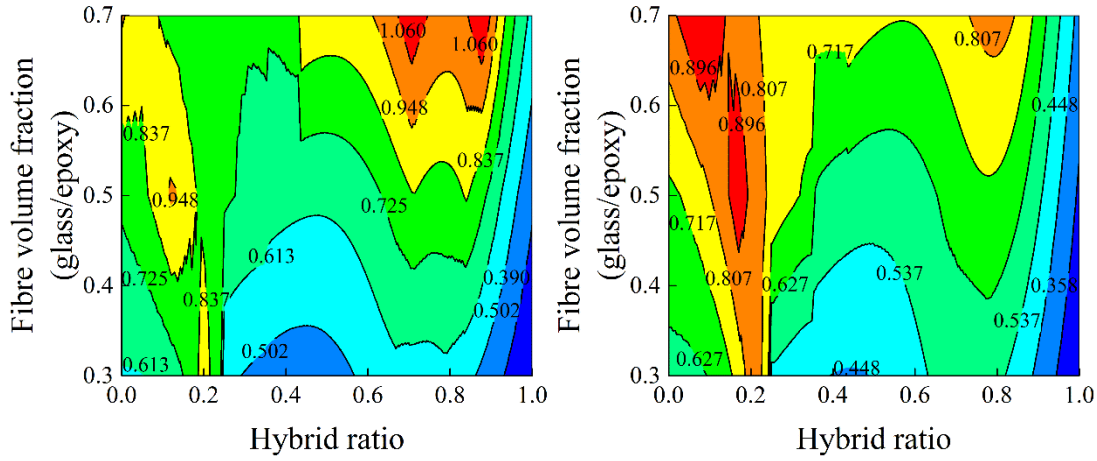


**Figure 3-10: Left: normalised robust flexural strength; right: normalised robust specific flexural strength (the fibre volume fraction for carbon/epoxy section is 50%)**

### 3.4.3. Monte Carlo Simulation

A number of hybrid composites are simulated to show the effect of parameter variations on the flexural strength or specific flexural strength. For all cases, the laminate is 2 mm thick and consists of 8 laminas of 0.25 mm thick. The CoV for the thickness is assumed to be 0.1. In each simulation, 1000 random data are generated and the resulting distributions are plotted.

The first case is the fibre volume fractions for both the carbon/epoxy and glass/epoxy sections are 50% and the hybrid ratio is 0.25, which corresponds to stacking sequence $[0_{2G}/0_{6C}]$. The nominal flexural strength and specific flexural strength are 1417 MPa and 928 kNm/kg, which are close to the maximum. The distributions of the flexural strength and specific flexural strength are shown in Figure 3-11. It is seen large variations are induced due to parameter variations. The distributions are negatively skewed. The minimum flexural strength and specific flexural strength are 1278 MPa

and 821 kNm/kg. 83.8% of the samples have flexural strength lower than the nominal value, and 80% of the samples have specific flexural strength lower than the nominal value. This indicates that if the nominal values are the design criteria, most samples will fail to meet the design requirement.

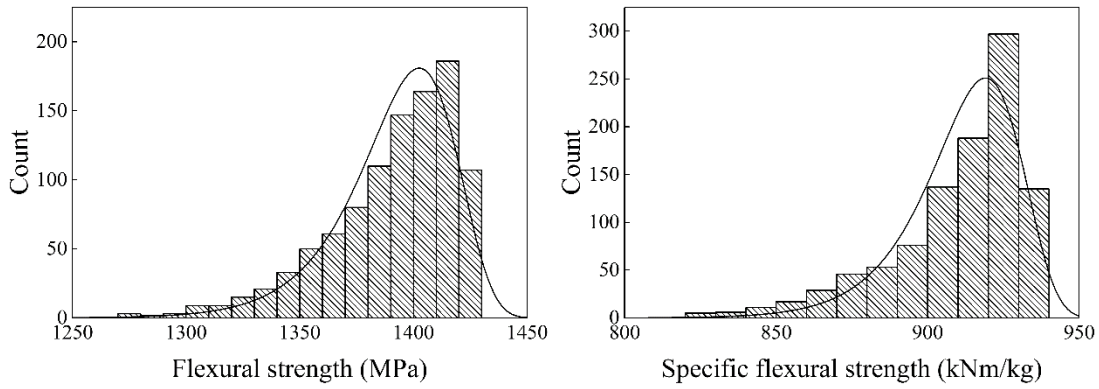


**Figure 3-11: Distributions of the flexural strength and specific flexural strength (the fibre volume fractions for both the carbon/epoxy and glass/epoxy sections are 50% and the hybrid ratio is 0.25)**

If the fibre volume fractions are kept constant but the hybrid ratio is changed to 0.625, which corresponds to stacking sequence $[0_{5G}/0_{3C}]$, the nominal flexural strength and specific flexural strength are 1114 MPa and 675 kNm/kg, and the distributions of the flexural strength and specific flexural strength are shown in Figure 3-12. It is seen the variations are much less than those of the previous case and the distributions are positively skewed. The minimum flexural strength and specific flexural strength are 1113 MPa and 669 kNm/kg. 33.6% of the samples have flexural strength lower than the nominal value, and 51.1% of the samples have specific flexural strength lower than the nominal value. This case is considered to be one of the most robust.

If the hybrid ratio is changed to 0.5, which corresponds to stacking sequence $[0_{4G}/0_{4C}]$, the nominal flexural strength and specific flexural strength are 1131 MPa and 703 kNm/kg. The distributions of the flexural strength and specific flexural strength are shown in Figure 3-13. The distributions are positively skewed. The minimum flexural strength and specific flexural strength are 1113 MPa and 677 kNm/kg. 49.6% of the samples have flexural strength lower than the nominal value,

and 51.2% of the samples have specific flexural strength lower than the nominal value. This is the case between cases 1 and 2.

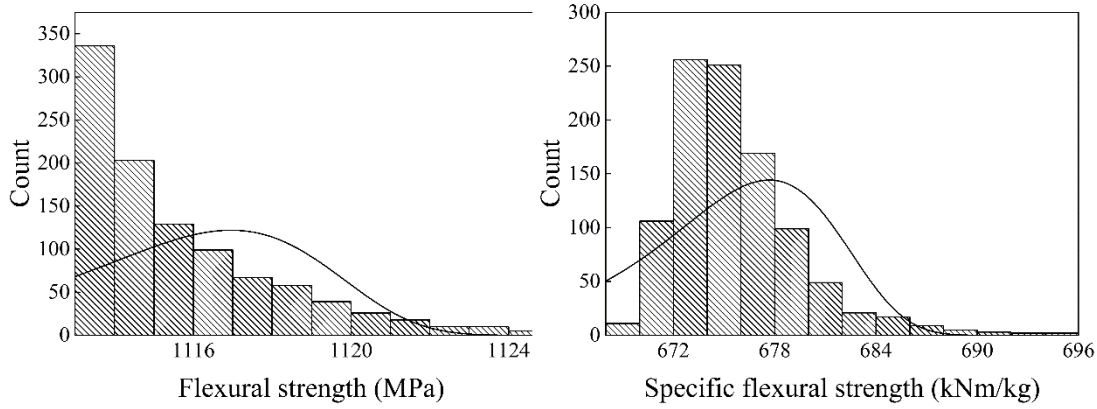


**Figure 3-12: Distributions of the flexural strength and specific flexural strength (fibre volume fractions for both the carbon/epoxy and glass/epoxy are 50% and the hybrid ratio is 0.625)**

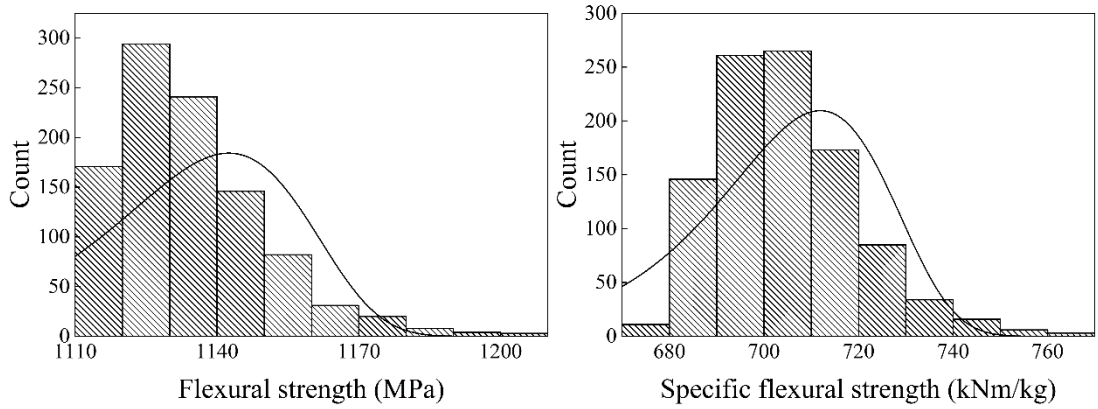


**Figure 3-13: Distributions of the flexural strength and specific flexural strength (the fibre volume fractions for both the carbon/epoxy and glass/epoxy sections are 50% and the hybrid ratio is 0.5)**

Re-considering case 1, if a minimum flexural strength of 1417 MPa needs to be achieved, the fibre volume fractions for the carbon/epoxy and glass/epoxy sections are increased to 55% and 65%, respectively, and the hybrid ratio is set to 0.5417, which corresponds to stacking sequence $[0_{4G}/0_{4C}]$. The distribution of the flexural strength is shown in Figure 3-14. It is seen a more robust design is achieved.

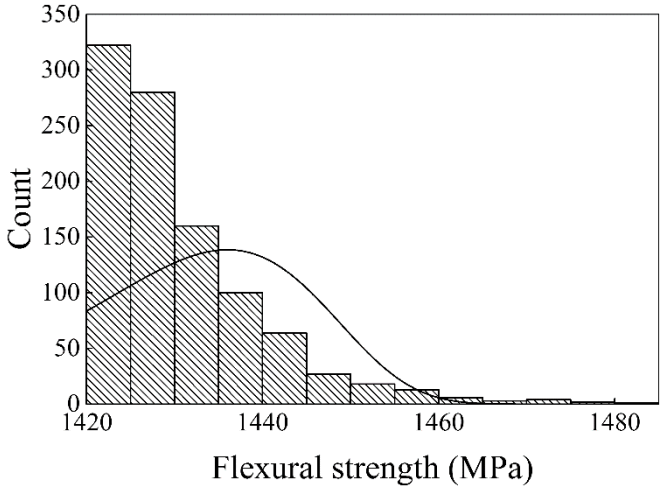


**Figure 3-14: Distributions of flexural strength (the fibre volume fractions for the carbon/epoxy and glass/epoxy sections are 55% and 65%, respectively, and the hybrid ratio is 0.5417)**

If a minimum specific flexural strength of 928 kNm/kg needs to be achieved, using the same fibre volume fractions, the hybrid ratio is set to 0.2826, which corresponds to stacking sequence $[0_{2G}/0_{6C}]$. The distribution of the flexural strength is shown in Figure 3-15. All of the samples meet the design requirement.

It is seen that the robust optima for the flexural strength and specific flexural strength are different.

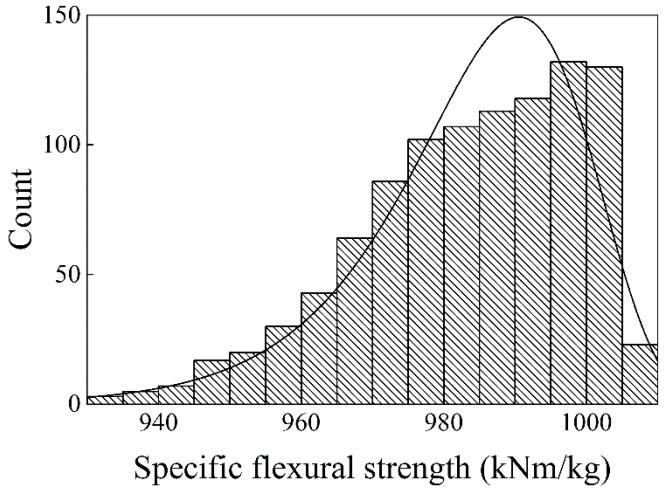


**Figure 3-15: Distributions of specific flexural strength (the fibre volume fractions for the carbon/epoxy and glass/epoxy sections are 55% and 65%, respectively, and hybrid ratio is 0.2826)**

## 3.5. Conclusions

A study on the robustness of unidirectional S-2 glass and T700S carbon reinforced epoxy hybrid composites under flexural loading is presented in this chapter. The flexural properties are computed using an approach based on the CLT, and the computed data for the hybrid effect are fitted to a regression model. With the aid of developed regression model, the robustness can be conveniently evaluated using the introduced robust index. The concept of robust strength is introduced to address both the strength and robustness criteria, with which the design guideline for robust hybrid composites is given. The influence of parameter variations on the flexural strength and specific flexural strength and how to improve the robustness are illustrated through a number of simulation cases.

Although carbon and glass fibres are used in this study, the methodology is suitable for other fibre types provided they have different strains-to-failure. Future work includes multi-objective optimisation study is needed to achieve the best design depending on the requirement of optimum and robustness.

## 3.6. References

[1] Marom G, Fischer S, Tuler FR, Wagner HD. Hybrid effects in composites: conditions for positive or negative effects versus rule-of-mixtures behaviour. Journal of Materials Science. 1978;13:1419-1426.

[2] Dong C, Davies IJ. Flexural properties of glass and carbon fiber reinforced epoxy hybrid composites. Proceedings of the Institution of Mechanical Engineers, Part L: Journal of Materials: Design and Applications. 2013;227:308-317.

[3] Dong C, Davies IJ. Flexural properties of E glass and TR50S carbon fiber reinforced epoxy hybrid composites. Journal of materials engineering and performance. 2013;22:41-49.

[4] Dong C, Duong J, Davies IJ. Flexural properties of S-2 glass and TR30S carbon fiber-reinforced epoxy hybrid composites. Polymer Composites. 2012;33:773-781.

[5] Dong C, Ranaweera-Jayawardena HA, Davies IJ. Flexural properties of hybrid composites reinforced by S-2 glass and T700S carbon fibres. Composites Part B: Engineering. 2012;43:573-581.

[6] Dong C, Davies IJ. Optimal design for the flexural behaviour of glass and carbon fibre reinforced polymer hybrid composites. Materials & Design. 2012 May 31;37:450-457.

[7] Dong C, Davies IJ. Flexural and tensile strengths of unidirectional hybrid epoxy composites reinforced by S-2 glass and T700S carbon fibres. Materials & Design. 2014;54:955-966.

[8] Dong C, Davies IJ. Flexural and tensile moduli of unidirectional hybrid epoxy composites reinforced by S-2 glass and T700S carbon fibres. Materials & Design. 2014;54:893-899.

[9] Pandya KS, Veerraju C, Naik NK. Hybrid composites made of carbon and glass woven fabrics under quasi-static loading. Materials & Design. 2011;32:4094-4099.

[10] Miwa M, Horiba N. Effects of fibre length on tensile strength of carbon/glass fibre hybrid composites. Journal of materials science. 1994;29:973-977.

[11] Chamis CC, Shiao MC. IPACS (Integrated Probabilistic Assessment of Composite Structures): Code development and applications. 1993.

[12] Chamis CC. Probabilistic simulation of multi-scale composite behavior. Theoretical and applied fracture mechanics. 2004;41:51-61.

[13] Chamis CC, Abumeri GH. Probabilistic dynamic buckling of composite shell structures. Composites Part A: Applied Science and Manufacturing. 2005;36:1368-1380.

[14] Shaw A, Sriramula S, Gosling PD, Chryssanthopoulos MK. A critical reliability evaluation of fibre reinforced composite materials based on probabilistic

micro and macro-mechanical analysis. Composites Part B: Engineering. 2010;41:446-453.

[15] Shiao MC, Chamis CC. Probabilistic evaluation of fuselage-type composite structures. Probabilistic engineering mechanics. 1999;14:179-187.

[16] Di Sciuva M, Lomario D. A comparison between Monte Carlo and FORMs in calculating the reliability of a composite structure. Composite Structures. 2003;59:155-162.

[17] Chiachio M, Chiachio J, Rus G. Reliability in composites–A selective review and survey of current development. Composites Part B: Engineering. 2012;43:902-913.

[18] Fertig RS, Jensen EM. Effect of fiber volume fraction variation across multiple length scales on composite stress variation: the possibility of stochastic multiscale analysis. in Proceedings-55th AIAA/ASMe/ASCE/AHS/SC Structures, Structural Dynamics, and Materials Conference. 2014.

[19] Spurgeon WA. Thickness and reinforcement fiber content control in composites by vacuum-assisted resin transfer molding fabrication processes. Army Research Lab Aberdeen Proving Ground MD; 2005.

[20] António CC, Hoffbauer LN. From local to global importance measures of uncertainty propagation in composite structures. Composite Structures. 2008;85:213-225.

[21] Sriramula S, Chryssanthopoulos MK. Quantification of uncertainty modelling in stochastic analysis of FRP composites. Composites Part A: Applied Science and Manufacturing. 2009;40:1673-1684.

[22] Chou TW. Microstructural design of fiber composites. Cambridge University Press; 2005.

[23] Mallick PK. Fiber-Reinforced Composites: Materials, manufacturing, and design. 3rd Edition. London: CRC press; 1993.

[24] Karahan M, Lomov SV, Bogdanovich AE, Mungalov D, Verpoest I. Internal geometry evaluation of non-crimp 3D orthogonal woven carbon fabric

composite. Composites Part A: Applied Science and Manufacturing. 2010;41:1301-1311.

[25] Hubert P, Poursartip A. Aspects of the compaction of composite angle laminates: an experimental investigation. Journal of Composite Materials. 2001;35:2-6.

p r d d d pr

# 4

# Numerical Investigation of the Hybridisation Mechanism in Fibre Reinforced Hybrid Composites Subjected to Flexural Load[1]

## 4.1. Introduction

Carbon and glass fibre reinforced polymer hybrid composites, which combine the advantages of the high specific strength of carbon fibres and high strain-to-failure of glass fibres, have become increasingly utilized in aerospace, civil and automotive applications. Since the strain-to-failure of glass fibres is higher than that of carbon fibres, it has proved possible to design hybrid composites with improved failure strain through the incorporation of glass fibres into carbon fibre reinforced polymer (CFRP) composites [1, 2].

The concept of a hybrid effect in composite materials was first noted by Hayashi [3] to take into account the deviation of properties from those predicted by the standard rule of mixtures (RoM). Research thus far has indicated that the properties of unidirectional carbon/glass fibre reinforced polymer matrix composites (PMCs) are affected by the stacking sequence and fibre volume fractions of the laminas [4-10] whilst recent work by the current authors [10, 11] has indicated that the flexural strength of carbon/glass fibre reinforced epoxy composites can be

[1] This Chapter has been published in Composites Part B: Engineering, Vol 102, 2016, Pages 100-111

improved by placing glass fibres at the compressive side. The fibre volume fractions of the laminas were also investigated and it was concluded that the fibre volume fraction of the glass/epoxy laminas should be higher than that of the carbon/epoxy laminas in order to achieve a hybrid composite with improved flexural strength [10].

In addition to unidirectional composites, recent studies [12, 13] on woven fabric carbon/glass hybrid composites indicated the presence of a positive hybrid effect for both tensile and flexural strength. For example, Zhang *et al.* [13] investigated the tensile and flexural strength of carbon/glass fibre hybrid composites with symmetrical stacking configurations containing eight woven fabric laminas and reported a positive hybrid effect when two carbon laminas were placed on the exterior. In contrast to woven hybrid fabric composites, Dong and Davies [14] reported no significant improvement for the flexural properties of bidirectional hybrid epoxy composites reinforced by T700S carbon and E glass fibres. However, their simulation studies did suggest that hybridisation of such composites could potentially improve the flexural strength under certain circumstances. Whilst the potential for a positive hybrid effect in composites is well known, the actual mechanisms that result in such an effect are still not well understood and thus no general rules exist to guide designers on how to design composites with an improved hybrid effect (such as that which might express itself in the form of improved flexural strength).

A number of analytical and numerical methods exist for the prediction of mechanical properties in hybrid composite laminates manufactured through the stacking of laminas containing different materials and/or fibre angles. Structural theories for such materials can be classified as “equivalent single-layer theories (ESL)”, “three dimensional elasticity theories” or “multiple model methods”. Among these theories, the classical lamination theory (CLT) remains one of the most popular ESL theories due to its simplicity and ability to adequately describe the static and kinematic behaviour of most laminates [15]. In addition to these structural theories, finite element analysis (FEA) has also been widely used to simulate the behaviour of composites. For example, several studies [1, 2, 10, 13, 15,

16] concerning the flexural and tensile modulus of carbon/glass fibre reinforced hybrid composite laminates have shown good agreement between the experimental results and predictions by CLT and FEA. Previous experimental studies indicated that for components with a large span-to-thickness ratio, shear stresses present in the laminas are negligible [16, 17] and thus CLT is able to accurately determine the stress and strain distributions within the laminas [16, 18].

In order to model the flexural strength of hybrid composites, once the stress distribution in the laminas has been determined (with the aid of CLT or FEA), an appropriate failure criterion is needed in order to estimate the maximum allowable load corresponding to failure of the laminas and thus the ultimate strength of the component. Amongst the failure theories proposed for the prediction of first ply failure (FPF) in composite laminates, the maximum stress, maximum strain, Azzi-Tsai-Hill and Tsai-Wu theories are most commonly used [18, 19]. However, detailed studies [20-23] have shown that not all of these theories are successful in predicting the failure strength of composites comprised of laminas with varying fibre orientations and materials. Therefore, with regards to the design process of laminate based composites, the lamina failure theories must first be evaluated with regards to their ability to predict the failure strength of a lamina and thus composite [24].

In this study, the mechanical behaviour of carbon and glass fibre reinforced hybrid composites with a relatively large span-to-thickness ratio under flexural loading was investigated numerically by FEA and analytically by CLT in order to determine the flexural modulus and stress distribution through the laminas. Two failure criteria which assume no stress interaction, namely, maximum stress and maximum strain theory, and two failure criteria which include full stress interaction, namely, Azzi-Tsai-Hill and Tsai-Wu, were used to estimate the FPF with the most appropriate criterion being chosen to determine the flexural strength. The effect of hybridisation of carbon and glass fibres on the flexural modulus and strength was investigated with the established approach then being used to elucidate the reasons behind the hybrid effect in hybrid composites with the aim of providing general rules for optimal design with respect to flexural strength. The general rules

derived in this study were then used to determine the stacking sequences in carbon/glass fibre reinforced epoxy hybrid composites that would be expected to exhibit improved flexural strength with the results being verified using CLT.

## 4.2. Hybrid Composite Model

In the present study, a carbon and glass fibre reinforced epoxy hybrid composite under three-point bending was investigated, as shown in Figure 4-1. Previous work by the current authors [2, 5, 10] has indicated a positive hybrid effect to exist with regards to the flexural strength of T700S carbon and S-2 glass fibre reinforced epoxy composites together with good agreement between CLT and FEA. Therefore, the same materials were used in the present study with the properties of the fibres and matrix being presented in Table 4-1. The thickness of each lamina, $h_i$, was chosen to be 0.2 mm with a relatively large span-to-thickness, $^{L}/_{h}$, ratio being used so that the component could be considered as a thin plate. Simple supports were used at both ends with a load, *F*, being applied at the mid-span.

Four out of the five elastic moduli for each transversely isotropic lamina, *i.e.*, longitudinal modulus, bulk modulus, longitudinal-transverse shear modulus and transverse-transverse shear modulus were calculated using Hashin's model whereas the transverse modulus was derived from the stress-strain relationship [25]. The longitudinal and transverse tensile strengths of each lamina were estimated based on the tensile failure of the fibres and matrix, respectively, whilst the transverse compressive strength of each lamina was calculated based on matrix failure with the longitudinal compressive strength being estimated from fibre micro-buckling in compression based on the Lo-Chim model [26].

It is shown from our previous study [5] that residual stresses have negligible effects on the flexural strength, and thus they are not included in the present model.

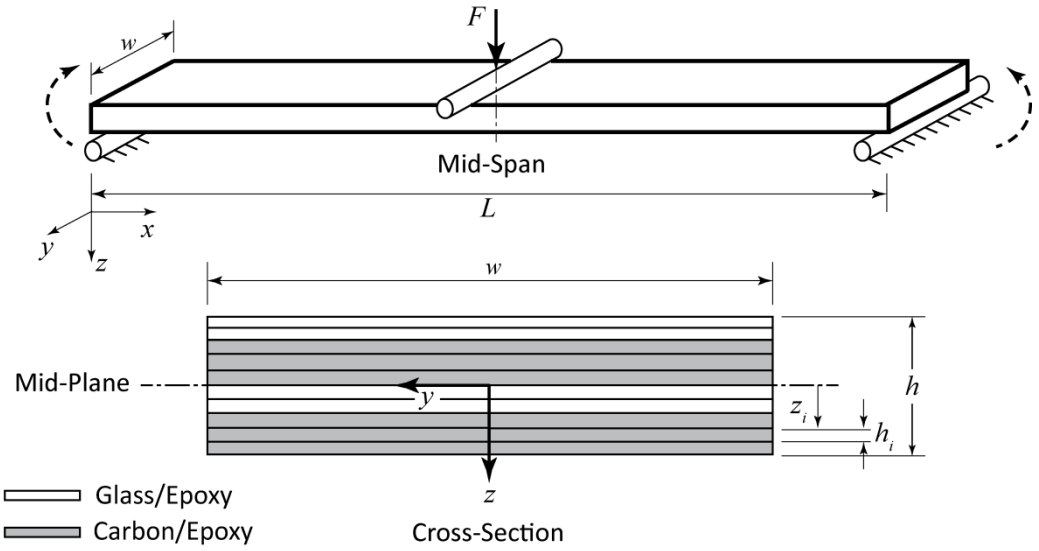


**Figure 4-1: Schematic representation of the carbon/glass fibre reinforced hybrid composite specimen in the three-point bend configuration.**

**Table 4-1: Assumed properties of the fibres and resin utilized in this work.**

| Material | Longitudinal Tensile Modulus, $E^f_{11}$ (GPa) | Transverse Tensile Modulus, $E^f_{22}$ (GPa) | Longitudinal / Transverse Poisson's Ratio, $\upsilon^f_{12}$ / $\upsilon^f_{21}$ | Tensile Strength (MPa) | Strain to Failure (%) |
|---|---|---|---|---|---|
| High strength carbon fibre [a] | 230 | 14.0 | 0.2 / 0.4 | 4900 | 2.1 |
| High strength glass fibre [b] | 86.9 | 86.9 | 0.2 / 0.2 | 4890 | 5.6 |
| High performance epoxy resin [c] | 3.10 | 3.10 | 0.3 / 0.3 | 69.60 | ~ 4 |

a T700S® 12K, Toray Industries, Inc., Tokyo, Japan.

b S-2 glass unidirectional Unitex plain weave UT-S500 fibre mat, SP System, Newport, Isle of Wight, UK.

c Kinetix R240 high performance epoxy resin with H160 hardener at a ratio of 4:1 by weight, ATL Composites Pty Ltd., Australia.

### 4.2.1. Classical Lamination Theory

The stress distribution across each lamina was calculated using CLT [19]. With reference to Figure 4-1, the *xy*-plane was taken to be within the plane of the hybrid composite with the z-axis being positive downwards and the direction of generated bending moment being shown as dashed arrows. Since the fibre angles may be

non-zero, global and principal material coordinate systems were defined separately as shown in Figure 4-2 with both a global *x-y-z* coordinate system and principal material *1-2-3* coordinate system being indicated. In formulating the CLT the out-of-plane stress components were considered to be negligible such that the strain distribution through the thickness of each lamina was linear. Since the component was assumed to be a thin plate, these assumptions would provide the in-plane normal and shear stresses to be sufficiently accurate in order to estimate the FPF. According to the Kirchhoff assumption for bending, after deformation the normal to the mid-plane remains straight and normal [15]. Thus, the strain at any point across the composite can be given in the following form:

$$\boldsymbol{\varepsilon} = \begin{Bmatrix} \varepsilon_x \\ \varepsilon_y \\ \gamma_{xy} \end{Bmatrix} = \boldsymbol{\varepsilon^0} + z\boldsymbol{\kappa} \tag{4-1}$$

where $\varepsilon^0$ is the strain vector of the mid-plane (membrane strain), $\kappa$ is the curvature vector of the mid-plane (vector of the second derivative of the displacement) and *z* is the distance from the mid-plane. The constitutive equations for a laminate composite subjected to bending moments, ***M***, and normal forces, ***N***, can be written as:

$$\begin{Bmatrix} \boldsymbol{N} \\ \boldsymbol{M} \end{Bmatrix} = \begin{bmatrix} \boldsymbol{A} & \boldsymbol{B} \\ \boldsymbol{B} & \boldsymbol{D} \end{bmatrix} \begin{Bmatrix} \boldsymbol{\varepsilon^0} \\ \boldsymbol{\kappa} \end{Bmatrix} \tag{4-2}$$

However, for a specimen subjected to three-point bending as shown in Figure 4-1 the normal force is zero and thus the composite constitutive equations can be simplified to:

$$\begin{Bmatrix} \boldsymbol{0} \\ \boldsymbol{M} \end{Bmatrix} = \begin{bmatrix} \boldsymbol{A} & \boldsymbol{B} \\ \boldsymbol{B} & \boldsymbol{D} \end{bmatrix} \cdot \begin{Bmatrix} \boldsymbol{\varepsilon^0} \\ \boldsymbol{\kappa} \end{Bmatrix} \tag{4-3}$$

where $\boldsymbol{M} = [M_{xx} \quad 0 \quad 0]^T$ when bending is applied in the *x* direction as shown in Figure 4-1 (or $[0 \quad M_{yy} \quad 0]^T$ when bending is applied in the *y* direction) and ***A***, ***B*** and ***D*** are the extensional stiffness matrix, extensional-bending coupling matrix and bending stiffness matrix, respectively. Given the external load being applied, the mid-plane strains, $\boldsymbol{\varepsilon^0}$, and curvatures, $\boldsymbol{\kappa}$, may be calculated. The strain at any location through the thickness can be found using Equation 4-1 whilst the stress components in each lamina may be given by:

$$\{\boldsymbol{\sigma}\}_{\boldsymbol{i}} = [\overline{\boldsymbol{Q}}]_{\boldsymbol{i}} \cdot \{\boldsymbol{\varepsilon}\}_{\boldsymbol{i}} \tag{4-4}$$

where $\{\boldsymbol{\sigma}\}_{\boldsymbol{i}}$ is the vector of in-plane normal and shear stresses in the *i*th lamina and $[\overline{\boldsymbol{Q}}]_{\boldsymbol{i}}$ is the transformed reduced stiffness matrix of the *i*th lamina.

Furthermore, the apparent flexural modulus was calculated using the following equation [15]:

$$E_{Fxx} = \frac{12}{h^3 D_{11}^*} \tag{4-5}$$

where *h* is the total thickness of the composite and $D_{11}^*$ is the first element of the inverse matrix of [**D]**.

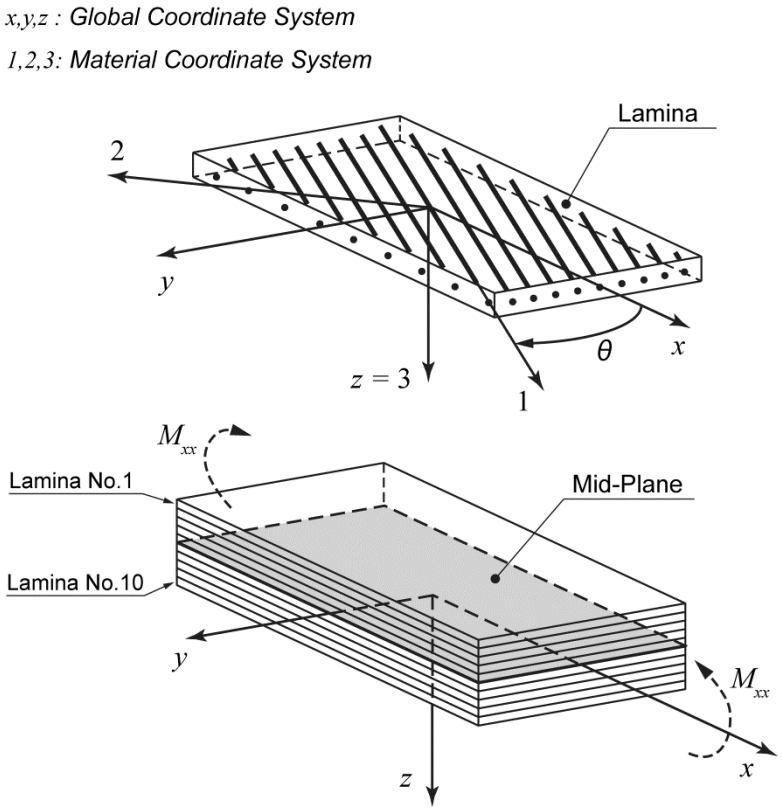


**Figure 4-2: Schematic representation of the global and material coordinate systems for a lamina and the composite laminate.**

### 4.2.2. Finite Element Analysis

For the purpose of validation, the flexural behaviour of the carbon/glass fibre reinforced hybrid composites was also studied using a commercial FEA software package (ANSYS). It was assumed that the centre load was distributed uniformly along the width of the component to approximate the contact pressure between the indenter and specimen with simply supported conditions being applied to both ends by constraining the displacement of the nodes as shown in Figure 4-3. With given mechanical properties of the fibres and matrix (Table 4-1) together with the fibre volume fraction ($V_f$), the mechanical properties of each lamina in three directions were calculated and all nine elastic constants of the laminas, *i.e.,* $E_{11}$, $E_{22}$, $E_{33}$, $G_{11}$, $G_{22}$, $G_{33}$, $\upsilon_{12}$, $\upsilon_{23}$, $\upsilon_{13}$) were used as the material properties in the FEA simulation.

Eight-node SHELL281 elements (with six degrees of freedom at each node) were used with the three dimensional state of stress being obtained and maximum stress

and strain at the mid-span being determined for all laminas and used to estimate the maximum allowable load based on the failure theories through an APDL script. The SHELL281 element was deemed to be suitable for the analysis of thin to moderately thick laminated composite shell structures [27] from consideration of the first order shear deformation theory (normally referred to as Mindlin-Reissner shell theory) [28].

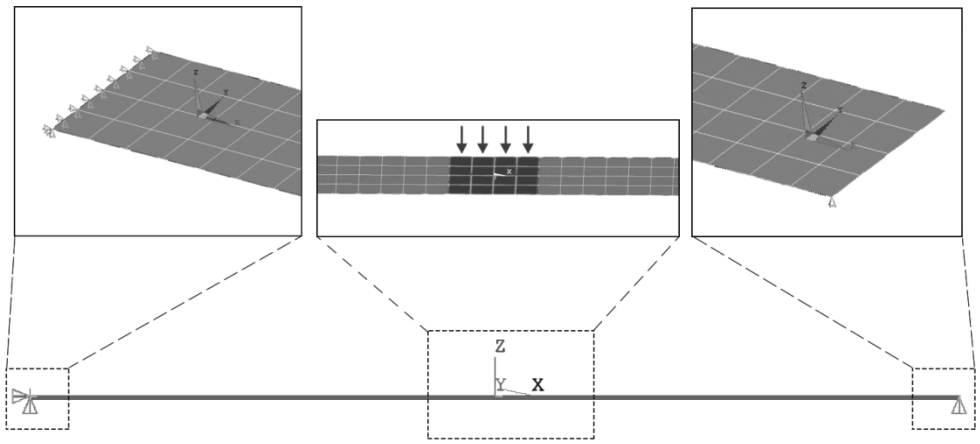


**Figure 4-3: Finite element analysis model indicating the displacement boundary conditions and distributed load applied on a small area.**

According to the Hertzian contact stress model, the maximum contact stress was estimated to be typically 5% of the longitudinal in-plane stress when the span-to-thickness ratio was 64 (which is a typical span-to-thickness ratio for high performance unidirectional polymer matrix composites). Thus, the contact stress was considered to have negligible effect in this case – this is in good agreement with previous experimental research by the present authors [5] that indicated the dominant failure mode for all similar hybrid composite specimens under three-point bending load to be in-plane failure for large span-to-thickness ratios. Therefore, as has been shown in previous research [2, 10] it was expected that the FEA model, in addition to the CLT method, would predict the allowable loads to a sufficient level of accuracy for the purpose of this study.

### 4.2.3. Failure Prediction

Once the stress components in each lamina have been determined, an appropriate failure criterion is needed in order to find the maximum allowable load before lamina failure. As mentioned previously, a number of theories have been proposed to predict failure in a lamina under plane stress conditions with the most common of these being maximum stress, maximum strain, Azzi-Tsai-Hill and Tsai-Wu.

In the present study, the applied stresses and strains in each lamina due to the bending moment were first calculated using CLT and FEA with the maximum values being found at the mid-span (where the moment equals its maximum value). Following this, the load was increased until such a point that the relevant failure criterion was satisfied for any of the laminas with this maximum allowable load at the first ply failure, $F_{max}$, being used to estimate the apparent flexural strength of the hybrid composite as follows:

$$S_F = \frac{3F_{max}L}{2wh^2} \tag{4-6}$$

where *L* is the span and *w* and *h* are the width and total thickness of the plate, respectively.

#### 4.2.3.1. Maximum stress failure theory

According to the maximum stress theory, when any stress component of a lamina in the principal material directions ($\sigma_{11}$, $\sigma_{22}$, $\tau_{12}$) is equal to or larger than the corresponding strength of the lamina, failure occurs, *i.e.*, FPF occurs if any of the following inequalities is not satisfied for any of the laminas:

$$\begin{aligned} -S_{Lc} \leq \sigma_{11} \leq S_{Lt} \\ -S_{Tc} \leq \sigma_{22} \leq S_{Tt} \\ -S_{LTs} \leq \tau_{12} \leq S_{LTs} \end{aligned} \tag{4-7}$$

where $S_{Lc}$ and $S_{Lt}$ are the ultimate compressive and tensile strengths of the lamina in the longitudinal (fibre) direction, respectively. Similarly, $S_{Tc}$ and $S_{Tt}$ are the ultimate compressive and tensile strengths of the lamina in the transverse (perpendicular to the fibres) direction, respectively, and $S_{LTs}$ is the ultimate shear stress of the lamina.

It is noteworthy that this theory does not consider the interactions between stress components.

#### 4.2.3.2. Maximum strain failure theory

According to the maximum strain theory, when any strain component of the lamina in the principal material directions ($\varepsilon_{11}$, $\varepsilon_{22}$, $\gamma_{12}$) is equal to or larger than the corresponding ultimate strain of the lamina, failure occurs, *i.e.*, FPF occurs if any of the following inequalities is not satisfied for any of the laminas:

$$\begin{aligned} -\varepsilon_{Lc} \leq \varepsilon_{11} \leq \varepsilon_{Lt} \\ -\varepsilon_{Tc} \leq \varepsilon_{22} \leq \varepsilon_{Tt} \\ -\gamma_{LTs} \leq \gamma_{12} \leq \gamma_{LTs} \end{aligned} \tag{4-8}$$

where $\varepsilon_{Lc}$ and $\varepsilon_{Lt}$ are the compressive and tensile ultimate strains of the lamina in the longitudinal (fibre) direction, respectively. Similarly, $\varepsilon_{Tc}$ and $\varepsilon_{Tt}$ are the compressive and tensile ultimate strains of the lamina in the transverse (perpendicular to the fibres) direction, respectively, and $\gamma_{LTs}$ is the ultimate shear strain of the lamina.

Similar to the maximum strain theory, this theory does not consider any interaction between stress components.

#### 4.2.3.3. Azzi-Tsai-Hill failure theory

Azzi and Tsai [19] proposed that if the stresses are tensile then failure occurs in an orthotropic lamina when the following equality is satisfied:

$$\frac{\sigma_{11}^2}{S_{Lt}^2} - \frac{\sigma_{11}\sigma_{22}}{S_{Lt}^2} + \frac{\sigma_{22}^2}{S_{Tt}^2} + \frac{\tau_{12}^2}{S_{LTs}^2} = 1 \qquad (4\text{-}9)$$

with the respective case for compressive stresses being:

$$\frac{\sigma_{11}^2}{S_{Lc}^2} - \frac{\sigma_{11}\sigma_{22}}{S_{Tc}^2} + \frac{\sigma_{22}^2}{S_{Tc}^2} + \frac{\tau_{12}^2}{S_{LTs}^2} = 1 \qquad (4\text{-}10)$$

The interaction between longitudinal and transverse stress components is included in the Azzi-Tsai-Hill theory.

#### 4.2.3.4. Tsai-Wu failure theory

The Tsai-Wu failure theory [29] predicts failure in an orthotropic lamina when the following equality is satisfied:

$$F_1\sigma_{11} + F_2\sigma_{22} + F_6\tau_{12} + F_{11}\sigma_{11}^2 + F_{22}\sigma_{22}^2 + F_{66}\tau_{12}^2 + 2F_{12}\sigma_{11}\sigma_{22} = 1 \qquad (4\text{-}11)$$

where $F_i$ and $F_{ij}$ are called the strength coefficients and given by:

$$F_1 = \frac{1}{S_{Lt}} - \frac{1}{S_{Lc}}\ , F_2 = \frac{1}{S_{Tt}} - \frac{1}{S_{Tc}}\ , F_6 = 0, F_{11} = \frac{1}{S_{Lt}S_{Lc}}$$

$$F_{22} = \frac{1}{S_{Tt}S_{Tc}}\ , F_{66} = \frac{1}{S_{LTs}^2}\ ,\ F_{12} \approx -\frac{\sqrt{F_{11}F_{22}}}{2}$$

It should be noted that the interaction between stresses is considered in this theory.

## 4.3. Results and Discussion

Two types of carbon/glass fibre reinforced hybrid composite with different stacking configurations were studied in this study. The first type was a unidirectional composite with the fibres being aligned along the *x* direction and the bending moment, $M_{xx}$, being applied as shown in Figure 4-1 to investigate the flexural behaviour of the material in the *x* direction. The second type was a bidirectional hybrid composite where the fibres were aligned in either the *x* or *y* directions and with the bending moments, $M_{xx}$ and $M_{yy}$, being applied to obtain the flexural properties in both *x* and *y* directions. Composites comprising of 10 laminas were investigated for the majority of the study with the number of laminas later being varied to investigate the applicability of the initial conclusions. The fibre volume fraction of the carbon/epoxy, $V_{fc}$, and glass/epoxy, $V_{fg}$, laminas were chosen to be 30% and 50%, respectively, in which case the unidirectional full carbon/epoxy and glass/epoxy composites would possess almost identical flexural strength of approximately 910 MPa. The properties of the carbon/epoxy and glass/epoxy laminas have been calculated and listed in Table 4-2. In order to indicate the material of each lamina in the stacking configurations, the subscripts C and G have been used to denote the carbon/epoxy and glass/epoxy laminas, respectively.

**Table 4-2: Properties of the carbon/epoxy and glass/epoxy laminas utilized in this work calculated from classical lamination theory.**

| Material | Fibre volume fraction (%) | Longitudinal / Transverse modulus (GPa) | Longitudinal / Transverse tensile strength (MPa) | Longitudinal / Transverse compressive strength (MPa) | Compressive strain-to-failure (%) |
|---|---|---|---|---|---|
| Carbon fibre reinforced epoxy | 30 | 71 / 5 | 1516 / 70 | 697 / 209 | 0.98 |
| Glass fibre reinforced epoxy | 50 | 45 / 5 | 1010 / 70 | 700 /209 | 1.55 |

Firstly, in order to show the effect of lamina material and orientation on the apparent flexural strength given by different failure theories, ten different stacking configurations were selected with the resulting flexural strength and number of the FPF according to each failure criterion being presented in Table 4-3. It can be observed from these results that the stacking configuration, *i.e.*, material and orientation of the fibres, significantly influenced the flexural strength and failure mode of the hybrid composites. For instance, the $[0_{2G}/0_{8C}]$ composite possessed a flexural strength of 1146 MPa which was almost 26% higher than that of $[0_C]_{10}$ and $[0_G]_{10}$ which indicated the presence of a positive hybrid effect. In contrast to this, the $[0_{8C}/0_{2G}]$ composite possessed a flexural strength 28% lower when compared to $[0_{2G}/0_{8C}]$ (despite having the same number of carbon/epoxy and glass/epoxy laminas) and 10% lower when compared to $[0_C]_{10}$ and $[0_G]_{10}$. Overall these results showed close agreement with previous studies on the topic [1, 2, 5] and thus indicated the validity of the techniques used in this work.

It should be noted that, in general, the results from FEA and CLT were in good agreement for all stacking configurations shown in Table 4-3. However, for some configurations the flexural strength predicted by the Tsai-Wu failure criterion was significantly different from that of the other criteria, especially for non-unidirectional composites. For example, the flexural strength of the $[(0/90)_C]_5$, $[(0/45/-45/90/0)_C]_s$ and $[0_{2G}/0_{2C}/(90/45/90_2/0_2)_C]$ composites predicted by the Tsai-Wu criterion were approximately 11% different compared to the other failure criteria. This difference is in agreement with previous experimental work [24] which

reported that the interactive failure criteria are sensitive to any variation of the matrix-dominated lamina strengths and that, for fibre-dominated laminates, maximum stress and maximum strain failure criteria outperform other failure criteria. According to experimental data [24], in addition to a personal communication [30], amongst all of the failure theories currently being applied to composite materials, the maximum strain failure theory is believed to be most appropriate and therefore was utilized for the remainder of the present study.

**Table 4-3: Comparison of the apparent flexural strength given by FEA and CLT for some selected stacking configurations *.**

| Stacking Configuration | Flexural Strength, $S_{Fxx}$ (MPa) (by FEA) | | | | Flexural Strength, $S_{Fxx}$ (MPa) (by CLT) | | | | FPF |
|---|---|---|---|---|---|---|---|---|---|
| | Max. Stress | Max. Strain | Azzi-Tsai-Hill | Tsai-Wu | Max. Stress | Max. Strain | Azzi-Tsai-Hill | Tsai-Wu | |
| $[0_C]_{10}$ | 910 | 910 | 910 | 909 | 907 | 907 | 907 | 907 | 1 |
| $[0_{2G}/0_{8C}]$ | 1148 | 1147 | 1146 | 1136 | 1143 | 1143 | 1144 | 1133 | 1 |
| $[0_{8C}/0_{2G}]$ | 821 | 821 | 821 | 823 | 818 | 818 | 818 | 821 | 1 |
| $[0_G/0_C]_5$ | 902 | 902 | 902 | 908 | 898 | 899 | 899 | 905 | 2 |
| $[0_G]_{10}$ | 913 | 913 | 913 | 913 | 910 | 910 | 910 | 910 | 1 |
| $[(0/90)_C]_5$ | 520 | 522 | 523 | 584 | 518 | 520 | 521 | 582 | 1 |
| $[0_G/90_C/90_G/0_C/0_G]_s$ | 502 | 501 | 502 | 500 | 500 | 499 | 500 | 499 | 8 |
| $[(0/90)_G]_5$ | 259 | 257 | 259 | 256 | 258 | 256 | 258 | 255 | 10 |
| $[(0/45/-45/90/0)_C]_s$ | 520 | 518 | 517 | 460 | 519 | 516 | 515 | 458 | 1 |
| $[0_{2G}/0_{2C}/(90/45/90_2/0_2)_C]$ | 1112 | 1116 | 1117 | 1232 | 1108 | 1112 | 1115 | 1232 | 1 |

* $V_{fg}$ = 50% and $V_{fc}$ = 30% for all configurations.

### 4.3.1. Unidirectional Hybrid Composites with Glass/Epoxy Laminas at the Compressive Side

Previous research [10] has indicated that a positive hybrid effect exists for the flexural strength of carbon/glass fibre reinforced epoxy hybrid composites when glass/epoxy laminas are placed at the compressive side and carbon/epoxy laminas at the tensile side. For the particular case when the carbon/epoxy and glass/epoxy

laminas possess equal strength, the flexural strength of such hybrid composites is higher than that of both the pure carbon/epoxy and pure glass/epoxy composites [10, 11]. In order to investigate the reason behind this phenomenon, carbon/epoxy and glass/epoxy laminas with nominally equal strengths ($V_{fc}$=30% and $V_{fg}$=50%) were chosen to form hybrid composites with the glass/epoxy laminas being placed at the top*, i.e.,* compressive side. The bending moment, $M_{xx}$, in the *x* direction was applied and the resulting mid-plane strain, $\varepsilon_{xx}^{0}$, and curvature, $\kappa_{xx}$, location of neutral axis, $z_{NA}$ (measured from the mid-plane and positive towards the tensile side), flexural modulus in the *x* direction, $E_{Fxx}$, apparent flexural strength in the *x* direction, $S_{Fxx}$, and first ply failed have been presented in Table 4-4 with the variation of $S_{Fxx}$ being presented in Figure 4-4.

**Table 4-4: The effect of replacing carbon/epoxy laminas with glass/epoxy laminas (going from the compressive to tensile side) on the flexural properties of carbon/glass fibre reinforced hybrid composites together with the pure carbon/epoxy and glass/epoxy composites.**

| Stacking configuration | $\varepsilon_{xx}^{0}$ (×10$^{-5}$) | $\kappa_{xx}$ (×10$^{-5}$) | $z_{NA}$ (mm) | $E_{Fxx}$ (GPa) | $S_{Fxx}$ (MPa) | FPF |
|---|---|---|---|---|---|---|
| $[0_C]_{10}$ | 0.000 | 21.076 | 0.00 | 71 | 907 | 1 |
| $[0_G/0_{9C}]$ | -0.798 | 23.241 | 0.03 | 65 | 986 | 2 |
| $[0_{2G}/0_{8C}]$ | -1.585 | 24.953 | 0.06 | 61 | 1143 | 1 |
| $[0_{3G}/0_{7C}]$ | -2.265 | 26.091 | 0.09 | 59 | 1070 | 1 |
| $[0_{4G}/0_{6C}]$ | -2.760 | 26.671 | 0.10 | 58 | 1030 | 1 |
| $[0_{5G}/0_{5C}]$ | -3.024 | 26.846 | 0.11 | 58 | 1016 | 1 |
| $[0_{6G}/0_{4C}]$ | -3.041 | 26.859 | 0.09 | 58 | 1015 | 1 |
| $[0_{7G}/0_{3C}]$ | -2.809 | 27.011 | 0.10 | 57 | 1017 | 1 |
| $[0_{8G}/0_{2C}]$ | -2.306 | 27.669 | 0.08 | 55 | 1012 | 1 |
| $[0_{9G}/0_C]$ | -1.454 | 29.391 | 0.05 | 51 | 983 | 1 |
| $[0_G]_{10}$ | 0.000 | 33.333 | 0.00 | 45 | 910 | 1 |

From Table 4-4 and Figure 4-4 it can be noted that a positive hybrid effect exists for all hybrid composites with the maximum hybrid effect (and thus the maximum flexural strength) being achieved for the hybrid composite with the $[0_{2G}/0_{8C}]$ stacking configuration.

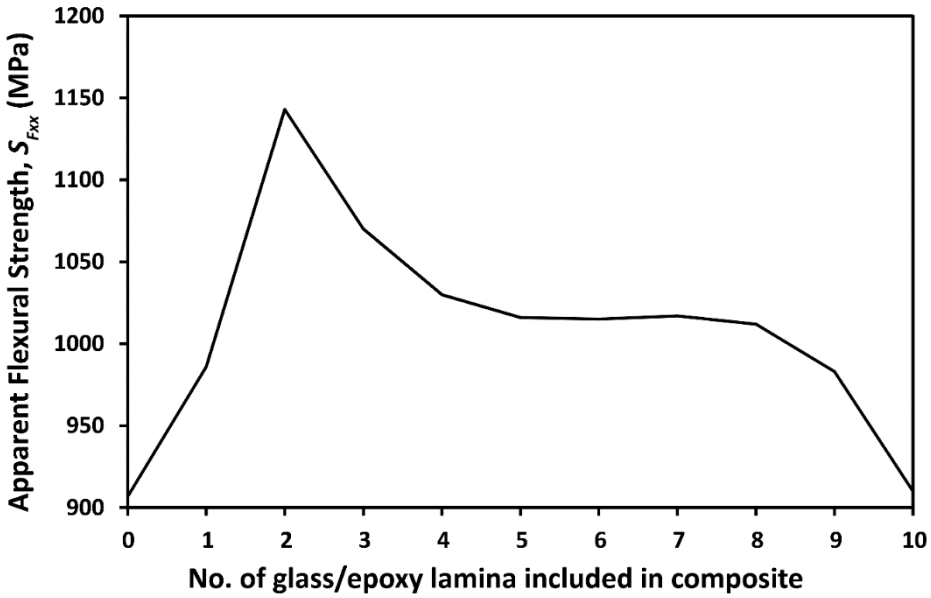


**Figure 4-4: Influence of replacing carbon/epoxy laminas with glass/epoxy laminas (going from the compressive to tensile side) on the flexural strength for a hybrid carbon/glass fibre reinforced epoxy matrix composite with $V_{fc}$ = 30% and $V_{fg}$ = 50%. (Data from Table 4-4)**

The stress distributions in the laminas in the global *x* direction due to a bending moment of $M_{xx}$= 10 N·m have been plotted for four stacking sequences, namely $[0_C]_{10}$, $[0_{1G}/0_{9C}]$, $[0_{2G}/0_{8C}]$ and $[0_{3G}/0_{7C}]$, in Figure 4-5 with it being noted that replacing one or two carbon/epoxy laminas at the compressive side with glass/epoxy laminas resulted in a significant stress reduction in these laminas. The stress reduction within the glass/epoxy laminas is attributed to the lower modulus of the glass/epoxy laminas when compared to the carbon/epoxy laminas. Furthermore, the stress distribution across the entire composite was changed when glass/epoxy laminas were introduced.

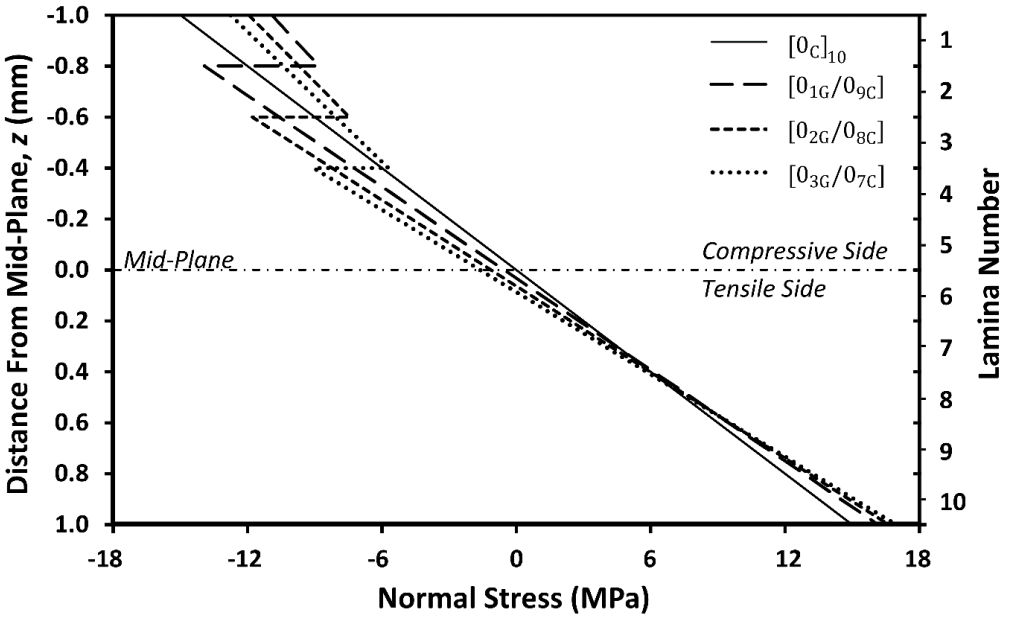


**Figure 4-5: Distribution of the normal stress in the global *x* direction (0˚) through the thickness of selected composites for a bending moment of $M_{xx}$=10 N·m. (Glass/epoxy laminas are placed at the top)**

Among the four stacking sequences shown in Figure 4-5 it can be observed that the lowest compressive and tensile stresses occurred with $[0_{1G}/0_{9C}]$ and $[0_C]_{10}$, respectively, whilst the stresses at the compressive side of the $[0_{2G}/0_{8C}]$ and $[0_{3G}/0_{7C}]$ composites were between those of $[0_C]_{10}$ and $[0_{1G}/0_{9C}]$. However, it can be seen from Table 4-4 that the critical lamina (*i.e.*, FPF) occurred at the compressive side for all configurations which indicates that the maximum compressive stress was the limiting factor for failure and that any small increase in the tensile stress was insufficient to cause failure at the tensile side, *i.e.*, lamina number 10. On the other hand, the FPF for $[0_{1G}/0_{9C}]$ was the second lamina at the compressive side, *i.e.*, the first carbon/epoxy lamina under compression. Therefore, whilst a significant reduction in the maximum compressive stress in the $[0_{1G}/0_{9C}]$ configuration was observed for lamina number 1, it was the magnitude of the compressive stress in the critical lamina number 2 that was the limiting factor for the flexural strength. Also of note is that the highest flexural strength was achieved for the $[0_{2G}/0_{8C}]$ configuration which possessed relatively low maximum compressive stress in both the glass/epoxy and carbon/epoxy laminas.

From comparison of the stacking sequences in Figure 4-5 it can be concluded that, through partial substitution of the carbon/epoxy laminas at the compressive side with glass/epoxy laminas, the stress distribution through the laminas changed in such a way that the normal stress in the critical lamina, *i.e.*, laminas at the compressive side, decreases significantly and thus allowed the hybrid composite to make more efficient use of the remaining laminas to carry a larger applied moment. On the other hand, by using a smaller or larger than optimum number of glass/epoxy laminas, *e.g.*, $[0_{1G}/0_{9C}]$ and $[0_{3G}/0_{7C}]$ compared to $[0_{2G}/0_{8C}]$, the stresses within the critical lamina increased and thus led to a decreased flexural strength. In summary, the replacement of carbon/epoxy laminas at the compressive side with glass/epoxy laminas led to two competing factors which affected the hybrid composite:

(i) The maximum compressive stress in the higher modulus lower strain-to-failure (HMLS) material (carbon/epoxy) decreased as the HMLS material was moved away from the compressive side, leading to increased flexural strength. Also, when a lamina with the HMLS material (carbon/epoxy) was replaced by a lower modulus higher strain-to-failure (LMHS) material (glass/epoxy) then the stress in that lamina became significantly lower as can be concluded from the jumps in the stress distribution curves shown in Figure 4-5.

(ii) The maximum compressive stress in the LMHS material (glass/epoxy) increased with the proportion of LMHS material. (This can also be explained by the overall composite stiffness decreasing with increasing proportion of LMHS material. Under the same load, a decreased overall stiffness would lead to a higher compressive strain and higher compressive stress). Such a phenomenon would tend to decrease the composite flexural strength.

Based on these two conflicting factors, an optimal value for the number of glass/epoxy laminas at the compressive side with regards to flexural strength can be determined. The optimal stacking sequence previously proposed by Dong and Davies [10] can now be explained by the aforementioned conflicting factors.

The increase in flexural strength of such hybrid composites can also be described in terms of the strain distribution through the laminas. On one hand, the strain-to-failure of the glass/epoxy laminas is much higher than that of the carbon/epoxy laminas, thus the glass/epoxy laminas at the compressive side (critical lamina number 1) can undergo greater strain before failure. On the other hand, by using more glass/epoxy laminas, the flexural modulus of the overall hybrid composite decreased (as shown in Table 4-4) and thus the curvature and strain in all laminas increased (including the critical lamina). As a result of these two effects, when one or two glass/epoxy laminas with a lower modulus and higher elongation were placed at the compressive side, the flexural strength of the overall composite improved. However, including more than two glass/epoxy laminas resulted in the strain increase becoming a dominant factor and thus the overall composite flexural strength was reduced.

The conclusions reached above for carbon and glass fibre reinforced epoxy hybrid composites are applicable to hybrid composites with other fibre types. For example, Davies and Hamada [31] studied the flexural properties of hybrid unidirectional composites in which a proportion of carbon/epoxy layers were replaced by silicon carbide (SiC)/epoxy layers. They prepared hybrid composites contained 67% fibre volume fraction for both lamina types with an elastic modulus of 160 GPa and 122 GPa and strain-to-failure of 0.86% and 1.31% for the carbon/epoxy and SiC/epoxy laminas, respectively. With these specifications, the flexural strengths of the full carbon/epoxy and full SiC/epoxy composites were found to be 1722 MPa and 1985 MPa, respectively, for a span-to-thickness ratio of 64. Since the SiC/epoxy lamina has a lower modulus and higher elongation to failure, replacing carbon/epoxy lamina at the compressive side with SiC/epoxy lamina would be expected to improve the flexural strength. Indeed, they reported an increased flexural strength of 2104 MPa for the $[0_{SiC}/0_{7C}]$ stacking configuration (the C and SiC subscripts denote carbon/epoxy and SiC/epoxy lamina, respectively) which was 22% higher compared to the $[0_C]_8$ configuration [31]. The analytical results for the same material based on the method in the present study indicated

the flexural strength to be 1796 MPa for $[0_C]_8$, 2146 MPa for $[0_{SiC}/0_{7C}]$ and 2071 for $[0_{SiC}]_8$ which are in good agreement with the experimental data.

### 4.3.2. Unidirectional Hybrid Composites with the Glass/Epoxy Laminas Close to the Mid-Plane at the Tensile Side

Since the laminas close to the neutral axis are not the main load carrying layers under bending load, they do not have a significant effect on the flexural modulus of the whole material. This can be inferred from Table 4-4 where the flexural modulus decreased with increasing number of glass/epoxy laminas for all cases except for the stacking configurations $[0_{5G}/0_{5C}]$ and $[0_{6G}/0_{4C}]$. It should also be noted that the $[0_{7G}/0_{3C}]$ composite exhibited a higher flexural strength when compared to $[0_{6G}/0_{4C}]$. That is, increasing the number of glass/epoxy laminas at the tensile side and close to the mid-plane improved the flexural strength without reducing the flexural modulus, significantly.

In order to investigate the reason behind this phenomenon and the possibility of improving the composite flexural strength by placing one or more glass/epoxy laminas close to the mid-plane, two stacking sequences, $[0_{5C}/0_{2G}/0_{3C}]$ and $[0_{5C}/0_{3G}/0_{2C}]$, were investigated and the corresponding flexural behaviour compared with that of $[0_C]_{10}$. The stress distributions have been plotted in Figure 4-6 whereas the corresponding mid-plane strain, $\varepsilon_{xx}^0$, and curvature, $\kappa_{xx}$, location of the neutral axis, $z_{NA}$ , flexural modulus, $E_{Fxx}$, flexural strength, $S_{Fxx}$, and the FPF have been presented in Table 4-5. It can be seen that the neutral axis for the $[0_C]_{10}$ configuration was located at the mid-plane, *i.e.,* $z_{NA}$= 0, but when carbon/epoxy laminas were replaced with glass/epoxy laminas below the mid-plane, the neutral axis was slightly shifted towards the top surface/compressive side. The distances of the neutral axis from the mid-plane for $[0_{5C}/0_{2G}/0_{3C}]$ and $[0_{5C}/0_{3G}/0_{2C}]$ were -0.01 mm and -0.03 mm, respectively. This movement of the neutral axis caused a reduction in the strain and stress within the laminas at the compressive side. Simultaneously, introducing glass/epoxy laminas reduced the overall stiffness of the composite and thus increased the strain. Due to these two competing mechanisms, the highest flexural strength for the three stacking sequences occurred with

$[0_{5C}/0_{2G}/0_{3C}]$ which was slightly higher than that of $[0_C]_{10}$. Whilst the authors acknowledge that such a minor increase may well be masked by the influence of manufacturing variations during practical use for this particular hybrid composite system, there may exist other hybrid composite systems where this phenomenon is more pronounced.

It can be concluded from these results that when carbon/epoxy laminas close to the neutral axis at the tensile side are replaced by glass/epoxy laminas, there exists two competing factors which affect the flexural properties:

(i) Increasing strength attributed to movement of the neutral axis towards the compressive side when glass/epoxy laminas are introduced below the mid-plane;

(ii) Reducing strength due to decreased overall flexural modulus of the hybrid composite.

Based on these two conflicting factors, the optimal number of glass/epoxy laminas below the neutral axis for the purpose of maximizing the flexural strength was found to be 2, *i.e.*, the optimal stacking configuration for this type of hybrid composite was $[0_{5C}/0_{2G}/0_{3C}]$.

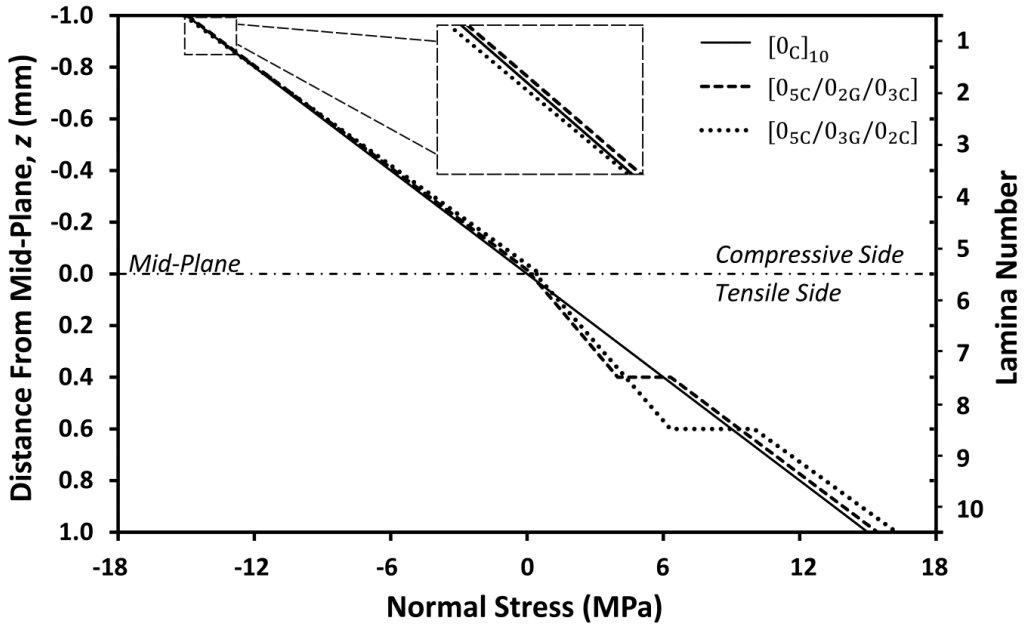


**Figure 4-6: Distribution of the normal stress in the global *x* direction (0˚) through the thickness of selected composites for a bending moment of $M_{xx}$=10 N·m.**
**(Glass/epoxy laminas are placed at the top)**

**Table 4-5: Detailed information concerning the stacking configurations shown in Figure 4-6.**

| Stacking configuration | $\varepsilon^0_{xx}$ (×10$^{-5}$) | $\kappa_{xx}$ (×10$^{-5}$) | $z_{NA}$ (mm) | $E_{Fxx}$ (GPa) | $S_{Fxx}$ (MPa) | FPF |
|---|---|---|---|---|---|---|
| $[0_C]_{10}$ | 0.000 | 21.076 | 0.00 | 71 | 907 | 1 |
| $[0_{5C}/0_{2G}/0_{3C}]$ | 0.339 | 21.342 | -0.01 | 70 | 910 | 1 |
| $[0_{5C}/0_{3G}/0_{2C}]$ | 0.819 | 22.033 | -0.03 | 68 | 901 | 1 |

### 4.3.3. Unidirectional Hybrid Composites with the Glass/Epoxy Laminas at both Compressive and Tensile Sides

Thus far it has been shown that the flexural strength of a full carbon/epoxy composite can be improved when two carbon/epoxy laminas at either the top surface (outer surface on compressive side) or below the neutral axis are replaced with glass/epoxy laminas. However, it may be possible to superimpose these two effects in order to take advantage of hybridisation. In order to investigate this, a hybrid composite with stacking sequence $[0_{2G}/0_{3C}]_2$ was studied and, as expected,

the flexural strength of this configuration (1146 MPa) was slightly higher than that of $[0_{2G}/0_{8C}]$ and approximately 26% higher than that of the fully carbon/epoxy composite. The through-thickness stress distributions for the fully carbon/epoxy composite and the proposed stacking sequence, *i.e.*, $[0_{2G}/0_{3C}]_2$, have been shown in Figure 4-7.

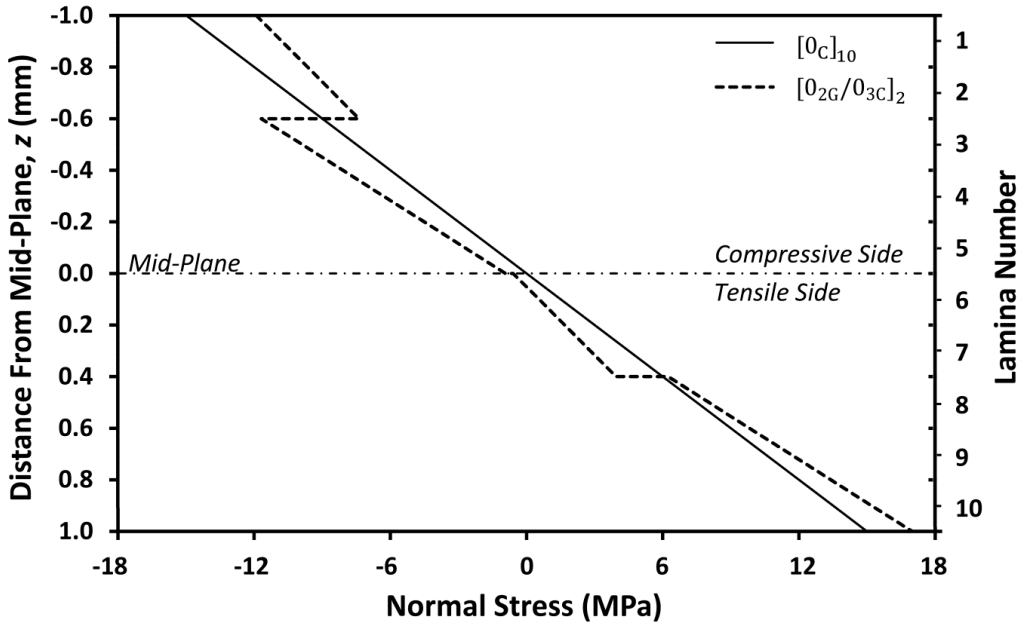


**Figure 4-7: Distribution of the normal stress in the global *x* direction (0˚) through the thickness of the composites for a bending moment of $M_{xx}$=10 N·m. (Glass/epoxy laminas are placed at the top and middle)**

### 4.3.4. Bidirectional Hybrid Composites

Previous research [14] has reported the possibility of improving the flexural strength of unidirectional carbon/glass epoxy hybrid composites by choosing a suitable material sequence. Likewise, it is expected that the flexural strength of bidirectional full carbon/epoxy composites, *i.e.*, $[(0/90)_5]_C$, can be improved by placing higher elongation glass/epoxy laminas at the compressive side. In order to investigate this hypothesis, three different composites with stacking configurations, $[(0/90)_5]_C$, $[(0/90)_G/(0/90)_{4C}]$ and $[(0/90)_{2G}/(0/90)_{3C}]$, were analysed with Figure 4-8 presenting the stress distributions through the laminas when a bending moment of $M_{xx}$=10 N·m was applied in the *x* direction with the corresponding data including the FPF being listed in Table 4-6. Similarly, the stress distributions through the

laminas when a bending moment of $M_{yy}$=10 N·m was applied in the *y* direction have been plotted in Figure 4-9 with the corresponding mid-plane strain, $\varepsilon_{yy}^{0}$, and curvature, $\kappa_{yy}$, location of the neutral axis, $z_{NA}$, flexural modulus, $E_{Fyy}$, flexural strength, $S_{Fyy}$, and the FPF being listed in Table 4-7.

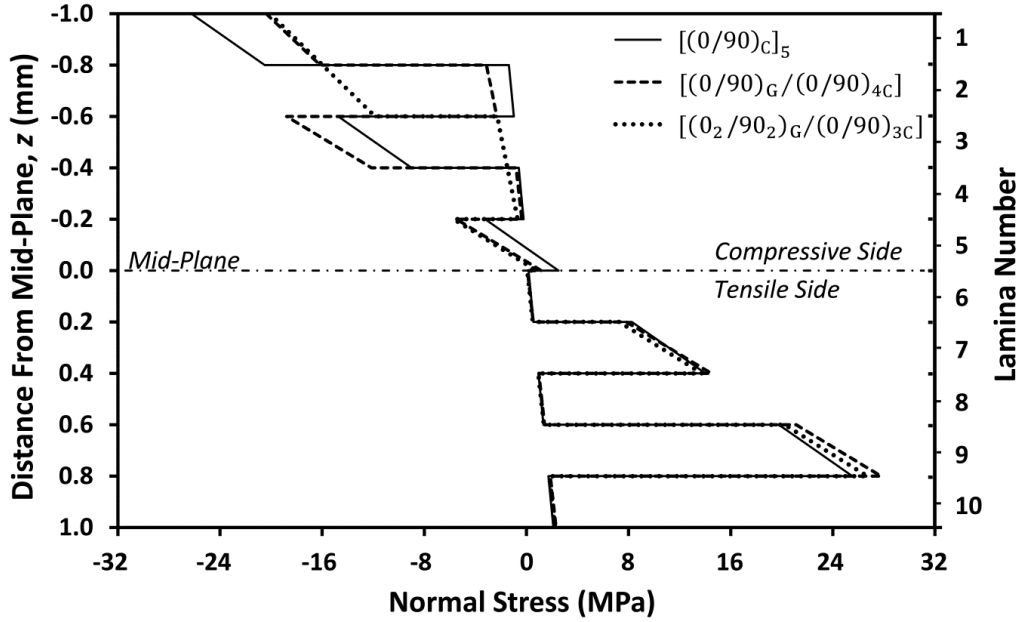


**Figure 4-8: Distribution of the normal stress in the global *x* direction (0˚) through the thickness of the composites for a bending moment of $M_{xx}$=10 N·m. (Glass/epoxy laminas are placed at the top)**

**Table 4-6: Detailed information about the stacking configurations shown in Figure 4-8.**

| Stacking configuration | $\varepsilon_{xx}^{0}$ (×10$^{-5}$) | $\kappa_{xx}$ (×10$^{-5}$) | $z_{NA}$ (mm) | $E_{Fxx}$ (GPa) | $S_{Fxx}$ (MPa) | FPF |
|---|---|---|---|---|---|---|
| $[(0/90)_C]_5$ | 3.513 | 40.245 | -0.010 | 38 | 520 | 1 |
| $[(0/90)_G/(0/90)_{4C}]$ | 1.632 | 46.528 | -0.003 | 32 | 583 | 10 |
| $[(0_2/90_2)_G/(0/90)_{3C}]$ | 1.071 | 45.379 | -0.002 | 33 | 605 | 10 |

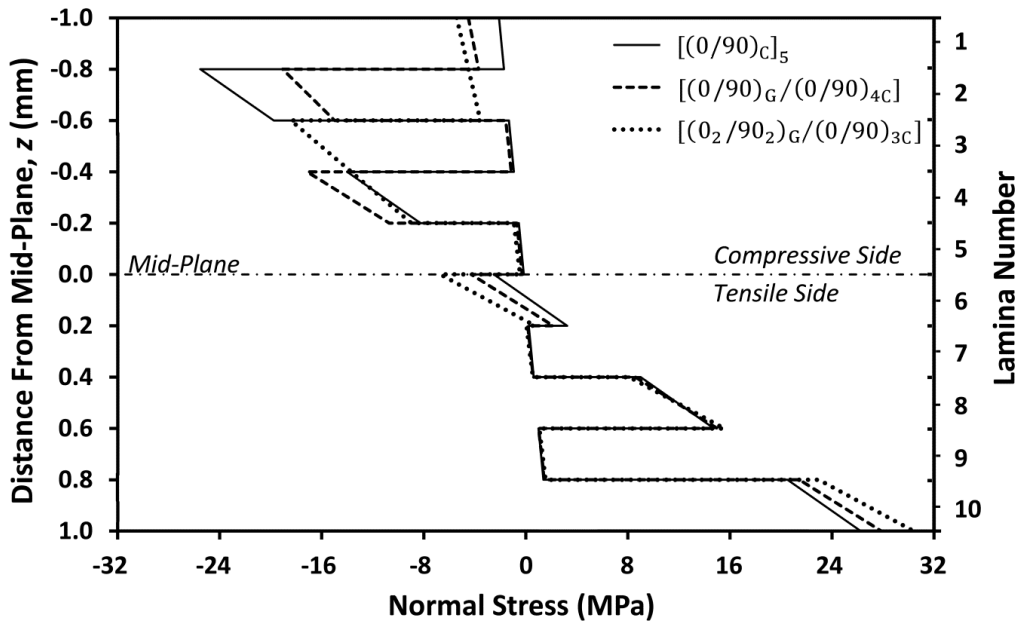


**Figure 4-9: Distribution of the normal stress in the global *y* direction (90˚) through the thickness of the composites for a bending moment of $M_{yy}$=10 N·m. (Glass/epoxy laminas are placed on the top)**

**Table 4-7: Detailed information about the stacking configurations in Figure 4-9.**

| Stacking configuration | $\varepsilon^0_{yy}$ (×10$^{-5}$) | $\kappa_{yy}$ (×10$^{-5}$) | $z_{NA}$ (mm) | $E_{Fyy}$ (GPa) | $S_{Fyy}$ (MPa) | FPF |
|---|---|---|---|---|---|---|
| $[(0/90)_C]_5$ | -3.513 | 40.245 | 0.184 | 38 | 535 | 2 |
| $[(0/90)_G/(0/90)_{4C}]$ | -5.998 | 44.984 | 0.193 | 35 | 723 | 2 |
| $[(0_2/90_2)_G/(0/90)_{3C}]$ | -9.402 | 51.930 | 0.199 | 32 | 748 | 3 |

From these results it can be noted that the bidirectional hybrid composites with glass/epoxy laminas at the compressive side in the 0° and 90° directions followed the same rules as for the unidirectional hybrid composites as evidenced by the flexural strengths of the $[(0/90)_G/(0/90)_{4C}]$ and $[(0_2/90_2)_G/(0/90)_{3C}]$ configurations in both the *x* and *y* directions being improved when compared to the $[(0/90)_C]_5$ composite.

Form Figure 4-8 and Table 4-6, when the $[(0/90)_C]_5$ composite is compared with the $[(0/90)_G/(0/90)_{4C}]$ case, it can be noted that by placing glass/epoxy laminas at the top of the composite the normal stress in the *x* direction was significantly reduced

in lamina number 1 and this lamina was no longer the critical one with the failure mode switching from compressive failure in lamina number 1 to tensile failure in lamina number 10. The failure mode in lamina number 10 with a 90° fibre angle and an applied moment in the *x* direction was "transverse tensile failure" which can be described based on the effect of the reduction in flexural stiffness of the composite when more glass/epoxy laminas were included (as mentioned before). That is, the strain and stress increased in the bottom carbon/epoxy laminas and this resulted in initial matrix failure in lamina number 10 instead of fibre failure in lamina number 1. It should be noted that the transverse strength of the carbon/epoxy lamina was less than 5% of its longitudinal strength and therefore even a small increase in the stress within the transverse direction may cause transverse failure. A similar situation was noted for the $[(0_2/90_2)_G/(0/90)_{3C}]$ configuration subject to a bending moment in the *x* direction. However, the flexural strength in the *x* direction slightly increased from 583 MPa to 605 MPa when compared to $[(0/90)_G/(0/90)_{4C}]$ and this was attributed to additional glass/epoxy laminas at the top surface causing the neutral axis to move towards the tensile side and thus reduce the strain in the tensile side laminas. Since lamina number 10 at the tensile side is the critical lamina, the reduction in strain within this lamina caused an improvement in the overall composite flexural strength. In contrast to the *x* direction, when the moment was applied in the global *y* direction (Figure 4-9 and Table 4-7), the failure mode remained unchanged and was the same for all stacking configurations, *i.e.*, compressive failure in the longitudinal direction due to micro-buckling of the fibres. This was attributed to the existence of carbon fibres in the loading direction (90°) at the bottom surface, *i.e.*, lamina number 10, which were aligned along the *y* axis. Therefore, $S_{Fyy}$ was considerably higher than $S_{Fxx}$ (723 MPa and 748 MPa compared to 583 MPa and 605 MPa, respectively).

Similar to the conclusions for unidirectional hybrid composites, the flexural strength of bidirectional hybrid composites could be improved by replacing carbon/epoxy lamina at the tensile side below the neutral axis by lower modulus glass/epoxy lamina. This hypothesis was investigated by analysing the properties of hybrid composites with stacking configurations of $[(0/90)_G/(0/90/0)_C/90_G/(0/90)_{2C}]$ and

$[(0_2/90_2)_G/0_C/90_G/(0/90)_{2C}]$ with resulting flexural strengths of 585 MPa and 606 MPa, respectively, in the *x* direction, *i.e.*, the flexural strength slightly increased for both configurations as expected. However, it should be noted that the improvement was not as significant as for those configurations with glass/epoxy laminas placed at the top.

It should be noted that the transverse modulus of a unidirectional lamina is much lower than the longitudinal modulus and thus changing the orientation of a lamina should have the same effect on shifting the location of the neutral axis as would changing the material of the lamina, *i.e.*, instead of replacing some of the carbon/epoxy layers with glass/epoxy lamina, changing the orientation of the carbon/epoxy laminas would play the same role in shifting the neutral axis and possibly improve the composite flexural strength. However, changing the orientation of 0° laminas close to the outer surfaces, which are the main load carrying components under bending load, may cause a significant reduction in the flexural strength. In contrast to this, laminas close to the mid-plane are not the main load carrying components and therefore changing their orientation from 0° to 90° would be expected to shift the location of the neutral axis and reduce the stress within the top or bottom laminas and thus may improve the composite flexural strength. This hypothesis was verified by comparing two stacking configurations, $[0_{2G}/0_{8C}]$ and $[0_{2G}/0_{3C}/90_{2C}/0_{3C}]$, with their flexural strengths being 1143 MPa and 1153 MPa, respectively, which indicated a small improvement due to this effect. It should also be noted that the flexural strength of the latter configuration was 166 MPa in the *y* direction compared to 104 MPa for the first configuration. That is, rotating the fibre angle of the laminas at the tensile side below the mid-plane by 90° improved the composite flexural strength in both directions.

### 4.3.5. General Rules for Improving the Flexural Strength of Hybrid Composites

According to what has been discussed so far, when low modulus laminas, *e.g.* glass/epoxy or SiC/epoxy, with relatively high elongation-to-failure are combined with high modulus laminas, *e.g.* carbon/epoxy, to form a hybrid composite, four

main factors exist which affect the stress and strain distributions in the laminas and thus either improve or degrade the composite flexural strength. These factors can be summarised as follows:

1. The stress in the low modulus laminas is generally less than that in the high modulus laminas. Thus, replacing the critical lamina, *i.e.*, the lamina that limits the composite flexural strength (which is normally at the compressive surface of the composite), by a LMHS lamina will tend to improve the flexural strength of the hybrid composite. However, following this procedure may cause another non-replaced HMLS lamina to become the critical lamina within the composite.
2. Laminas closer to the mid-plane experience lower stress. Therefore, the compressive stress within a HMLS lamina under any given load may be decreased if the HMLS lamina is placed closer to the mid-plane whilst the LMHS laminas are placed at the compressive face away from the mid-plane.
3. The inclusion of low modulus laminas reduces the flexural modulus of the overall composite and this leads to higher compressive strain and stress which thus causes the flexural strength of the hybrid composite to be reduced.
4. The inclusion of low modulus laminas (or else changing the fibre angle) changes the location of the neutral axis with the result that stresses in all the laminas will be changed. If the neutral axis is shifted towards the critical lamina then the stress in that critical lamina may be reduced – this would result in an increased hybrid composite flexural strength.

Based on the above-mentioned factors, four general rules have been proposed for the design of both unidirectional and bidirectional hybrid composites with improved flexural strength. These general rules can be summarised as follows:

1. The placement of laminas with a lower modulus and higher elongation, *e.g.*, glass/epoxy and SiC/epoxy, at the surface of the compressive side can increase the flexural strength of the hybrid composite when compared with the simple composite containing only high modulus laminas, *e.g.*, full carbon/epoxy. Based on this rule, it was shown that hybrid composites with stacking configurations of

$[0_{2G}/0_{8C}]$, $[0_{SiC}/0_{7C}]$, $[(0_2/90_2)_G/(0/90)_{3C}]$ and $[(0/90)_G/(0/90)_{4C}]$ possessed a higher flexural strength than that of a full carbon/epoxy composite with the same fibre orientation.

2. The placement of laminas with a lower modulus and higher elongation close to the neutral axis at the tensile side can improve the flexural strength of the hybrid composite when compared with the simple composite containing only high modulus laminas. Stacking configurations such as $[0_{5C}/0_{2G}/0_{3C}]$, which has a higher flexural strength than that of full carbon/epoxy, is an example of the application of this rule. A similar effect can be achieved in a full high modulus fibre composite, *e.g.*, CFRP, by changing the angle of the laminas from $0^o$ to $90^o$ close to the neutral axis at the tensile side.
3. Rules 1 and 2 have no conflictions and can be combined, *i.e.*, by placing low modulus laminas at both locations, *i.e.*, surface at compressive side and close to the neutral axis at the tensile side, the flexural strength can be improved. The improved flexural strength of a hybrid composite with stacking sequence $[0_{2G}/0_{3C}]_2$ was designed based on this rule.
4. The effect of Rule 1 is significantly higher than that of Rule 2, *i.e.*, the flexural strength of hybrid composites with stacking configurations such as $[0_G/0_{9C}]$ and $[0_{2G}/0_{8C}]$ is much higher than those of $[0_{5C}/0_G/0_{4C}]$ and $[0_{5C}/0_{2G}/0_{3C}]$.

The optimum level of hybridisation, *i.e.*, the number of high modulus and low modulus laminas and the fibre volume fraction for each lamina, which provide the maximum flexural strength, should be determined through an optimization process.

In order to investigate the applicability of the rules mentioned above to composites with different number of layers, hybrid composites with eight and eighteen laminas and the same individual lamina thickness were investigated with the results for flexural strength being presented in Table 4-8 and 4-9, respectively. It can be seen that the general rules were still valid in these cases, *i.e.*, the hybrid composites with glass/epoxy laminas at the outer surface of the compressive side and/or glass/epoxy laminas close to the neutral axis at the tensile side possessed higher flexural strength compared to the full carbon/epoxy composite.

The actual number of glass/epoxy lamina required for maximum flexural strength depends on the total number of laminas within the composite. For example, from Table 4-4 it can be seen in order for the unidirectional hybrid composites with ten laminas to achieve their maximum flexural strength, two glass/epoxy laminas would be required at the compressive side, whereas the values for composites containing eight and eighteen laminas were found to be two and four, respectively. However, as would be expected, the maximum strength achieved for these composites was not the same with a value of 1101 MPa for $[0_{2G}/0_{6C}]$ compared to 1143 MPa for the original $[0_{2G}/0_{8C}]$ and 1123 MPa for $[0_{4G}/0_{14C}]$. The fact that the optimum hybrid ratio (with respect to laminate thickness) within this system was found to be approximately 20% (Table 4-4) resulted in the maximum flexural strength of the 18 lamina composite being slightly lower than that of the 10 lamina composite due the fact that a 20% hybrid ratio was not be possible for the 18 lamina composite – the closest values available being 16.7% for $[0_{3G}/0_{15C}]$ and 22.2% for $[0_{4G}/0_{14C}]$. However, it should be noted that, in general, hybrid composites containing larger numbers of laminas would be more likely to achieve a higher flexural strength, *i.e.*, large positive hybrid effect, due to the finer control of the hybrid ratio. Therefore, should a solution through optimization not be possible, it would be beneficial for hybrid composite designers to use larger numbers of lamina, for example, by choosing a smaller fibre tow in order to reduce the individual lamina thickness and thus maintain a similar composite component thickness whilst increasing the lamina number.

**Table 4-8: Comparison of flexural strength and stiffness for hybrid composites containing 8 laminas.**

| Stacking configuration | $S_{Fxx}$ (MPa) | $S_{Fyy}$ (MPa) | $E_{Fxx}$ (GPa) | $E_{Fyy}$ (GPa) |
|---|---|---|---|---|
| $[0_C]_8$ | 907 | 90 | 71 | 5 |
| $[0_{2G}/0_{6C}]$ | 1101 | 105 | 60 | 7 |
| $[0_{4C}/0_{1G}/0_{3C}]$ | 910 | 92 | 60 | 7 |
| $[0_{2G}/0_{2C}/0_{1G}/0_{3C}]$ | 1103 | 108 | 60 | 7 |
| $[(0/90)_C]_4$ | 526 | 546 | 38 | 38 |

| Stacking configuration | $S_{Fxx}$ (MPa) | $S_{Fyy}$ (MPa) | $E_{Fxx}$ (GPa) | $E_{Fyy}$ (GPa) |
|---|---|---|---|---|
| $[(0/90)_G/(0/90)_{3C}]$ | 555 | 723 | 31 | 35 |
| $[(0/90)_{2C}/(0/90)_G/(0/90)_C]$ | 531 | 549 | 38 | 37 |

**Table 4-9: Comparison of flexural strength and stiffness for hybrid composites containing 18 laminas.**

| Stacking configuration | $S_{Fxx}$ (MPa) | $S_{Fyy}$ (MPa) | $E_{Fxx}$ (GPa) | $E_{Fyy}$ (GPa) |
|---|---|---|---|---|
| $[0_C]_{18}$ | 907 | 90 | 71 | 5 |
| $[0_{3G}/0_{15C}]$ | 1085 | 103 | 62 | 6 |
| $[0_{4G}/0_{14C}]$ | 1123 | 104 | 60 | 7 |
| $[0_{4G}/0_{6C}/0_{2G}/0_{6C}]$ | 1126 | 107 | 60 | 7 |
| $[(0/90)_C]_9$ | 507 | 515 | 38 | 38 |
| $[(0/90)_{2G}/(0/90)_{7C}]$ | 616 | 682 | 33 | 34 |
| $[(0_2/90_2)_G/(0/90)_{7C}]$ | 632 | 736 | 34 | 33 |
| $[(0/90)_{4C}/0_C/(0/90/0)_G/(0/90)_{3C}]$ | 509 | 517 | 38 | 38 |

## 4.4. New Stacking Configurations for Bidirectional Hybrid Composite with Equal Properties in both Directions

In many applications it would be beneficial for a bidirectional composite to have nominally equal properties in the *x* and *y* directions. However, the flexural strengths in the *x* direction, $S_{Fxx}$, for the bidirectional hybrid composites proposed in Table 4-6 were lower than those in the *y* direction (Table 4-7). Based on the proposed general rules, and noting that the FPF in the $[(0_2/90_2)_G/(0/90)_{3C}]$ and $[(0/90)_G/(0/90)_{4C}]$ stacking configurations was lamina number 10 at the tensile side (Table 4-6), it would be expected that the strength of the hybrid composite in the *x* direction could be improved by rotating one of the 90° laminas at the tensile side to 0°. Since the two laminas at the top and bottom are the main load carrying laminas, instead the orientation of lamina number 8 was changed to 0° in order to achieve two new stacking configurations, namely $[(0/90)_G/(0/90)_{2C}/(0/0/0/90)_C]$ and

$[(0_2/90_2)_G/(0/90/0/0/0/90)_C]$, with improved strength in the *x* direction. The results for these two new stacking configurations have been listed in Table 4-10 and, as expected, the flexural strength in the *x* direction was significantly improved without any major reduction in strength in the *y* direction. In the case of the $[(0_2/90_2)_G/(0/90/0/0/0/90)_C]$ composite, although the failure mode was tensile failure in the transverse direction, the flexural strength in the *y* direction was still high compared to the *x* direction.

**Table 4-10: Detailed information about the two proposed stacking configurations for improving $S_{Fxx}$.**

| Stacking configuration | $E_{Fxx}$ (GPa) | $S_{Fxx}$ (MPa) | $FPF_x$ | $E_{Fyy}$ (GPa) | $S_{Fyy}$ (MPa) | $FPF_y$ |
|---|---|---|---|---|---|---|
| $[(0/90)_G/(0/90)_{2C}/(0/0/0/90)_C]$ | 716 | 37 | 1 | 713 | 30 | 2 |
| $[(0_2/90_2)_G/(0/90/0/0/0/90)_C]$ | 717 | 38 | 1 | 706 | 27 | 9 |

By comparing the flexural strengths of the full carbon/epoxy and hybrid composites presented in Tables 4-6, 4-7 and 4-8 it can be concluded that a positive hybrid effect exists for the case of bidirectional hybrid composites, similar to the situation in unidirectional hybrid composites. For instance, the flexural strength of the $[(0/90)_G/(0/90)_{2C}/(0/0/0/90)_C]$ configuration in the *x* and *y* directions was 716 MPa and 713 MPa, respectively, which was approximately 38% and 33% higher compared to that of $[(0/90)_C]_5$.

## 4.5. Conclusions

In this study, classical lamination theory and finite element analysis have been used to investigate the effect of stacking configuration (material and fibre angle) of laminas on the flexural strength of carbon/glass fibre reinforced epoxy hybrid composites with the hope of elucidating the mechanism behind the hybrid effect. The maximum allowable force at the mid-span, together with the corresponding apparent flexural strength, were estimated based on four common failure theories

with the Tsai-Wu failure criteria being noted to be different from the other failure theories under certain circumstances such as for hybrid composites with different fibre angles and lamina materials.

The reasons behind the presence of a hybrid effect in the flexural properties of composite laminates were investigated by comparing the strength, modulus and stress distribution within the laminas. Several factors were detected that contributed to the presence of a hybrid effect in hybrid composites with the effect of each factor on the apparent flexural strength of unidirectional and bidirectional hybrid composites being determined and with conflicting factors being indicated. Based on the conflicting factors the optimal level of hybridisation was found for each case and the optimal stacking configurations were determined.

Based on all factors, four general rules have been obtained for improving the flexural strength of hybrid composites which can be summarised as follows:

1. Placing laminas with a lower modulus and higher elongation at the surface of the compressive side will improve the composite flexural strength when compared with composite laminates containing only high modulus laminas.
2. Placing laminas with a lower modulus and higher elongation close to the neutral axis at the tensile side will improve the composite flexural strength when compared with composite laminates containing only high modulus laminas. A similar effect can be achieved by rotating a higher modulus and lower elongation lamina in the same location.
3. Rules 1 and 2 have no conflictions and can be combined, *i.e.*, placing low modulus fibres at both the surface at the compressive side and close to the neutral axis at the tensile side will improve the flexural strength.
4. The effect of Rule 1 is significantly higher than that of Rule 2.

Composites with different numbers of total laminas were investigated and it has been shown that they follow the same general rules. It was also noted that choosing a higher number of laminas within any given hybrid composite component would allow the designer to more accurately adjust the hybridization level in order to achieve the optimum configuration with maximum flexural strength.

Overall the results showed that a positive hybrid effect could be achieved for both unidirectional and bidirectional carbon/glass fibre reinforced epoxy hybrid composites. The authors suggest that the proposed rules can be utilized for the design of any continuous fibre hybrid polymer matrix composites with improved flexural strength.

## 4.6. References


[1] Dong C, Davies IJ. Flexural and tensile moduli of unidirectional hybrid epoxy composites reinforced by S-2 glass and T700S carbon fibres. Materials & Design. 2014;54:893-899.

[2] Dong C, Davies IJ. Flexural and tensile strengths of unidirectional hybrid epoxy composites reinforced by S-2 glass and T700S carbon fibres. Materials & Design. 2014;54:955-966.

[3] Hayashi T. On the improvement of mechanical properties of composites by hybrid composition. in Proceedings-8th International Reinforced Plastics Conferance. Brighton, UK: British Plastics Federation. 1972;149-152.

[4] Marom G, Fischer S, Tuler FR, Wagner HD. Hybrid effects in composites: conditions for positive or negative effects versus rule-of-mixtures behaviour. Journal of Materials Science. 1978;13:1419-1426.

[5] Dong C, Ranaweera-Jayawardena HA, Davies IJ. Flexural properties of hybrid composites reinforced by S-2 glass and T700S carbon fibres. Composites Part B: Engineering. 2012;43:573-581.

[6] Giancaspro JW, Papakonstantinou CG, Balaguru PN. Flexural response of inorganic hybrid composites with E-Glass and Carbon fibers. Journal of Engineering Materials and Technology. 2010;132:021005-1-021005-8.

[7] Tekalur SA, Shivakumar K, Shukla A. Mechanical behavior and damage evolution in E-glass vinyl ester and carbon composites subjected to static and blast loads. Composites Part B: Engineering. 2008;39:57-65.

[8] Isa MT, Ahmed AS, Aderemi BO, Taib RM, Mohammed-Dabo IA. Effect of fiber type and combinations on the mechanical, physical and thermal stability properties of polyester hybrid composites. Composites Part B: Engineering. 2013;52:217-223.

[9] Song JH. Pairing effect and tensile properties of laminated high-performance hybrid composites prepared using carbon/glass and carbon/aramid fibers. Composites Part B: Engineering. 2015;79:61-66.

[10] Dong C, Davies IJ. Optimal design for the flexural behaviour of glass and carbon fibre reinforced polymer hybrid composites. Materials & Design. 2012;37:450-457.

[11] Kalantari M, Dong C, Davies IJ. Multi-objective analysis for optimal and robust design of unidirectional glass/carbon fibre reinforced hybrid epoxy composites under flexural loading. Composites Part B: Engineering. 2016;84:130-139.

[12] Pandya KS, Veerraju Ch, Niak N.K. Hybrid composites made of carbon and glass woven fabrics under quasi-static loading. Materials & Design. 2011;32:4094-4099.

[13] Zhang J, Chaisombat K, He S, Wang CH. Hybrid composite laminates reinforced with glass/carbon woven fabrics for lightweight load bearing structures. Materials & Design. 2012;36:75-80.

[14] Dong C, Davies IJ. Flexural strength of bidirectional hybrid epoxy composites reinforced by E glass and T700S carbon fibres. Composites Part B: Engineering. 2015;72:65-71.

[15] Reddy JN. Mechanics of laminated composite plates and shells: theory and analysis. London: CRC press; 2004.

[16] Kretsis G. A review of the tensile, compressive, flexural and shear properties of hybrid fibre-reinforced plastics. Composites. 1987;18:13-23.

[17] Stevanovic MM, Stecenko TB. Mechanical behaviour of carbon and glass hybrid fibre reinforced polyester composites. Journal of Materials Science. 1992;27:941-946.

[18] Jones RM. Mechanics of composite materials. 2nd Edition. Philadelphia: Taylor & Francis; 1998.

[19] Mallick PK. Fiber-reinforced composites: materials, manufacturing, and design. 3rd Edition. London: CRC press; 1993.

[20] Lopez RH, Luersen MA, Cursi ES. Optimization of laminated composites considering different failure criteria. Composites Part B: Engineering. 2009;40:731-740.

[21] Soden PD, Hinton MJ, Kaddour AS. A comparison of the predictive capabilities of current failure theories for composite laminates. Composites Science and Technology. 1998;58:1225-1254.

[22] Hinton MJ, Kaddour AS, Soden PD. A comparison of the predictive capabilities of current failure theories for composite laminates, judged against experimental evidence. Composites Science and Technology. 2002;62:1725-1797.

[23] Reddy JN, Pandey AK. A first-ply failure analysis of composite laminates. Computers and Structures. 1987;25:371-393.

[24] Sun CT, Quinn BJ, Tao J, Oplinger DW. Comparative evaluation of failure analysis methods for composite laminates. Report No: DOT/FAA/AR-95/109, U.S. Department of Transportation. Washington; 1996.

[25] Hashin, Z. Analysis of composite materials - a survey. Journal of Applied Mechanics. 1983;50:481-505.

[26] Lo KH, Chim ESM. Compressive strength of unidirectional composites. Journal of Reinforced Plastics and Composites. 1992;11:838-896.

[27] ANSYS Mechanical APDL Element Reference. Release 15. November 2013.

[28] Wang CM, Lim GT, Reddy JN, Lee KH. Relationships between bending solutions of Reissner and Mindlin plate theories. Engineering Structures. 2001;23:838-849.

[29] Tsai SW, Wu EM. A general theory of strength for anisotropic materials. Journal of Composite Materials. 1971;5:58-80.

[30] Personal communication between the author (MK) and J. N. Reddy (Texas A&M University), June 18th 2015.

[31] Davies IJ, Hamada H. Flexural properties of a hybrid polymer matrix composite containing carbon and silicon carbide fibres. Advanced Composite Materials. 2001;10:77-96.

# 5

# Multi-Objective Analysis for Optimal and Robust Design of Unidirectional Glass/Carbon Fibre Reinforced Hybrid Epoxy Composites under Flexural Loading[1]

## 5.1. Introduction

The term “hybrid composite” is used to indicate a composite where the matrix has been reinforced by at least two types of fibre with the aim being to provide a synergistic effect between the multiple fibre types, e.g., improved strength. It is known that the flexural strength of unidirectional carbon fibre-reinforced polymer matrix composites (PMCs) can be improved by replacing carbon fibre at the compressive side with higher compressive strength fibres such as glass [1-4] or silicon carbide [5] whereas, conversely, the flexural strength of glass fibre-reinforced PMCs can be improved through the addition of carbon fibres on the tensile side [6]. Recent work by the current authors [4, 7, 8] has focussed on the effect of fibre volume fraction, span-to-depth ratio and number of glass laminas on the flexural strength and modulus of hybrid carbon/glass fibre-reinforced PMCs using finite element analysis (FEA) and classical lamination theory (CLT) with the hybrid ratio and fibre volume fractions for maximum positive hybrid effect being determined.

[1] This Chapter has been published in Composites Part B: Engineering, Vol 84, 2016, Pages 130-139

Research has indicated that the mechanical properties of hybrid composites, e.g., strength and modulus of elasticity, differ from those predicted by the standard rule of mixtures (RoM) [9-17] with the concept of a "hybrid effect" being introduced to take into account the difference between the properties of hybrid PMCs when compared to the RoM. This hybrid effect was first noted by Hayashi [16] in 1972 and is known to influence several composite properties related to strength such as the specific flexural strength and robustness. However, experience has shown that these parameters may not always be compatible and the optimal design of hybrid composites therefore requires a multi-criteria decision analysis.

The hybridization of PMCs influences not only mechanical properties such as strength, elastic modulus and strain to failure but other properties as well such as weight and cost. Maximizing the strength and reliability of hybrid PMCs, whilst minimizing their weight and cost, would be of fundamental concern for the design and manufacture of such composites. One significant topic of research for hybrid composites has concerned the minimisation of cost and weight whilst maximizing the strength and reliability [18-28]. For example, Adali and Verijenko [19] used the positive hybrid effect to improve the fundamental frequency and material cost of glass/graphite hybrid composites. Walker et al. [20] used a sequential optimization procedure to minimize the weight and cost of carbon/glass/Kevlar hybrid composites with the use of a limited amount of Kevlar fibre being noted to reduce the cost and weight of hybrid composites whilst simultaneously improving their buckling load. In contrast to this, the optimization of flexural strength for a hybrid composite reinforced by S-2 glass and T700S carbon fibres [23] indicated the maximum hybrid effect to be 56.1%, i.e., 56.1% greater than that predicted by the RoM, for the case of Vfc = 0.4748 and Vfg = 0.6329.

More recently, Hemmatian et al. [24, 25] applied different algorithms to solve the multi-objective optimization of carbon/glass hybrid composites in order to achieve minimum weight and cost. They considered first natural frequency as a constraint and used the weighted sum method (WSM) to construct Pareto-optimal fronts [29-

30]. WSM is the simplest, and possible the most widely used, classical approach in multi-objective optimization problems [31] and essentially scalarizes a set of objectives into a single objective by multiplying each objective by a weighting factor that is defined by the designer.

Most studies in the field of design and optimization of hybrid composites have used traditional design methods based on a deterministic approach with a large factor of safety being incorporated to account for expected variations in material and processing parameters. For example, it is well known that any deviation in composite performance can often be linked to variations in the constituent properties, fibre distribution, structural geometry, loading conditions and manufacturing process [32]. Fertig et al. [33] showed that microstructural variations, particularly for the volume fraction (which typically varies by ±1% [34, 35]), can lead to significant increases in stress within the composite. Another important source of manufacturing related variation is ply thickness. According to Chamis [36], the coefficient of variation (CoV) can be as high as 5% for this parameter. Thus, highly optimized composites designed with the assumption of deterministic parameters may not be achievable in practice with a resulting decrease in robustness and reliability. Therefore, an alternative approach based on probabilistic design [35-39] may be required which allows the estimation of reliability and incorporation of stochastic variability [40].

Robust design optimization (RDO) was first investigated by Taguchi [41] and aims to improve the product quality through controlling variations in parameters and/or minimizing the effect of variations on the performance of optimum design. Several attempts have been made to incorporate the effect of uncertainties in design variables on the optimization of composite materials [42-50]. For example, Walker and Hamilton [42] introduced a technique for optimally designing laminated structures for maximum buckling load taking into account manufacturing uncertainty in fibre angle whereas Adali et al. [43] incorporated load uncertainties within the robust design optimization of laminated composites for maximum buckling load. These researchers concluded that the performance of composites designed by RDO subjected to uncertain loading conditions was significantly higher

when compared to composites obtained by deterministic design. However, thus far there has been little discussion about the optimal and robust design of hybrid composites.

The present study aimed to numerically evaluate the effect of replacing carbon fibre laminas with glass fibre laminas on the flexural performance, cost, weight and robustness of the resulting hybrid composites. Classical lamination theory (CLT) was employed to calculate the stress distribution amongst the laminas with the materials being selected to be T700 carbon and S-2 glass as fibres and epoxy as the matrix in order to be comparable with previous research [1, 4, 7, 8, 23]. A multi-objective optimization problem was defined and solved by WSM with the weighting factors being calculated from the analytical hierarchy process (AHP) [51, 52], which has been extensively applied in various scenarios involving multi-criteria decision making (MCDM). Five different example scenarios were examined as an illustration for this technique with the corresponding optimal stacking sequences being obtained for each scenario.

## 5.2. Model Development

### 5.2.1. Laminate Configuration

The subject of this work was a hybrid unidirectional laminated composite under three-point bending as shown in Figure 5-1 with a normal force, *P*, applied at the mid-span. The stacking configuration for the hybrid composite was obtained by partially replacing carbon/epoxy laminas on the compressive side of the component by glass/epoxy laminas with the height of the glass/epoxy section, $h_g$, being varied from zero to *h* to reach a full glass/epoxy composite.

In order to quantify the degree of hybridization, the hybrid ratio was defined to be the relative ratio of glass fibres to all fibres, *i.e.*,

$$r_h = \frac{h_g V_{fg}}{h_g V_{fg} + h_c V_{fc}} \tag{5-1}$$

with $r_h$ = 0 and $r_h$ = 1 corresponding to full carbon/epoxy and glass/epoxy composites, respectively. Thus, the thicknesses of the respective carbon/epoxy and glass/epoxy sections can be written as:

$$h_c = \frac{(1-r_h)V_{fg}h}{r_h V_{fc}+(1-r_h)V_{fg}} \tag{5-2}$$

$$h_g = \frac{r_h V_{fc}h}{r_h V_{fc}+(1-r_h)V_{fg}} \tag{5-3}$$

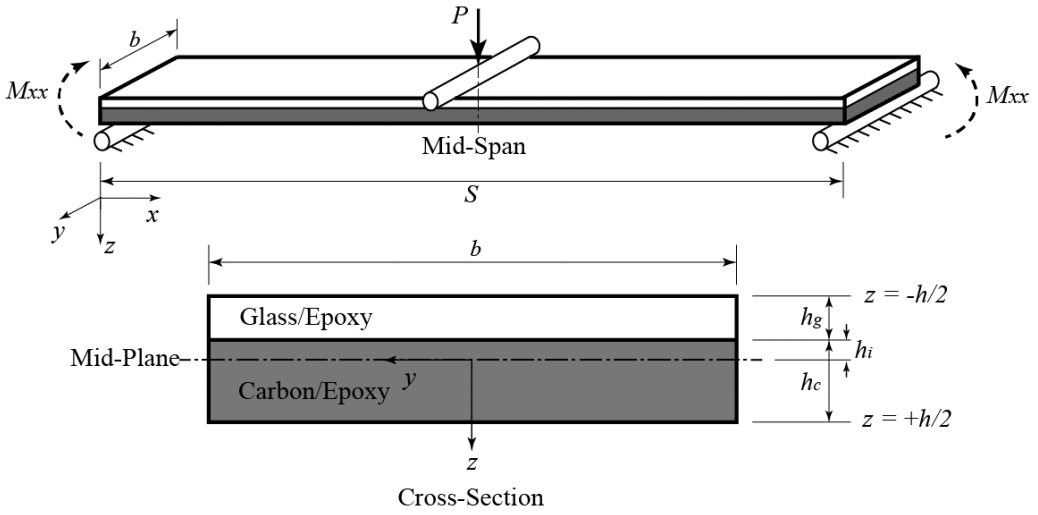


**Figure 5-1: Schematic representation of the hybrid composite specimen in the three-point bending configuration.**

### 5.2.2. Material Properties

As mentioned earlier, the hybrid composites investigated in this study were chosen to be comprised of T700S carbon and S-2 glass fibres and epoxy matrix [1, 4, 7, 8, 23] with the properties of the fibres and matrix being shown in Table 5-1. From this data the carbon/epoxy and glass/epoxy lamina properties, including the longitudinal modulus, $E_{xx}$, and shear modulus, $G_{xy}$, were derived using Hashin's model [53] and used in the subsequent laminate analysis.

**Table 5-1: Assumed properties of the fibres and resin utilized in this work.**

| Material | Tensile modulus (GPa) | Tensile strength (MPa) | Strain to failure | Density (kg/m$^3$) | Cost [58] ($/litre) |
|---|---|---|---|---|---|
| Toray T700S 12K carbon fibre | 230 | 4900 | 0.021 | 1800 | 22.0 |
| S-2 glass unidirectional Unitex plain weave UT-S500 fibre mat | 86.9 | 4890 | 0.056 | 2460 | 23.3 |
| Kinetix R240 high performance epoxy resin with H160 hardener at a ratio of 4:1 by weight | 3.10 | 69.60 | 0.022 | 1090 | 34.1 |

### 5.2.3. Classical Lamination Theory (CLT)

The CLT was used to simulate the flexural behaviour of the component and to calculate the stress distribution across the laminas [55]. With reference to Figure 5-1, the *xy*-plane was taken to be within the plane of the hybrid composite with the *z*-axis being positive downwards and the bending moment, $M_{xx}$, being generated as shown. In formulating the theory, the laminas were assumed to be perfectly bonded together whilst the strains and displacements were assumed to be small such that the composite deformed according to the Kirchhoff assumption for bending, *i.e.* after deformation the normal to the mid-plane remained straight and normal [56]. Given the external load being applied, the mid-plane strains, $\boldsymbol{\epsilon^0}$, and curvatures, $\boldsymbol{\kappa}$, can be calculated. The strain and stress at any location through the thickness can be found accordingly.

### 5.2.4. Flexural Strength and Hybrid Effect

Whilst the strength of a composite is dependent on the failure mode, analysis of failure modes for a laminated composite subjected to pure bending indicates that failure would occur at the compressive side with the most common failure mode being micro-buckling of fibres or kinking [5, 8]. Therefore, in the present model the compressive strength of each composite was predicted using the Lo-Chim model [57] as a previous study [4] indicated this model to be in good agreement with

experimental results. According to the Lo-Chim model, the longitudinal compressive strength of a unidirectional laminated composite can be given by:

$$S_C = \frac{G_{12}}{1.5+12(6/\pi)^2(G_{12}/E_{11})} \quad (5\text{-}4)$$

However, using the Weibull statistical strength theory, the ratio of flexural and compressive strength for unidirectional composites is known to be approximately 1.3 [58] and the compressive strength of the composite can therefore be modified to:

$$S_{Cm} = 1.3S_C \quad (5\text{-}5)$$

In order to determine the flexural strength of the hybrid composite specimen, the stress in each lamina due to *P* was calculated with the maximum value of compressive stress at the mid-span (where the moment is maximum) being found. The load was then gradually increased until the maximum compressive stress within any lamina reached the modified compressive strength of the lamina. It should be noted that the maximum compressive stress was calculated for each lamina of the hybrid composite and thus both the glass/epoxy and carbon/epoxy sections were analysed with the maximum compressive stress in each lamina being compared to the compressive strength of the particular lamina in order to determine the lamina in which failure initiated.

The apparent flexural strength of the hybrid composite could thus be estimated from the maximum load required to initiate failure, $P_{max}$, together with the specimen geometry.

No significant end forces are present in the simulation so that the flexural strength of the hybrid composite can be given by [56]:

$$S_F = \frac{3P_{max}S}{2bh^2} \quad (5\text{-}6)$$

In contrast to this, the flexural strength of the hybrid composites predicted from the RoM would be given by:

$$S_{FRoM} = S_{Fc}(1 - r_h) + S_{Fg}r_h \quad (5\text{-}7)$$

The hybrid effect is defined as the fractional deviation of the hybrid flexural strength (Equation 5-6) compared to that estimated from the RoM (Equation 5-7) and can be thus given by:

$$e_h = \frac{S_F}{S_{FRoM}} - 1 \quad (5\text{-}8)$$

The flexural strength for the hybrid composite may be rewritten in terms of the hybrid effect, hybrid ratio and the strength of each section, *i.e.,*

$$S_F = (1 + e_h)\left[S_{Fc} + \left(S_{Fg} - S_{Fc}\right)r_h\right] \quad (5\text{-}9)$$

Previous work by the authors has indicated that a positive hybrid effect exists (*i.e.*, $e_h > 0$) for the flexural strength of carbon/glass fibre epoxy composites [4, 7, 8, 23, 59-61].

The concept of dimensionless flexural strength refers to the flexural strength at any given hybrid ratio divided by the flexural strength of a reference material, which in

this work was arbitrarily chosen to be the flexural strength of a fully carbon/epoxy with a fibre volume fraction of 0.50, *i.e.,*

$$\underline{S_F} = \frac{S_F}{S_{F_{ref}}} \tag{5-10}$$

### 5.2.5. Robustness Index

The existence of a positive hybrid effect makes it possible to improve the flexural strength of such composites by utilising hybridisation. In order to clearly illustrate this effect, the fibre volume fractions of the pure carbon/epoxy and glass/epoxy composites were chosen so that they possessed the same flexural strength, *i.e.*, according to the RoM every combination of hybrid composite should have an identical flexural strength. Choosing the fibre volume fraction of the pure carbon/epoxy composite, $V_{fc}$, to arbitrarily be 0.30, this resulted in the fibre volume fraction of the pure glass/epoxy composite, $V_{fg}$, being 0.498 in order to maintain an identical flexural strength. According to the present analysis, combining these types of laminate into a hybrid composite showed a significant variation in flexural strength as a function of hybrid ratio as shown in Figure 5-2. Whereas the flexural strength for both of the pure composites was estimated to be 907 MPa, a maximum value of 1145 MPa was predicted for a hybrid ratio of 0.292, suggesting a maximum hybrid effect of 0.262 to be achievable when compared to the RoM value.

Whilst the analysis thus far has implicitly assumed that the geometry and quality of the composite laminates can be controlled to an arbitrarily high precision, in reality the manufacture of composite components will inevitably introduce variations in the lamina fibre volume fraction and thickness amongst other factors. From the definition of the hybrid ratio it is apparent that these variations in lamina fibre volume fraction and thickness will lead to a variation in the hybrid ratio. Since an increase in lamina fibre volume fraction can be considered equivalent to a decrease of lamina thickness, both of these parameter variations can be characterised by their influence on the variation of hybrid ratio. Thus, given that the hybrid ratio may

include some inherent variation during manufacturing processing it is important to understand the sensitivity of the flexural strength to the hybrid ratio in order to develop robust hybrid composites, *i.e.*, composites where the flexural strength is least sensitive to variations in manufacturing conditions.

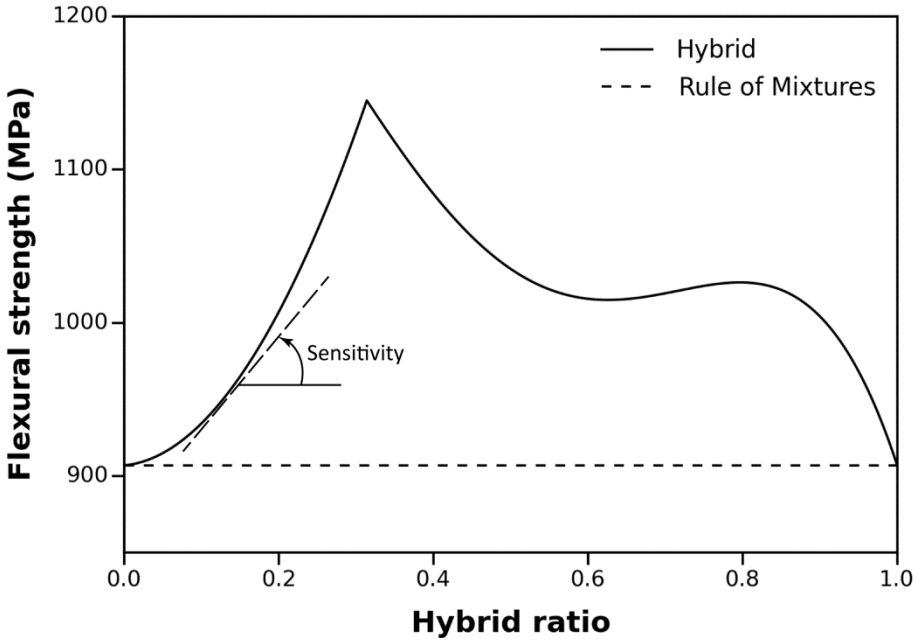


**Figure 5-2: Influence of hybrid ratio on the predicted flexural strength for a hybrid carbon/glass fibre-reinforced epoxy matrix composite with $V_{fc}$ = 30% and $V_{fg}$ = 49.8%. Note that the sensitivity of the flexural strength to hybrid ratio is the slope of the curve.**

In this study, the automatic differentiation (AD) technique [62] was used to calculate the local sensitivity of flexural strength with the sensitivity of the flexural strength to the hybrid ratio being characterised by the slope of the tangent of the curve, *i.e.*, the first derivative of flexural strength with respect to hybrid ratio. From this it can be deduced that hybrid composites where the first derivative of flexural strength is close to zero should be more stable and less sensitive to uncertainties concerning the ply thickness and fibre volume fraction and thus can be used as an indicator of robustness.

The influence of hybrid ratio on the first derivative of flexural strength has been presented in Figure 5-3. It is clear from the data that, from the point of view of robustness, hybrid ratios in the range of approximately 0.6 to 0.8 would possess the

least sensitivity to uncertainties in lamina thickness and fibre volume fraction due to the first derivative of flexural strength being relatively small in this range with crossover points at hybrid ratios of 0.676 and 0.803. In contrast to this, the hybrid ratio of 0.292 associated with the maximum flexural strength was noted to be most sensitive to the indicated uncertainties and would be a poor design choice from the point of view of robustness.

It can be seen from Figure 5-3 that a large range exists for the first derivative of flexural strength with respect to hybrid ratio as the value is derived from a tangent value which can approach infinity under certain conditions. For better applicability to optimal and robust design, the authors proposed the robustness index to be defined as the following:

$$RI = \frac{2\,tan^{-1}\left|\frac{d\underline{S}_F}{dr_h}\right|}{\pi} \tag{5-11}$$

where it is noted that the robustness index is taken to be the arctangent of the derivative of dimensionless flexural strength divided by its maximum value with $tan^{-1}\left|\frac{d\underline{S}_F}{dr_h}\right|$ possessing a maximum value of $\frac{\pi}{2}$ and thus *RI* having a maximum value of unity. As was the case for the first derivative of flexural strength, a smaller robustness index is preferred with a value close to zero implying that the composite design is more stable or robust against any variations in the lamina fibre volume fraction and thickness.

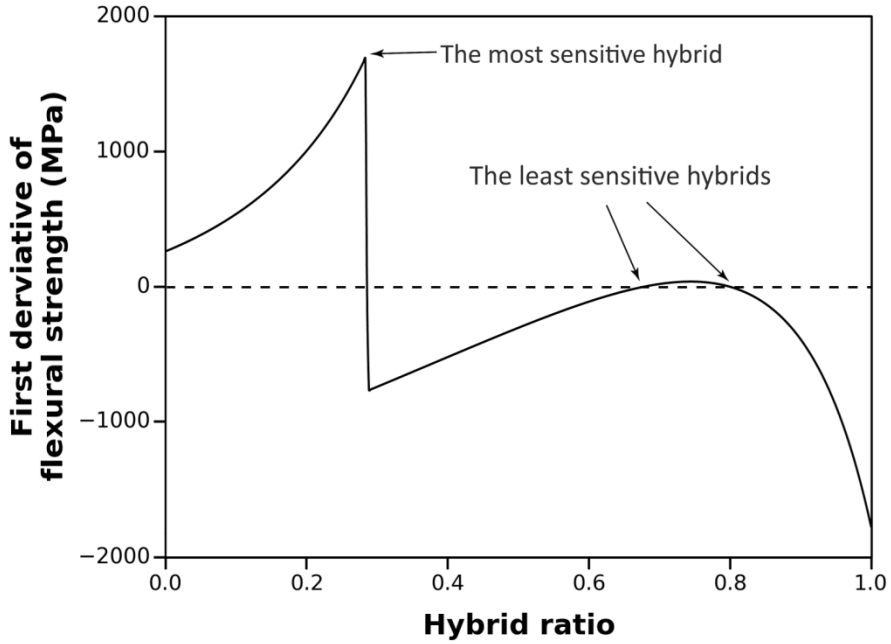


**Figure 5-3: Influence of hybrid ratio on the first derivative of flexural strength for a hybrid carbon/glass fibre-reinforced epoxy matrix composite with $V_{fc}$ = 30% and $V_{fg}$ = 49.8%.**

### 5.2.6. Density

One important criterion for composite design is weight which can be alternatively characterized by the density. A RoM can be used to determine the density of composite materials with the density of the current carbon/glass fibre-reinforced epoxy matrix composite being given by:

$$\rho_c = \rho_m + \frac{V_{fc}V_{fg}}{r_h V_{fc}+(1-r_h)V_{fg}}\left(\rho_{fc} - \rho_m\right) + \frac{r_h V_{fc}V_{fg}}{r_h V_{fc}+(1-r_h)V_{fg}}\left(\rho_{fg} - \rho_{fc}\right) \qquad (5\text{-}12)$$

### 5.2.7. Cost

Cost is another important criterion in the design of hybrid composites and is known to be influenced by a combination of design and manufacturing parameters. The key cost drivers for design can be summarized as material selection, geometry configuration and complexity. Whereas the key cost drivers for manufacturing would be related to labour and equipment costs, automation and production volume, these manufacturing parameters are generally not under the control of the

designer. If it is considered that approximately 40% of the composite cost is due to material cost [63] then material cost may be used as a reasonable proxy for the cost index.

The material cost for a hybrid composite is the summation of its constituent costs and thus the material cost per unit volume for a hybrid composite would be a function of hybrid ratio and thickness as follows:

$$C_{mat} = \frac{C_c(1-r_h)V_{fg}V_{fc}+C_g r_h V_{fc}V_{fg}+C_m[r_h V_{fc}(1-V_{fg})+(1-r_h)V_{fg}(1-V_{fc})]}{r_h V_{fc}+(1-r_h)V_{fg}} \quad (5\text{-}13)$$

with typical costs for the constituent materials under investigation being shown in Table 5-1.

## 5.3. Optimization

### 5.3.1. Objective Functions

The principal aims in the design of any composite structure would normally be minimization of the weight and cost and maximization of the strength and robustness. Multiple conflicting objectives are therefore present and a multi-objective optimization problem needs to be formulated. In general, the solution to a multi-objective problem is not a single optimal solution but instead a set of optimal solutions known as Pareto-optimal solutions [30].

To solve the multi-objective optimization problem in this study a weighted sum method (WSM) was utilized. This method is classified as a preference-based classic method which scalarizes a set of objectives into a single objective function. Each objective is normalized (*i.e.*, converted to values of similar order) and multiplied by a proper weighting factor (to take into account its relative importance). This method is simple and the most widely used classical approach [31]. Although this method is simple, setting values for the weighting factors is of primary concern and

requires a multiple-objective decision making process that will be described in Section 3.2.

Four objectives, namely flexural strength, weight, cost, and robustness were defined for the optimization problem in this study. It is a requirement that all objectives should be in the form of the smaller-the-better target (STB) [64] and thus, as the flexural strength needs to be maximized and based on the duality principle [65] in the context of optimization, the maximization problem can be converted to a minimization scenario by multiplying the objective function by −1. The objective function for the flexural strength was therefore chosen to be:

$$minimize\ [F_1(r_h) = -\frac{S_F}{S_{F_{ref}}}] \tag{5-14}$$

where $S_F$ is the flexural strength of the hybrid composite calculated from Equation 5-9 and $S_{F_{ref}}$ is the flexural strength of the reference composite, *i.e.*, full carbon/epoxy composite with a fibre volume fraction of 0.50. It should be noted that normalizing the objective function with respect to $S_{F_{ref}}$ allowed $F_1(r_h)$ to be on the order of unity.

With regards to weight minimization, the (closely related) density of the hybrid composite was considered to be the objective function with the normalized weight index and objective function for weight being defined as:

$$minimize\ [F_2(r_h) = \frac{\rho_c}{\rho_{c_{ref}}}] \tag{5-15}$$

with $\rho_c$ being obtained from Equation 5-12 and $\rho_{c_{ref}}$ being the density of the reference composite mentioned previously.

As discussed in the previous section, since approximately 40% of the composite cost can be attributed to material cost, the cost index was considered to be a function of material cost with the normalized objective function for cost being given by:

$$minimize\ [F_3(r_h) = \frac{C_{mat}}{C_{ref}}] \tag{5-16}$$

where $C_{mat}$ is the material cost calculated from Equation 5-13 and $C_{ref}$ is the material cost of the reference composite.

The robustness index was previously defined in Section 2.5 and may be calculated from Equation 5-11. A lower robustness index indicates that the hybrid composite is less sensitive to the mentioned manufacturing uncertainties and thus the objective is to minimize the robustness index, *i.e.*,

$$minimize\ [F_4(r_h) = RI] \tag{5-17}$$

Regarding the four objective functions mentioned above, the multi-objective optimization problem can be written as:

$$\textit{Minimize} \qquad [F_1(r_h)\ , F_2(r_h), F_3(r_h), F_4(r_h)] \tag{5-18}$$

$$\textit{Subjected to} \qquad 0 \leq r_h \leq 1$$

Using the weighted sum method, the objectives can be converted to a single objective function as follows:

*Minimize* $DI = \sum w_i F_i(r_h), \quad i = 1, 2, 3, 4$ (5-19)

*Subjected to* $0 \leq r_h \leq 1$

where $DI$ is the design index and $F_i$ are the objective functions measuring the flexural strength index, weight index, cost index and robustness index of the hybrid composite and $w_i$ are the weighting factors. An individual or series of Pareto-optimal solutions can therefore be found by varying the weighting factors to minimize $DI$. In the present study, only a single design variable was considered, *i.e.*, hybrid ratio, although other design variables could be incorporated if required. The total thickness of the hybrid composite was considered to be constant throughout the analysis.

### 5.3.2. Weighting Factors

The weighting factors in WSM are known to be dependent on two parameters, namely the importance and scaling factor of each objective. For a situation when the objectives are of different orders of magnitude, appropriate scaling factors should be introduced in order to achieve values of similar order. This was achieved in the present work by normalising each objective function such that the weighting factor for each objective was proportional to the relative importance of that objective. In general, a designer would use a decision making method in order to determine the preference of objectives with AHP being utilized in the present study to determine the weighting factor for each objective. AHP was developed by Saaty [52] in 1990 and has been used extensively in different fields for the analysis of multi-criteria decisions. Through use of the AHP method, objectives may be arranged in a hierarchical structure based on mathematics and psychology.

In this study, the AHP method was implemented based on pairwise comparison between the objectives from a preference point of view in order to determine the weighting factors in WSM. Four different preference levels were chosen with the corresponding scores being assigned based on a 1 to 9 scale as shown in Table 5-2.

Based on the preference levels and corresponding scores, a pairwise comparison matrix was derived by considering the rows and columns of the matrix as the objectives. Each cell of the matrix was filled by comparing objectives for different scenarios and using the scores in Table 5-2. For example, Table 5-3 illustrates the case of a comparison matrix when the flexural strength of the hybrid composite was extremely preferred by the designer compared to weight, cost and robustness.

**Table 5-2: Preference levels and scores for the weighting factors.**

| Preference level | Score |
|---|---|
| Equally preferred | 1 |
| Moderately preferred | 3 |
| Strongly preferred | 6 |
| Extremely preferred | 9 |

Elements on the main diagonal of the matrix are comparisons between the same objectives and thus must always equal one. Since flexural strength in Table 5-3 was extremely preferred compared to the other objectives, all other elements apart from flexural strength in the first row were set to have a value of nine which is equal to “Extremely preferred” in accordance with Table 5-2. The corresponding elements in the flexural strength column were then set to 1/9. Since the cost, weight, and robustness were equally preferred, values for these elements above the main diagonal of the matrix were set equal to one with the remaining values being set to reciprocal values depending on their previous assignment. Once this has been carried out, the summation of each row indicates the priority of the objective with the weighting factors being calculated by normalizing with respect to the summation of all priorities as shown in the final column of Table 5-3. The calculated weighting factors were then utilized in the WSM in order to determine the solution of the multi-objective optimization problem.

**Table 5-3: Pairwise comparison matrix for objectives for the case when flexural strength is extremely preferred to other considerations.**

| | Flexural Strength | Weight | Cost | Robustness | Priority | Weighting factor |
|---|---|---|---|---|---|---|
| Flexural Strength | 1 | 9 | 9 | 9 | 28.000 | 0.750 |
| Weight | 1/9 | 1 | 1 | 1 | 3.111 | 0.083 |
| Cost | 1/9 | 1 | 1 | 1 | 3.111 | 0.083 |
| Robustness | 1/9 | 1 | 1 | 1 | 3.111 | 0.083 |
| | | | | *Sum* | *37.333* | *1.00* |

### 5.3.3. Implementation

Figure 5-4 illustrates the procedure for calculating the flexural strength for a hybrid carbon/glass fibre-reinforced epoxy matrix composite and evaluating the objective functions for all hybrid ratios between zero to one in order to determine the optimum hybrid ratio based on the preference of each objective.

In the present study a computer routine was developed in MATLAB in order to calculate mechanical properties such as the flexural strength and solve multi-objective optimization problems with the hybrid ratio being allowed to vary from zero to one. The first step of the procedure was to calculate the stiffness and strength of the carbon/epoxy and glass/epoxy laminas using Hashin's model and Lo-Chim's model, respectively. Secondly, a load corresponding to a bending moment in the longitudinal direction was applied with the mid-span stresses within each lamina being determined based on CLT. With knowledge of the strength and stress components, factors of safety were then calculated at the top, middle and bottom of each lamina. The load was then gradually increased until failure initiated in order to calculate the failure load. These steps were carried out as the hybrid ratio was gradually increased from zero to one with the failure load, and hence, flexural strength being determined as a function of hybrid ratio. In parallel to this, the predicted flexural strength obtained from standard RoM was also calculated with the resulting flexural strengths from CLT and RoM being utilized to determine the

hybrid effect as a function of hybrid ratio. In addition to this, other necessary parameters such as density, cost and robustness were also evaluated with the resulting design index being calculated taking in account the weighting factors obtained from AHP.

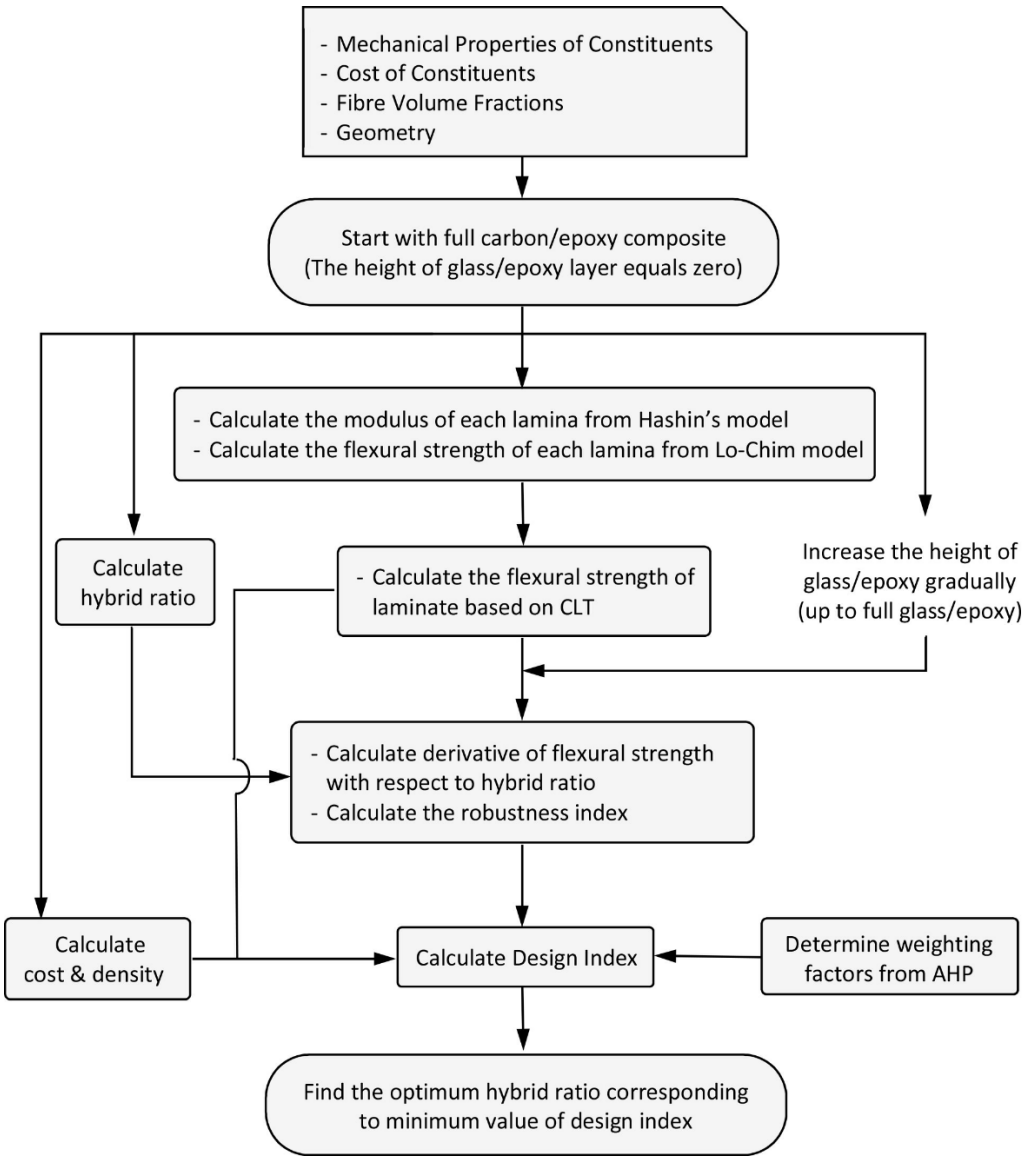


**Figure 5-4: Flowchart illustrating the main steps used to determine the optimum hybrid ratio for a hybrid carbon/glass fibre-reinforced epoxy matrix composite.**

## 5.4. Results and Discussion

Whilst the optimization problem under consideration may be solved for any fibre volume fraction, in this section the authors have selected two cases for study as

examples of the technique. The conditions of the first case were $V_{fc} = 0.30$ and $V_{fg} = 0.498$ in which the full carbon/epoxy and glass/epoxy composites would possess identical flexural strength (and previously highlighted in Figure 5-2 and 5-3).

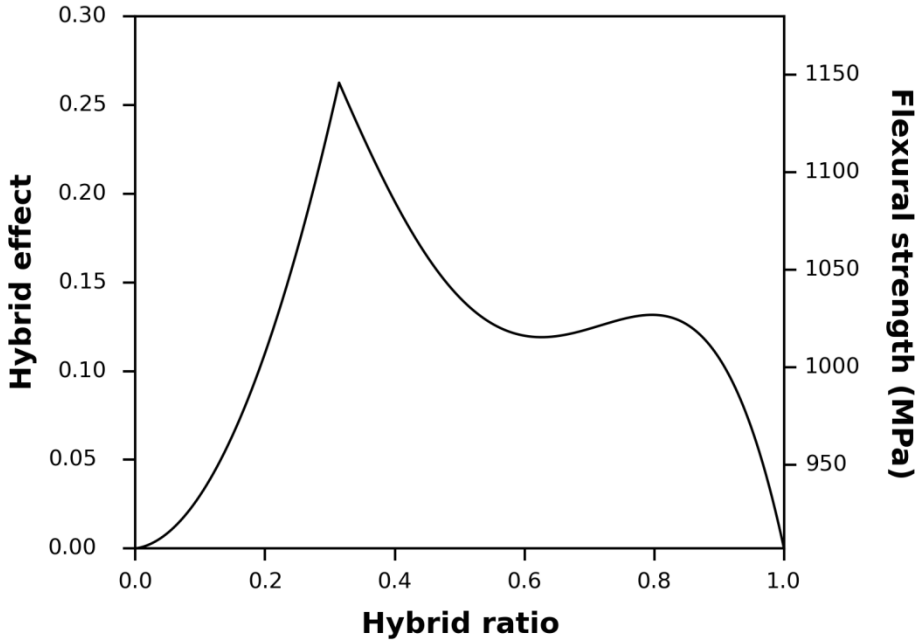


**Figure 5-5: Influence of hybrid ratio on hybrid effect and flexural strength for a hybrid carbon/glass fibre-reinforced epoxy matrix composite in Case 1 ($V_{fc}$ = 30% and $V_{fg}$ = 49.8%).**

In the second case, the fibre volume fractions for the carbon/epoxy and glass/epoxy laminas were chosen to be 0.50 and 0.65, respectively, with this representing a high volume fraction (and thus, high flexural strength) composite. The influence of hybrid ratio on hybrid effect and flexural strength, density, cost and robustness index for a hybrid carbon/glass fibre-reinforced epoxy matrix composite in Case 1 ($V_{fc}$=0.30 and $V_{fg}$=0.498) has been shown in Figures 5-5 to 5-8, respectively.

As previously mentioned, the weighting factors in the WSM were determined based on the preference of each objective. In this study, five different example scenarios have been presented in Table 5-4 with the preference of the objectives and the respective weighting factors being determined based on AHP and shown in Table 5-5. The design index for each of the scenarios was then calculated as a function of hybrid ratio with the minimum value of the design index being the proposed

optimal solution. The hybrid ratio corresponding to the minimum value of design index would therefore be designated as the best laminate configuration.

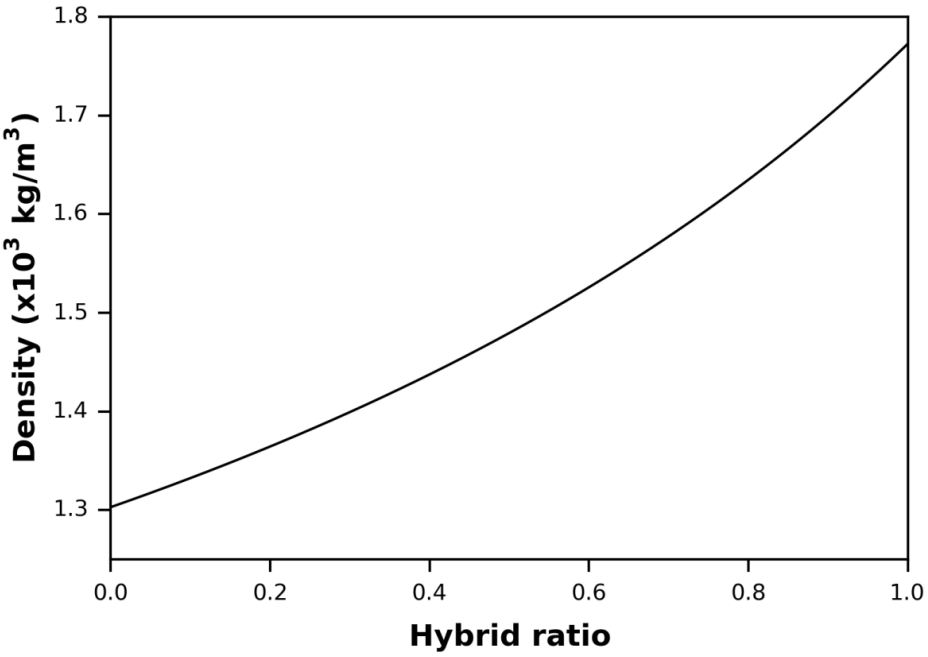


**Figure 5-6: Influence of hybrid ratio on density for a hybrid carbon/glass fibre-reinforced epoxy matrix composite in Case 1 ($V_{fc}$ = 30% and $V_{fg}$ = 49.8%).**

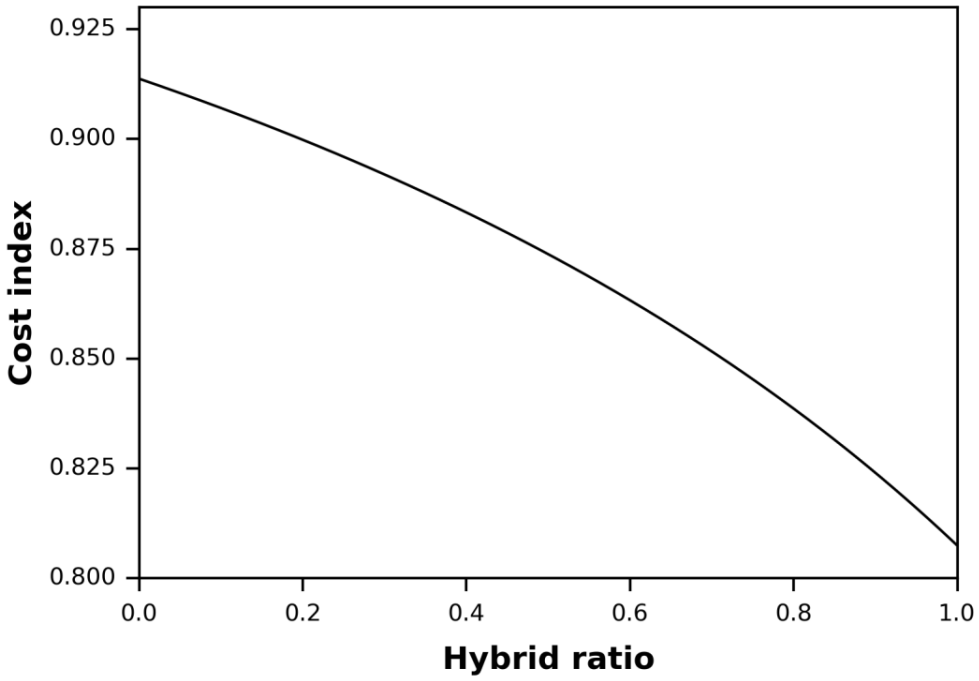


**Figure 5-7: Influence of hybrid ratio on cost index for a hybrid carbon/glass fibre-reinforced epoxy matrix composite in Case 1 ($V_{fc}$ = 30% and $V_{fg}$ = 49.8%).**

**Table 5-4: Scenarios and preference of the objectives for a hybrid carbon/glass fibre-reinforced epoxy matrix composite.**

| Scenario No. | Scenario Description | Preference |
|---|---|---|
| 1 | Two objectives are preferred | Strength and weight are extremely preferred to all others. |
| 2 | | Strength and cost are extremely preferred to all others. |
| 3 | | Strength and robustness are extremely preferred to all others. |
| 4 | One objective is not preferred | All objectives are extremely preferred to weight. |
| 5 | | All objectives are extremely preferred to cost. |

Results illustrating the influence of hybrid ratio on design index for each of the five scenarios in Case 1 have been presented in Figure 5-9 with the minimum design index value, $DI_{min}$, and corresponding hybrid ratio, $r_{h,opt}$, being listed in Table 5-6. In order to convert the data in Table 5-6 into example design specifications, if the hybrid composite was comprised of eight equal laminas of 0.25 mm thickness then the heights of the carbon and glass sections, $h_c$ and $h_g$ respectively, together with the corresponding stacking sequence in each scenario would be as shown in Table 5-6. Likewise, results for the high strength composite Case 2 study with $V_{fc}$ = 0.50 and $V_{fg}$ = 0.65 have been presented in Figure 5-10 and Table 5-7.

**Table 5-5: Weighting factors from AHP for each scenario for a hybrid carbon/glass fibre-reinforced epoxy matrix composite.**

| Weighting factors | Scenario | | | | |
|---|---|---|---|---|---|
| | 1 | 2 | 3 | 4 | 5 |
| $w_1$ (strength) | 0.450 | 0.450 | 0.450 | 0.321 | 0.321 |
| $w_2$ (weight) | 0.450 | 0.050 | 0.050 | 0.037 | 0.321 |
| $w_3$ (cost) | 0.050 | 0.450 | 0.050 | 0.321 | 0.037 |
| $w_4$ (robustness) | 0.050 | 0.050 | 0.450 | 0.321 | 0.321 |

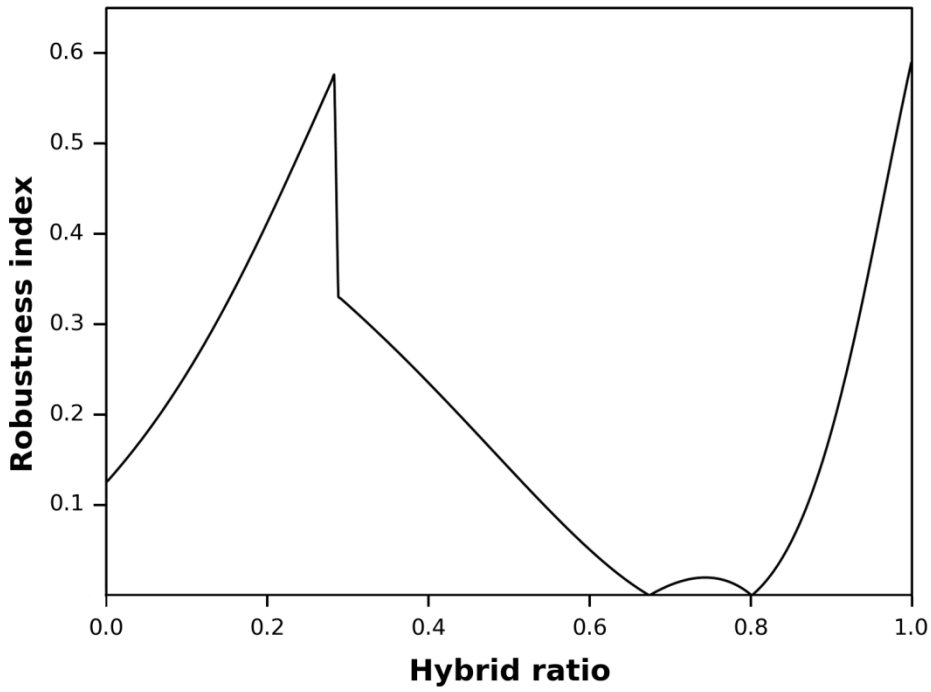


**Figure 5-8: Influence of hybrid ratio on robustness index for a hybrid carbon/glass fibre-reinforced epoxy matrix composite in Case 1 ($V_{fc}$ = 30% and $V_{fg}$ = 49.8%).**

From the results of both cases, it can be observed that extreme preference for strength and weight (Scenario 1) or strength and cost (Scenario 2) resulted in an optimal hybrid ratio of approximately 0.3 which corresponded to a stacking configuration of $[0_{2G}/0_{6C}]$. Such a hybrid ratio correlates closely with the maximum hybrid effect and is in good agreement with a previous study [23]. However, when strength and robustness (Scenario 3) or all objectives but the weight (Scenario 4) are extremely preferred then the optimal hybrid ratio is found to be approximately 0.8 which corresponds to a stacking configuration of $[0_{6G}/0_{2C}]$. Finally, when cost is not the main concern (Scenario 5), the optimal hybrid ratio was found to be approximately 0.68 in Case 1 which corresponded to a stacking configuration of $[0_{4G}/0_{4C}]$, and 0.01 in Case 2 which corresponded to full carbon/epoxy ($[0_{8C}]$), *i.e.*, entirely higher cost carbon fibres will be used.

**Table 5-6: Optimal hybrid ratio and stacking sequence for each scenario in Case 1 for an eight lamina hybrid carbon/glass fibre-reinforced epoxy matrix composite ($V_{fc}$ = 30% and $V_{fg}$ = 49.8%) with a lamina thickness of 0.25 mm.**

| Scenario | $DI_{min}$ | $r_{h,opt}$ | $h_c$ (mm) | $h_g$ (mm) | Stacking sequence |
|---|---|---|---|---|---|
| 1 | 0.109 | 0.292 | 1.60 | 0.40 | $[0_{2G}/0_{6C}]$ |
| 2 | 0.080 | 0.292 | 1.60 | 0.40 | $[0_{2G}/0_{6C}]$ |
| 3 | −0.244 | 0.803 | 0.58 | 1.42 | $[0_{6G}/0_{2C}]$ |
| 4 | 0.066 | 0.803 | 0.58 | 1.42 | $[0_{6G}/0_{2C}]$ |
| 5 | 0.153 | 0.676 | 0.90 | 1.10 | $[0_{4G}/0_{4C}]$ |

**Table 5-7: Optimal hybrid ratio and stacking sequence for each scenario in Case 2 for an eight lamina hybrid carbon/glass fibre-reinforced epoxy matrix composite ($V_{fc}$ = 50% and $V_{fg}$ = 65%) with a lamina thickness of 0.25 mm.**

| Scenario | $DI_{min}$ | $r_{h,opt}$ | $h_c$ (mm) | $h_g$ (mm) | Stacking sequence |
|---|---|---|---|---|---|
| 1 | 0.010 | 0.312 | 1.48 | 0.52 | $[0_{2G}/0_{6C}]$ |
| 2 | −0.048 | 0.312 | 1.48 | 0.52 | $[0_{2G}/0_{6C}]$ |
| 3 | −0.380 | 0.781 | 0.53 | 1.47 | $[0_{6G}/0_{2C}]$ |
| 4 | −0.023 | 0.781 | 0.53 | 1.47 | $[0_{6G}/0_{2C}]$ |
| 5 | 0.038 | 0.007 | 1.99 | 0.01 | $[0_{8C}]$ |

It should be noted that any difference in design index between individual scenarios would generally be of little concern to composite designers. The reason for this being that the designer would normally only be interested in a single scenario for any given application. Therefore, in general only the variation of design index for a single scenario would be of importance (as compared to the variation of design index against multiple scenarios).

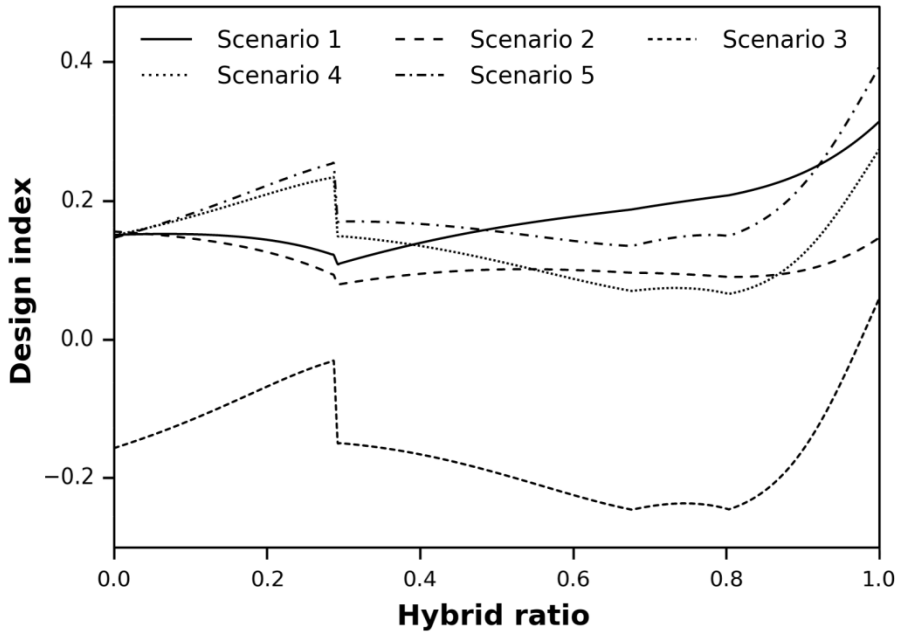


**Figure 5-9: Influence of hybrid ratio on design index for each scenario in Case 1 for a hybrid carbon/glass fibre-reinforced epoxy matrix composite ($V_{fc}$ = 30% and $V_{fg}$ = 49.8%).**

## 5.5. Conclusions

In this study, a multi-objective analysis has been presented to evaluate the optimal and robust design for unidirectional hybrid S-2 glass and T700S carbon fibre-reinforced epoxy composites with respect to the flexural properties. The robustness index was derived and formulated to take account the effect of uncertainties in the lamina fibre volume fractions and thickness on the flexural strength of the composite. Four objectives, namely, flexural strength, weight, cost and robustness were considered with WSM being used to convert the problem into a single objective optimization with the weighting factors being determined using AHP. Two example cases, each with five different scenarios, were studied in order to illustrate the effect of different objective preferences on the composite design. The results suggested that the optimal design is not always at the critical hybrid ratio with the maximum flexural strength or hybrid effect but depends on the objective preferences.

The authors suggest that the proposed method is a powerful tool that can be utilized to design more stable and realistic components with minimal weight, cost

and variability of response when subjected to manufacturing uncertainties in material design parameters.

## 5.6. References


[1] Sudarisman, Davies IJ. The effect of processing parameters on the flexural properties of unidirectional carbon fibre-reinforced polymer (CFRP) composites. Materials Science and Engineering A. 2008;498:65-68.

[2] Subagia I.D.G, Kim Y, Tijing LD, Kim CS, Shon HK. Effect of stacking sequence on the flexural propertiesof hybrid composites reinforced with carbon and balast fibres. Composites Part B: Engineering. 2014;58:251-258.

[3] Manders PW, Bader MG. The strength of hybrid glass/carbon fibre composites - Part 1 Failure strain enhancement and failure mode. Journal of Materials Science. 1981;16:2233-2245.

[4] Dong C, Ranaweera-Jayawardena HA, Davies IJ. Flexural properties of hybrid composites reinforced by S-2 glass and T700S carbon fibres. Composites Part B: Engineering. 2012;43:573-581.

[5] Davies IJ, Hamada H. Flexural properties of a hybrid polymer matrix composite containing carbon and silicon carbide fibres. Advanced Composite Materials. 2001;10:77-96.

[6] Giancaspro JW, Papakonstantinou CG, Balaguru PN. Flexural response of inorganic hybrid composites with E-Glass and Carbon fibers. Journal of Engineering Materials and Technology. 2010;132:021005-1-8.

[7] Dong C, Davies IJ. Flexural and tensile moduli of unidirectional hybrid epoxy composites reinforced by S-2 glass and T700S carbon fibres. Materials & Design. 2014;54:893-899.

[8] Dong C, Davies IJ. Flexural and tensile strengths of unidirectional hybrid epoxy composites reinforced by S-2 glass and T700S carbon fibres. Materials & Design. 2014;54:955-966.

[9] Jarukumjorn K, Suppakarn N. Effect of glass fibre hybridization on properties of sisal fibre-polypropylene composites. Composites Part B: Engineering. 2009;40:623-627.

[10] Banerjee S, Sankar BV. Mechanical properties of hybrid composites using finite element method based micromechanics. Composites Part B: Engineering. 2014;58:318-327.

[11] Pandya KS, Veerraju C, Naik NK. Hybrid composites made of carbon and glass woven fabrics under quasi-static loading. Materials and Design. 2011;32:4094-4099.

[12] Kim HS, Hong SI, Kim SJ. On the rule of mixtures for predicting the mechanical properties of composites with homogeneously distributed soft and hard particles. Journal of Materials Processing Technology. 2001;112:109-113.

[13] Zweben C. Tensile strength of hybrid composites. Journal of Materials Science. 1977;12:1325-1337.

[14] Summerscales J, Short D. Carbon fibre and glass fibre hybrid reinforced plastics. Composites. 1978;9:157-166.

[15] Phillips LN. The hybrid effect — does it exist? Composites. 1976;7:7-8.

[16] Hayashi T. On the improvement of mechanical properties of composites by hybrid composition. in Proceedings-8th International Reinforced Plastics Conference. Brighton, UK: British Plastics Federation. 1972;149-152.

[17] Peijs AAJM, De Kok JMM. Hybrid composites based on polyethylene and carbon fibres. Part 6: Tensile and fatigue behaviour. Composites. 1993;24:19-32.

[18] Oh JH, Kim YG, Lee DG. Optimum bolted joints for hybrid composite materials. Composite Structures. 1997;38:329-341.

[19] Adali S, Verijenko VE. Optimum stacking sequence design of symmetric hybrid laminates undergoing free vibrations. Composite Structures. 2001;54:131-138.

[20] Walker M, Reiss T, Adali S. A procedure to select the best material combinations and optimally design hybrid composite plates for minimum weight and cost. Engineering Optimization. 1997;29:65-83.

[21] Conceição António CA. A hierarchical genetic algorithm with age structure for multimodal optimal design of hybrid composites. Structural and Multidisciplinary Optimization. 2006;31:280-94.

[22] Abachizadeh M, Tahani M. An ant colony optimization approach to multi-objective optimal design of symmetric hybrid laminates for maximum fundamental frequency and minimum cost. Structural and Multidisciplinary Optimization. 2009;37:367-376.

[23] Dong C, Davies IJ. Optimal design for the flexural behaviour of glass and carbon fibre reinforced polymer hybrid composites. Materials & Design. 2012;37:450-457.

[24] Hemmatian H, Fereidoon A, Sadollah A, Bahreininejad A. Optimization of laminate stacking sequence for minimizing weight and cost using elitist ant system optimization. Advances in Engineering Software. 2013;57:8-18.

[25] Hemmatian H, Fereidoon A, Assareh E. Optimization of hybrid laminated composites using the multi-objective gravitational search algorithm (MOGSA). Engineering Optimization. 2014;46:1169-1182.

[26] Sfiso Radebe I, Adali S. Minimum cost design of hybrid cross-ply cylinders with uncertain material properties subject to external pressure. Ocean Engineering. 2014;88:310-317.

[27] Tserpes K.I, Koumpias A.S. A numerical methodology for optimizing the geometry of composite structural parts with regard to strength. Composites Part B: Engineering. 2015;68:176-184.

[28] Lopez R.H, Luersen M.A, Cursi E.S. Optimization of laminated composites considering different failure criteria. Composites Part B: Engineering. 2009;40:731-740.

[29] Smale S. Global Analysis and Economics I: Pareto Optimum and a Generalization of Morse Theory. In: Peixoto MM, editor. Dynamical Systems: Academic Press. 1973;531-544.

[30] De Melo W. Stability and optimization of several functions. Topology. 1976;15:1-12.

[31] Deb K. Multi-objective optimization using evolutionary algorithms: John Wiley & Sons; 2001.

[32] Chiachio M, Chiachio J, Rus G. Reliability in composites – A selective review and survey of current development. Composites Part B: Engineering. 2012;43:902-913.

[33] Ray SF, Eric MJ. Effect of fiber volume fraction variation across multiple length scales on composite stress variation: the possibility of stochastic multiscale analysis. in Proceedings-55th AIAA/ASMe/ASCE/AHS/SC Structures, Structural Dynamics, and Materials Conference: American Institute of Aeronautics and Astronautics. 2014.

[34] Spurgeon WA. Thickness and reinforcement fiber content control in composites by vacuum-assisted resin transfer molding fabrication processes. DTIC Document: Army Research Lab Aberdeen Proving Ground MD. 2005.

[35] Shaw A, Sriramula S, Gosling PD, Chryssanthopoulos MK. A critical reliability evaluation of fibre reinforced composite materials based on probabilistic micro and macro-mechanical analysis. Composites Part B: Engineering. 2010;41:446-453.

[36] Chamis CC. Probabilistic simulation of multi-scale composite behavior. Theoretical and Applied Fracture Mechanics. 2004;41:51-61.

[37] Chamis CC, Shiao MC. IPACS – integrated probabilistic assessment of composite structures: Code development and application. in Proceedings-Third NASA Advanced Composite Technology Conference 1992;987-999.

[38] Chamis CC, Abumeri GH. Probabilistic dynamic buckling of composite shell structures. Composites Part A: Applied Science and Manufacturing. 2005;36:1368-1380.

[39] Shiao MC, Chamis CC. Probabilistic evaluation of fuselage-type composite structures. Probabilistic Engineering Mechanics. 1999;14:179-187.

[40] Di Sciuva M, Lomario D. A comparison between Monte Carlo and FORMs in calculating the reliability of a composite structure. Composite Structures. 2003;59:155-162.

[41] Taguchi G. Performance analysis design. International Journal of Production Research. 1978;16:521-530.

[42] Walker M, Hamilton R. A methodology for optimally designing fibre-reinforced laminated structures with design variable tolerances for maximum buckling strength. Thin-Walled Structures. 2005;43:161-174.

[43] Adali S, Lene F, Duvaut G, Chiaruttini V. Optimization of laminated composites subject to uncertain buckling loads. Composite Structures. 2003;62:261-269.

[44] Liao YS, Chiou CY. Robust optimum designs of fiber-reinforced composites using constraints with sensitivity. Journal of Composite Materials. 2006;40:2067-2081.

[45] António CC, Hoffbauer LN. An approach for reliability-based robust design optimisation of angle-ply composites. Composite Structures. 2009;90:53-59.

[46] Lee MCW, Mikulik Z, Kelly DW, Thomson RS, Degenhardt R. Robust design - A concept for imperfection insensitive composite structures. Composite Structures. 2010;92:1469-1477.

[47] Lee D, Morillo C, Oller S, Bugeda G, Oñate E. Robust design optimisation of advance hybrid (fiber-metal) composite structures. Composite Structures. 2013;99:181-192.

[48] Lekou D.J, Philippidis T.P. Mechanical property variability in FRP laminates and its effect on failure prediction. Composites Part B: Engineering. 2008;39:1247-1256.

[49] Shaw A, Sriramula S, Gosling PD, Chryssanthopoulos MK. A critical reliability evaluation of fibre reinforced composite materials based on probabilistic micro and macro-mechanical analysis. Composites Part B: Engineering. 2010;41:446-453.

[50] Chiachio M, Chiachio J, Rus G. Reliability in composites – A selective review and survey of current development. Composites Part B: Engineering. 2012;43:902-913.

[51] Saaty TL. Axiomatic foundation of the analytic hierarchy process. Management Science. 1986;32:841-855.

[52] Saaty TL. How to make a decision: The analytic hierarchy process. European Journal of Operational Research. 1990;48:9-26.

[53] Chou T-W. Microstructural design of fiber composites. Cambridge University Press; 2005.

[54] Gurit. Guid to composites, www.gurit.com, Accessed: 5 June 2014

[55] Mallick PK. Fiber-Reinforced Composites: Materials, Manufacturing, and Design. 3rd edition. London: CRC press; 1993.

[56] Reddy JN. Mechanics of laminated composite plates and shells: theory and analysis: CRC press; 2004.

[57] Lo KH, Chim ESM. Compressive strength of unidirectional composites. Journal of Reinforced Plastics and Composites. 1992;11:838-896.

[58] Bullock RE. Strength ratios of composite materials in flexure and in tension. Journal of Composite Materials. 1974;8:200-206.

[59] Dong C, Davies IJ. Flexural properties of glass and carbon fiber reinforced epoxy hybrid composites. Proceedings of the Institution of Mechanical Engineers, Part L: Journal of Materials: Design and Applications. 2013;227:308-317.

[60] Dong C, Sudarisman, Davies IJ. Flexural properties of E glass and TR50S carbon fiber reinforced epoxy hybrid composites. Journal of Materials Engineering and Performance. 2013;22:41-49.

[61] Dong C, Duong J, Davies IJ. Flexural properties of S-2 glass and TR30S carbon fiber-reinforced epoxy hybrid composites. Polymer Composites. 2012;33:773-781.

[62] Frey HC, Patil SR. Identification and review of sensitivity analysis methods. Risk Analysis. 2002;22:553-578.

[63] Karlsson M. The development of a technical cost model for composites. Stockholm, Sweden: KTH Royal Institute of Technology; 2013.

[64] Murphy T, Tsui K-L, Allen J. A review of robust design methods for multiple responses. Research Engineering Design. 2005;15:201-215.

[65] Rao S. Engineering Optimization: Theory and Practice: New Age International; 1996.

# 6

# Multi-Objective Robust Optimization of Unidirectional Carbon/Glass Fibre Reinforced Hybrid Composites Under Flexural Loading[1]

## 6.1. Introduction

Hybrid composite laminates, which contain more than one type of reinforcement phase, *e.g.*, carbon and glass fibre, are widely used in applications requiring high strength, low weight and low cost. For example, since glass fibres possess a lower modulus and higher strain-to-failure when compared to carbon fibres, the flexural strength of carbon fibre-reinforced polymer (CFRP) composites can be significantly improved by replacing some of the carbon fibre laminas at the compressive side of the composite by glass fibre laminas [1-6].

However, the effect of hybridization in fibre-reinforced composites is not always positive [7] and finding the optimum level of hybridization would be of fundamental concern for the design of such materials. The hybrid effect is defined as the deviation of a certain property from the rule of mixtures (RoM) equation. The general rule of mixtures is the weighted mean of a material property with respect to the volume fraction of the constituents. Dong *et al.* [3, 4, 8] investigated the optimal design of carbon and glass fibre-reinforced hybrid composites under

[1] This Chapter has been published in Composite Structures, Vol 138, 2016, Pages 264-275

bending load and concluded that the fibre volume fraction of the glass/epoxy laminas must be higher than that of the carbon/epoxy laminas in order to achieve a positive hybrid effect on flexural strength. They also determined the critical level of hybridization (the critical hybrid ratio) in which the hybrid effect is maximized.

The hybridization of carbon and glass fibre influences not only the flexural strength and stiffness but other properties such as cost and weight. Since the glass fibres are heavier and cheaper than carbon fibres, hybridization of a CFRP composite through the incorporation of glass fibres leads to a lower material cost but higher density. Minimization of weight and cost as two conflicting objectives is a continuing concern in the design process of hybrid composite structures. Several studies have attempted to define and solve the multi-objective optimization of hybrid composites with regards to minimum cost and/or weight [9-16].

An optimization problem involving more than one simultaneous objective function is referred to as multi-objective optimization with the solution for such a problem being achieved through the trade-off between objectives. A set of trade-off solutions that cannot be improved with respect to one objective without hurting another objective is known as a Pareto set and referred to as a Pareto optimal front when plotted in the design space [17]. The multi-objective optimizers aim to find the optimal solutions which form the ideal Pareto set with respect to all objectives. The majority of classical multi-objective optimization methods avoid the complexities of multiple objectives and simply transform the problem into a single objective using *a priori* methods and preference-based strategies [18]. However, choosing a reliable and accurate preference of the objectives requires higher-level information which may not be available during the initial stages of the design process [17]. Unlike *a priori* methods, *a posteriori* methods aim at generating the Pareto optimal sets regardless of the objective preferences. Thus, sets of trade-off solutions can be generated which allow additional evaluation and comparison by the designer in order to make a final decision. To this end, a multi-objective optimization evolutionary algorithm (MOEA), which is classified as an *a posteriori* method, can be utilized to produce a set of Pareto optimal sets in a single simulation and hence improve the solutions in a number of evolutions without

considering any preference of objectives. There are a number of MOEAs available, *e.g.*, strength Pareto evolutionary algorithm (SPEA-II) [19], Pareto archived evolutionary strategies (PAES) [20] and non-dominated sorting genetic algorithm (NSGA-II) [21], which have been applied in order to generate optimal Pareto sets. Amongst these, NSGA-II is the most popular due to its effectiveness and simplicity with this algorithm being based on non-domination and crowding distance sorting and generates populations through the use of genetic operators, thus leading to optimal solutions, in a number of iterations known as a generation. However, there is no guarantee that population members progress in all iterations. To overcome the convergence problem and make the overall procedure faster the NSGA-II process should be combined with one or more mathematical optimization methods having local convergence properties [17, 22].

Most of the research in the field of multi-objective optimization of composites has used preference-based classical methods to convert the multi-objective optimization problem into a single objective form [15, 16, 23-28]. For example, Hemmatian *et al*. [15, 16] applied a gravitational search algorithm and elitist ant system to solve the multi-objective optimization of carbon/glass fibre hybrid composites in order to achieve designs with minimum weight and cost. They considered first natural frequency as a constraint and simply used the weighted sum method (WSM) to construct Pareto-optimal fronts. In contrast to this, Walker *et al*. [26] used a sequential optimization procedure to minimize the weight and cost of symmetric carbon/glass/Kevlar hybrid laminated plates subject to a buckling load. Relatively little research has been conducted in this area using evolutionary methods such as Lakshmi and Rao [29] who used a new hybridized version of NSGA-II to minimize the weight and cost of laminated hybrid composite cylindrical shells with the hybrid algorithm being superior in performance. Visweswaraiah *et al*. [30] used both *a priori* and *a posteriori* methods to optimize a composite helicopter blade and demonstrated the trade-off designs given by their evolutionary non-dominated sorting hybrid algorithm (NSHA) which could not be achieved by *a priori* classical methods. Recently, Madeira *et al.* [31] used the Direct MultiSearch (DMS) method based on a derivative free solver for multi-objective optimization problems

to find the optimal design of viscoelastic laminated sandwich composite panels for maximum modal damping, minimum mass and material cost.

Traditionally, studies in the field of optimization of composites have assumed deterministic values for design variables and ignored uncertainties in material properties and geometry tolerances. However, practical engineering design optimization problems in the field of composite materials contain variations in design parameters due to reasons such as manufacturing tolerances, defects, voids, fibre misalignment and the presence of resin rich regions [32-35]. Such variations in manufacturing and material properties will generally degrade the performance of the optimal design. Thus, the mechanical properties of highly optimized composites designed with the assumption of deterministic parameters may be significantly lower in practice and fail to satisfy the required performance constraints. Robust design philosophy, which was introduced by Taguchi [36], aims to obtain optimal solutions that are insensitive to such material and manufacturing variations. Methods for the modelling of material uncertainties may be classified into probabilistic and non-probabilistic. For the case of probabilistic methods, a probability distribution for the uncertain parameters is assumed with the variation of the objective(s) being minimized and the mean value of the objective(s) being optimized. However, accurate estimates of probability distributions in the early stages of the design process may be difficult or sometimes impossible to achieve [37]. On the other hand, non-probabilistic methods do not require the estimation of any probability distributions but instead utilize information concerning the bounds of any uncertain parameters to ensure the suitability of optimum solutions when the uncertainties are taken into account [38]. Several studies have attempted to investigate the robust optimization of composites [39-45] such as Radebe *et al.* [39] who studied hybrid cross-ply cylinders subject to external pressure and considered uncertainties in the elastic constants of the materials. They determined the worst-case combination of material uncertainties to find the minimum buckling load. The elastic constants were considered as uncertain-but-bounded variables with the minimum cost designs being found. Recently, the current authors proposed a robustness index for the consideration of uncertainties in lamina thickness in

optimization problems [45]. However, the multi-objective optimization problem was converted to a single objective form by using the WSM whilst uncertainties in fibre angles were not included.

In the present study, a hybrid multi-optimization evolutionary algorithm was proposed by modifying and combining the NSGA-II process with a local search which uses the fractional factorial design method in order to improve the convergence rate. The original NSGA-II and modified algorithms were employed to find the robust Pareto optimal sets of carbon and glass fibre-reinforced epoxy hybrid composite plates under bending load and their performance was evaluated and compared. The conflicting objectives of the optimization were to minimize the weight and cost subject to the constraint that the flexural strength be greater than a specified value. The fibre volume fraction and thickness of the carbon and glass epoxy lamina were considered as the design variables with the thickness of the lamina and fibre angle being considered to be uncertain-but-bounded variables. Uncertainties were modelled using the worst-case analysis as a non-probabilistic method. The optimization problem was formulated and solved for several flexural strengths with the Pareto optimal sets being determined. Three example scenarios were considered to show the applicability of the solutions in *a posteriori* methods.

## 6.2. Model Development

In this study, a unidirectional carbon and glass fibre-reinforced epoxy laminate hybrid composite under three-point bending was investigated. Recent work by the current authors [1, 3, 4] has indicated that a positive hybrid effect for the flexural strength can be achieved by replacing a portion of the carbon fibres by glass fibres at the compressive side of the specimen. Therefore, the same stacking configuration was used in the present work as shown in Figure 6-1 with the properties of the fibres and matrix being presented in Table 6-1. The span-to-depth ratio, $L/h$, was relatively large so that the plate can be considered as a thin plate. Roller supports were used at both ends with a load, $F$, being applied at the mid-span. The thicknesses of the carbon/epoxy, $h_c$, and glass/epoxy, $h_g$, sections, in

addition to the fibre orientations, were considered as uncertain variables that varied about their nominal value.

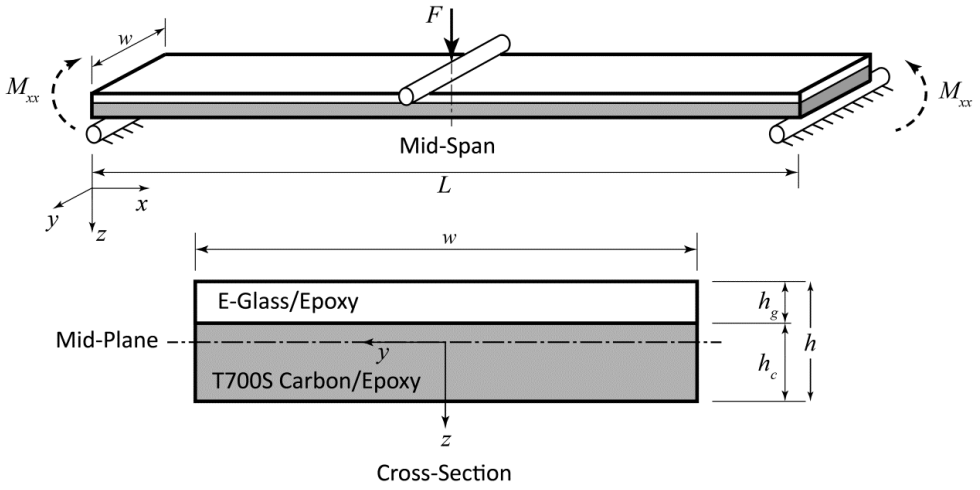


**Figure 6-1: Schematic representation of the hybrid composite specimen in the three-point bending configuration.**

**Table 6-1: Assumed properties of the fibres and matrix utilized in this work.**

| Material | Tensile Modulus (GPa) | Tensile Strength (MPa) | Strain to Failure | Density (kg/m$^3$) | Cost [46] ($/litre)* |
|---|---|---|---|---|---|
| Toray T700S 12K carbon fibre | 230 | 4900 | 0.021 | 1800 | 151.2 |
| E glass unidirectional fibre | 72 | 3450 | 0.048 | 2580 | 10.8 |
| Kinetix R240 high performance epoxy resin with H160 hardener at a ratio of 4:1 by weight | 3.10 | 69.60 | 0.022 | 1090 | 26.2 |

* All material prices were converted to US$.

For any given fibre volume fraction the Young's moduli and shear moduli of a lamina were derived using Hashin's model [47] based on the composite cylinder assemblage (CCA). In the CCA model, the basic element is a composite cylinder

comprising of an inner fibre cylinder and outer matrix shell. Using this approach, the effective moduli of composites are derived by variational principles.

### 6.2.1. Flexural Strength

For the plate subjected to pure bending the stress components across each lamina were calculated based on the classical lamination theory (CLT) [48]. It should be noted that the transverse and shear components of stress are not necessarily zero due to fibre misalignment. Thus, simple unidirectional compressive or tensile failure criteria could not be used to accurately estimate the failure load. Thus the Tsai-Wu failure criterion [49] was employed to consider the contribution of all stress components and their interaction during failure.

The Tsai-Wu failure theory predicts failure in an orthotropic lamina when the following equality is satisfied:

$$F_1\sigma_{11} + F_2\sigma_{22} + F_6\tau_{12} + F_{11}\sigma_{11}^2 + F_{22}\sigma_{22}^2 + F_{66}\tau_{12}^2 + 2F_{12}\sigma_{11}\sigma_{22} = 1 \qquad (6\text{-}1)$$

where $F_i$ and $F_{ij}$ are known as the strength coefficients and given by:

$$F_1 = \frac{1}{S_{Lt}} - \frac{1}{S_{Lc}}\ , F_2 = \frac{1}{S_{Tt}} - \frac{1}{S_{Tc}}\ , F_6 = 0, F_{11} = \frac{1}{S_{Lt}S_{Lc}}$$

$$F_{22} = \frac{1}{S_{Tt}S_{Tc}}\ , F_{66} = \frac{1}{S_{Lts}^2}\ ,\ F_{12} \approx -\frac{\sqrt{F_{11}F_{22}}}{2}$$

and $S_{ij}$ are the strength components in the lamina.

In order to determine the flexural strength of the hybrid composite specimen based on Tsai-Wu theory, the stress components in each lamina due to the bending moment were calculated using CLT with the maximum value of stress components at the mid-span (where the moment equals its maximum value) being found.

Following this, the load was gradually increased until such a point that the failure criteria (Equation 1) was satisfied for either the carbon/epoxy or glass/epoxy lamina with this maximum allowable load, $F_{max}$, being used to estimate the apparent flexural strength of the hybrid composite as follows:

$$\mathrm{S} = \frac{3\mathrm{F_{max}L}}{2\mathrm{wh}^2} \tag{6-2}$$

where *L* is the span and *w* and *h* are the width and total thickness of the plate, respectively.

### 6.2.2. Hybrid Effect

One important issue in dealing with hybrid composites is the *hybrid effect* which is defined as the fractional deviation of a behaviour of hybrid composites compared to that predicted from the RoM equation.

There are several possible ways to define the degree of hybridization in hybrid composite materials. However, whilst the strength and modulus of unidirectional fibre composites are proportional to the number of fibres, *i.e.*, the fibre volume fraction and thickness [3, 4], the hybrid ratio in the present study was defined to be the relative ratio of glass fibres to all fibres, *i.e.*

$$r_h = \frac{h_g V_{fg}}{h_g V_{fg} + h_c V_{fc}} \tag{6-3}$$

where $V_{fc}$ and $V_{fg}$ denote the fibre volume fraction of carbon/epoxy and glass/epoxy laminas, respectively. Thus, $r_h$ = 0 and $r_h$ = 1 correspond to fully carbon/epoxy and fully glass/epoxy composites, respectively. Based on the definition of the hybrid ratio, the flexural strength of hybrid composites predicted from RoM is simply given by:

$$S_{FRoM} = S_c(1 - r_h) + S_g r_h \quad (6\text{-}4)$$

where $S_c$ and $S_g$ are the flexural strength of the carbon and glass lamina, respectively.

Then, the hybrid effect is given by:

$$e_h = \frac{S}{S_{FRoM}} - 1 \quad (6\text{-}5)$$

where $S$ is the apparent flexural strength of the hybrid composite and can be calculated from Equation (2).

The hybrid effect can be either positive or negative which means that the property of the hybrid composite is higher (positive) or lower (negative) than that estimated from the RoM. Many researchers have noted the existence of a hybrid effect for the flexural strength of unidirectional carbon/glass fibre-reinforced hybrid composites [1-8]. In order to clearly illustrate the hybrid effect on the flexural strength, a hybrid composite has been analysed in three different cases and the variation of both the actual flexural strength based on CLT and Tsai-Wu failure theory (Equation (1) and (2)) and the flexural strength based on the RoM (Equation (4)) have been presented in Figure 6-2. In case 1 the fibre volume fractions of the pure carbon/epoxy and glass/epoxy composites were chosen to be 30% and 56.63%, respectively, so that they possessed an identical flexural strength. In case 2 a low fibre volume fraction carbon/epoxy (30%) and a high fibre volume fraction glass/epoxy (70%) were selected and in case 3 the fibre volume fractions of both laminas were 30%. According to the present analysis, combining these types of laminate into a hybrid composite produced a significant variation in flexural strength as a function of the hybrid ratio as shown in Figure 6-2. The section of the curve in case 3 which is below the RoM line corresponds to a negative hybrid effect. In this work the term

"critical hybrid ratio" will be used to define the hybrid ratio corresponding to the peak of the curves.

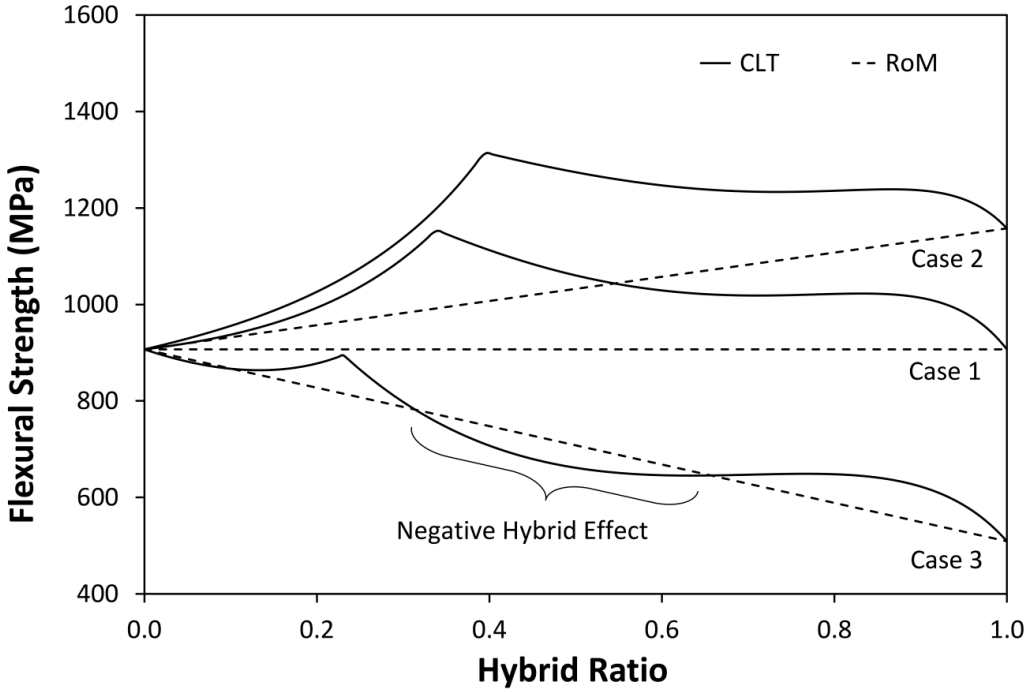


**Figure 6-2: Influence of hybrid ratio on the flexural strength for a hybrid carbon/glass fibre-reinforced epoxy matrix composite with $V_{fc}$ = 30%: Case 1 - $V_{fg}$ = 56.63%; Case 2 - $V_{fg}$ = 70%; Case 3 - $V_{fg}$ = 30%.**

### 6.2.3. Density

The weight of a composite may be characterized by the density which can be determined by RoM. Considering the definition of hybrid ratio in this study (Equation 3), the density for the current carbon/glass fibre-reinforced epoxy matrix composites can be derived as:

$$\rho_c = \rho_m + \frac{V_{fc}V_{fg}}{r_h V_{fc}+(1-r_h)V_{fg}}\left(\rho_{fc} - \rho_m\right) + \frac{r_h V_{fc}V_{fg}}{r_h V_{fc}+(1-r_h)V_{fg}}\left(\rho_{fg} - \rho_{fc}\right) \qquad (6\text{-}6)$$

It should be noted that the density of hybrid composites (using the current definition of hybrid ratio) is generally a nonlinear function of hybrid ratio.

### 6.2.4. Cost

The cost of composites is known to be influenced by a combination of design and manufacturing parameters. From the point of view of design parameters, the material cost is a key cost driver which is under the control of the designer. In this study the material cost was thus used as a composite cost index.

The material cost of a hybrid composite is the summation of its constituent costs and thus the material cost per unit volume for a hybrid composite would be a function of hybrid ratio and thickness as follows:

$$C_{mat} = \frac{C_c(1-r_h)V_{fg}V_{fc}+C_g r_h V_{fc}V_{fg}+C_m[r_h V_{fc}(1-V_{fg})+(1-r_h)V_{fg}(1-V_{fc})]}{r_h V_{fc}+(1-r_h)V_{fg}} \quad (6\text{-}7)$$

where $C_c$, $C_g$ and $C_m$ are the cost per volume of carbon fibre, glass fibre and epoxy, respectively, with typical costs for the constituent materials under investigation being shown in Table 6-1.

## 6.3. Multi-Objective Robust Optimization Problem Definition

Minimization of weight and cost whilst maintaining a minimum strength would be a principal aim for the design of many composite structures. When compared to carbon fibres, glass fibres have a relatively higher strain to failure but are cheaper. Thus, the strength, cost and price of hybrid composites can be improved by choosing an appropriate fibre volume fraction and hybrid ratio. Therefore, multiple objectives are present simultaneously and a multi-objective optimization problem needs to be formulated and solved. As mentioned earlier, the solutions of a multi-objective optimization problem, known as Pareto optimal sets, are achieved by a trade-off between the objectives.

On the other hand, robust optimization (RO) aims to obtain optimum solutions which are as good as possible whilst keeping the values of the objectives and/or constraints within an acceptable range when uncertainties exist. The optimal

solution of a multi-objective robust optimization is called the *robust Pareto optimal solutions* or *set* and when plotted in the objective space is known as a *robust Pareto optimal front*.

A typical multi-objective robust optimization (MORO) problem can be formulated as follows:

$$Minimize\ f_i(\boldsymbol{x}, \boldsymbol{u}) \qquad i = 1, \dots, M$$
$$Subject\ to\ contraints:$$

$$g_j(\boldsymbol{x}, \boldsymbol{u}) \leq 0 \qquad j = 1, \dots, N \tag{6-8}$$
$$\boldsymbol{x}_L \leq \boldsymbol{x} \leq \boldsymbol{x}_U$$
$$\boldsymbol{u}_0 - \Delta\boldsymbol{u} \leq \boldsymbol{u} \leq \boldsymbol{u}_0 + \Delta\boldsymbol{u}$$

where $f_i$ and $g_j$ are objective functions and constraints, respectively, $\boldsymbol{x}$ is the vector of design variables with upper and lower bounds being $\boldsymbol{x}_U$ and $\boldsymbol{x}_L$, respectively, $\boldsymbol{u}$ is the vector of uncertain variables and represented by a nominal value, $\boldsymbol{u}_0$, and half range of variation, $\Delta\boldsymbol{u}$.

The aim of MORO in this study was to find the solutions which satisfied two criteria:

(i) **Feasibility robustness**: For a given range of variation of uncertain parameters, the constraints remain feasible, *i.e.*, inequality constraints in Equation (8) ($g_j(\boldsymbol{x}, \boldsymbol{u}) \leq 0$) still hold.

(ii) **Optimality**: For the mean value of uncertain parameters, the objective functions form a Pareto optimal set.

With these requirements, the simple multi-objective optimization corresponding to Equation (8) can be transformed to a MORO as follows [38]:

$$
\left.
\begin{aligned}
&Minimize\ f_i(\boldsymbol{x}, \boldsymbol{u}_0) \qquad\qquad i = 1, \dots, M \\
&Subject\ to\ contraints: \\
&\eta_g \leq 0 \\
&where\ \eta_g = \max\left\{ \max_u\ g_j(\boldsymbol{x}, \boldsymbol{u}), j = 1, \dots, N \right\} \\
&\qquad \boldsymbol{x}_L \leq \boldsymbol{x} \leq \boldsymbol{x}_U \\
&\qquad \boldsymbol{u}_0 - \Delta\boldsymbol{u} \leq \boldsymbol{u} \leq \boldsymbol{u}_0 + \Delta\boldsymbol{u}
\end{aligned}
\right\} \quad (6\text{-}9)
$$

In the present work the objectives were minimization of the weight and cost with the only constraint being a specified minimum flexural strength. As mentioned earlier, the density of the hybrid composite, $\rho_c$, and the material cost, $C_{mat}$, were chosen as the weight and cost index, respectively, with the requirement for the flexural strength of the hybrid composite to be larger than a prescribed value, $S_0$. The constraint was treated as an objective with violation of the constraint being minimized and only feasible solutions being selected.

There are several manufacturing factors that may result in uncertainties in the material properties of composites. In the present study, the uncertain variables were considered to be the laminas thicknesses, $h_c$ and $h_g$, and fibre angles, $\theta_c$ and $\theta_g$. The ranges of variation for the thicknesses and fibre angles were assumed to be ±10% and ±3˚, respectively, which is typical to that obtained experimentally [32-35]. The nominal value of the total thickness, $h^{nom}$ , was considered to be fixed with the variation in total thickness of the hybrid composite being due to variations in the thickness of the carbon and glass laminas. The design variables were the lamina thickness and fibre volume fraction of the laminas. Noting that the nominal value of the thickness of carbon/epoxy lamina, $h_c^{nom}$, depends on the nominal value of the

thickness of glass/epoxy lamina, $h_g^{nom}$. Therefore, these two variables are not independent and only one of them is sufficient to be used as a design variable. Here the thickness of glass/epoxy lamina, $h_g^{nom}$, and the fibre volume fractions, $V_{fc}^{nom}$ and $V_{fg}^{nom}$ were chosen as the design variables.

Thus, the MORO can be rewritten as:

$$\left.\begin{array}{l} Minimize \begin{cases} \rho_c\left(h_g^{nom}, V_{fc}^{nom}, V_{fg}^{nom}\right) \\ C_{mat}\left(h_g^{nom}, V_{fc}^{nom}, V_{fg}^{nom}\right) \end{cases} \\ Subject\ to\ contraints: \\ \quad \eta_g \le 0 \\ where\ \ \eta_g = \max\left\{-S\left(h_g, V_{fc}, V_{fg}, \theta_c, \theta_g\right) + S_0\right\} \\ and \quad h_c^{nom} = h^{nom} - h_g^{nom} \end{array}\right\} \quad (6\text{-}10)$$

with the upper and lower bound of the variables being listed in Table 6-2.

**Table 6-2: The range of variables for the present robust optimization problem.**

| Variable | Lower Bound | Upper Bound |
|---|---|---|
| $h_g^{nom}$ | 0 | $h^{nom}$ |
| $V_{fc}^{nom}$ | 30% | 70% |
| $V_{fg}^{nom}$ | 30% | 70% |
| $h_c$ | $h_c^{nom} - 0.1h_c^{nom}$ | $h_c^{nom} + 0.1h_c^{nom}$ |
| $h_g$ | $h_g^{nom} - 0.1h_g^{nom}$ | $h_g^{nom} + 0.1h_g^{nom}$ |
| $\theta_c$ | $-3^o$ | $+3^o$ |
| $\theta_g$ | $-3^o$ | $+3^o$ |

$S$, $\rho_c$ and $C_{mat}$ in Equation (10) are the flexural strength, density and material cost of the hybrid composite and given by Equations (2), (6) and (7), respectively.

The number of fibres was considered to be constant with any variation in lamina thickness being attributed to a variation in the amount of epoxy. Therefore, the variation of thicknesses, $h_c$ and $h_g$, affects the fibre volume fractions, $V_{fc}$ and $V_{fg}$. The flexural strength, which is influenced by the variation of laminate thicknesses, fibre angles and fibre volume fractions, was to be kept larger than $S_0$.

Since the uncertainties have little effect on the cost and weight of the composite, the robust design methodology could be simplified to the robustness of the constraint, *i.e.*, robustness of objectives (weight and cost) was not considered in the present study, although it could have been incorporated if required.

### 6.3.1. Optimization Method

An *a posteriori* method was used in this study to find the Pareto optimal solution of the MO and MORO problems, *i.e.* the objective preference was not considered in the early stages of the solution, instead, the set of trade-offs between the solution were obtained and then a preference based strategy used to determine the final single optimum solution. *A posteriori* methods can be classified into mathematical programing-based and evolutionary algorithms. The evolutionary algorithms produce the Pareto optimal set in a single run and thus are generally faster with NSGA-II being selected in the present case although some modifications were performed (discussed later) to improve its performance.

NSGA-II starts with an initial population and tries to improve the results in a number of generations based on non-domination and crowding distance sorting. A detailed description of NSGA-II can be found in other references [17, 22] with the schematic of the non-dominated solutions (Pareto optimal front) and the crowding distance being illustrated in Figure 6-3.

To improve the rate of convergence and make the overall procedure faster, NSGA-II (like other MOEAs) must be combined with other optimizers with local search capabilities [22]. Thus far, several studies have focused on combining NSGA-II with a local search algorithm to improve the convergence rate [50-52]. In the present

study, three modifications have been carried out to the NSGA-II in order to improve its performance.

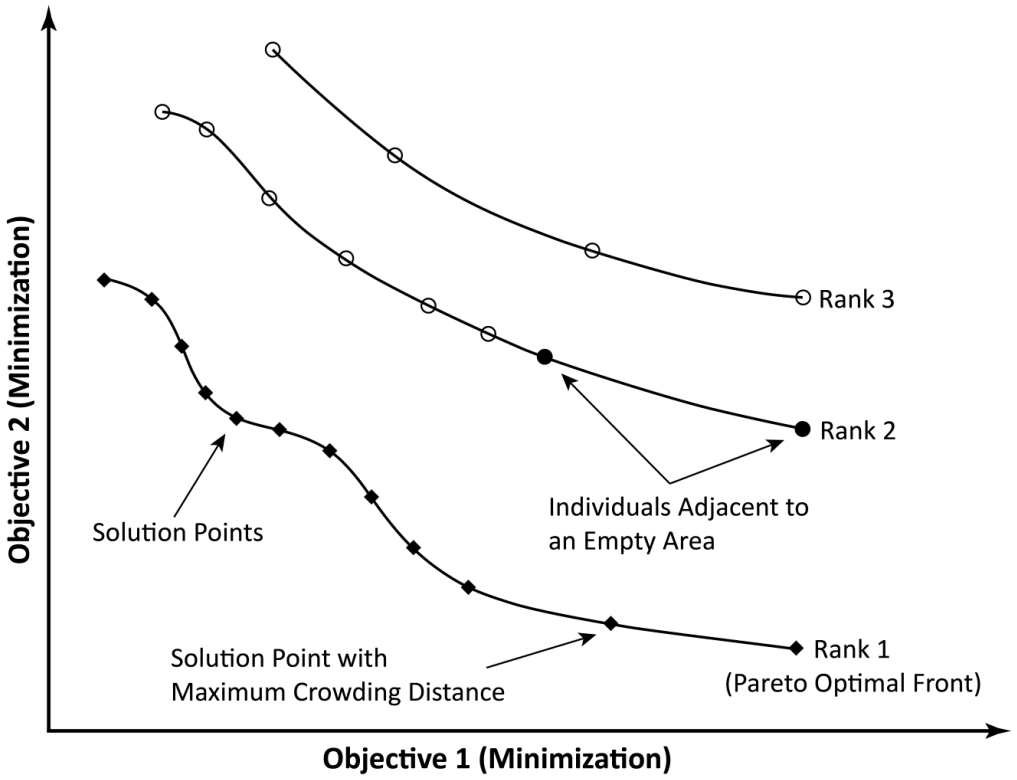


**Figure 6-3: The Pareto optimal front compared to other solution sets (ranks and crowding distance illustrated).**

1- Evaluate the upper and lower bounds

The optimal solution of many optimization problems is located on the boundary of the feasible domain and most of the time the boundary corresponds to the upper or lower limit of the design variables. However, NSGA-II does not evaluate the boundary points during the process unless GA operators can create offspring near or on the boundaries. Thus, sometimes it takes many generations to reach the boundary points. In order to overcome this difficulty, the algorithm was modified to explore the upper and lower bound of the variables by choosing some of the population members at random and generating four new

offspring such that the fibre volume fractions, $V_{fc}$ and $V_{fg}$, changed to their minimum and maximum values.

2- Hybridizing the NSGA-II algorithm with the fractional factorial design method

The concept of fractional factorial design [53] was used as a local search to explore the vicinity of the populations. For this purpose, a number of solution points were selected at random in each generation and six new offspring was generated for each point. Each offspring was generated by varying one of the variables. This process has been illustrated in Figure 6-4 by changing $V_i$ to $V_i + \delta V_i$ and $V_i - \delta V_i$. The new offspring together with the original solution point form a small population. The rank of each member in the small population was determined and the member with rank 1 was moved directly to the next generation. If there was more than one offspring with rank 1 then another new offspring would be generated by combining those offspring and using the new value of the variables ($V_i + \delta V_i$ or $V_i - \delta V_i$). Based on the factorial design method, the new offspring was expected to take the advantages of all parents and indicates the possible path of improvement; thus it was moved to the next generation with the hope of being one of the optimal solutions.

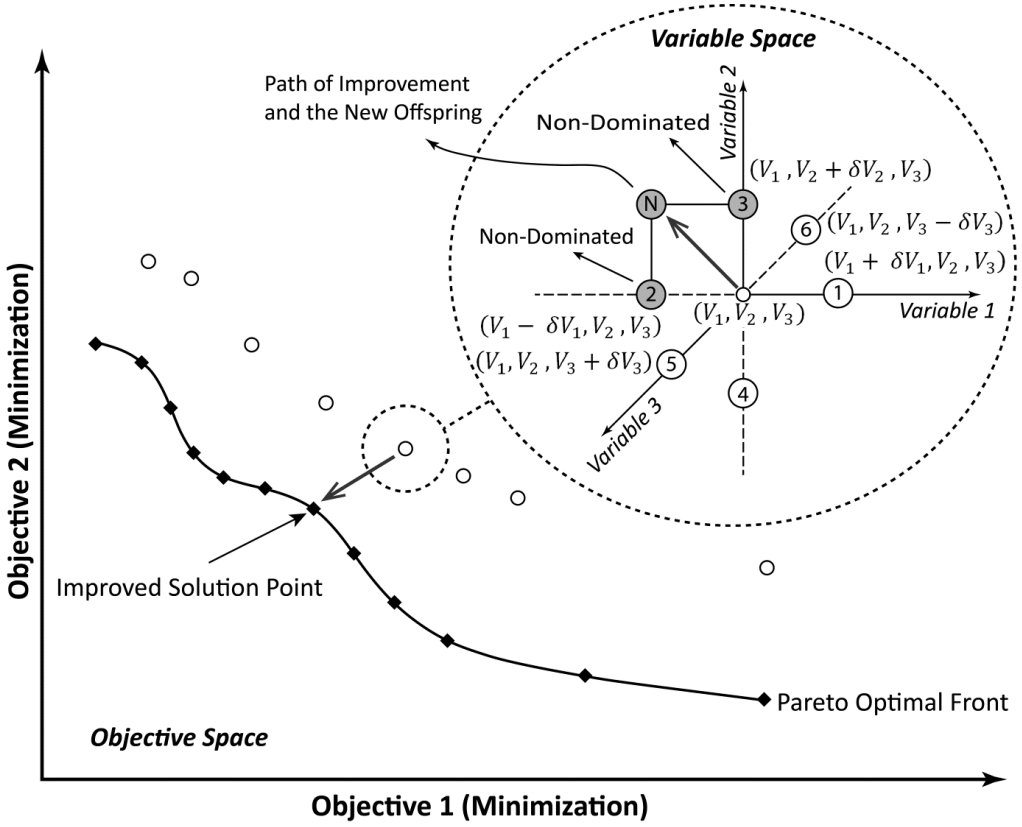


**Figure 6-4: The fractional factorial design method illustrating the path of improvement in generating new offspring.**

3- Choose parents adjacent to empty areas

In the original NSGA-II, the selection of parents to fill the mating pool for producing offspring is at random. Selecting the individual at random means in a number of generations that individuals near the empty areas (with the maximum crowding distance) might not be selected. Therefore, the algorithm is not able to explore these areas intensively and a good diversity in the solution points on the optimal front will not be efficiently achieved. Normally, the possibility of generating an offspring in an empty area is higher when parents are selected close to that area. Therefore, in the proposed modified hybrid algorithm, in addition to individuals which were chosen at random, the individuals adjacent to empty areas were found and selected as parents to create a separate mating pool with new offspring being generated. This operation improves the diversity of the solution points by forcing the algorithm to choose points adjacent to empty areas as the parents.

The main steps of the original NSGA-II and the proposed modified hybrid algorithm with three modifications have been shown in Figure 6-5. The modified hybrid algorithm was employed to find the robust Pareto optimal sets for the MORO problem defined by Equation (10).

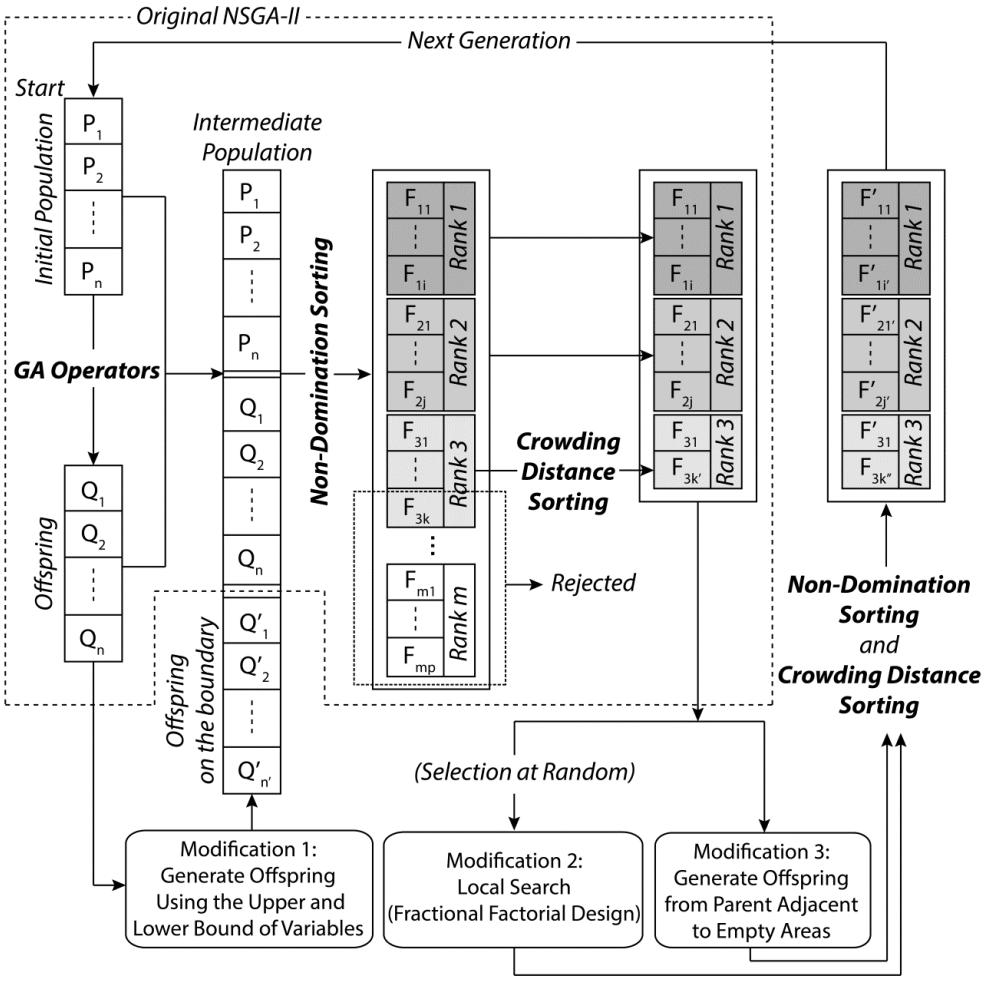


**Figure 6-5: Schematic of the original NSGA-II and the proposed modified hybrid algorithm.**

## 6.4. Results and Discussion

As mentioned above, the objectives of the present study were to minimize the weight and cost of a hybrid composite plate subject to the constraint that the flexural strength should be greater than a prescribed value, $S_0$, and considering the uncertainties in the thickness and fibre angle of both the carbon/epoxy and glass/epoxy laminas.

Firstly, the performance of the proposed modified hybrid algorithm was compared with that of the original NSGA-II. For this reason, both algorithms were employed to find the robust Pareto optimal sets of the same problem defined by Equation (10) with the material being T700S carbon and E glass fibre-reinforced epoxy with the minimum strength being 1000 MPa. The initial population and number of generations were chosen to be 50 and 200, respectively, for both algorithms and were gradually increased to converge to the solution points. In the modified hybrid algorithm, 20 solution points were selected in every other generation for fractional factorial design with the variation, $\delta V_i$, for local search being set to ±1% for fibre volume fraction and ±0.1 mm for thickness for the initial generations and decreased during the evolutionary process. Considering two levels of each variable and three design variables ($V_{fc}$, $V_{fg}$ and $h_g$), six offspring were generated corresponding to each individual as the fractional factorial design. The problem was solved by using both algorithms with the number of generations required so that the solutions did not improve significantly, *i.e.*, convergence was reached, being recorded.

Results indicated that the original NSGA-II required a minimum initial population of 1000 in order to converge during 1000 generations. In contrast to this, the proposed modified hybrid algorithm was able to converge to the optimal solution after 500 generations with an initial population of 50 and only required approximately 5% of the computational time compared to the NSGA-II case. Since the evolutionary algorithms are stochastic and use random data, there is no guarantee that the converged Pareto set is the Pareto optimal solution in each run. Thus, both algorithms were executed 10 times with the same input parameter settings and the best Pareto set obtained amongst all of the executions was considered to be the Pareto optimal set with these robust Pareto optimal fronts being presented in Figure 6-6. It can be seen from this figure that the proposed modified hybrid algorithm has superior performance compared to the original NSGA-II, *i.e.*, not only it is significantly faster but the number of solutions, diversity and convergence of the solution points are better. Therefore, the modified hybrid algorithm was used for the remainder of this study.

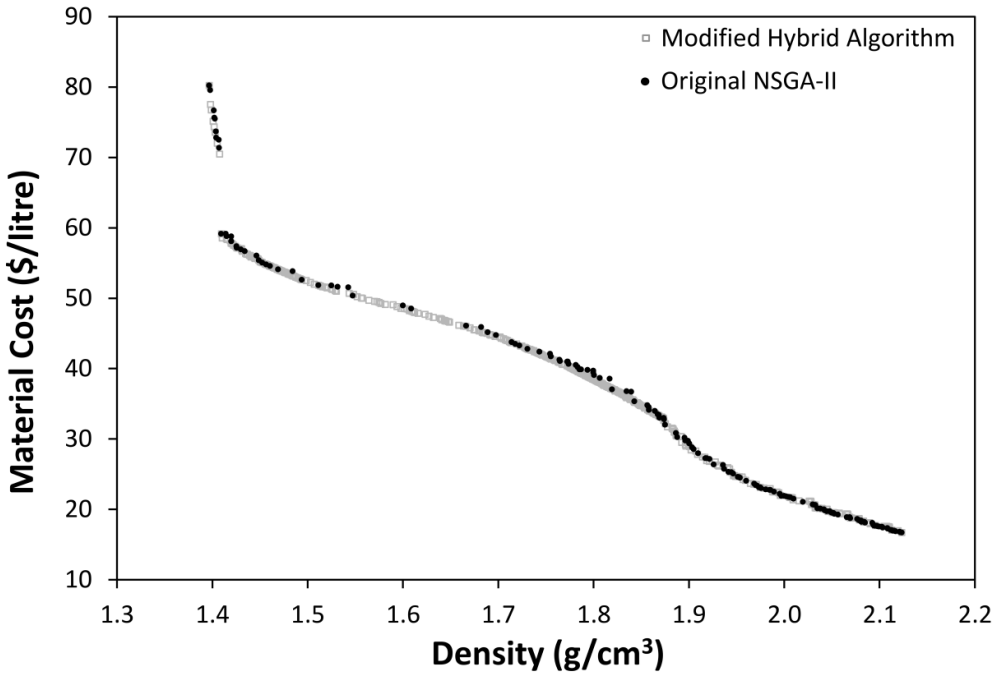


**Figure 6-6: Comparison between the Pareto optimal fronts obtained by the original version of NSGA-II and the modified hybrid algorithm for the MORO of T700S carbon/E glass fibre-reinforced epoxy composites ($S_0$=1000 MPa).**

In order to investigate the effect of uncertainties in lamina thickness and fibre angle on the objectives, the optimization problem was solved for three levels of minimum required strength, namely 700 MPa, 1000 MPa and 1300 MPa which represent low, medium and high strength hybrid composites. The Pareto fronts in each case have been presented in Figures 6-7 to 6-9 with the data corresponding to some of the solution points being listed in Tables 6-3 to 6-5. Note that for comparison the figures include Pareto fronts for the cases of: (i) no uncertainties in angle or thickness, (ii) uncertainty in angle or thickness and (iii) uncertainty in both angle and thickness. As might be expected the Pareto fronts with the assumption of no uncertainties in angle or thickness produced the highest performing designs whereas the introduction of one or more uncertainty tended to reduce the performance of the optimal designs, *i.e.*, the composites tended to be heavier and/or more expensive for the case of one or more uncertainties, particularly for the 1000 MPa and 1300 MPa cases.

For the low strength composites ($S_0$=700 MPa) the Pareto optimal front is linear between point 1 and point 2 and also between point 5 and 6 in Figure 6-7. These

sections of Pareto optimal front correspond to low weight and low cost composites. In both of these composites, the strength is an inactive constraint and its value is more than the required value, *i.e.*, 700MPa, so that the strength constraint does not affect the optimal solutions at these two sections and therefore the optimal solution points are insensitive to uncertainties. For the low weight composites, the only driving factor is the hybrid ratio and the fibre volume fractions equal their minimum value. In contrast to this, the low cost composites are pure glass/epoxy composites with the only driving factor being the glass fibre volume fraction. In both sections all of the data points are identical which means that the uncertainties have no effect on the objectives. This is in good agreement with a previous study [54] which concluded that material and manufacturing uncertainties have no practical importance for composites with very low load and strength requirements. In contrast to this, for high strength composites the strength is an active constraint and designs with either the minimum values of fibre volume fractions or the fully glass/epoxy composite fail to satisfy the strength constraint. In this situation the consideration of uncertainties becomes important as they decrease the strength. Thus, the fibre volume fraction and/or thickness of the laminas must be increased in order to achieve the minimum required strength - this has the undesired effect of also increasing the weight and/or cost of the composite.

From the selected data points in Table 6-3 to 6-5 it can be concluded that including uncertainties leads to higher material cost. For example, for data points 3 in Table 6-4 with the same density, the material cost equals $34.08 per litre when uncertainties are not considered and increases to $44.48 per litre when both uncertainties are considered. Likewise, for the high strength (1300 MPa) hybrid composites, the lightest composite achieved by robust optimization (considering uncertainties) from Table 6-5 has a cost of $107.20 per litre and density of 1.550 g/cm$^3$ compared to the cost and weight of the lightest non-robust design which is $87.08 per litre and 1.436 g/cm$^3$.

By comparing the Pareto optimal fronts for composites with different strengths (Figure 6-7 to 6-9) it can be observed that as the strength constraint increases from 700 MPa to 1300 MPa the difference between the curves increases. That is, high

strength composites are more sensitive to uncertainties when compared to low strength composites. Also, low strength composites are more sensitive to thickness variation (compared to fibre angle variation) whereas medium and high strength composites do not follow a general rule for their sensitivity to fibre angle and lamina thickness.

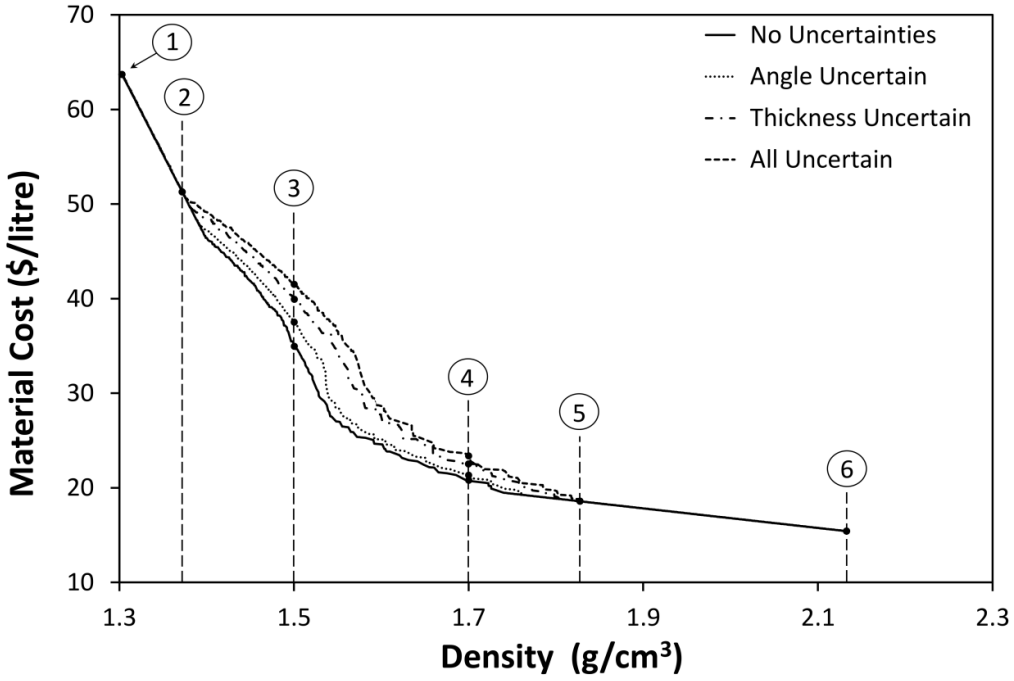


**Figure 6-7: The effect of uncertainties on the Pareto optimal fronts for low strength T700S carbon/E glass fibre-reinforced epoxy composites ($S_0$=700 MPa).**

The hybrid ratio of optimal designs for low and medium strength composites (Table 6-3 and 6-4) has a wide range from 0 to 1 including the critical hybrid ratio (*i.e.*, hybrid ratio corresponding to the peak of the strength curves in Figure 6-2) which is approximately 0.3 in most configurations. This feature was attributed to the fact that when the required strength is not too high the feasible domain is relatively large and the solutions can be obtained from numerous solutions with any hybrid ratio. In contrast to this, when uncertainties are included for high strength composites (Table 6-5) the hybrid ratios for all optimal designs are less than 0.280. That is, all optimal solutions have the hybrid ratio less than the critical hybrid ratio with this being attributed to the feasible domain being limited to the designs with the highest strength and least sensitivity. Therefore, the optimal designs converge

to relatively low carbon and high glass fibre volume fractions near the critical hybrid ratio. These results are in good agreement with previous studies by the current authors [6, 8].

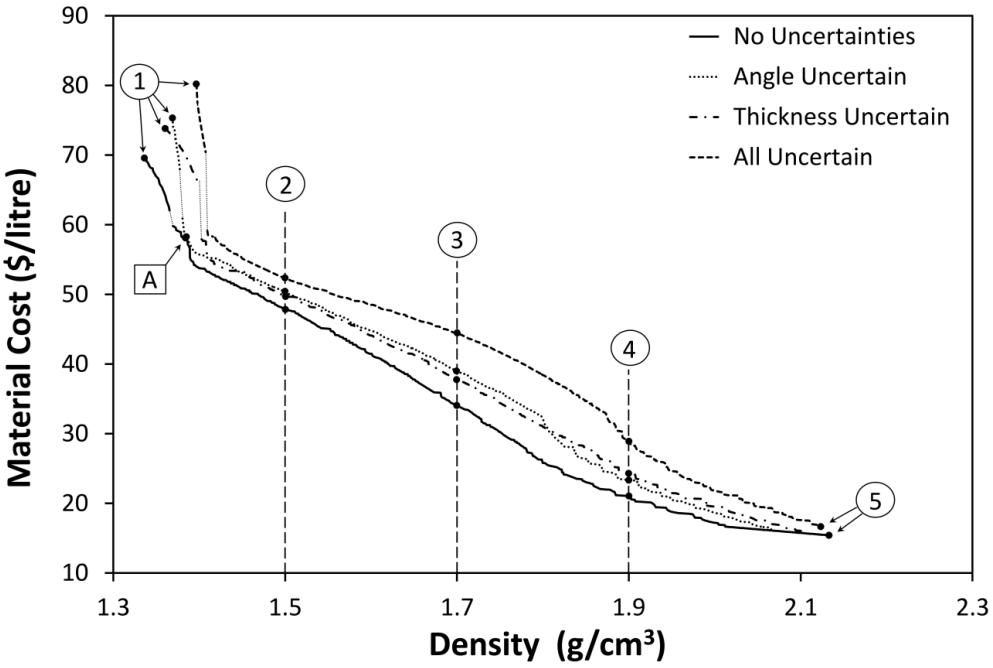


**Figure 6-8: The effect of uncertainties on the Pareto optimal fronts for medium strength T700S carbon/E glass fibre-reinforced epoxy composites ($S_0$=1000 MPa).**

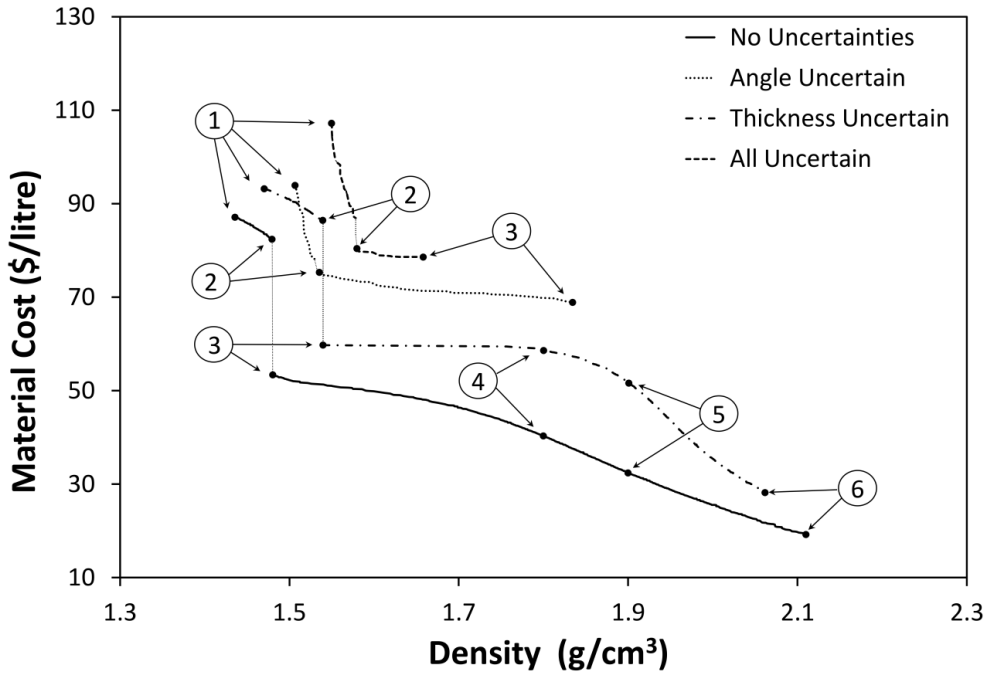


**Figure 6-9: The effect of uncertainties on the Pareto optimal fronts for high strength T700S carbon/E glass fibre-reinforced epoxy composites ($S_0$=1300 MPa).**

**Table 6-3: Selected data from Figure 6-7 for solution points on the Pareto optimal solution when $S_0$=700 MPa.**

| | Data Point | Design Variables | | | | | Objectives | | Constraint |
|---|---|---|---|---|---|---|---|---|---|
| | | $V_{fg}$ | $V_{fc}$ | $h_g$ (mm) | $h_c$ (mm) | Hybrid ratio | Density (g/cm$^3$) | Material Cost ($/litre) | Strength (MPa) |
| Uncertainties not Considered | 1 | - | 30.0% | 0.000 | 2.000 | 0.000 | 1.303 | 63.70 | 907 |
| | 2 | 30.0% | 30.0% | 0.590 | 1.410 | 0.295 | 1.372 | 51.27 | 804 |
| | 3 | 34.0% | 30.0% | 1.345 | 0.655 | 0.699 | 1.500 | 34.96 | 701 |
| | 4 | 40.6% | 60.0% | 1.979 | 0.021 | 0.985 | 1.700 | 20.80 | 700 |
| | 5 | 49.5% | - | 2.000 | 0.000 | 1.000 | 1.828 | 18.58 | 790 |
| | 6 | 70.0% | - | 2.000 | 0.000 | 1.000 | 2.133 | 15.42 | 1158 |
| Uncertainty in Thickness | 1 | - | 30.0% | 0.000 | 2.000 | 0.000 | 1.303 | 63.70 | 852 |
| | 2 | 30.0% | 30.0% | 0.590 | 1.410 | 0.295 | 1.372 | 51.27 | 742 |
| | 3 | 38.5% | 30.0% | 1.095 | 0.905 | 0.608 | 1.500 | 39.92 | 702 |
| | 4 | 42.0% | 37.0% | 1.890 | 0.110 | 0.951 | 1.700 | 22.63 | 707 |
| | 5 | 49.5% | - | 2.000 | 0.000 | 1.000 | 1.828 | 18.58 | 721 |
| | 6 | 70.0% | - | 2.000 | 0.000 | 1.000 | 2.133 | 15.42 | 1033 |
| Uncertainty in Fibre Angle | 1 | - | 30.0% | 0.000 | 2.000 | 0.000 | 1.303 | 63.70 | 854 |
| | 2 | 30.0% | 30.0% | 0.590 | 1.410 | 0.295 | 1.372 | 51.27 | 771 |
| | 3 | 36.1% | 30.0% | 1.217 | 0.783 | 0.651 | 1.500 | 37.51 | 702 |
| | 4 | 41.2% | 58.0% | 1.970 | 0.030 | 0.979 | 1.700 | 21.32 | 701 |
| | 5 | 49.5% | - | 2.000 | 0.000 | 1.000 | 1.828 | 18.58 | 762 |
| | 6 | 70.0% | - | 2.000 | 0.000 | 1.000 | 2.133 | 15.42 | 1066 |
| Uncertainty in Fibre Angle and Thickness | 1 | - | 30.0% | 0.000 | 2.000 | 0.000 | 1.303 | 63.70 | 809 |
| | 2 | 30.0% | 30.0% | 0.590 | 1.410 | 0.295 | 1.372 | 51.27 | 717 |
| | 3 | 40.4% | 30.0% | 1.015 | 0.985 | 0.581 | 1.500 | 41.51 | 703 |
| | 4 | 43.5% | 30.0% | 1.825 | 0.175 | 0.938 | 1.700 | 23.37 | 702 |
| | 5 | 49.5% | - | 2.000 | 0.000 | 1.000 | 1.828 | 18.58 | 700 |
| | 6 | 70.0% | - | 2.000 | 0.000 | 1.000 | 2.133 | 15.42 | 967 |

**Table 6-4: Selected data from Figure 6-8 for solution points on the Pareto optimal solution when $S_0$=1000 MPa.**

| | | Design Variables | | | | | Objectives | | Constraint |
|---|---|---|---|---|---|---|---|---|---|
| | Data Point | $V_{fg}$ | $V_{fc}$ | $h_g$ (mm) | $h_c$ (mm) | Hybrid Ratio | Density (g/cm$^3$) | Material Cost ($/litre) | Strength (MPa) |
| Uncertainties not Considered | 1 | - | 34.7% | 0.000 | 2.000 | 0.000 | 1.336 | 69.58 | 1002 |
| | 2 | 52.4% | 30.0% | 0.696 | 1.304 | 0.482 | 1.500 | 47.84 | 1003 |
| | 3 | 55.3% | 30.0% | 1.287 | 0.713 | 0.769 | 1.700 | 34.08 | 1000 |
| | 4 | 53.9% | 70.0% | 1.930 | 0.070 | 0.955 | 1.890 | 21.25 | 1000 |
| | 5 | 70.0% | - | 2.000 | 0.000 | 1.000 | 2.133 | 15.42 | 1158 |
| | A | 59.9% | 30.0% | 0.240 | 1.760 | 0.213 | 1.384 | 58.10 | 1000 |
| Uncertainty in Thickness | 1 | - | 38.1% | 0.000 | 2.000 | 0.000 | 1.361 | 73.83 | 1000 |
| | 2 | 58.3% | 30.0% | 0.603 | 1.398 | 0.456 | 1.501 | 49.70 | 1000 |
| | 3 | 62.7% | 30.0% | 1.100 | 0.900 | 0.719 | 1.700 | 37.76 | 1003 |
| | 4 | 57.2% | 54.3% | 1.820 | 0.180 | 0.914 | 1.900 | 24.30 | 1003 |
| | 5 | 70.0% | - | 2.000 | 0.000 | 1.000 | 2.133 | 15.42 | 1032 |
| Uncertainty in Fibre Angle | 1 | - | 39.3% | 0.000 | 2.000 | 0.000 | 1.369 | 75.33 | 1001 |
| | 2 | 61.1% | 30.0% | 0.565 | 1.435 | 0.445 | 1.500 | 50.45 | 1002 |
| | 3 | 65.6% | 30.0% | 1.038 | 0.963 | 0.702 | 1.700 | 39.01 | 1000 |
| | 4 | 56.6% | 56.4% | 1.852 | 0.148 | 0.926 | 1.900 | 23.34 | 1001 |
| | 5 | 70.0% | - | 2.000 | 0.000 | 1.000 | 2.133 | 15.42 | 1003 |
| | A | 62.2% | 30.0% | 0.230 | 1.770 | 0.212 | 1.385 | 58.29 | 1005 |
| Uncertainty in Fibre Angle and Thickness | 1 | - | 43.2% | 0.000 | 2.000 | 0.000 | 1.397 | 80.20 | 1001 |
| | 2 | 70.0% | 30.1% | 0.473 | 1.527 | 0.419 | 1.500 | 52.37 | 1001 |
| | 3 | 70.0% | 34.3% | 0.918 | 1.083 | 0.633 | 1.700 | 44.48 | 1001 |
| | 4 | 57.3% | 69.8% | 1.760 | 0.240 | 0.857 | 1.900 | 28.91 | 1003 |
| | 5 | 70.0% | 57.4% | 1.970 | 0.030 | 0.988 | 2.123 | 16.66 | 1001 |

One point of note is that of Point A in Figure 6-8 for the 1000 MPa curves which indicates the solutions for the cases of no uncertainties considered and just angle uncertainties considered to be very close to each other. The values of the variables corresponding to this point in both curves have been noted in Table 6-4. The reason for these two designs possessing the same density and cost is that the E glass fibres are cheaper than the epoxy matrix and thus increasing the fibre volume fraction of glass fibre simultaneously increases the strength and reduces the cost. Therefore, it would be possible to achieve a hybrid composite through the addition of glass fibres at Point A that possessed simultaneously higher strength and lower material cost.

The MORO problem and the multi-objective optimization problem without any uncertainty, *i.e.*, using nominal values and a deterministic approach, were also solved for different levels of minimum required flexural strength from 700 MPa to 1300 MPa with the results for the Pareto optimal fronts being presented in Figures 6-10 and 6-11. As was expected, it can be seen from these figures that the cost and density both increase with the strength. When the strength constraint equals 700 MPa, the fibre volume fractions of the optimal solutions were found to be 30% for both carbon and glass fibres at the first section of the curve. By increasing the flexural strength constraint the Pareto optimal fronts move away from the origin which means that the designs are heavier and/or more expensive. A sudden drop can be observed in the 1100 MPa, 1200 MPa, 1300 MPa curves as indicated by the broken lines. To highlight the importance of these broken lines, the values corresponding to the points exactly before and after the drops in the 1300 MPa curve have been presented in Table 6-5 (data points 2 and 3 in the case when uncertainties were not considered). For these data points the density equals 1.479 g/cm$^3$ and 1.480 g/cm$^3$ and the material cost equals \$82.39 per litre and \$53.38 per litre, respectively. That is, the density is almost the same for both designs but the material cost of data point 2 is more than 50% higher and thus it makes sense to choose data point 3 as the final optimal solution in this part of the curve.

**Table 6-5: Selected data from Figure 6-9 for the solution points on the Pareto optimal solution when $S_0$=1300 MPa**

| | Data Point | Design Variables | | | | | Objectives | | Constraint |
|---|---|---|---|---|---|---|---|---|---|
| | | $V_{fg}$ | $V_{fc}$ | $h_g$ (mm) | $h_c$ (mm) | Hybrid Ratio | Density (g/cm$^3$) | Material Cost ($/litre) | Strength (MPa) |
| **Uncertainties not Considered** | 1 | - | 48.7% | 0.000 | 2.000 | 0.000 | 1.436 | 87.08 | 1300 |
| | 2 | 70.0% | 48.6% | 0.128 | 1.873 | 0.089 | 1.479 | 82.39 | 1301 |
| | 3 | 70.0% | 30.0% | 0.428 | 1.573 | 0.388 | 1.480 | 53.38 | 1301 |
| | 4 | 70.0% | 37.7% | 1.141 | 0.859 | 0.712 | 1.800 | 40.28 | 1300 |
| | 5 | 70.0% | 36.9% | 1.404 | 0.596 | 0.817 | 1.900 | 32.38 | 1300 |
| | 6 | 70.0% | 66.9% | 1.920 | 0.080 | 0.962 | 2.110 | 19.20 | 1303 |
| **Uncertainty in Thickness** | 1 | - | 53.6% | 0.000 | 2.000 | 0.000 | 1.471 | 93.20 | 1301 |
| | 2 | 70.0% | 54.3% | 0.195 | 1.805 | 0.122 | 1.540 | 86.41 | 1304 |
| | 3 | 70.0% | 37.7% | 0.470 | 1.530 | 0.363 | 1.540 | 59.72 | 1300 |
| | 4 | 70.0% | 57.4% | 0.953 | 1.047 | 0.526 | 1.800 | 58.59 | 1301 |
| | 5 | 70.0% | 64.4% | 1.208 | 0.793 | 0.624 | 1.901 | 51.59 | 1300 |
| | 6 | 70.0% | 69.7% | 1.740 | 0.260 | 0.870 | 2.062 | 28.15 | 1300 |
| **Uncertainty in Fibre Angle** | 1 | 68.3% | 56.1% | 0.060 | 1.940 | 0.036 | 1.507 | 93.91 | 1300 |
| | 2 | 64.1% | 48.6% | 0.330 | 1.670 | 0.207 | 1.536 | 75.30 | 1302 |
| | 3 | 70.0% | 69.8% | 0.910 | 1.090 | 0.456 | 1.835 | 68.85 | 1300 |
| **Uncertainty in Fibre Angle and Thickness** | 1 | - | 64.8% | 0.000 | 2.000 | 0.000 | 1.550 | 107.20 | 1300 |
| | 2 | 70.0% | 53.6% | 0.330 | 1.670 | 0.205 | 1.580 | 80.37 | 1301 |
| | 3 | 70.0% | 58.3% | 0.490 | 1.510 | 0.280 | 1.658 | 78.58 | 1303 |

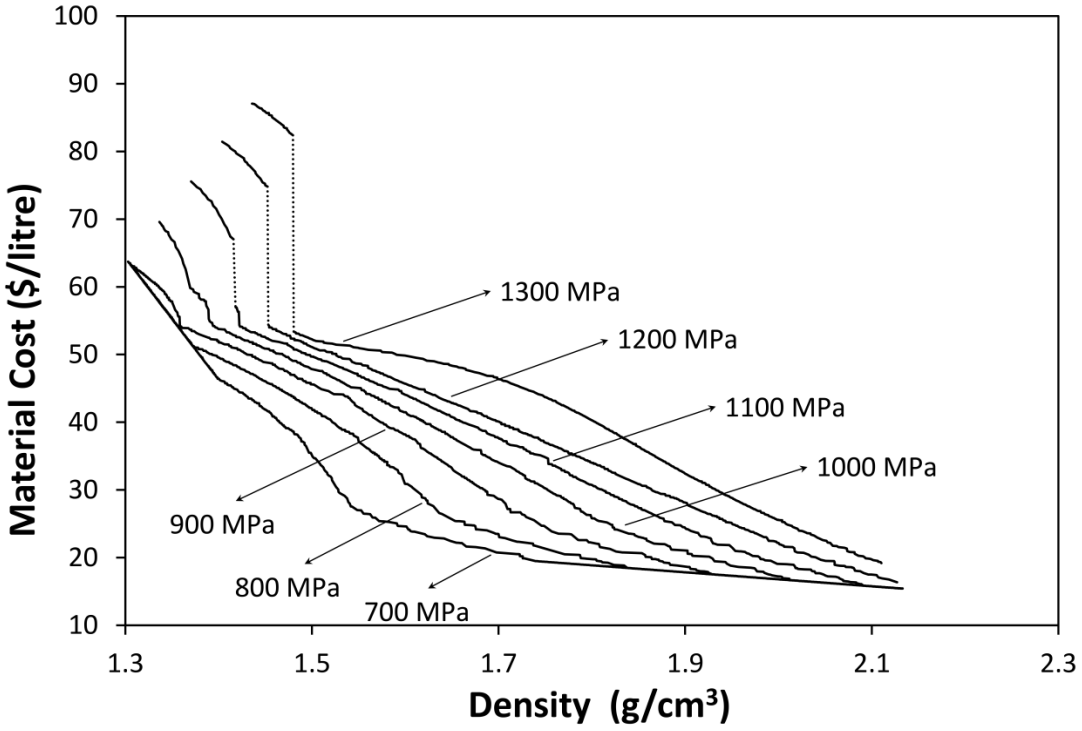


**Figure 6-10: Pareto optimal fronts for T700S carbon/E glass fibre-reinforced epoxy composites as a function of minimum strength requirement (uncertainties were not included).**

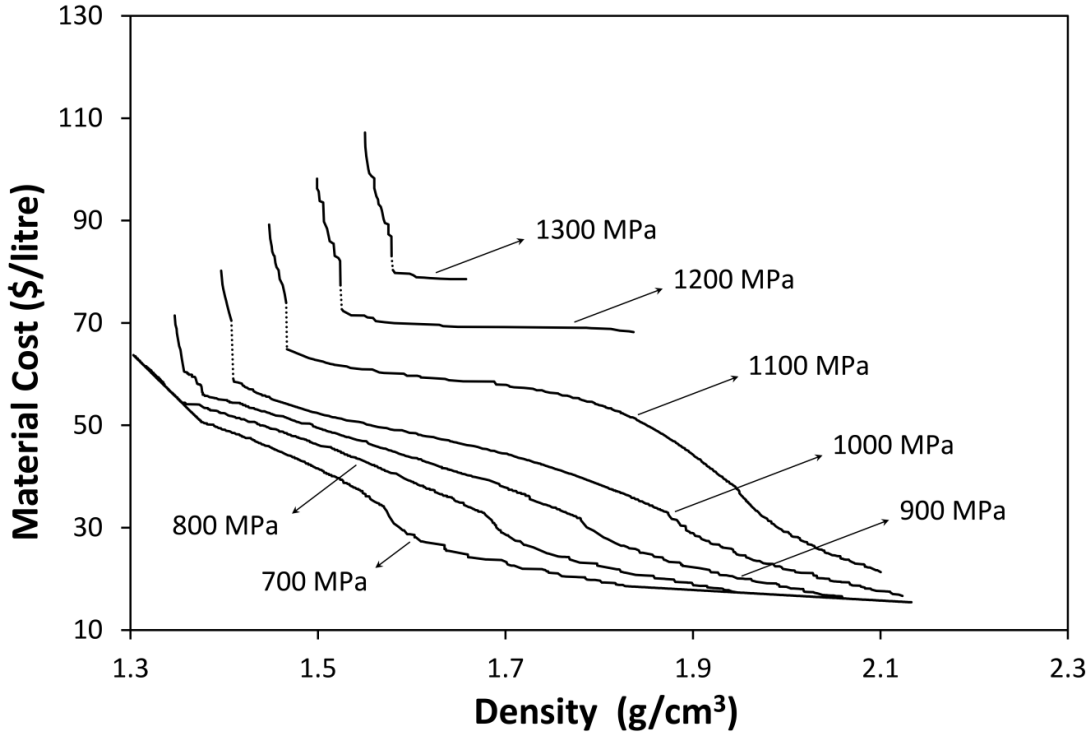


**Figure 6-11: Robust Pareto optimal front for T700S carbon/E glass fibre-reinforced epoxy composites as a function of minimum strength requirement (both uncertainties were included).**

By comparing Figure 6-10 and 6-11 it can also be noted that the length of the fronts is considerably shorter for strengths greater than 1100 MPa which indicates the number of optimal solution points to be more limited. This was attributed to the feasible domain being highly influenced by the strength constraint with the feasible domain being more limited and thus the obtained Pareto front being shorter as the strength increased. This effect became even more pronounced when both uncertainties were considered (Figure 6-11).

It is noteworthy that the fully glass/epoxy composite was not among the optimal solutions present in Table 6-4 and 6-5, *i.e.*, when the minimum required strength was 1000 MPa or 1300 MPa, which highlights the importance of hybridization when medium and high strength composites are required.

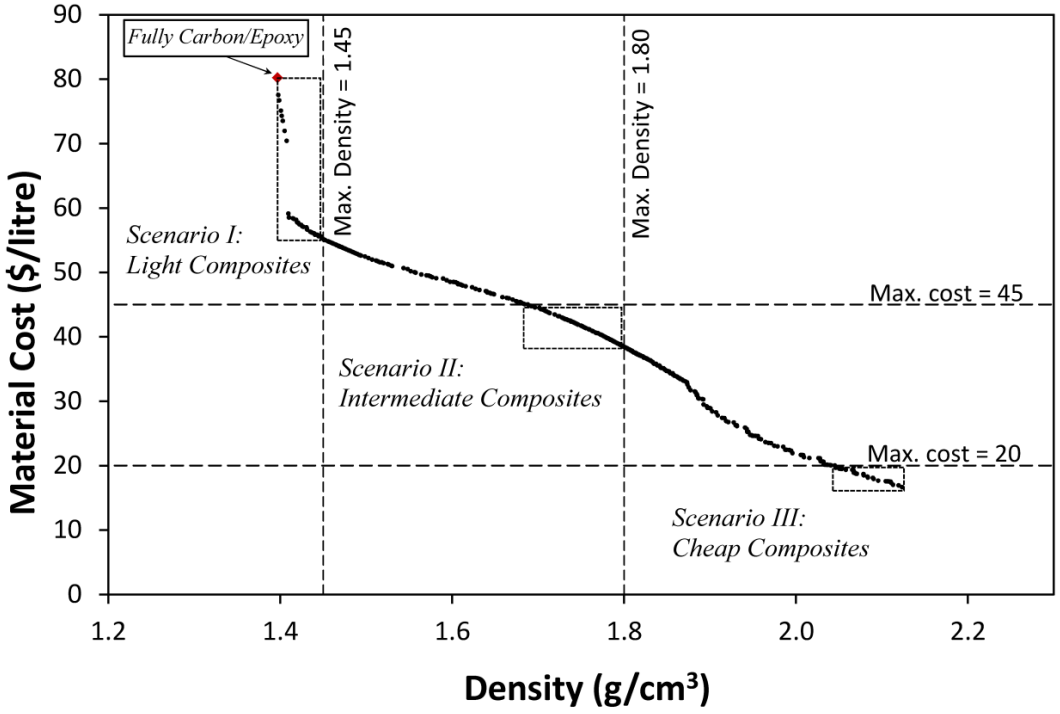


**Figure 6-12: The robust Pareto optimal front for the T700S carbon/E glass fibre-reinforced epoxy composites with $S_0$=1000 MPa and three scenarios (both uncertainties were included).**

The Pareto optimal sets found in this study can be used to determine a single preferred solution in the *a posteriori* approach. In such an *a posteriori* approach, which has been widely used in the field of optimization of composite materials [30,55,56], after the Pareto optimal sets have been found, preference information

(which can be based on non-technical and/or qualitative considerations) can be used to select the final optimal solution. To demonstrate the applicability of this approach, three different example scenarios have been considered for the hybrid composite with a flexural strength greater than 1000 MPa as follows:

I- *Light hybrid composites*: Optimal composites with a density less than 1.450 g/cm$^3$.

II- *Intermediate hybrid composites*: Optimal composites with a density less than 1.800 g/cm$^3$ and a material cost less than $45 per litre.

III- *Cheap hybrid composites*: Optimal composites with a material cost less than $20 per litre.

The robust Pareto optimal front together with the acceptable solution points according to each scenario have been indicated in Figure 6-12 with the corresponding data being listed in Table 6-6.

From these example scenarios it can be seen that, with a given preference for each scenario, the design options will be limited to a few solutions. The pros and cons of each solution point might be evaluated based on higher level information and the final design selected from among these limited solutions. For example, from Table 6-6 the density and material cost are respectively 1.396 g/cm$^3$ and $80.11 per litre for optimal solution 1 and 1.408 g/cm$^3$ and $70.44 per litre for optimal solution 2, *i.e.*, optimal solution 2 is less than 1% heavier but more than 12% cheaper. Thus, it can be considered the best optimal design among the light composites. However, for certain applications, *e.g.*, aerospace and automotive, the weight of the component is a primary concern and even a 1% increase in component weight may not be offset by the increase in cost. Therefore, in this type of case the optimal solution 1 would be the final optimal design. If further carbon fibres are replaced by glass fibres in scenario I, no significant change will be observed in the density but the cost will be reduced by 31%. For scenarios II and III the range of variation is very narrow and there is no significant difference between the designs. In these cases, other factors and properties rather than the density and cost (such as manufacturing limitations) could be considered. For scenarios I and II (light and

intermediate composites) the general conclusion is that the fibre volume fraction of the glass/epoxy lamina should be set to maximum in all cases whereas the fibre volume fraction of the carbon/epoxy lamina should be set to some value between 30% and 40%. However, in scenario III with a thin layer of carbon/epoxy at the tensile side, the fibre volume fraction of the glass/epoxy lamina can be slightly less than its maximum, *i.e.*, 70%, but the fibre volume fraction of the carbon/epoxy lamina must be higher (when compared to scenarios I and II) in order to achieve a strength of greater than 1000 MPa.

In order to compare the optimal results with simple non-hybrid laminates, the best fully carbon/epoxy composite has been indicated in Figure 6-12. As can be seen, there are many hybrid composites within scenario I which are slightly heavier, but significantly more economical, when compared to the fully carbon/epoxy composite.

**Table 6-6: Solution points for different scenarios as shown in Figure 6-12.**

| Scenario | No. | Design Variables | | | | Hybrid Ratio | Objectives | | Constraint |
|---|---|---|---|---|---|---|---|---|---|
| | | $V_{fg}$ | $V_{fc}$ | $h_g$ (mm) | $h_c$ (mm) | | Density (g/cm$^3$) | Material Cost ($/litre) | Strength (MPa) |
| I | 1 | - | 43.1% | 0.000 | 2.000 | 0.000 | 1.396 | 80.11 | 1000 |
| | 2 | 70.0% | 38.2% | 0.120 | 1.880 | 0.105 | 1.408 | 70.44 | 1001 |
| | 3 | 70.0% | 31.1% | 0.240 | 1.760 | 0.235 | 1.410 | 59.12 | 1001 |
| | 4 | 70.0% | 30.0% | 0.354 | 1.646 | 0.334 | 1.450 | 55.15 | 1000 |
| II | 1 | 70.0% | 34.0% | 0.890 | 1.110 | 0.623 | 1.688 | 44.99 | 1000 |
| | 2 | 70.0% | 35.0% | 1.050 | 0.950 | 0.689 | 1.756 | 41.32 | 1001 |
| | 3 | 70.0% | 35.2% | 1.160 | 0.840 | 0.733 | 1.800 | 38.43 | 1000 |
| III | 1 | 65.4% | 69.5% | 1.920 | 0.080 | 0.958 | 2.045 | 20.00 | 1001 |
| | 2 | 67.5% | 70.0% | 1.953 | 0.047 | 0.975 | 2.084 | 18.13 | 1000 |
| | 3 | 70.0% | 57.4% | 1.970 | 0.030 | 0.988 | 2.124 | 16.66 | 1001 |

## 6.5. Conclusions

The multi-objective robust optimization of T700S carbon/E glass fibre-reinforced epoxy hybrid composites with respect to minimum weight and cost and subject to a prescribed minimum flexural strength has been investigated through the aid of a newly modified hybrid evolutionary algorithm based on NSGA-II and enhanced through the incorporation of fractional factorial design based on a local search. Uncertainties in the fibre angle and thickness of the laminas have been considered and results for optimal solution points and the Pareto optimal front obtained using the NSGA-II and modified hybrid algorithm have been presented and compared. Results indicated that the modified algorithm is significantly more efficient when compared to NSGA-II.

A sensitivity analysis for two uncertain variables (fibre angle and lamina thickness) was performed and the effect of uncertainty in each variable on the objectives was investigated by using a non-probabilistic model based on worst-case analysis. Results for low strength, medium strength and high strength composites were presented and indicated that the low strength composites are more sensitive to variations in lamina thickness than to fibre angle.

The Pareto optimal fronts for the multi-objective problem with and without considering uncertainties have also been compared and it was indicated that uncertainties increase the weight and cost of the hybrid composites.

The Pareto optimal sets for different levels of minimum flexural strength have been presented and it was concluded that the fully carbon/epoxy or fully glass/epoxy composites are not necessarily the best solutions. This result emphasizes that the hybridization of CFRP composites through the partial substitution of carbon fibres by glass fibres (and *vice versa*) not only improves the flexural strength but can also optimize the weight and cost of the composite structure.

The robust Pareto optimal sets obtained in this study can assist designers in their decision making procedure. In practice, the optimal solutions can be used to evaluate the pros and cons of each design based on non-technical and qualitative considerations in order to make an informed choice. Three different example

scenarios were considered and the optimal solution points were investigated to illustrate the applicability of the results.

## 6.6. References


[1] Dong C, Ranaweera-Jayawardena HA, Davies IJ. Flexural properties of hybrid composites reinforced by S-2 glass and T700S carbon fibres. Composites Part B: Engineering 2012;43(2):573-581.

[2] Giancaspro JW, Papakonstantinou CG, Balaguru PN. Flexural response of inorganic hybrid composites with E-Glass and Carbon fibers. Journal of Engineering Materials and Technology 2010;132(2):0210051-02100518.

[3] Dong C, Davies IJ. Flexural and tensile moduli of unidirectional hybrid epoxy composites reinforced by S-2 glass and T700S carbon fibres. Materials & Design 2014;54:893-899.

[4] Dong C, Davies IJ. Flexural and tensile strengths of unidirectional hybrid epoxy composites reinforced by S-2 glass and T700S carbon fibres. Materials & Design 2014;54:955-966.

[5] Summerscales J, Short D. Carbon fibre and glass fibre hybrid reinforced plastics. Composites 1978;9(3):157-166.

[6] Dong C, Kalantari M, Davies IJ. Robustness for unidirectional carbon/glass fibre reinforced hybrid epoxy composites under flexural loading. Composite Structures 2015;128:354-362.

[7] Marom G, Fischer S, Tuler FR, Wagner HD. Hybrid effects in composites: conditions for positive or negative effects versus rule-of-mixtures behaviour. Journal of Materials Science 1978;13(7):1419-1426.

[8] Dong C, Davies IJ. Optimal design for the flexural behaviour of glass and carbon fibre reinforced polymer hybrid composites. Materials & Design 2012;37:450-457.

[9] Oh JH, Kim YG, Lee DG. Optimum bolted joints for hybrid composite materials. Composite Structures 1997;38(1-4):329-341.

[10] Adali S, Verijenko VE. Optimum stacking sequence design of symmetric hybrid laminates undergoing free vibrations. Composite Structures 2001;54(2-3):131-138.

[11] Le Riche R, Haftka RT. Optimization of laminate stacking sequence for buckling load maximization by genetic algorithm. AIAA journal 1993;31(5):951-956.

[12] Antonio CAC. A hierarchical genetic algorithm with age structure for multimodal optimal design of hybrid composites. Structural and Multidisciplinary Optimization 2006;31(4):280-294.

[13] Abachizadeh M, Tahani M. An ant colony optimization approach to multi-objective optimal design of symmetric hybrid laminates for maximum fundamental frequency and minimum cost. Structural and Multidisciplinary Optimization 2009;37(4):367-376.

[14] Rahul, Sandeep G, Chakraborty D, Dutta A. Multi-objective optimization of hybrid laminates subjected to transverse impact. Composite Structures 2006;73(3)360-369.

[15] Hemmatian H, Fereidoon A, Sadollah A, Bahreininejad A. Optimization of laminate stacking sequence for minimizing weight and cost using elitist ant system optimization. Advances in Engineering Software 2013;57:8-18.

[16] Hemmatian H, Fereidoon A, Assareh E. Optimization of hybrid laminated composites using the multi-objective gravitational search algorithm (MOGSA). Engineering Optimization 2014;46(9):1169-1182.

[17] Deb K. Multi-objective optimization using evolutionary algorithms: John Wiley & Sons, 2001.

[18] Sen P, Yang JB. Multiple criteria decision support in engineering design. Springer, London, 1998.

[19] Zitzler E, Laumanns M, Thiele L. SPEA2: Improving the strength Pareto evolutionary algorithm. Tech Rep 103, Computer Engineering and Networks

Laboratory (TIK). Swiss Federal Institute of Technology (ETH), Zurich, Switzerland, 2001.

[20] Knowles J, Corne D. The Pareto archived evolution strategy: a new baseline algorithm for multi-objective optimisation. In: Proceedings of the 1999 congress on evolutionary computation. IEEE Press, Piscataway, 2002;99-105.

[21] Deb K, Pratap A, Agarwal S, Meyarivan T. A fast and elitist multi-objective genetic algorithm: NSGA-II. IEEE Transactions on Evolutionary Computation 2002;6(2):182-197.

[22] Deb K. "Multi-objective optimisation using evolutionary algorithms: an introduction." In: Wang L, Amos HC. Ng, Deb K, editors. Multi-objective evolutionary optimisation for product design and manufacturing. London: Springer, 2011. p. 3-34.

[23] Adali S, Walker M, Verijenko VE. Multi-objective optimization of laminated plates for maximum pre buckling, buckling and post buckling strengths using continuous and discrete ply angles. Composite Structures 1996;35(1):117-130.

[24] Walker M, Smith R. A technique for the multiobjective optimization of laminated composite structures using genetic algorithms and finite element analysis. Composite Structures 2003;62(1):123-128.

[25] Walker M, Reiss T, Adali S. Multi-objective design of laminated cylindrical shells for maximum torsional and axial buckling loads. Computers & Structures 1997;62(2):237-242.

[26] Walker M, Reiss T, Adali S. A procedure to select the best material combinations and optimally design hybrid composite plates for minimum weight and cost. Engineering Optimization 1997;29(1-4):65-83.

[27] Almeida F.S, Awruch A.M. Design optimization of composite laminated structures using genetic algorithms and finite element analysis. Composite Structures 2009;88(3):443-454.

[28] Kaufmann M, Zenkert D, Wennhage P. Integrated cost/weight optimization of aircraft structures. Structural and Multidisciplinary Optimization 2010;41(2):325-334.

[29] Lakshmi K, Rama Mohan Rao A. Multi-objective optimal design of laminated composite skirt using hybrid NSGA. Meccanica 2013;48(6):1431-1450.

[30] Visweswaraiah S. B, Ghiasi H, Pasini D, Lessard L. Multi-objective optimization of a composite rotor blade cross-section. Composite Structures 2013;96:75-81.

[31] Madeira JFA, Araújo AL, Mota Soares CM, Mota Soares CA, Ferreira AJM. Multiobjective design of viscoelastic laminated composite sandwich panels. Composites Part B: Engineering 2015;77:391-401.

[32] Chamis CC. Probabilistic simulation of multi-scale composite behavior. Theoretical and Applied Fracture Mechanics 2004;41(1-3):51-61.

[33] Spurgeon WA. Thickness and reinforcement fiber content control in composites by vacuum-assisted resin transfer molding fabrication processes. DTIC Document: Army Research Lab Aberdeen Proving Ground MD, 2005.

[34] Shaw A, Sriramula S, Gosling PD, Chryssanthopoulos MK. A critical reliability evaluation of fibre reinforced composite materials based on probabilistic micro and macro-mechanical analysis. Composites Part B: Engineering 2010;41(6):446-453.

[35] Fertig R.S, Jensen E.M, Malusare K.A. Effect of fiber volume fraction variation across multiple length scales on composite stress variation: the possibility of stochastic multiscale analysis. 55th AIAA/ASMe/ASCE/AHS/SC Structures, Structural Dynamics, and Materials Conference: American Institute of Aeronautics and Astronautics. 2014.

[36] Taguchi G. Performance analysis design. International Journal of Production Research 1978;16(6):521-530.

[37] Beyer H-G, Sendhoff B. Robust optimization–a comprehensive survey. Computer methods in applied mechanics and engineering 2007;196(33-34):3190-3218.

[38] Cheng S, Zhou J, Li M. A new hybrid algorithm for multi-objective robust optimization with interval uncertainty. Journal of Mechanical Design 2015;137:021401-021401.

[39] Radebe IS, Adali S. Minimum cost design of hybrid cross-ply cylinders with uncertain material properties subject to external pressure. Ocean Engineering 2014;88:310-317.

[40] Walker M, Hamilton R. A methodology for optimally designing fibre-reinforced laminated structures with design variable tolerances for maximum buckling strength. Thin-Walled Structures 2005;43(1):161-174.

[41] Zhang X-M, Ding H. Design optimization for dynamic response of vibration mechanical system with uncertain parameters using convex model. Journal of Sound and Vibration 2008;318(1-2):406-415.

[42] Adali S, Lene F, Duvaut G, Chiaruttini V. Optimization of laminated composites subject to uncertain buckling loads. Composite Structures 2003;62(3-4):261-269.

[43] António CC, Hoffbauer LN. An approach for reliability-based robust design optimisation of angle-ply composites. Composite Structures 2009;90(1):53-59.

[44] Lee D, Morillo C, Oller S, Bugeda G, Oñate E. Robust design optimisation of advance hybrid (fiber-metal) composite structures. Composite Structures 2013;99:181-192.

[45] Kalantari M, Dong C, Davies IJ. Multi-objective analysis for optimal and robust design of unidirectional glass/carbon fibre reinforced hybrid epoxy composites under flexural loading. Composites Part B: Engineering 2016;84:130-139.

[46] Gurit. Guide to composites, www.gurit.com, Accessed: 7 April 2015.

[47] Chou T-W. Microstructural design of fiber composites: Cambridge University Press, 2005.

[48] Reddy JN. Mechanics of laminated composite plates and shells: Theory and analysis: CRC press, 2004.

[49] Tsai S.W, Wu E.M. A general theory of strength for anisotropic materials. Journal of composite materials. 1971;5:58-80.

[50] Bechikh S, Belgasmi N, Ben Said L, Ghédira K. PHC-NSGA-II: a novel multi-objective memetic algorithm for continuous optimization. In: Proceedings of 20th IEEE International Conference on Tools with Artificial Intelligence. 2008;1:180-189.

[51] Ghiasi H., Pasini D, Lessard L. A non-dominated sorting hybrid algorithm for multi-objective optimization of engineering problems. Engineering Optimization 2011;43(1):39-59.

[52] Hu X, Huang Z, Wang Z. Hybridization of the multi-objective evolutionary algorithms and the gradient-based algorithms. In: Proceedings of the IEEE Congress on Evolutionary Computation (CEC 2003), 8–12 December, Canberra, Australia. New York: IEEE Press. 2003:870–877.

[53] Montgomery D.C. Design and analysis of experiments. New York: John Wiley & Sons, 2008.

[54] Latalski J. Ply thickness tolerances in stacking sequence optimization of multilayered laminate plates. Journal of theoretical and applied mechanics 2013;51(4):1039-1052.

[55] Vučina D, Lozina Z, Vlak F. NPV-based decision support in multi-objective design using evolutionary algorithms. Engineering Applications of Artificial Intelligence 2010;23(1):48-60.

[56] Lanzi L, Giavotto V. Post-buckling optimization of composite stiffened panels: Computations and experiments. Composite Structures 2006;73(2):208-220.

# 7

# Multi-Objective Robust Optimization of Multi-Directional Carbon/Glass Fibre-Reinforced Hybrid Composites with Manufacture Related Uncertainties under Flexural Loading[1]

## 7.1. Introduction

Hybrid composite materials that comprise two or more fibre types have shown great potential as a substitute for traditional composites in many engineering applications requiring high strength, low weight and low cost. However, problems such as the complexity in the design process of optimal and reliable composites together with high manufacturing costs have thus far restricted their use. The complexity in the design of hybrid composite materials has been mainly attributed to the emergence of a so-called “hybrid effect” such that the standard Rule of Mixtures (RoM) is not applicable for many hybrid composite properties.

Whilst hybrid composite laminate materials can be designed for tailored mechanical properties, the optimal design of such materials requires proper selection of design variables such as fibre type, fibre orientation angle and fibre volume fraction of each lamina with an optimization problem being solved in order to find the best stacking configuration. The optimization of laminate stacking configurations has been of continuing concern within the design process of

[1] This Chapter has been published in Composite Structures, Vol 182, 2017, Pages 132-142

composite materials and structures with various objective functions and constraints being used such as stiffness [1], strength [2], cost [3] and weight [4]. A review of the optimal stacking configuration design for composite materials and optimization methods can be found elsewhere [5].

In real applications of composite structures, it is usual that more than one objective may be involved with all of these objectives being considered to be important and sometimes conflicting. Such an optimization problem which simultaneously deals with the minimizing or maximizing of two or more conflicting objectives is known as a multi-objective optimization problem. Unlike single objective optimization, the result of multi-objective optimization problem is not a unique solution but instead a set of trade-off solutions. Such a set of trade-off solutions that cannot be improved with respect to one objective without compromising another objective(s) is known as a Pareto optimal set or Pareto optimal solutions and referred to as a Pareto optimal front when plotted in the design space [6]. A Pareto optimal set is in fact a set of best possible solutions in terms of all objectives and can be evaluated by designers in order to make the final design choice based on other higher-level information and criteria.

Several methods have been proposed and applied for the solving of multi-objective optimization problems in the field of composite materials [5]. However, most of the research has used classical optimization methods and avoided the complexity of multi-objective optimization by transforming the problem into a single objective using preference-based classical methods [7-15]. For example, Adali *et al.* [9] used the weighted sum method (WSM) by defining weighting factors based on the priority of the objectives to obtain a design index and considering it as a single objective function for optimizing composite laminates subject to uniaxial loads. A similar method was used by Walker and Smith [10] to minimise the mass and deflection of fibre-reinforced structures. They used the weighted average of objectives as a design index for the objective function with a genetic algorithm (GA) being linked to finite element analysis to solve the problem. Hemmatian *et al*. [7, 8] used the WSM to construct Pareto optimal fronts for multi-objective optimization

of carbon/glass fibre hybrid composites with minimum weight and cost being chosen as objectives and first natural frequency as a constraint.

Preference-based classical methods require relatively accurate estimation of objective preferences at the beginning of the design process which is almost impossible to achieve in practice due to a lack of information concerning the optimal solutions. In contrast to this, multi-objective optimization evolutionary algorithms (MOEA) do not require the preference of the objectives at the early stage of design with Pareto optimal sets being achieved in a single run and through evolution of a random initial population in a number of iterations called generations. There are a number of MOEAs available, *e.g.*, strength Pareto evolutionary algorithm (SPEA-II) [16], Pareto archived evolutionary strategy (PAES) [17] and the non-dominated sorting GA (NSGA) [18]. A modified version of the NSGA, known as NSGA-II, is one of the most popular MOEAs due to its simplicity and efficiency [18]. The evolution in this algorithm is based on non-domination and crowding distance sorting with the genetic operators being used to generate new population members in each generation. Despite the popularity of MOEAs, little attention has been paid to MOEAs in the field of optimization of composite materials such the case of Lakshmi and Rao [19] who used a new hybridized version of NSGA-II to minimize the weight and cost of a laminated hybrid composite cylinder. Visweswaraiah *et al*. [20] proposed an evolutionary non-dominated sorting hybrid algorithm (NSHA) and employed it to optimize a composite helicopter blade whereas Vosoughi and Nikoo [21] combined the differential quadrature method (DQM) and NSGA-II to develop a hybrid method for the optimal design of laminated composite plates with the fundamental natural frequency and thermal buckling temperature being chosen as objective functions.

Objective functions and constraints in optimization problems are mathematical models that approximate the real world with the assumption of deterministic parameters. However, in real applications of composite materials the design variables are not always deterministic with uncertainties existing due to manufacturing tolerance and the presence of defects such as matrix voids and resin rich regions [22-25]. Therefore, idealised optimal designs in the traditional sense

may be extremely sensitive to any variation of design variables. In light of this, robust design optimization (RDO) aims to consider uncertainties and achieve designs which are less sensitive to these uncertainties and yet still optimum [26].

Modelling of uncertainties in design variables may be classified into probabilistic and non-probabilistic. Probabilistic methods are used when the probability distribution of uncertainties is known or else can be estimated with the goal being to minimize variation of objective function(s) whilst their nominal value is being optimized. However, this distribution may not be available or else difficult to achieve [27]. In contrast to this, non-probabilistic methods do not require the probability distribution but only utilize information concerning the bound of any uncertain variables [28]. In the non-probabilistic approach, the optimization problem can be solved based on the worst-case of the objective(s) and feasibility of the constraint(s).

In order to find the worst-case design for RDO based on non-probabilistic approach, the combination of upper and lower bounds of all variables should be evaluated. This process may be very time consuming especially when the number of uncertain variables and/or the range of their nominal values are large. In such a situation the anti-optimization method [29-35], which aims to efficiently determine the worst case design under specified uncertainties and the corresponding value of objective(s) and constraint function(s), can be used with these values being incorporated within the optimization problem to find optimal and robust designs (*i.e.,* the best of the worst). Liao and Chiou [30] combined optimization and anti-optimization sub-problems and proposed a method for finding robust optimal designs of fibre-reinforced composites subject to uncertainties in design variables by including uncertainties in the modified constraint. Likewise, Elishakoff *et al.* [35] used hybrid optimization and anti-optimization methods to solve the optimal design of composite cylindrical shells subject to uncertainties.

Although the robust optimization of simple composite materials has been addressed in a number of studies [36-41], little attention has been paid to hybrid composites such as Radebe *et al.* [36] who considered uncertainties in the elastic constants of the constituent laminas of hybrid cross-ply cylinders subject to

external pressure with worst-case analysis being used to find the minimum buckling load. It should be noted that RDO problems applied to hybrid composites may be more complex due to the presence of a hybrid effect for some properties.

The hybrid effect is defined as the deviation of a property from the standard RoM and it has been reported by many researchers to exist in the flexural properties of hybrid composites contain different reinforcements such as carbon/glass [42], carbon/basalt [43] and carbon/SiC [44]. Because the hybrid is not always positive [45], determining the optimal level of hybridization to achieve improved properties would be one of the greatest challenges in the design of hybrid composites. Dong and Davies [46] investigated the flexural properties of unidirectional carbon and glass fibre-reinforced epoxy hybrid composites under flexural load and determined the critical level of hybridization in which the hybrid effect was maximized. It was also found that the fibre volume fractions of the carbon/epoxy and glass/epoxy laminas played an important role in the hybrid effect with respect to flexural properties [47, 48].

In addition to the flexural stiffness and strength, other properties such as the weight and cost of hybrid composites may be affected by the level of hybridization. For instance, glass fibres are heavier and cheaper compared to carbon fibres, therefore, hybridization of a carbon fibre-reinforced polymer (CFRP) composite through the incorporation of glass fibres would lead to lower material cost but higher density and, should an appropriate amount of glass fibres be used, the flexural strength will also be improved. The minimization of weight and cost as two conflicting objectives subject to strength as a constraint is a major concern when designing composite structures [49-54]. Previous work by the present authors [55-57] proposed methods for the multi-objective robust optimization of unidirectional hybrid composites through the development of a new evolutionary hybrid algorithm and also by defining a robust index and converting the multi-objective optimization problem into a single optimization problem. However, these studies were restricted to unidirectional composites with very little being known about the multi-objective robust optimization of multi-directional hybrid composites.

In the present study, a hybrid multi-objective robust optimization evolutionary algorithm was proposed by combining the NSGA-II process for multi-objective optimization with a GA as an anti-optimizer in order to find the robust Pareto optimal sets of multi-directional carbon and glass fibre-reinforced epoxy hybrid composite plates subject to flexural loading. The conflicting objectives of the optimization were to minimize the weight and cost subject to the constraint that the flexural strength was greater than specified values of 500 MPa, 600 MPa, 700 MPa or 800 MPa in both the longitudinal and transverse directions. These values of flexural strength were chosen to represent a range from low strength to high strength multidirectional composites. The fibre type, fibre orientation angle and fibre volume fraction of the laminas were considered as the design variables with the thickness of the lamina and fibre orientation angle being considered to be uncertain-but-bounded variables. The optimization problem was formulated and solved for the required minimum flexural strengths with the Pareto optimal sets being determined.

## 7.2. Hybrid Composite Model

Fibre-reinforced epoxy hybrid laminates containing six laminas under three-point bending load (as shown in Figure 7-1) were investigated. High strength T700S carbon and S-2 glass fibres were chosen for the laminas in order to ensure the possibility of achieving a positive hybrid effect as shown previously [42]. The properties of the fibres and matrix used in this study have been listed in Table 7-1.

### 7.2.1. Flexural strength

The mechanical properties of the laminas (*e.g.*, modulus of elasticity) were calculated using Hashin's model from the constituent properties and fibre volume fraction with the strength of the laminas being determined based on the strain-to-failure and Lo-Chim model for micro-buckling. The classical lamination theory (CLT) was employed to determine the stress distribution in each lamina when a bending moment of unity in one direction (along the *x* axis or *y* axis) was applied. The span-

to-thickness ratio of the specimen was considered to be large enough to neglect the effect of inter-laminar shear and contact stresses.

**Table 7-1: Mechanical properties and cost of the fibres and matrix utilized in this study.**

| Material | High strength carbon fibre [a] | High strength glass fibre [b] | High performance epoxy matrix [c] |
|---|---|---|---|
| Tensile Modulus (GPa) | *Long.* 230<br>*Trans.* 14 | 86.9 | 3.1 |
| Poisson's Ratio | *Long.* 0.2<br>*Trans.* 0.4 | 0.2 | 0.3 |
| Tensile Strength (MPa) | 4900 | 4890 | 69.6 |
| Strain to Failure (%) | 2.1 | 5.6 | ~4 |
| Density (kg/m$^3$) | 1800 | 2460 | 1090 |
| Cost ($/litre)* | 151.2 | 103.3 | 26.2 |

* All material prices were converted to US$.

a T700S® 12K, Toray Industries, Inc., Tokyo, Japan

b S-2 glass unidirectional Unitex plain weave UT-S500 fibre mat, SP System, Newport, Isle of Wight, UK.

c Kinetix R240 high performance epoxy resin with H160 hardener at a ratio of 4:1 by weight, ATL Composites Pty Ltd., Australia.

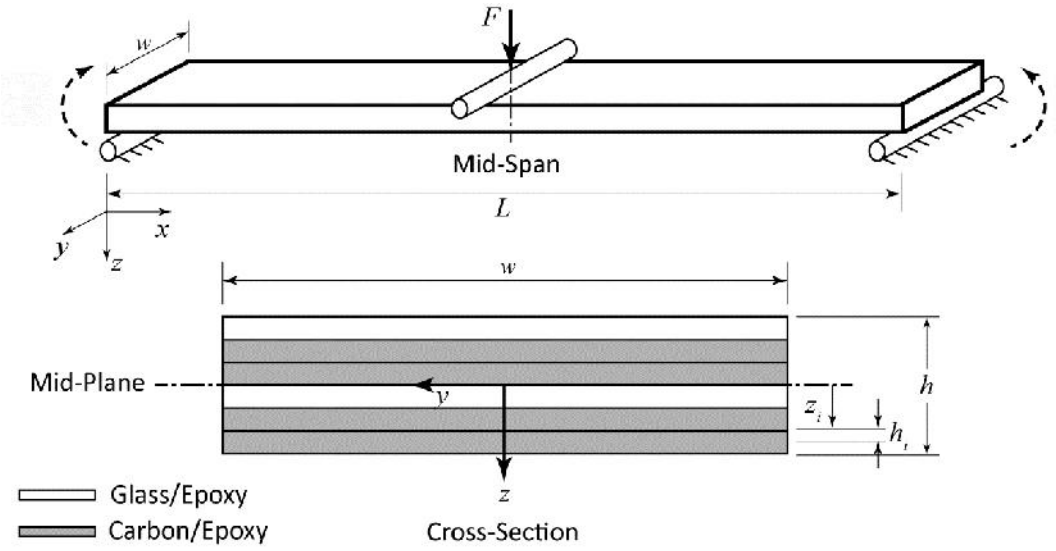


**Figure 7-1: Schematic representation of the carbon/glass fibre-reinforced hybrid composite specimen in the three-point bending configuration.**

The maximum allowable bending moment, $M_{max}$, and thus the maximum allowable force, $F_{max}$, in which first ply failure (FPF) occurred was determined based on the maximum strain failure theory [59]. The failure load, $F_{max}$, was then used to calculate the apparent flexural strength, $S_F$, of the composite as follows:

$$S_F = \frac{3F_m \ L}{2wh^2} \tag{7-1}$$

where $L$, $w$ and $h$ are the span, width and total thickness of the composite, respectively. Although the stress distribution is not linear through the thickness of the composite laminates, the apparent flexural strength defined by Equation (7-1) was chosen as a suitable normalized value of the maximum load at the point of failure for comparison purposes. The flexural strength in both the *x* and *y* directions was determined with the smaller value being considered as the flexural strength of the hybrid composite.

### 7.2.2. Density

In most applications of composite materials the weight is a limiting factor with one of the objectives of designing the composites being to minimize the total weight. The weight is directly proportional to the density and thus it can be characterised by the density. The density of a hybrid composite, $\rho_c$, can be derived based on RoM as follows:

$$\rho_c = \frac{1}{h}\sum_{i=1}^{n} h_i\left(V_f \,.\, \rho_f \ + (1 - V_f \,).\, \rho_m\right) \tag{7-2}$$

where $h_i$, $V_f$ and $\rho_f$ are the thickness, fibre volume fraction and fibre density of the *i*th lamina, respectively, and $\rho_m$ is the density of the matrix. *n* and *h* are the number of laminas and total thickness of the specimen, respectively. The density of the constituent materials under investigation has been presented in Table 7-1.

### 7.2.3. Cost

The material cost plays an important role in the application of composite materials. The final cost of a composite may be influenced by several parameters including design parameters and manufacturing parameters. Material cost is the most important controllable design parameter which directly influences the total cost of the component. As material cost can be decreased by using an optimal design (for example, by using cheaper constituents which still satisfy the design requirements), it is expected that the total cost will be reduced. In this study, the material cost was used as an indicator of the total composite cost.

The material cost can be determined by adding the cost of all constituents, *i.e.*, for carbon/glass fibre-reinforced epoxy hybrid composites the material cost is the summation of the total costs of the carbon fibre, glass fibre and epoxy. Therefore, the material cost for such hybrid composites would be a function of the fibre volume fraction and thickness of the laminas as well as the cost of the constituent materials, *i.e.*, carbon fibre, glass fibre and epoxy.

Thus, the material cost per unit volume of a carbon/glass hybrid composite, $C_c$, can be given by:

$$C_c = \frac{1}{h}\sum_{i=1}^{n} h_i\left(V_{fi}.C_{fi} + (1 - V_{fi}).C_m\right) \qquad (7\text{-}3)$$

where $C_{fi}$ and $C_m$ are the cost per volume of fibres in the *i*th lamina and epoxy, respectively, with typical costs for the constituent materials under investigation being shown in Table 7-1.

### 7.2.4. Robust Design Optimization

The strength, cost and weight of a hybrid composite can be improved by choosing appropriate fibre orientation angles, materials (fibre type), volume fractions and stacking configurations. The present study aimed to minimize the density and cost of carbon/glass fibre-reinforced epoxy hybrid composites whilst simultaneously

subject to the constraint of a minimum flexural strength. The design variables were the fibre type, fibre orientation angle and fibre volume fraction of each lamina. On the other hand, the aim of robust design optimization (RDO) is to find the optimal design for which the objectives and constraints are kept feasible in the presence of uncertainties. The fibre orientation and thickness of the laminas were considered to be uncertain-but-bounded variables with the variation of the fibre orientation angle and the thickness from their nominal value being within ±3° and ±10%, respectively, which is typical for manufacturing situations. The nominal values of the fibre orientation angles were chosen to be 0°, ±45° and 90° with the nominal value of the thickness being taken to be 0.2 mm for all laminas. The nominal values of the fibre volume fraction of the laminas were considered to be between 30% and 70% with an increment of 5%. During the manufacture of composite laminates, any variation in lamina thickness would be mostly due to the presence of excess resin or else a variation in the curing pressure, therefore the number of fibres and thus the nominal fibre volume fraction would normally be fixed with the actual fibre volume fraction of the laminas being affected by the thickness. Hence, in this study the actual value of the fibre volume fraction was defined as a function of the actual thickness and nominal fibre volume fraction. The upper and lower bounds of the variables have been listed in Table 7-2.

The multi-objective robust optimization problem was formulated in the following form:

$$\left.\begin{array}{l} Minimize \begin{cases} \rho_c\left(m_i, V_{fi}^{nom}, \theta_i^{nom}\right) \\ C_c\left(m_i, V_{fi}^{nom}, \theta_i^{nom}\right) \end{cases} \\ Subject\ to\ contraints: \\ \quad \eta_g \leq 0 \\ where\ \ \eta_g = \max\left\{-S\left(m_i, h_i^{act}, V_{fi}^{act}, \theta_i^{act}\right) + S_0\right\} \\ and \quad V_{fi}^{act} = V_{fi}^{nom} \frac{h_i^{nom}}{h_i^{act}} \end{array}\right\} \quad (7\text{-}4)$$

where $\rho_c$, $C_c$ and $S$ are the density, cost and actual flexural strength of the hybrid composite from Equations (7-2), (7-3) and (7-1), respectively. $S_0$ is the minimum required flexural strength as a constraint and $V_{fi}$, $\theta_i$and $m_i$ are the fibre volume fraction, fibre orientation angle and fibre type of the *i*th lamina, respectively. Superscripts *nom* and *act* indicate the nominal and actual values.

Whilst the total number of fibres were considered to be fixed in the laminas, the material cost and density would not be significantly affected by variation in lamina thickness (and obviously fibre orientation angle) and therefore objective robustness is not considered in Equation (7-4).

**Table 7-2: The range and nominal values of the variables used in this robust optimization problem.**

| Variable | Lower Bound | Upper Bound | Nominal Value Domain |
|---|---|---|---|
| $h_i$ | $h_i^{nom} - 0.1h_i^{nom}$ | $h_i^{nom} + 0.1h_i^{nom}$ | $h_i^{nom} = 0.2$ mm |
| $V_{fi}$ | $\frac{h_i^{nom}}{\max(h_i)} V_{fi}^{nom}$ | $\frac{h_i^{nom}}{\min(h_i)} V_{fi}^{nom}$ | $\{30\%, 35\%, \ldots, 65\%, 70\%\}$ |
| $\theta_i$ | $\theta_i^{nom} - 3^o$ | $\theta_i^{nom} + 3^o$ | $\{0°, 45°, -45°, 90°\}$ |

The variable $\eta_g$ in Equation (7-4) is the maximum violation of the strength constraint and was defined to make sure that the optimal solution in the worst case would not violate the constraint when uncertainties were incorporated. The worst case of the strength for each set of nominal values of design variables is a combination of the nominal, upper and lower values of the uncertain variables for which the strength is its minimum value, *i.e.*, the worst. Since the composites comprised six laminas with two uncertain variables, *i.e.*, $\theta_i$ and $h_i$, and three possible values (nominal, lower and upper bound) there exists $3^{12}$ possible combinations for each set of nominal values. Evaluation of all combinations to find the worst case would be extremely time consuming as this evaluation would be required for each population member in the multi-objective optimizer, *i.e.*, NSGA II. Instead of evaluating all combinations, a GA was used as an internal anti-optimizer

to find the worst case of the strength for each optimal solution and a hybrid robust optimization algorithm was proposed by combining optimization and anti-optimization elements. A flowchart of the combined optimization and anti-optimization algorithm has been presented in Figure 7-2. It was found during initial testing that for anti-optimization, a GA with an initial population of 100 and 8 generations would be sufficient to find the worst case with the computational time being decreased by a factor of 600 when compared to evaluating all 531,441 cases.

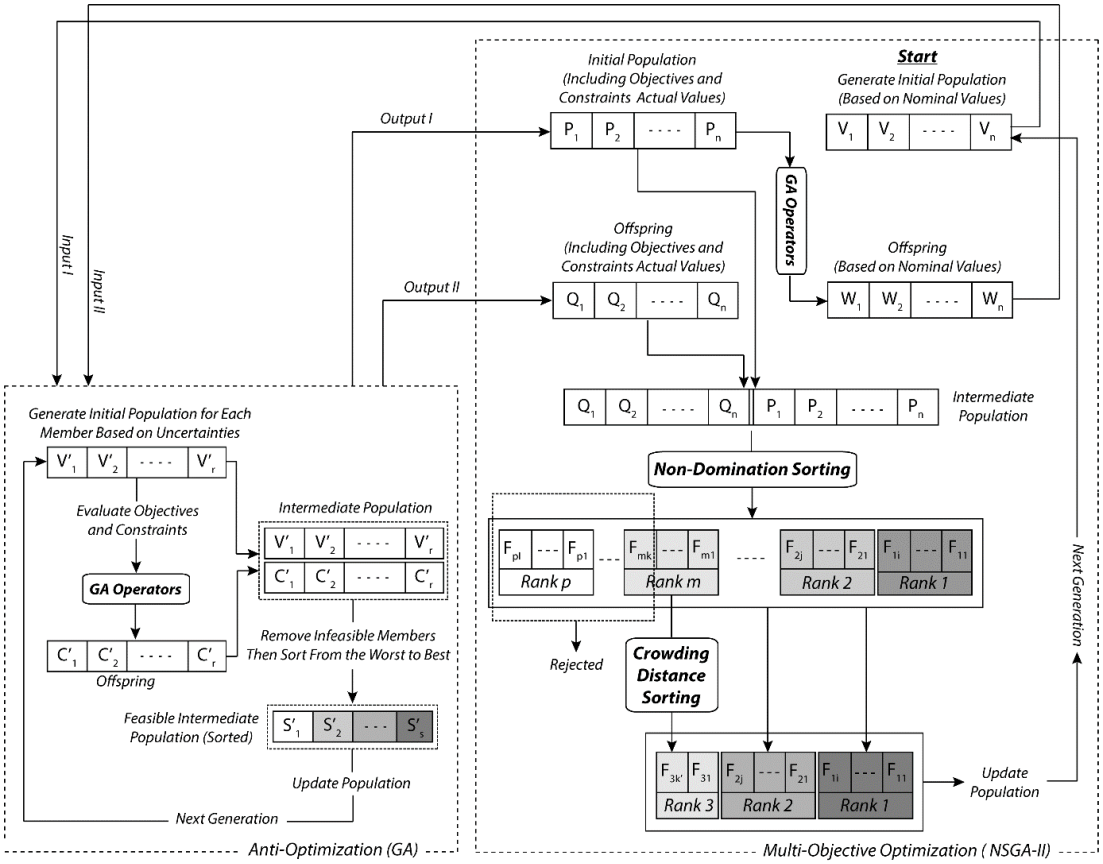


**Figure 7-2: Combined optimization and anti-optimization algorithm used for the multi-objective robust optimization.**

## 7.3. Results and Discussion

Through utilizing the proposed method outlined above, the multi-objective robust optimization problem was considered for hybrid composites with six laminas and four levels of minimum required bidirectional strength, $S_0$, namely 500 MPa, 600 MPa, 700 MPa and 800 MPa. In particular, four situations concerning uncertainties

in the variables were considered, namely, no uncertainties (NU), uncertainty in lamina thickness (UT), uncertainty in fibre orientation angle (UA) and uncertainties in both fibre orientation angle and lamina thickness (UAT), with the first case containing no uncertainties (NU) being solved using a deterministic approach. Pareto optimal fronts for each of the minimum required bidirectional strengths have been presented in Figures 7-3 to 7-6 whilst corresponding data has been presented in Tables 7-3 to 7-6, respectively.

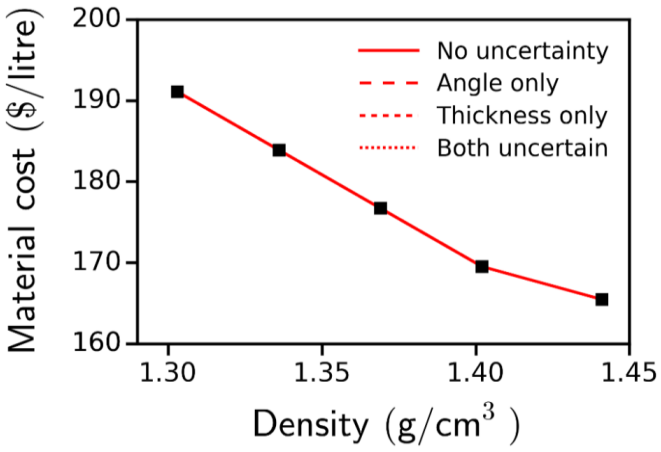


**Figure 7-3: The effect of uncertainties on the Pareto optimal fronts for multi-directional T700S carbon/S-2 glass fibre-reinforced epoxy composites ($S_0$ = 500 MPa).**

From comparison of Figures 7-4 to 7-6, which represent $S_0$ values of 600, 700 and 800 MPa, respectively, it can be noted that when uncertainties in lamina thickness and/or fibre orientation angles were incorporated, the Pareto optimal fronts shifted away from the origin which indicated that the performance of the composite had degraded, *i.e.*, the cost and/or density increased for the same value of required strength. However, this situation was not valid for the lowest strength composites of $S_0$ = 500 MPa as shown in Figure 7-3 in which the Pareto optimal fronts were essentially identical irrespective of whether or not the uncertainties were taken into account. Such a phenomenon was attributed to the flexural strength at the minimum fibre volume fraction, *i.e.*, 30%, being higher than the required flexural strength for all cases.

**Table 7-3: Pareto optimal solutions for multi-directional T700S carbon/S-2 glass fibre-reinforced epoxy composites and minimum required strength of 500 MPa.**

| | ID | Stacking Configuration, $\theta^{\text{Vf \%}}_{\text{fibre type}}$ | Density (g/cm³) | Cost ($/litre) | $S_{Fxx}$ (MPa) | $S_{Fyy}$ (MPa) | FPF* |
|---|---|---|---|---|---|---|---|
| No Uncertainties | NU 1 | $0_c^{30\%}$ / $90_c^{30\%}$ / $+45_c^{30\%}$ / $0_c^{30\%}$ / $0_c^{30\%}$ / $90_c^{30\%}$ | 1.303 | 63.70 | 510 | 574 | 1-X |
| | NU 2 | $0_c^{30\%}$ / $90_g^{30\%}$ / $+45_c^{30\%}$ / $-45_c^{30\%}$ / $0_c^{30\%}$ / $90_c^{30\%}$ | 1.336 | 61.30 | 521 | 519 | 2-Y |
| | NU 3 | $0_c^{30\%}$ / $90_c^{30\%}$ / $+45_g^{30\%}$ / $+45_g^{30\%}$ / $0_c^{30\%}$ / $90_c^{30\%}$ | 1.369 | 58.91 | 523 | 570 | 1-X |
| | NU 4 | $0_c^{30\%}$ / $0_g^{30\%}$ / $-45_g^{30\%}$ / $90_g^{30\%}$ / $0_c^{30\%}$ / $90_c^{30\%}$ | 1.402 | 56.51 | 574 | 584 | 1-X |
| | NU 5 | $0_g^{30\%}$ / $90_g^{30\%}$ / $-45_g^{30\%}$ / $0_g^{30\%}$ / $90_c^{35\%}$ / $0_c^{30\%}$ | 1.441 | 55.16 | 520 | 510 | 1-Y |
| Uncertainty in Thickness | UT 1 | $0_c^{30\%}$ / $-45_c^{30\%}$ / $0_c^{30\%}$ / $90_c^{30\%}$ / $0_c^{30\%}$ / $90_c^{30\%}$ | 1.303 | 63.70 | 507 | 553 | 1-X |
| | UT 2 | $0_c^{30\%}$ / $90_c^{30\%}$ / $0_c^{30\%}$ / $90_c^{30\%}$ / $0_c^{30\%}$ / $90_c^{30\%}$ | 1.303 | 63.70 | 502 | 530 | 1-X |
| | UT 3 | $0_c^{30\%}$ / $-45_c^{30\%}$ / $0_g^{30\%}$ / $90_c^{30\%}$ / $0_c^{30\%}$ / $90_c^{30\%}$ | 1.336 | 61.30 | 502 | 566 | 1-X |
| | UT 4 | $0_c^{30\%}$ / $90_c^{30\%}$ / $0_c^{30\%}$ / $-45_g^{30\%}$ / $0_c^{30\%}$ / $90_c^{30\%}$ | 1.336 | 61.30 | 502 | 531 | 1-X |
| | UT 5 | $0_c^{30\%}$ / $-45_g^{30\%}$ / $0_c^{30\%}$ / $90_g^{30\%}$ / $0_c^{30\%}$ / $90_c^{30\%}$ | 1.369 | 58.91 | 506 | 587 | 1-X |
| | UT 6 | $0_c^{30\%}$ / $-45_g^{30\%}$ / $0_g^{30\%}$ / $90_g^{30\%}$ / $0_c^{30\%}$ / $90_c^{30\%}$ | 1.402 | 56.51 | 501 | 594 | 1-X |
| Uncertainty in Angle | UA 1 | $0_c^{30\%}$ / $0_c^{30\%}$ / $+45_c^{30\%}$ / $90_c^{30\%}$ / $0_c^{30\%}$ / $90_c^{30\%}$ | 1.303 | 63.70 | 549 | 529 | 4-Y |
| | UA 2 | $0_c^{30\%}$ / $90_c^{30\%}$ / $0_c^{30\%}$ / $+45_c^{30\%}$ / $0_c^{30\%}$ / $90_c^{30\%}$ | 1.303 | 63.70 | 528 | 549 | 1-X |
| | UA 3 | $0_c^{30\%}$ / $0_c^{30\%}$ / $-45_g^{30\%}$ / $90_c^{30\%}$ / $0_c^{30\%}$ / $90_c^{30\%}$ | 1.336 | 61.30 | 548 | 521 | 4-Y |
| | UA 4 | $0_c^{30\%}$ / $0_c^{30\%}$ / $90_g^{30\%}$ / $90_c^{30\%}$ / $0_c^{30\%}$ / $90_c^{30\%}$ | 1.336 | 61.30 | 547 | 577 | 6-X |
| | UA 5 | $0_c^{30\%}$ / $90_g^{30\%}$ / $90_c^{30\%}$ / $0_c^{30\%}$ / $0_c^{30\%}$ / $90_c^{30\%}$ | 1.336 | 61.30 | 507 | 704 | 1-X |
| | UA 6 | $0_c^{30\%}$ / $0_g^{30\%}$ / $90_g^{30\%}$ / $90_c^{30\%}$ / $0_c^{30\%}$ / $90_c^{30\%}$ | 1.369 | 58.91 | 546 | 589 | 6-X |
| | UA 7 | $0_c^{30\%}$ / $0_g^{30\%}$ / $0_g^{30\%}$ / $90_g^{30\%}$ / $0_c^{30\%}$ / $90_c^{30\%}$ | 1.402 | 56.51 | 550 | 540 | 1-Y |
| | UA 8 | $0_c^{30\%}$ / $0_g^{30\%}$ / $-45_g^{30\%}$ / $90_g^{30\%}$ / $0_c^{30\%}$ / $90_c^{30\%}$ | 1.402 | 56.51 | 549 | 561 | 6-X |
| | UA 9 | $0_c^{30\%}$ / $0_g^{30\%}$ / $90_g^{30\%}$ / $90_g^{30\%}$ / $0_c^{30\%}$ / $90_c^{30\%}$ | 1.402 | 56.51 | 548 | 528 | 3-Y |
| | UA 10 | $0_c^{30\%}$ / $90_g^{30\%}$ / $90_g^{30\%}$ / $0_g^{30\%}$ / $0_c^{30\%}$ / $90_c^{30\%}$ | 1.402 | 56.51 | 515 | 562 | 1-X |
| Uncertainties in Angle and Thickness | UAT 1 | $0_c^{30\%}$ / $0_c^{30\%}$ / $+45_c^{30\%}$ / $90_c^{30\%}$ / $0_c^{30\%}$ / $90_c^{30\%}$ | 1.303 | 63.70 | 525 | 513 | 4-Y |
| | UAT 2 | $0_c^{30\%}$ / $0_c^{30\%}$ / $90_g^{30\%}$ / $90_c^{30\%}$ / $0_c^{30\%}$ / $90_c^{30\%}$ | 1.336 | 61.30 | 523 | 544 | 6-X |
| | UAT 3 | $0_c^{30\%}$ / $0_g^{30\%}$ / $90_g^{30\%}$ / $90_c^{30\%}$ / $0_c^{30\%}$ / $90_c^{30\%}$ | 1.369 | 58.91 | 522 | 555 | 6-X |
| | UAT 4 | $0_c^{30\%}$ / $0_g^{30\%}$ / $0_g^{30\%}$ / $90_g^{30\%}$ / $0_c^{30\%}$ / $90_c^{30\%}$ | 1.402 | 56.51 | 525 | 528 | 1-X |
| | UAT 5 | $0_c^{30\%}$ / $0_g^{30\%}$ / $-45_g^{30\%}$ / $90_g^{30\%}$ / $0_c^{30\%}$ / $90_c^{30\%}$ | 1.402 | 56.51 | 524 | 548 | 1-X |

* First ply failure (Ply No. - Failure Direction); X:[0] and Y:[90]

However, whilst the fibre volume fraction and Pareto optimal fronts were identical for the minimum required strength of 500 MPa in all cases (Figure 7-3), it was interesting to note that the fibre types and fibre orientation angles in Table 7-3 were found to depend on the type of uncertainties being considered – this highlights the importance of choosing a suitable stacking configuration for

laminated hybrid composites. For example, when uncertainties were not considered (NU) the fibre orientation angles of the first two laminas at the compressive side were found to be 0° and 90° whereas incorporation of the uncertainties led to the fibre orientation angle of these laminas both approaching 0° in order to maintain the required level of strength. Furthermore, in all cases of $S_0$ = 500 MPa except NU5, the outermost lamina at the compressive side and the two outermost laminas at the tensile side were all noted to be carbon/epoxy. The cost and density for these (low strength) hybrid composites could thus be adjusted by choosing carbon/epoxy or glass/epoxy of the same fibre volume fraction for the three remaining (internal) laminas.

In contrast to the lowest strength composites, the fibre volume fraction was noted to vary for the higher strength composites (Tables 7-4 to 7-6) depending on the uncertainties considered. For example, when uncertainties were considered, the fibre volume fraction within the outer one or two laminas at the compressive side generally increased whereas that of the remaining laminas stayed almost unchanged. For instance, in Table 7-4 for the hybrid composite with a minimum required strength of 600 MPa, when uncertainties were not considered (NU) the fibre volume fraction of the first lamina at the compressive side was 40% and increased to 45~50% when uncertainties were included whereas the fibre volume fraction of the other laminas remained unchanged in most configurations. These results are in good agreement with previous experimental and numerical studies [42, 48] which indicated that the mode of failure in unidirectional fibre-reinforced hybrid composites under flexural loading was compressive failure due to micro-buckling of fibres and that the flexural strength of such materials could be enhanced through improvement of strain-to-failure at the compressive surface without much loss of stiffness. The hybrid composites with minimum strengths of 700 MPa and 800 MPa (Tables 7-5 and 7-6) followed the same rule as for the 600 MPa case; therefore, it can be concluded that, in general, an additional 5-10% increase in fibre volume fraction within the outer one or two laminas at the compressive side would be required to achieve optimal and robust hybrid composites compared to optimal and non-robust hybrid composites (*i.e.*,

deterministic approach) for the same value of minimum strength. That is, the detrimental effect of manufacturing uncertainties for fibre orientation angle, fibre volume faction and lamina thickness can be negated through increasing the fibre volume fraction within the outer one or two laminas at the compressive side as mentioned above.

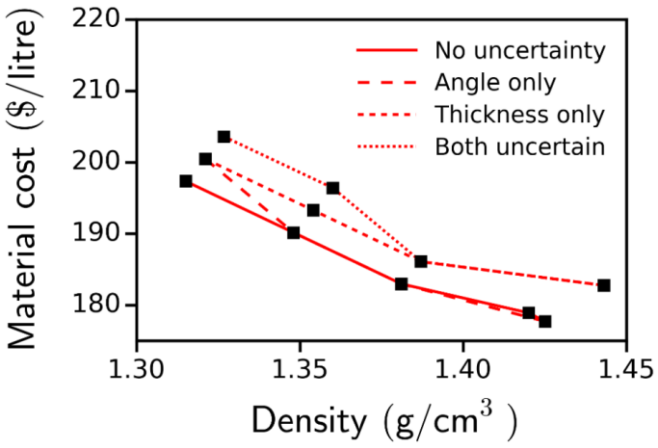


**Figure 7-4: The effect of uncertainties on the Pareto optimal fronts for multi-directional T700S carbon/S-2 glass fibre-reinforced epoxy composites ($S_0$ = 600 MPa).**

The hybrid composites presented in each of Tables 7-3 to 7-6 have been ordered from lowest to highest density. Since carbon fibres have a lower density and higher cost, stacking configurations containing higher amounts of carbon fibres would be listed first with the cost conversely tending to decrease. The first composite listed in each table would thus be full carbon/epoxy, *i.e.*, not hybrid, for all required strengths in both the deterministic and RDO approaches. Thus, it can be concluded that full carbon/epoxy composites with appropriate fibre volume fractions and lamina fibre orientation angles were the lightest optimal and robust materials in all cases. However, the existence of a positive hybrid effect can be noted through comparing the strength of the full carbon/epoxy and other composites. For example, the hybrid composite listed as UAT2 in Table 7-4 had the same fibre orientation and fibre volume fraction as those of composite UAT1 with the only difference being that the second lamina (90°) in UAT1 was carbon/epoxy which changed to glass/epoxy in composite UAT2 which resulted in the 0° strength remaining almost unchanged but the 90° strength increased from 638 MPa to 677

MPa, *i.e.*, although the strength of the carbon/epoxy laminas are higher than glass/epoxy laminas, replacing a carbon/epoxy lamina with a glass/epoxy lamina resulted in a hybrid composite with a higher flexural strength. Such an increase in 90° flexural strength is an example of a positive hybrid effect and was attributed to the higher elongation of the glass/epoxy laminas which has been investigated in several studies [42, 47, 48].

**Table 7-4: Pareto optimal solutions for multi-directional T700S carbon/S-2 glass fibre-reinforced epoxy composites and minimum required strength of 600 MPa.**

| | ID | Stacking Configuration, $\theta^{\text{Vf \%}}_{\text{fibre type}}$ | Density (g/cm³) | Cost ($/litre) | $S_{xx}$ (MPa) | $S_{yy}$ (MPa) | FPF* |
|---|---|---|---|---|---|---|---|
| No Uncertainties | **NU 1** | $0_c^{40\%} / 90_c^{30\%} / 90_c^{30\%} / 90_c^{30\%} / 0_c^{30\%} / 90_c^{30\%}$ | 1.315 | 65.78 | 614 | 669 | 1-X |
| | **NU 2** | $0_c^{40\%} / 90_c^{30\%} / 90_c^{30\%} / +45_c^{30\%} / 0_c^{30\%} / 90_c^{30\%}$ | 1.315 | 65.78 | 612 | 682 | 1-X |
| | **NU 3** | $0_c^{40\%} / 90_g^{30\%} / 90_c^{30\%} / 90_c^{30\%} / 0_c^{30\%} / 90_c^{30\%}$ | 1.348 | 63.39 | 615 | 641 | 1-X |
| | **NU 4** | $0_c^{40\%} / 90_c^{30\%} / 90_c^{30\%} / 0_g^{30\%} / 0_c^{30\%} / 90_c^{30\%}$ | 1.348 | 63.39 | 605 | 682 | 1-X |
| | **NU 5** | $0_c^{40\%} / 90_g^{30\%} / 90_c^{30\%} / 0_g^{30\%} / 0_c^{30\%} / 90_c^{30\%}$ | 1.381 | 60.99 | 607 | 733 | 1-X |
| | **NU 6** | $0_c^{40\%} / 90_g^{30\%} / 90_c^{30\%} / 90_g^{30\%} / 0_c^{30\%} / 90_c^{30\%}$ | 1.381 | 60.99 | 615 | 636 | 1-X |
| | **NU 7** | $0_c^{40\%} / 90_g^{35\%} / 90_g^{30\%} / 0_g^{30\%} / 0_c^{30\%} / 90_c^{30\%}$ | 1.425 | 59.24 | 608 | 616 | 1-X |
| | **NU 8** | $0_c^{40\%} / 90_g^{35\%} / 90_g^{30\%} / 90_g^{30\%} / 0_c^{30\%} / 90_c^{30\%}$ | 1.425 | 59.24 | 616 | 627 | 1-X |
| Uncertainty in Thickness | **UT 1** | $0_c^{45\%} / 90_c^{30\%} / 90_c^{30\%} / -45_c^{30\%} / 0_c^{30\%} / 90_c^{30\%}$ | 1.321 | 66.82 | 613 | 647 | 1-X |
| | **UT 2** | $0_c^{45\%} / 90_g^{30\%} / 90_c^{30\%} / 90_c^{30\%} / 0_c^{30\%} / 90_c^{30\%}$ | 1.354 | 64.43 | 601 | 694 | 6-X |
| | **UT 3** | $0_c^{45\%} / 90_g^{30\%} / 90_c^{30\%} / 90_g^{30\%} / 0_c^{30\%} / 90_c^{30\%}$ | 1.387 | 62.03 | 602 | 690 | 6-X |
| | **UT 4** | $0_c^{45\%} / 90_g^{30\%} / 90_c^{30\%} / 0_g^{30\%} / 0_c^{30\%} / 90_c^{30\%}$ | 1.387 | 62.03 | 608 | 687 | 6-X |
| | **UT 5** | $0_c^{45\%} / 90_g^{40\%} / 90_g^{30\%} / 90_g^{30\%} / 0_c^{30\%} / 90_c^{30\%}$ | 1.443 | 60.92 | 603 | 618 | 6-X |
| Uncertainty in Angle | **UA 1** | $0_c^{45\%} / 90_c^{30\%} / 90_c^{30\%} / 0_c^{30\%} / 0_c^{30\%} / 90_c^{30\%}$ | 1.321 | 66.82 | 640 | 672 | 1-X |
| | **UA 2** | $0_c^{40\%} / 90_c^{35\%} / 0_c^{30\%} / 0_c^{30\%} / 0_c^{30\%} / 90_c^{30\%}$ | 1.321 | 66.82 | 601 | 605 | 1-X |
| | **UA 3** | $0_c^{40\%} / 90_c^{30\%} / 90_c^{30\%} / 0_g^{30\%} / 0_c^{30\%} / 90_c^{30\%}$ | 1.348 | 63.39 | 603 | 668 | 1-X |
| | **UA 4** | $0_c^{40\%} / 90_g^{30\%} / 90_c^{30\%} / 0_g^{30\%} / 0_c^{30\%} / 90_c^{30\%}$ | 1.381 | 60.99 | 604 | 716 | 1-X |
| | **UA 5** | $0_c^{40\%} / 90_c^{30\%} / 90_g^{30\%} / 0_g^{30\%} / 0_c^{30\%} / 90_c^{30\%}$ | 1.381 | 60.99 | 603 | 607 | 1-X |
| | **UA 6** | $0_c^{40\%} / 90_g^{35\%} / 90_g^{30\%} / 0_g^{30\%} / 0_c^{35\%} / 90_c^{30\%}$ | 1.425 | 59.24 | 605 | 609 | 1-X |
| Uncertainties in Angle and Thickness | **UAT 1** | $0_c^{50\%} / 90_c^{30\%} / 90_c^{30\%} / 0_c^{30\%} / 0_c^{30\%} / 90_c^{30\%}$ | 1.327 | 67.87 | 637 | 638 | 1-X |
| | **UAT 2** | $0_c^{50\%} / 90_g^{30\%} / 90_c^{30\%} / 0_c^{30\%} / 0_c^{30\%} / 90_c^{30\%}$ | 1.360 | 65.47 | 638 | 677 | 1-X |
| | **UAT 3** | $0_c^{45\%} / 90_g^{30\%} / 90_c^{30\%} / +45_c^{30\%} / 0_c^{35\%} / 90_c^{30\%}$ | 1.360 | 65.47 | 617 | 670 | 1-X |
| | **UAT 4** | $0_c^{45\%} / 90_g^{30\%} / 90_c^{30\%} / 0_g^{30\%} / 0_c^{30\%} / 90_c^{30\%}$ | 1.387 | 62.04 | 605 | 671 | 1-X |
| | **UAT 5** | $0_c^{45\%} / 90_g^{40\%} / 90_g^{30\%} / 0_g^{30\%} / 0_c^{30\%} / 90_c^{30\%}$ | 1.443 | 60.92 | 607 | 604 | 2-Y |

* First ply failure (Ply No. - Failure Direction); X:[0] and Y:[90]

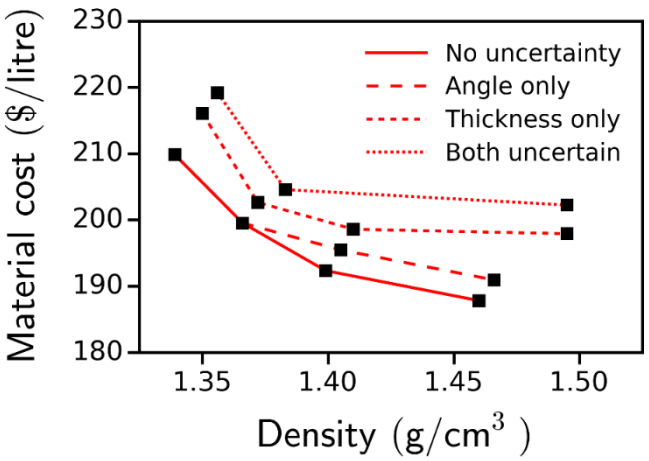


**Figure 7-5: The effect of uncertainties on the Pareto optimal fronts for multi-directional T700S carbon/S-2 glass fibre-reinforced epoxy composites ($S_0$ = 700 MPa).**

It should be noted that, due to the limited number of fibre volume fractions used in the optimization problem (*i.e.*, 5% increment in $V_f$), the difference between Pareto optimal fronts when the fibre orientation angle or lamina thickness were uncertain could not be detected for intermediate strength composites (600 MPa and 700 MPa); however, it could be identified from corresponding data in Tables 7-4 and 7-5. For instance, regarding the optimal solution for a minimum strength of 600 MPa in Table 7-4, the hybrid composites NU4 and UA3 had the same cost and density. Although the strength in the latter composite was slightly lower due to uncertainties, both strengths were still greater than the required value of 600 MPa. Similar configurations were also achieved for composites UT4 and UAT4 and thus the data points on the Pareto optimal fronts were identical. Should more accurate Pareto optimal fronts be required, additional fibre volume fraction levels should be included within the optimization and anti-optimization problem although this would be achieved at the expense of significantly increased computational time.

**Table 7-5: Pareto optimal solutions for multi-directional T700S carbon/S-2 glass fibre-reinforced epoxy composites and minimum required strength of 700 MPa.**

| | ID | Stacking Configuration, $\theta^{\mathrm{Vf\,\%}}_{\mathrm{fibre\ type}}$ | Density (g/cm³) | Cost ($/litre) | $S_{xx}$ (MPa | $S_{yy}$ (MPa) | FPF* |
|---|---|---|---|---|---|---|---|
| No Uncertainties | NU 1 | $0_c^{50\%}$ / $90_c^{30\%}$ / $90_c^{35\%}$ / $0_c^{30\%}$ / $0_c^{35\%}$ / $90_c^{30\%}$ | 1.339 | 69.95 | 704 | 706 | 1-X |
| | NU 2 | $0_c^{55\%}$ / $90_c^{35\%}$ / $90_c^{30\%}$ / $0_c^{30\%}$ / $0_c^{30\%}$ / $90_c^{30\%}$ | 1.339 | 69.95 | 744 | 721 | 2-Y |
| | NU 3 | $0_c^{55\%}$ / $90_g^{30\%}$ / $90_c^{30\%}$ / $0_c^{30\%}$ / $0_c^{30\%}$ / $90_c^{30\%}$ | 1.366 | 66.51 | 744 | 755 | 1-X |
| | NU 4 | $0_c^{55\%}$ / $90_g^{30\%}$ / $90_c^{30\%}$ / $0_g^{30\%}$ / $0_c^{30\%}$ / $90_c^{30\%}$ | 1.399 | 64.12 | 715 | 755 | 6-X |
| | NU 5 | $0_c^{50\%}$ / $90_g^{45\%}$ / $90_g^{30\%}$ / $0_g^{30\%}$ / $0_c^{30\%}$ / $90_c^{30\%}$ | 1.460 | 62.61 | 701 | 709 | 6-X |
| Uncertainty in Thickness | UT 1 | $0_c^{60\%}$ / $90_c^{40\%}$ / $90_c^{30\%}$ / $0_c^{30\%}$ / $0_c^{30\%}$ / $90_c^{30\%}$ | 1.350 | 72.03 | 731 | 705 | 2-Y |
| | UT 2 | $0_c^{60\%}$ / $90_g^{30\%}$ / $90_c^{30\%}$ / $0_c^{30\%}$ / $0_c^{30\%}$ / $90_c^{30\%}$ | 1.372 | 67.55 | 731 | 707 | 2-Y |
| | UT 3 | $0_c^{65\%}$ / $90_g^{30\%}$ / $90_c^{30\%}$ / $0_g^{30\%}$ / $0_c^{30\%}$ / $90_c^{30\%}$ | 1.410 | 66.20 | 702 | 715 | 6-X |
| | UT 4 | $0_c^{55\%}$ / $90_g^{50\%}$ / $90_g^{35\%}$ /-$45_g^{30\%}$ / $0_c^{35\%}$ / $90_c^{30\%}$ | 1.495 | 65.98 | 701 | 715 | 6-X |
| Uncertainty in Angle | UA 1 | $0_c^{55\%}$ / $90_c^{35\%}$ / $90_c^{30\%}$ / $0_c^{30\%}$ / $0_c^{30\%}$ / $90_c^{30\%}$ | 1.339 | 69.95 | 740 | 705 | 2-Y |
| | UA 2 | $0_c^{50\%}$ / $90_c^{35\%}$ / $90_c^{30\%}$ / $0_c^{30\%}$ / $0_c^{35\%}$ / $90_c^{30\%}$ | 1.339 | 69.95 | 701 | 701 | 2-Y |
| | UA 3 | $0_c^{55\%}$ / $90_g^{30\%}$ / $90_c^{30\%}$ / $0_c^{30\%}$ / $0_c^{30\%}$ / $90_c^{30\%}$ | 1.366 | 66.51 | 740 | 737 | 2-Y |
| | UA 4 | $0_c^{55\%}$ / $90_g^{30\%}$ / $90_c^{30\%}$ / $0_g^{30\%}$ / $0_c^{35\%}$ / $90_c^{30\%}$ | 1.405 | 65.16 | 721 | 738 | 6-X |
| | UA 5 | $0_c^{50\%}$ / $90_g^{45\%}$ / $90_g^{30\%}$ / $0_g^{30\%}$ / $0_c^{35\%}$ / $90_c^{30\%}$ | 1.446 | 63.65 | 708 | 700 | 2-Y |
| Uncertainties in Angle and Thickness | UAT 1 | $0_c^{60\%}$ / $90_c^{40\%}$ / $90_c^{35\%}$ / $0_c^{30\%}$ / $0_c^{30\%}$ / $90_c^{30\%}$ | 1.356 | 73.08 | 721 | 700 | 2-Y |
| | UAT 2 | $0_c^{60\%}$ / $90_g^{35\%}$ / $90_c^{30\%}$ / $0_c^{30\%}$ / $0_c^{30\%}$ / $90_c^{30\%}$ | 1.383 | 68.20 | 721 | 714 | 2-Y |
| | UAT 3 | $0_c^{65\%}$ / $90_g^{50\%}$ / $90_g^{30\%}$ / $0_g^{30\%}$ / $0_c^{35\%}$ / $90_c^{30\%}$ | 1.495 | 67.42 | 711 | 703 | 2-Y |

* First ply failure (Ply No. - Failure Direction); X:[0] and Y:[90]

From Figures 4 to 6 it can also be observed that all curves for the uncertainties in lamina thickness case were above those of the uncertainties in fibre orientation angle case, thus indicating that intermediate and high strength hybrid composites (*i.e.*, excluding the 500 MPa composite) were more sensitive to uncertainties in thickness than to fibre orientation angle. As discussed before, the lowest strength composites, *i.e.*, 500 MPa, were insensitive to any of the uncertainties considered. Therefore, from the point of view of manufacturing, controlling the thickness of laminas is more critical than controlling the fibre orientation angle, especially for the case of high strength hybrid composites considered in this work.

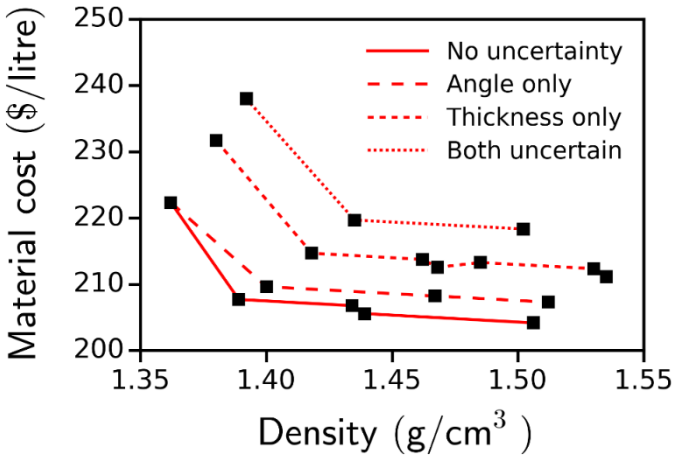


**Figure 7-6: The effect of uncertainties on the Pareto optimal fronts for multi-directional T700S carbon/S-2 glass fibre-reinforced epoxy composites ($S_0$ = 800 MPa).**

Pareto optimal fronts for all levels of minimum required strength (500 to 800 MPa) in two specific cases, namely when no uncertainties were included (NU, deterministic approach with nominal values) and when uncertainties in both fibre orientation angle and lamina thickness were included (UAT), have been presented in Figure 7-7. As would be expected, in both cases the weight and/or cost of the resulting composites increased with increasing required strength *i.e.*, the Pareto optimal fronts moved away from the origin. This highlights the fact that higher strength hybrid composites are more expensive and/or heavier that their lower strength counterparts. However, closer examination of Figure 7-7(a) and (b) showed that the distances between the individual curves achieved by RDO (UAT, Figure 7-7(b)) were greater than those achieved through the deterministic approach (NU, Figure 7-7(a)), *i.e.*, the minimum required strength had a stronger effect on density and/or cost of materials when uncertainties were considered. This difference can also be verified by comparing the corresponding data in Tables 7-4 to 7-6.

**Table 7-6: Pareto optimal solutions for T700S carbon/S-2 glass fibre-reinforced epoxy composites and minimum required strength of 800 MPa.**

| | ID | Stacking Configuration, $\theta^{\text{Vf \%}}_{\text{fibre type}}$ | Density (g/cm³) | Cost ($/litre) | $S_{xx}$ (MPa) | $S_{yy}$ (MPa) | FPF No. |
|---|---|---|---|---|---|---|---|
| No Uncertainties | NU 1 | $0_c^{60\%} / 90_c^{50\%} / 90_c^{30\%} / \; 0_c^{30\%} / 0_c^{30\%} / 90_c^{30\%}$ | 1.362 | 74.12 | 801 | 824 | 1-X |
| | NU 2 | $0_c^{65\%} / 90_g^{35\%} / 90_c^{30\%} / \; 0_c^{30\%} / 0_c^{30\%} / 90_c^{30\%}$ | 1.389 | 69.24 | 844 | 800 | 2-Y |
| | NU 3 | $0_c^{70\%} / 90_g^{35\%} / 90_c^{30\%} / \; 0_g^{30\%} / 0_c^{35\%} / 90_c^{30\%}$ | 1.434 | 68.93 | 821 | 811 | 2-Y |
| | NU 4 | $0_c^{65\%} / 90_g^{40\%} / 90_c^{30\%} / \; 0_g^{30\%} / 0_c^{35\%} / 90_c^{30\%}$ | 1.439 | 68.53 | 810 | 832 | 6-X |
| | NU 5 | $0_c^{65\%} / 90_g^{55\%} / 90_g^{30\%} / \; 0_g^{30\%} / 0_c^{35\%} / 90_c^{30\%}$ | 1.506 | 68.06 | 810 | 829 | 6-X |
| Uncertainty in Thickness | UT 1 | $0_c^{70\%} / 90_c^{55\%} / 90_c^{30\%} / \; 0_c^{30\%} / 0_c^{30\%} / 90_c^{30\%}$ | 1.380 | 77.24 | 815 | 804 | 2-Y |
| | UT 2 | $0_c^{70\%} / 90_g^{45\%} / 90_c^{30\%} / \; 0_c^{30\%} / 0_c^{30\%} / 90_c^{30\%}$ | 1.418 | 71.57 | 815 | 802 | 2-Y |
| | UT 3 | $0_c^{70\%} / 90_g^{45\%} / 90_c^{30\%} / \; 0_g^{30\%} / 0_c^{40\%} / 90_c^{30\%}$ | 1.462 | 71.25 | 848 | 802 | 2-Y |
| | UT 4 | $0_c^{65\%} / 90_g^{50\%} / 90_c^{30\%} / 0_g^{30\%} / 0_c^{40\%} / 90_c^{30\%}$ | 1.468 | 70.85 | 822 | 827 | 1-X |
| | UT 5 | $0_c^{70\%} / 90_g^{60\%} / 90_g^{30\%} / 0_c^{30\%} / 0_c^{30\%} / 90_c^{30\%}$ | 1.485 | 71.10 | 815 | 803 | 2-Y |
| | UT 6 | $0_c^{70\%} / 90_g^{60\%} / 90_g^{30\%} / 0_g^{30\%} / 0_c^{40\%} / 90_c^{30\%}$ | 1.530 | 70.79 | 848 | 802 | 2-Y |
| | UT 7 | $0_c^{65\%} / 90_g^{65\%} / 90_g^{30\%} / 0_g^{30\%} / 0_c^{40\%} / 90_c^{30\%}$ | 1.535 | 70.39 | 827 | 840 | 1-X |
| Uncertainty in Angle | UA 1 | $0_c^{60\%} / 90_c^{50\%} / 90_c^{30\%} / \; 0_c^{30\%} / 0_c^{35\%} / 90_c^{30\%}$ | 1.362 | 74.12 | 811 | 806 | 2-Y |
| | UA 2 | $0_c^{60\%} / 90_g^{40\%} / 90_c^{30\%} / \; 0_c^{30\%} / 0_c^{35\%} / 90_c^{30\%}$ | 1.400 | 69.88 | 811 | 807 | 2-Y |
| | UA 3 | $0_c^{60\%} / 90_g^{55\%} / 90_g^{30\%} / \; 0_c^{30\%} / 0_c^{35\%} / 90_c^{30\%}$ | 1.467 | 69.41 | 812 | 816 | 1-X |
| | UA 4 | $0_c^{60\%} / 90_g^{55\%} / 90_g^{30\%} / \; 0_g^{30\%} / 0_c^{45\%} / 90_c^{30\%}$ | 1.512 | 69.10 | 850 | 816 | 2-Y |
| Uncertainties in Angle and Thickness | UAT 1 | $0_c^{70\%} / 90_c^{60\%} / 90_c^{30\%} / \; 0_c^{30\%} / 0_c^{35\%} / 90_c^{30\%}$ | 1.392 | 79.33 | 801 | 821 | 6-X |
| | UAT 2 | $0_c^{70\%} / 90_g^{50\%} / 90_c^{30\%} / \; 0_c^{30\%} / 0_c^{35\%} / 90_c^{30\%}$ | 1.435 | 73.23 | 802 | 819 | 1-X |
| | UAT 3 | $0_c^{70\%} / 90_g^{65\%} / 90_g^{30\%} / \; 0_c^{30\%} / 0_c^{35\%} / 90_c^{30\%}$ | 1.502 | 72.78 | 803 | 840 | 6-X |

* First ply failure (Ply No. - Failure Direction); X:[0] and Y:[90]

In order to clearly highlight the relationship between optimal solutions and minimum required strength, the lightest composites in both cases (deterministic approach, *i.e.*, NU and RDO) were selected with the corresponding cost and density being presented in Figure 7-8. Although all of these composites were full carbon/epoxy they can still be used for comparison purposes. From Figure 7-8 it can be concluded that, in general, both the cost and density increased with the minimum required strength (note that the cost axis has been reversed for clarity). As discussed earlier, the 500 MPa composites were found to be insensitive to

uncertainties with the density and cost being the same for both the RDO and deterministic cases. In addition, the difference between both the density and cost curves also increased with the minimum required strength. It can thus be concluded that high strength composites were more significantly affected for any given level of uncertainty, *i.e.*, the application of higher manufacturing tolerances is more significant in the control of cost and weight of such high strength materials. These results are in good agreement with previous research for unidirectional T700S carbon/E-glass epoxy hybrid composites [57] which indicated that consideration of uncertainties in fibre orientation angle and lamina thickness was more important when higher strength was required.

In order to verify that the same conclusion could be inferred for unidirectional T700S carbon/S-2 glass fibre-reinforced epoxy composites, the method presented in the previous study [57] was utilized to find the optimal and robust optimal designs for the present case. The unidirectional hybrid composites in that specific problem [57] comprised a section of glass/epoxy laminas at the compressive side and a section of carbon/epoxy at the tensile side with the design variables being the height of the glass/epoxy section and the volume fraction of glass/epoxy and carbon/epoxy laminas (with each section consisting of one or more laminas). The nominal value of total height (the nominal thickness) was considered to be fixed and uncertainties in fibre orientation angle and lamina thickness were considered using an RDO approach. Results for the lightest achieved composites in both cases (RDO and deterministic) and three levels of strength, *i.e.*, 700 MPa, 1000 MPa and 1300 MPa, have been presented in Figure 7-9 with the corresponding data being listed in Table 7-7. Similar to that concluded for multi-directional hybrid composites using the method presented in this work, it can be observed from Figure 7-9 that the difference between density and cost for unidirectional hybrid composites increased with increasing strength level with the low strength unidirectional hybrid composite, *i.e.*, 700 MPa, being insensitive to uncertainties. It is noteworthy that for intermediate and high strength unidirectional hybrid composites, *i.e.*, 1000 MPa and 1300 MPa, the optimal designs were not full carbon/epoxy and included glass/epoxy layers. This phenomenon was attributed to the existence of a

significant hybrid effect within unidirectional carbon/glass hybrid composites [42, 47, 48]. However, in contrast to this, experimental research [60] has reported no significant hybrid effect in bi-directional carbon/glass epoxy hybrid composites and therefore the lightest optimal designs in the present study were fully carbon/epoxy. This difference between the makeup of the unidirectional (carbon/epoxy and glass/epoxy) and multi-directional (carbon/epoxy) composites was attributed to the presence of a significant hybrid effect for the unidirectional case as mentioned above.

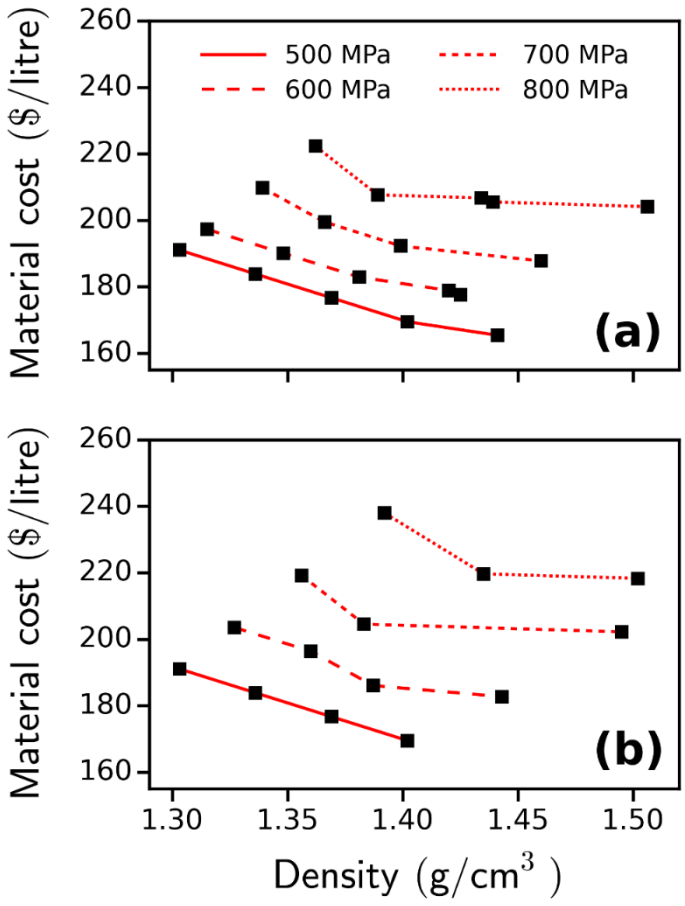


**Figure 7-7: Pareto optimal fronts for multi-directional T700S carbon/S-2 glass fibre-reinforced epoxy composites as a function of minimum strength requirement: (a) uncertainties were not included and (b) uncertainties in both fibre orientation angle and lamina thickness were included.**

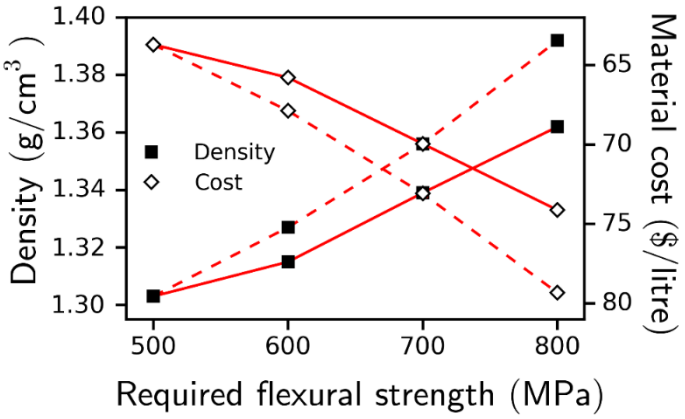


**Figure 7-8: Comparison of the effect of uncertainties on the cost and density of the lightest optimum composites for multi-directional T700S carbon/S-2 glass epoxy composites (Dash lines: RDO; Solid lines: Deterministic approach).**

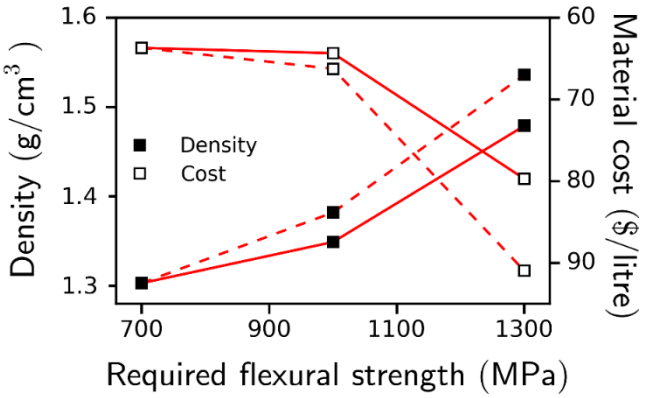


**Figure 7-9: Comparison of the effect of uncertainties on the cost and density of the lightest optimum composites for unidirectional T700S carbon/S-2 glass epoxy composites (Dash lines: RDO; Solid lines: Deterministic approach).**

**Table 7-7: Comparison of the effect of uncertainties for unidirectional S-2 glass/T700S carbon epoxy composites on the cost and density of the lightest optimum composites.**

| Minimum required Strength (MPa) | No Uncertainties (Deterministic approach) | | Uncertainties in Angle and Thickness (RDO) | | % change $(\frac{RDO-\text{Deterministic}}{\text{Deterministic}} \times 100)$ | |
|---|---|---|---|---|---|---|
| | Density (g/cm$^3$) | Cost ($/litre) | Density (g/cm$^3$) | Cost ($/litre) | Density Ratio (%) | Cost Ratio (%) |
| 700 | 1.303 ($V_{fg}$: N/A, $V_{fc}$: 30%, $h_g/h$: 0) | 63.70 | 1.303 ($V_{fg}$: N/A, $V_{fc}$: 30%, $h_g/h$: 0) | 63.70 | 0 | 0 |
| 1000 | 1.349 ($V_{fg}$: 60%, $V_{fc}$: 30%, $h_g/h$: 7.5%) | 64.36 | 1.382 ($V_{fg}$: 60%, $V_{fc}$: 31%, $h_g/h$: 11.5%) | 66.26 | 2.45 | 2.95 |
| 1300 | 1.479 ($V_{fg}$: 59%, $V_{fc}$: 44%, $h_g/h$: 15.5%) | 79.73 | 1.536 ($V_{fg}$: 70%, $V_{fc}$: 53%, $h_g/h$: 12.0%) | 90.98 | 3.85 | 14.11 |

## 7.4. Conclusions

The multi-objective robust optimization of multi-directional T700S carbon/S-2 glass fibre-reinforced epoxy hybrid composites with respect to minimum weight and cost and subject to a prescribed flexural strength has been investigated using a combined optimization and anti-optimization evolutionary algorithm. The material (fibre type), fibre orientation angle and fibre volume fraction within each lamina were considered as design variables with the manufacture related uncertainties in fibre orientation angle and lamina thickness (and thus in fibre volume fraction) being incorporated.

The worst case for the flexural strength was determined through an anti-optimization method using a GA optimizer. The multi-objective robust optimization problem for the minimum cost and density of the hybrid composites considering the uncertainties was formulated with the optimum results being found using the modified non-dominated sorting algorithm (NSGA-II).

Results indicated that consideration of manufacturing uncertainties increased the material cost and density with this increase being greater for higher strength

composites, *i.e.*, uncertainties become more important when higher strength composites were required. It was also shown that the hybrid composites investigated in this study were more sensitive to uncertainty in thickness than to uncertainty in fibre orientation angle. Therefore, from the viewpoint of manufacturing, improving the tolerance of the lamina thickness would be of increased benefit.

The results for stacking configuration showed that, in general, when uncertainties were included the fibre volume fractions of only the first one or two laminas at the compressive side should be increased in order to obtain an optimal and robust hybrid composite with the same required strength, *i.e.*, the robust optimal configurations can be achieved by adjusting only the fibre volume fraction of these laminas. Furthermore, a positive hybrid effect was observed in some stacking configurations when carbon/epoxy laminas at the compressive side were replaced with glass/epoxy laminas.

The combination of optimization and anti-optimization methods was found to be a robust and efficient approach to solving the robust design optimization of hybrid composite materials when a large number of design variables and uncertainties are involved.

## 7.5. References


[1] Dutra TA, Almeida SFM. Composite plate stiffness multicriteria optimization using lamination parameters. Composite Structures. 2015;133:166-177.

[2] Le-Manh T, Lee J. Stacking sequence optimization for maximum strengths of laminated composite plates using genetic algorithm and isogeometric analysis. Composite Structures. 2014;116:357-363.

[3] Velea MN, Wennhage P, Zenkert D. Multi-objective optimization of vehicle bodies made of FRP sandwich structures. Composite Structures, 2014;111:75-84.

[4] Madeira JFA, Araújo AL, Mota Soares CM, Mota Soares CA, Ferreira AJM. Multiobjective design of viscoelastic laminated composite sandwich panels, Composites Part B: Engineering. 2015;77:391-401.

[5] Ghiasi H, Pasini D, Lessard L. Optimum stacking sequence design of composite materials part i: Constant stiffness design. Composite Structures 2009;90:1-11.

[6] Deb K. Multi-objective optimization using evolutionary algorithms: John Wiley & Sons, 2001.

[7] Hemmatian H, Fereidoon A, Sadollah A, Bahreininejad A. Optimization of laminate stacking sequence for minimizing weight and cost using elitist ant system optimization. Advances in Engineering Software 2013;57:8-18.

[8] Hemmatian H, Fereidoon A, Assareh E. Optimization of hybrid laminated composites using the multi-objective gravitational search algorithm (MOGSA). Engineering Optimization 2014;46(9):1169-1182.

[9] Adali S, Walker M, Verijenko VE. Multi-objective optimization of laminated plates for maximum pre buckling, buckling and post buckling strengths using continuous and discrete ply angles. Composite Structures 1996;35(1):117-130.

[10] Walker M, Smith R. A technique for the multiobjective optimization of laminated composite structures using genetic algorithms and finite element analysis. Composite Structures 2003;62(1):123-128.

[11] Walker M, Reiss T, Adali S. Multi-objective design of laminated cylindrical shells for maximum torsional and axial buckling loads. Computers & Structures 1997;62(2):237-242.

[12] Walker M, Reiss T, Adali S. A procedure to select the best material combinations and optimally design hybrid composite plates for minimum weight and cost. Engineering Optimization 1997;29(1-4):65-83.

[13] Almeida FS, Awruch AM. Design optimization of composite laminated structures using genetic algorithms and finite element analysis. Composite Structures 2009;88(3):443-454.

[14] Kaufmann M, Zenkert D, Wennhage P. Integrated cost/weight optimization of aircraft structures. Structural and Multidisciplinary Optimization 2010;41(2):325-334.

[15] Rouhi M, Ghayoor H, Hoa SV, Hojjati M. Multi-objective design optimization of variable stiffness composite cylinders, Composites Part B: Engineering. 2015;69:249-255.

[16] Zitzler E, Laumanns M, Thiele L. SPEA2: Improving the strength Pareto evolutionary algorithm. Tech Rep 103, Computer Engineering and Networks Laboratory (TIK). Swiss Federal Institute of Technology (ETH), Zurich, Switzerland, 2001.

[17] Knowles J, Corne D. The Pareto archived evolution strategy: a new baseline algorithm for multi-objective optimisation. In: Proceedings of the 1999 congress on evolutionary computation. IEEE Press, Piscataway, 2002;99-105.

[18] Deb K, Pratap A, Agarwal S, Meyarivan T. A fast and elitist multi-objective genetic algorithm: NSGA-II. IEEE Transactions on Evolutionary Computation 2002;6(2):182-197.

[19] Lakshmi K, Rama Mohan Rao A. Multi-objective optimal design of laminated composite skirt using hybrid NSGA. Meccanica 2013;48(6):1431-1450.

[20] Visweswaraiah SB, Ghiasi H, Pasini D, Lessard L. Multi-objective optimization of a composite rotor blade cross-section. Composite Structures 2013;96:75-81.

[21] Vosoughi AR, Nikoo MR. Maximum fundamental frequency and thermal buckling temperature of laminated composite plates by a new hybrid multi-objective optimization technique. Thin-Walled Structures. 2015;95:408-415.

[22] Chamis CC. Probabilistic simulation of multi-scale composite behavior. Theoretical and Applied Fracture Mechanics 2004;41(1-3):51-61.

[23] Spurgeon WA. Thickness and reinforcement fiber content control in composites by vacuum-assisted resin transfer molding fabrication processes. DTIC Document: Army Research Lab Aberdeen Proving Ground MD, 2005.

[24] Shaw A, Sriramula S, Gosling PD, Chryssanthopoulos MK. A critical reliability evaluation of fibre-reinforced composite materials based on probabilistic micro and macro-mechanical analysis. Composites Part B: Engineering 2010;41(6):446-453.

[25] Fertig RS, Jensen EM, Malusare KA. Effect of fiber volume fraction variation across multiple length scales on composite stress variation: the possibility of stochastic multiscale analysis. 55th AIAA/ASMe/ASCE/AHS/SC Structures, Structural Dynamics, and Materials Conference: American Institute of Aeronautics and Astronautics. 2014.

[26] Taguchi G. Performance analysis design. International Journal of Production Research 1978;16(6):521-530.

[27] Beyer H-G, Sendhoff B. Robust optimization–a comprehensive survey. Computer methods in applied mechanics and engineering 2007;196(33-34):3190-31218.

[28] Cheng S, Zhou J, Li M. A new hybrid algorithm for multi-objective robust optimization with interval uncertainty. Journal of Mechanical Design 2015;137: 021401-021401.

[29] Elishakoff I, Ohsaki M. Optimization and anti-optimization of structures under uncertainty. 3rd edition. London: Imperial College Press; 2010.

[30] Liao Y-S, Chiou C-Y. Robust optimum designs of fiber-reinforced composites using constraints with sensitivity. Journal of Composite Materials 2006;40(22):2067-2080.

[31] Lombardi M, Haftka, RT. Anti-optimization technique for structural design under load uncertainties. Computer Methods in Applied Mechanics and Engineering 1998;157(1-2):19-31.

[32] Defaria AR. Buckling optimization and anti-optimization of composite plates -uncertain loading combination. International Journal for Numerical Methods in Engineering 2002;53(3):719-732.

[33] Elishakoff IE, Li YW, Starners JH. Deterministic method to predict the effect of unknown-but-bounded elastic moduli on the buckling of composite structures. Computer Methods in Applied Mechanics and Engineering 1994;111(1-2):155-167.

[34] Elishakoff IE, Haftka RT, Fang J. Structural design under bounded uncertainty - optimization with anti-optimization. Computers and Structures 1994;53(5):1401-1405.

[35] Elishakoff IE, Kriegesmann B, Rolfes R, Huhne C, Kling A. Optimization and antioptimization of buckling load for composite cylindrical shells under uncertainties. AIAA Journal, 2012;50(7):1513-1524.

[36] Radebe IS, Adali S. Minimum cost design of hybrid cross-ply cylinders with uncertain material properties subject to external pressure. Ocean Engineering 2014;88:310-317.

[37] Walker M, Hamilton R. A methodology for optimally designing fibre-reinforced laminated structures with design variable tolerances for maximum buckling strength. Thin-Walled Structures 2005;43(1):161-174.

[38] Zhang X-M, Ding H. Design optimization for dynamic response of vibration mechanical system with uncertain parameters using convex model. Journal of Sound and Vibration 2008;318(1-2):406-415.

[39] Adali S, Lene F, Duvaut G, Chiaruttini V. Optimization of laminated composites subject to uncertain buckling loads. Composite Structures 2003;62(3-4):261-269.

[40] António CC, Hoffbauer LN. An approach for reliability-based robust design optimisation of angle-ply composites. Composite Structures 2009;90(1):53-59.

[41] Lee D, Morillo C, Oller S, Bugeda G, Oñate E. Robust design optimisation of advance hybrid (fiber-metal) composite structures. Composite Structures 2013;99:181-192.

[42] Dong C, Ranaweera-Jayawardena HA, Davies IJ. Flexural properties of hybrid composites reinforced by S-2 glass and T700S carbon fibres. Composites Part B: Engineering 2012;43(2):573-581.

[43] Ary Subagia IDG, Kim Y, Tijing LD, Kim CS, Shon HK. Effect of stacking sequence on the flexural properties of hybrid composites reinforced with carbon and basalt fibers. Composites Part B: Engineering 2014;58:251-258.

[44] Davies IJ, Hamada H. Flexural properties of a hybrid polymer matrix composite containing carbon and silicon carbide fibres. Advanced Composite Materials. 2001;10:77-96.

[45] Marom G, Fischer S, Tuler FR, Wagner HD. Hybrid effects in composites: conditions for positive or negative effects versus rule-of-mixtures behaviour. Journal of Materials Science 1978;13(7):1419-1426.

[46] Dong C, Davies IJ. Optimal design for the flexural behaviour of glass and carbon fibre reinforced polymer hybrid composites. Materials & Design 2012;37:450-457.

[47] Dong C, Davies IJ. Flexural and tensile moduli of unidirectional hybrid epoxy composites reinforced by S-2 glass and T700S carbon fibres. Materials & Design 2014;54:893-899.

[48] Dong C, Davies IJ. Flexural and tensile strengths of unidirectional hybrid epoxy composites reinforced by S-2 glass and T700S carbon fibres. Materials & Design 2014;54:955-966.

[49] Oh JH, Kim YG, Lee DG. Optimum bolted joints for hybrid composite materials. Composite Structures 1997;38(1-4):329-341.

[50] Adali S, Verijenko VE. Optimum stacking sequence design of symmetric hybrid laminates undergoing free vibrations. Composite Structures 2001;54(2-3):131-138.

[51] Walker M, Reiss T, Adali S. A procedure to select the best material combinations and optimally design hybrid composite plates for minimum weight and cost. Engineering Optimization 1997;29(1-4):65-83.

[52] Antonio CAC. A hierarchical genetic algorithm with age structure for multimodal optimal design of hybrid composites. Structural and Multidisciplinary Optimization 2006;31(4):280-294.

[53] Abachizadeh M, Tahani M. An ant colony optimization approach to multi-objective optimal design of symmetric hybrid laminates for maximum fundamental frequency and minimum cost. Structural and Multidisciplinary Optimization 2009;37(4):367-376.

[54] Rahul, Sandeep G, Chakraborty D, Dutta A. Multi-objective optimization of hybrid laminates subjected to transverse impact. Composite Structures 2006;73(3):360-369.

[55] Dong C, Kalantari M, Davies IJ. Robustness for unidirectional carbon/glass fibre reinforced hybrid epoxy composites under flexural loading. Composite Structures 2015;128:354-362.

[56] Kalantari M, Dong C, Davies IJ. Multi-objective analysis for optimal and robust design of unidirectional glass/carbon fibre reinforced hybrid epoxy composites under flexural loading. Composites Part B: Engineering 2016;84:130-139.

[57] Kalantari M, Dong C, Davies IJ. Multi-objective robust optimization of unidirectional carbon/glass fibre reinforced hybrid composites under flexural loading. Composite Structures 2016;138:264-275.

[58] Gurit. Guide to composites, www.gurit.com, Accessed: 7 April 2015.

[59] Mallick PK. Fiber-reinforced composites: materials, manufacturing, and design. 3rd edition. London: CRC press; 1993.

[60] Dong C, Davies IJ. Flexural strength of bidirectional hybrid epoxy composites reinforced by E glass and T700S carbon fibres. Composites Part B: Engineering 2015;72:65-71.

# 8

# Effect of matrix voids, fibre misalignment and thickness variation on multi-objective robust optimization of carbon/glass fibre-reinforced hybrid composites under flexural loading[1]

## 8.1. Introduction

Advanced composite materials have successfully replaced metals in many applications that require a combination of high strength and low density, particularly in the fields of aerospace, marine and automotive engineering [1]. Among the different types of composite materials available, hybrid composites such as those based on carbon/glass fibre-reinforced epoxy, have become increasingly popular due to their ability to exploit the properties of multiple fibre types. However, complexities in the design and manufacture of such hybrid composite materials have thus far limited their widespread application.

Difficulties related with the manufacture of carbon/glass fibre-reinforced epoxy laminated composites are mainly associated with the existence of defects such as voids, resin rich regions and fibre misalignment. These defects have a detrimental effect on the performance of hybrid composites and lead to an undesired variation in the resulting mechanical properties [2-5]. Whilst several researchers have attempted to optimize the manufacturing process of composites through the

[1] This Chapter has been published in Composites Part B: Engineering, Vol 123, 2017, Pages 136-147

minimization of defects [6-8], in practice, it is impossible to eliminate all defects and produce a “perfect” component.

The presence of voids is undesirable in most applications of composite materials with the void content typically being restricted below 5% [4]. However, in some aerospace applications, even a void content of 1% is considered unacceptable [9, 10]. Thus far, several studies have investigated the relationship between void content and strength of composite materials with it being concluded that matrix-dominated properties, *e.g.*, flexural and compressive strength, are more influenced by voids when compared to fibre-dominated properties, *e.g.*, longitudinal tensile strength [11]. In particular, flexural strength and modulus are extremely sensitive to void content [3, 10-13]; therefore, consideration of the effect of matrix voids on mechanical properties is an important parameter in the design of composite materials. Dong [11] recently employed a finite element model based on representative volume elements (RVE) and proposed a simple regression model for predicting the strength of composite laminates with voids. This model was used in the present study to incorporate the degrading effect of void content within the optimization problem.

Other manufacturing related uncertainties and defects, such as resin rich regions and fibre misalignment, also affect the performance of composite products. Inspection of fibre-reinforced polymer (FRP) composite laminates produced by conventional manufacturing methods has shown that ±10% variation in the lamina thickness and ±3º deviation in fibre orientation angle from nominal values to be common [14,15].

Such manufacturing related uncertainties of the resulting composite properties are known to degrade the performance of optimum designs. Therefore, following manufacture, highly optimized composites designed on the basis of nominal values of the design variables may exhibit lower performance than that originally predicted. Robust design optimization (RDO), which was first proposed by Taguchi [16], aims to find optimal solutions that are less sensitive to uncertainties in design variables and manufacturing methods. RDO methods are classified into probabilistic and non-probabilistic approaches. Probabilistic approaches use the probability

distribution of the uncertain variables whereas non-probabilistic approaches only use information about the range of uncertain variables. Since in most cases the distribution of the design variables is not available at the early stage of the design process, non-probabilistic methods are generally considered more practical. One of the most popular non-probabilistic approaches is to consider uncertain inputs as bounded variables, *i.e.*, uncertain-but-bounded, and find the worst combination of the bounds which results in the lowest performance of the design, *i.e.*, the worst case [17].

Optimization of hybrid composite laminates is not a simple problem due to the contribution of several variables such as fibre type, orientation angle and volume fraction of individual laminas together with the existence of the hybrid effect [18]. This hybrid effect is defined as the deviation of a property from that calculated based on the rule of mixtures (RoM) [19] and has recently been explained in terms of the stress profile through the thickness of the composite [18]. Therefore, efficient optimization tools will be required to achieve the optimal and robust design of such composite materials. Several studies have investigated the problem of optimizing composite materials with different objectives and constraints such as maximizing strength, stiffness and buckling load capacity, and minimizing weight and cost [20-27].

In most actual applications of optimization problems, more than one objective is normally incorporated and hence the optimization problem is multi-objective. Unlike single-objective optimization, the result of a multi-objective problem is not unique and a set of optimum results would be expected. Such a set of optimal results obtained from multi-objective optimization is called a Pareto optimal set. Existing methods for finding the Pareto optimal set for multi-objective optimization problems are classified into “preference-based classical methods” and “multi-objective evolutionary algorithms (MOEA)” [28]. Whilst preference-based classical methods are easier to solve compared to MOEAs, a disadvantage is that they require the preference of objectives as an input, which is not always clear to the designer without prior knowledge of the optimal results. In contrast to this, MOEAs start with initial random data and converge to a Pareto optimal set through a

number of evolutions without using the preference of objectives. Once a Pareto optimal set has been obtained, different options can be compared and the final choice, *i.e*, optimum solution, can be determined. Several MOEAs have been proposed thus far, *e.g.*, strength Pareto evolutionary algorithm (SPEA-II) [29], Pareto archived evolutionary strategy (PAES) [30] and the non-dominated sorting genetic algorithm (NSGA) [31]. A modified version of NSGA, NSGA-II, is one of the most popular MOEAs and has been used by several researchers in the field of composite optimization.

The present study is a continuation of previous research by the current authors [18, 32-34] and aims to investigate the multi-objective optimization and robust design of multi-directional carbon/glass fibre-reinforced hybrid composites when different sources of uncertainties are considered. The effects of three sources of uncertainties, namely, existence of matrix voids, fibre misalignment and thickness variation, on optimal and robust designs were studied with the main focus being the influence of matrix voids. For this purpose, a modified version of the non-dominated sorting genetic algorithm (NSGA-II) was employed for multi-objective optimization and the worst case of the uncertainties was found through an anti-optimization method [35] using a simple genetic algorithm (GA). The density and material cost were chosen as objectives and hybrid composites with different minimum required values of flexural strength were studied.

## 8.2. Hybrid Composite Model

### 8.2.1. Flexural Strength

Fibre-reinforced epoxy hybrid composites containing six laminas under three-point bending load were investigated as shown in Figure 8-1 where *L*, *w* and *h* are the span, width and total thickness of the composite, respectively. High strength T700S carbon and S-2 glass fibres were chosen for the laminas in order to ensure the possibility of achieving a positive hybrid effect as noted previously [18, 32, 33]. The properties of the fibres and matrix used in this study are presented in Table 8-1.

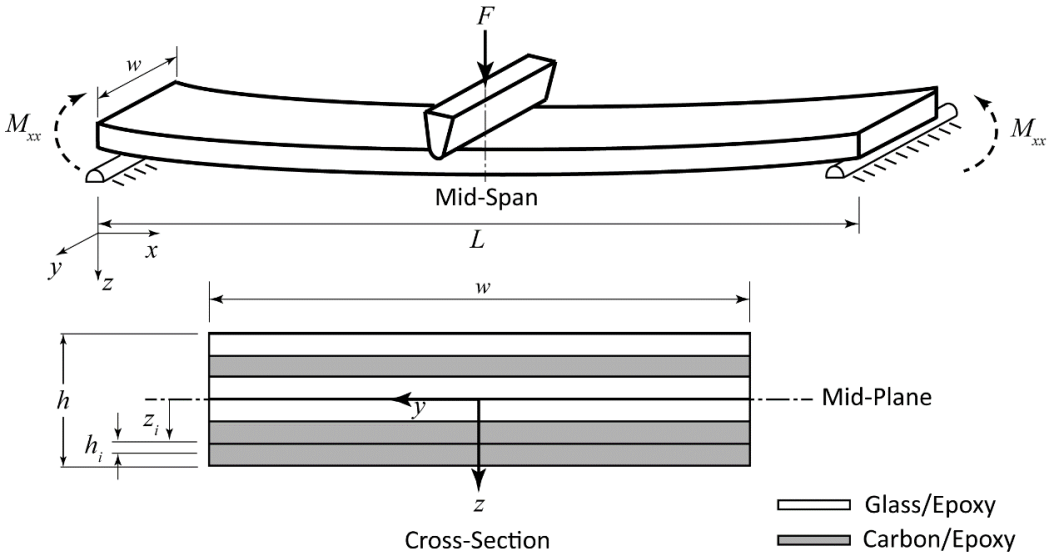


**Figure 8-1: Schematic representation of the carbon/glass fibre-reinforced hybrid composite specimen in the three-point bending configuration.**

**Table 8-1: Mechanical properties and cost of the fibres and matrix utilized in this study [32].**

| Material | High strength carbon fibre [a] | High strength glass fibre [b] | High performance epoxy matrix [c] |
|---|---|---|---|
| Tensile Modulus (GPa) | *Long.* 230<br>*Trans.* 14 | 86.9 | 3.1 |
| Poisson's Ratio | *Long.* 0.2<br>*Trans.* 0.4 | 0.2 | 0.3 |
| Tensile Strength (MPa) | 4900 | 4890 | 69.6 |
| Strain to Failure (%) | 2.1 | 5.6 | ~4 |
| Density (kg/m$^3$) | 1800 | 2460 | 1090 |
| Cost ($/litre)* | 151.2 | 103.3 | 26.2 |

* All material prices were converted to US$.

a T700S® 12K, Toray Industries, Inc., Tokyo, Japan

b S-2 glass unidirectional Unitex plain weave UT-S500 fibre mat, SP System, Newport, Isle of Wight, UK.

c Kinetix R240 high performance epoxy resin with H160 hardener at a ratio of 4:1 by weight, ATL Composites Pty Ltd., Australia.

### 8.2.2. Stiffness and Strength When Matrix Voids Are Present

The main role of the matrix in fibre-reinforced composite material is to transfer load between the fibres and to support fibres under compressive load. Therefore, when voids exist within the matrix, the transverse and shear moduli and strengths, as well as the longitudinal compressive strength are significantly affected by voids [11] because they are strongly dependent on matrix properties and are so called "matrix-dominated properties". In contrast to this, the longitudinal tensile modulus and strength are mainly affected by fibre properties and are therefore known as "fibre-dominated properties" and, consequently, are not significantly affected by the presence of voids. However, in order to achieve accurate results in optimization problems, all these effects should be taken into account. Several researchers have predicted the effective stiffness and strength of composite laminates when voids are present [9-13]. In this study the void content, $V_v$, is defined to be with respect to the matrix only and the analytical model recently proposed by Dong [11] was used due to its simplicity and good agreement with experimental results. Dong used the Kerner model [36] to estimate the effective modulus and Poisson's ratio of the matrix when voids were present. Together with the effective modulus and Poisson's ratio of the matrix, the longitudinal, transverse and shear moduli of fibre-reinforced laminas were found by utilizing Hashin's circular cylinder model (CCM) [37].

The longitudinal tensile strength of a fibre-reinforced lamina is governed by the strain-to-failure of the fibres with the matrix properties having little effect. However, for high elongation fibres (*e.g.*, glass fibres), the possibility of matrix failure prior to fibre failure must also be evaluated.

For the transverse and shear strengths, as well as the longitudinal compressive strength, previous research [11] has indicated that these strength components can be predicted with a regression model as given by:

$$\overline{S} = \begin{cases} 1 & , \ V_v \leq 2\% \\ \left(0.4964 - \frac{0.02668}{V_f^2}\right) V_v^{-\left(0.1546 + \frac{0.02126}{V_f^2}\right)} & , \ V_v > 2\% \end{cases} \quad (8\text{-}1)$$

where $\overline{S}$ is the normalised strength, *i.e.* $\overline{S} = \frac{S}{S_0}$, and $S$ and $S_0$ are strengths with and without voids, respectively.

Equation (8-1) shows that the aforementioned strength components are not affected by matrix void contents up to 2% but decrease for matrix void contents greater than 2%. The normalised strength, $\overline{S}$, from Equation (8-1) can be used to calculate the corresponding strength when voids are present.

Knowing the strength and modulus components of the laminas, the stress distribution across each lamina due to an applied force, $F$, at the mid-span of the specimen could be determined using classical lamination theory (CLT). It was considered that the span-to-depth ratio of the specimen was sufficiently high as to neglect the effect of inter-laminar shear stress and contact stress in the proximity of the failure region, *i.e.*, mid-span, using CLT. Following this, maximum failure strength theory [1] was employed to estimate the maximum allowable force, $F_{max}$, which could be applied before first ply failure (FPF) occurred. Flexural strength is defined as the maximum allowable stress within the material prior to failure based on the assumption of a linear stress distribution through the thickness. Although the stress distribution is not linear in the composite specimens investigated in this study, for evaluating the maximum load before failure the apparent flexural strength, $S_F$, of the composite specimen was calculated using the following equation:

$$S_F = \frac{3F_{max}L}{2wh^2} \quad (8\text{-}2)$$

Since flexural strengths in both major directions, *i.e.*, *x* and *y*, are important in the real application of multi-directional composites, the flexural strengths in both directions were calculated individually and the lower value was considered to be the flexural strength of the composite.

It should be noted that, whilst the normalised strength of laminas is not changed for void contents of less than 2%, the lamina modulus is affected by even a small amount of voids and therefore the composite strength will change; such a relationship between lamina modulus and lamina strength was observed in a recent study [18].

### 8.2.3. Robust Design Optimization

In most applications of composite materials, cost, weight and strength are of main concern. However, the material cost and density of carbon/glass fibre hybrid composites are two conflicting objectives, *i.e.*, by incorporating additional carbon fibres instead of glass fibres the density will be reduced at the expense of material cost and *vice versa*. Furthermore, the density, material cost and flexural strength of such composites exhibit a non-linear relationship with the design variables and, thus, the problem of finding optimal stacking configurations will be arduous.

A robust design optimization (RDO) problem was defined to find the optimal stacking configurations for hybrid composites which possessed the minimum required strength while simultaneously minimizing their cost and weight. Carbon/glass fibre-reinforced hybrid composites with six laminas were studied as shown in Figure 8-1 with the fibre type, orientation angle and volume fraction of each lamina being considered as design variables. The lamina thickness and fibre orientation angle were considered to be uncertain-but-bounded variables due to manufacturing tolerances. The effect of uncertainties in the modulus and strength of the composites due to the presence of matrix voids was also incorporated into the model.

The material cost and density of the hybrid composites were considered to be objectives with the minimum required flexural strength being a constraint. Thus,

the multi-objective robust design optimization problem, when all sources of uncertainties were incorporated, could be formulated as follows:

$$\left.\begin{array}{l} Minimize \begin{cases} \rho_c\left(m_i, V_{fi}^{nom}, \theta_i^{nom}\right) \\ C_c\left(m_i, V_{fi}^{nom}, \theta_i^{nom}\right) \end{cases} \\ Subject\ to\ contraints: \\ \quad \eta_g \le 0 \\ where\ \ \eta_g = \max\left\{-S_F\left(m_i, h_i^{act}, V_{fi}^{act}, \theta_i^{act}, V_v\right) + S_{F0}\right\} \end{array}\right\} \quad (8\text{-}3)$$

$$and \quad V_{fi}^{act} = V_{fi}^{nom} \frac{h_i^{nom}}{h_i^{act}}$$

where $C_c$ is the material cost per unit volume and $\rho_c$ is the density of a carbon/glass hybrid composite. Values of $C_c$ and $\rho_c$ were calculated based on Rule of Mixtures (RoM) using the typical cost and density of the constituent materials shown in Table 8-1 in a similar manner to previous work [34]. $S_F$ is the actual flexural strength of the hybrid composite from Equation (8-2) and $S_{F0}$ is the minimum required flexural strength as a constraint. $V_{fi}$, $\theta_i$and $m_i$ are the fibre volume fraction, fibre orientation angle and fibre type of the *i*th lamina, respectively. The superscripts *nom* and *act* indicate the nominal and actual values, respectively, whilst $\eta_g$ is the maximum violation of the constraint.

Equation (8-3) is a generic form of robust and optimal design and can be used for both carbon fibre and glass fibre as well as for hybrid composites by adjusting $m_i$. For example, in the case of pure glass fibre composites, the fibre type of all laminas, $m_i$ (*i.e.*, $m_1$ to $m_6$), is set to glass fibre type. The nominal value of each variable, *i.e.*, the value if no uncertainties are present, together with the lower and upper limits of each variable used in this study are shown in Table 8-2.

**Table 8-2: The range and nominal values of the variables used in this robust optimization problem.**

| Variable | Lower Bound | Upper Bound | Nominal Value Domain |
|---|---|---|---|
| $h_i$ | $h_i^{nom} - 0.1h_i^{nom}$ | $h_i^{nom} + 0.1h_i^{nom}$ | $h_i^{nom} = 0.2$ mm |
| $V_{fi}$ | $\frac{h_i^{nom}}{\max(h_i)} V_{fi}^{nom}$ | $\frac{h_i^{nom}}{\min(h_i)} V_{fi}^{nom}$ | $\{30\%, 35\%, \ldots, 65\%, 70\%\}$ |
| $\theta_i$ | $\theta_i^{nom} - 3^o$ | $\theta_i^{nom} + 3^o$ | $\{0°, 45°, -45°, 90°\}$ |
| $V_v$ | - | - | {0%, 1%, 2%, 3%, 5%} |

It should be noted that in most manufacturing processes the number of fibres can be controlled and uncertainties in fibre volume fraction are therefore due to variations in the lamina thickness. Thus, the nominal values of the fibre volume fraction for each lamina would be fixed with their true value being affected by the actual thickness as shown in Table 8-2 and Equation (8-3).

The variable $\eta_g$ in Equation (8-3) is the maximum violation of the constraint and was defined to identify and reject those designs which violated the minimum strength constraint when uncertainties were considered. In order to calculate $\eta_g$, all combinations of the upper and lower bounds and nominal values of uncertain variables were evaluated with the worst case, *i.e.*, minimum strength, being determined. Flexural strength can be estimated from Equation (8-2). This equation has been derived based on static equilibrium when the maximum allowable load before failure is applied. When uncertain variables are involved, this equation will be still valid if variations of the uncertain variables are considered. For this reason, the actual value of the thickness, *h*, and maximum allowable force, $F_{max}$, associated with the worst case has been used in Equation (8-2). Then, those designs which did not violate the constraints even in the worst case when uncertainties were incorporated, are considered to be robust designs. In a robust optimization problem, the multi-objective optimization solver aims to find the optimal solutions among the robust designs.

Evolutionary algorithms offer an effective way of finding the solution of complex and large size optimization problems. GA is one of the most well-known evolutionary algorithms and has been widely used in various engineering fields [38-41]. As previously mentioned, among all MOEAs available, NSGA-II, which generates solutions through the use of genetic operators, is currently the most popular method for solving multi-objective optimization due to its simplicity, the ability of global searching, fast convergence and achieving well distributed non-dominated solutions in a single run. Therefore, NSGA-II was chosen in this study as the multi-objective optimizer. NSGA-II starts with a random set of variables, known as the initial population, and converges to optimal results (Pareto optimal set) through a number of generations. The number of generations and size of the initial population varies in different problems. In order to ensure that the obtained results were a global optimum, *i.e.*, not local optimum, the optimization problem would normally be run several times with the best results of each run being collected as the final result. For the problem investigated here, typically 500 generations were completed with an initial population of 300 members and the convergence was assessed by running each problem five times. Violation of individual designs must be evaluated in each generation in order to identify the worst cases and maintain the robust designs. The composite comprised of six laminas and for each lamina there were two uncertain variables, *i.e.*, fibre orientation angle, $\theta_i$, and lamina thickness, $h_i$, and for each variable there were three possible values (nominal, lower and upper bound). Thus, there existed $3^{2\times6}$ possible combinations for each design set. Calculating all combinations of uncertain variables for all individual members within each generation would be extremely time consuming. One solution to overcome this difficulty is through the use of an anti-optimization method [35]. Instead of calculating the strength of all members in order to determine the maximum violation, a simple GA was introduced within NSGA-II to find the minimum strength when uncertainties were incorporated, *i.e.*, the worst case. Hence, the multi-objective optimization algorithm (NSGA-II) was combined with an anti-optimization algorithm and a new hybrid algorithm was proposed. A flowchart of the combined optimization and anti-optimization algorithm has been presented in Figure 8-2. It was found that the GA anti-optimizer could find the

worst case after eight generations with an initial population of 100 members – this reduced the processing time by a factor of 600 when compared to evaluating all 531,441 (*i.e.*, $3^{2\times6}$) possible cases.

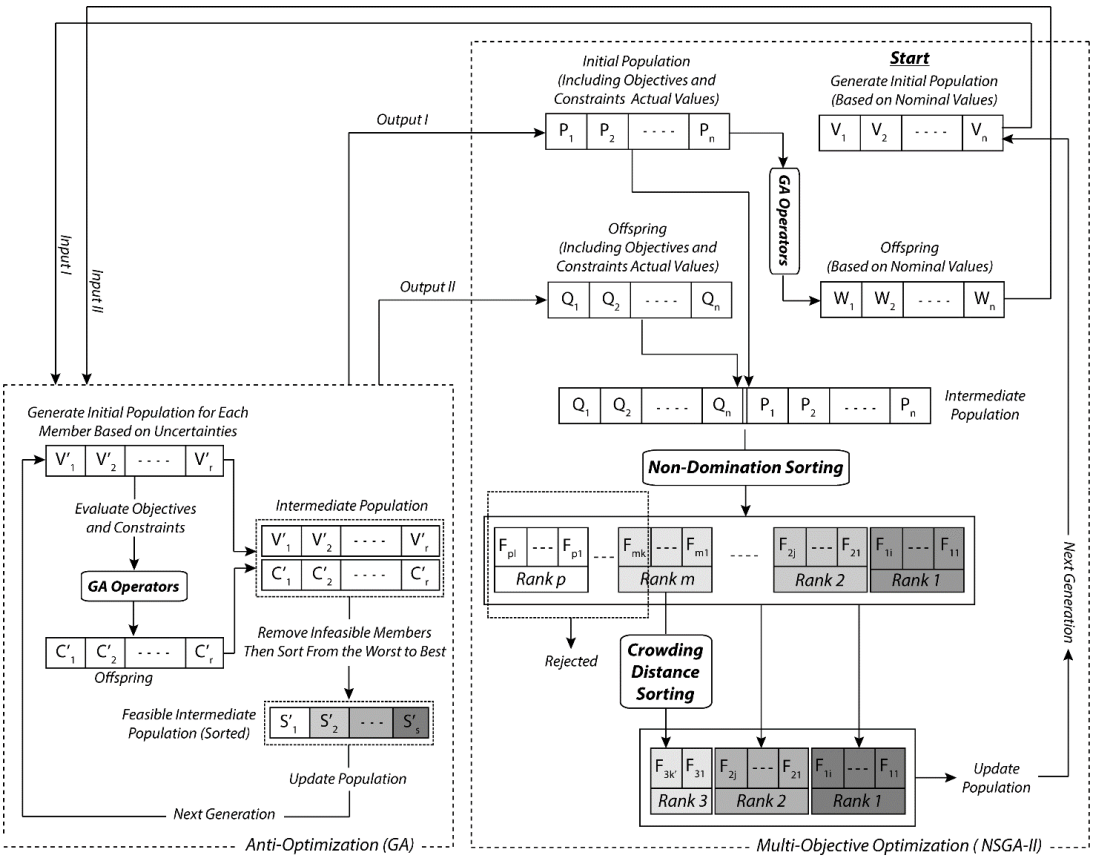


**Figure 8-2: Combined optimization and anti-optimization algorithm used for the multi-objective robust optimization.**

## 8.2.4. Model Validation

The CLT model presented in Section 2.2 was validated against experimental data for unidirectional glass/carbon hybrid composites investigated in a previous study [42]. Glass fibres were placed at the compressive side with the flexural strength being considered for three situations: (i) no uncertainties being considered (NU), (ii) uncertainties in fibre angle orientation and lamina thickness being considered (UAT) and (iii) uncertainties in fibre angle orientation and lamina thickness being considered together with the presence of 3% void content (UVAT). Flexural strengths obtained from the model are shown in Figure 8-3 together with experimental data as a comparison. It can be seen from Figure 8-3 that, by

replacing a thin carbon fibre lamina at the compressive side with a glass fibre lamina with higher fibre volume fraction, the flexural strength of the hybrid composite is improved and a positive hybrid effect is noted. However, when no uncertainties are included, *i.e.*, NU, the model prediction significantly overestimates the experimental results. In contrast to this, when uncertainties are included, *i.e.*, UAT and UVAT, the lower bounds are reduced significantly when compared to the nominal (NU) result. Therefore, in order to achieve a robust and reliable design it is necessary that the real lower bounds be determined through incorporating all uncertainties (UVAT).

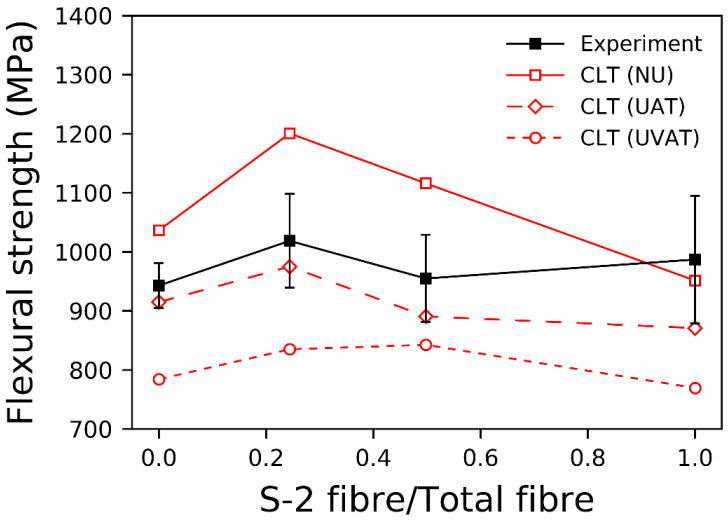


**Figure 8-3: Comparison of results for the flexural strength of unidirectional carbon/glass fibre-reinforced hybrid composite. (NU) - no uncertainties were included; (UAT) - uncertainties in fibre angle orientation and lamina thickness were included; (UVAT) - uncertainties in fibre angle orientation and lamina thickness were included together with the presence of 3% void content.**

The validated model and hybrid optimization and anti-optimization algorithms mentioned in Section 2.3 were then used to find solutions for the multi-objective robust optimization problem of carbon/glass fibre-reinforced epoxy hybrid composites comprising 6 laminas (as shown in Figure 8-1). Minimum required flexural strengths of 500 MPa, 600 MPa, 700 MPa and 800 MPa were investigated with Pareto optimal sets being obtained for each case. The effect of matrix voids at four different levels of void content, namely, 1%, 2%, 3% and 5%, together with the effects of ±10% variation in lamina thickness and ±3º variation in fibre orientation angle, were incorporated into the problem.

## 8.3. Results and Discussion

### 8.3.1. Effect of Voids

Given the aforementioned minimum required flexural strengths, the Pareto optimal fronts for hybrid composites with different levels of void content are presented in Figure 8-4.

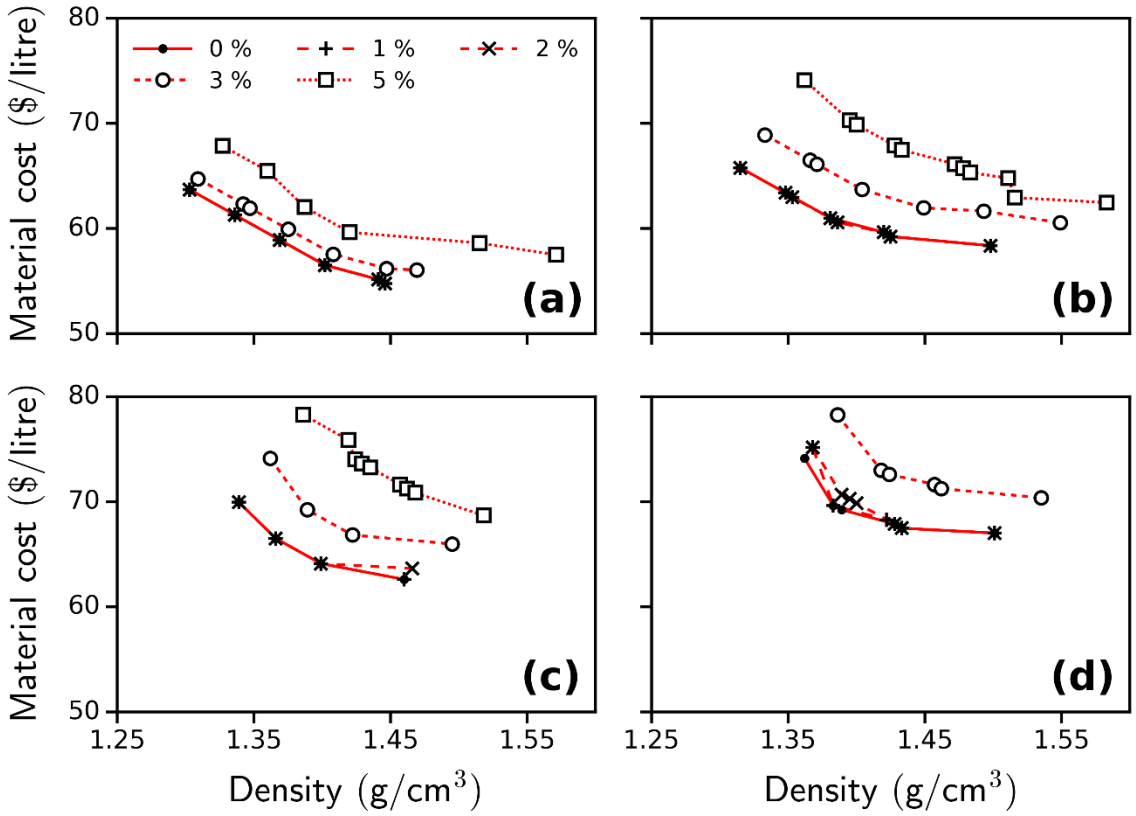


**Figure 8-4: The effect of void induced uncertainties on the Pareto optimal fronts for multi-directional T700S carbon/S-2 glass fibre-reinforced epoxy composites: (a) $S_0$ = 500 MPa, (b) $S_0$ = 600 MPa, (c) $S_0$ = 700 MPa and (d) $S_0$ = 800 MPa.**

It can be seen from Figure 8-4 that, in general, the presence of voids up to 2% does not significantly affect the performance of the optimal results with the Pareto optimal fronts for hybrid composites with $V_v$ = 0%, 1% and 2% being identical irrespective of the void content. However, for void contents of greater than 2%, *i.e.*, $V_v$ = 3% and 5%, the cost and/or weight of the optimal solutions for minimum required strengths of 500 MPa, 600 MPa and 700 MPa increased. In these cases, the Pareto optimal fronts moved away from the origin (intersection of the cost and

density axis), which is attributed to the degrading effect of voids for void contents of more than 2%. Furthermore, the distance between curves in each figure indicated the effectiveness of the voids, *i.e.*, the larger distance between the Pareto optimal fronts illustrated the higher degrading effect of the voids. By comparing Figures 8-4(a), 8-4(b) and 8-4(c), it can be observed that the distance between curves increased with the minimum required strength; therefore, it can be concluded that voids had a more serious degrading effect on the performance of the higher strength hybrid composites. It should be noted that in Figure 8-4(d) the Pareto front for a minimum required strength of 800 MPa and 5% void content could not be achieved due to the high degrading effect of such a large void content. However, the distances between the existing curves in Figure 8-4(d) were clearly visible which indicated the large negative effect of even small void contents (1% and 2%) on the cost and weight of high strength hybrid composites.

It has been shown [11] that whilst void contents less than 2% do not affect the strengths of composites, they do however reduce the moduli and hence it might be possible (based on the stacking configuration) that the presence of matrix voids could actually improve the composite flexural strength. On the other hand, it has been reported that lamina strength reduction due to voids decreases with increasing fibre volume fraction [11]. Thus, in certain cases for high strength hybrid composites with a high fibre volume fraction, the density and cost of the optimal composites may decrease when small amounts of voids are included. Such a phenomenon can be observed in Figure 8-5 for minimum required strengths of 700 MPa and 800 MPa when uncertainties in fibre angle orientation were also considered.

In Figure 8-5(a), the last optimal solutions for the 1% and 2% void contents are below the Pareto optimal front for 0% void content which shows that the presence of voids improves the strength and thus reduces the cost and/or weight of the material. The stacking sequence corresponding to the third data point in Figure 8-5(a) for the case without voids is given by $[0_c^{55\%}/90_g^{30\%}/90_c^{30\%}/0_g^{30\%}/0_c^{35\%}/90_c^{30\%}]$. When the void content is 2%, the respective stacking sequence is $[0_c^{50\%}/90_g^{30\%}/90_c^{30\%}/0_g^{30\%}/0_c^{35\%}/90_c^{30\%}]$. It is seen that the fibre volume fraction of

the first lamina decreases from 55% to 50% while all the other laminas remain unchanged. Similarly, in Figure 8-5(b), the Pareto optimal front for 2% void content is below that of the 1% case and the last solution point is even below the 0% curve. The stacking sequence corresponding to the fourth data point in Figure 8-5(b) for the case without voids is given by $[0_c^{60\%}/90_g^{55\%}/90_g^{30\%}/0_g^{30\%}/0_c^{45\%}/90_c^{30\%}]$. When the void content is 2%, the respective stacking sequence is $[0_c^{60\%}/90_g^{55\%}/90_g^{30\%}/0_g^{30\%}/0_c^{40\%}/90_c^{30\%}]$. It is seen that the fibre volume fraction of the fifth lamina decreases from 45% to 40% while all the other laminas remain unchanged. Thus, both the density and cost decrease when 2% void content is present.

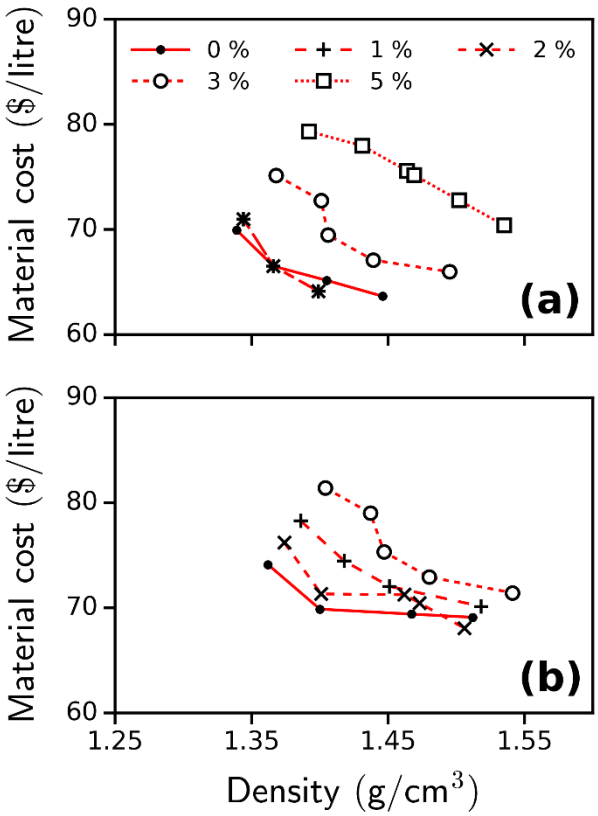


**Figure 8-5: Illustration of special cases in which small amounts of void content may improve composite flexural strength. Shown are Pareto optimal fronts for multi-directional T700S carbon/S-2 glass fibre-reinforced epoxy composites when uncertainties in fibre orientation angle and void content were considered: (a) $S_0$ = 700 MPa and (b) $S_0$ = 800 MPa.**

### 8.3.2. Effect of Uncertainty Sources

Uncertainties in other variables apart from void content, *e.g.*, fibre orientation angle and lamina thickness, also affect the strength, cost and weight of hybrid composites, and therefore the optimal solutions will be affected. In order to compare the effects of uncertainty sources, Pareto optimal fronts for the case of only one uncertainty source being present are plotted in Figure 8-6. Since it was shown previously that the effect of void contents less than 2% was usually negligible and that the Pareto optimal front for 5% void content could not be achieved for the 800 MPa composite strength, the level of void content for the curves in Figure 8-6 was chosen to be $V_v$ = 3%.

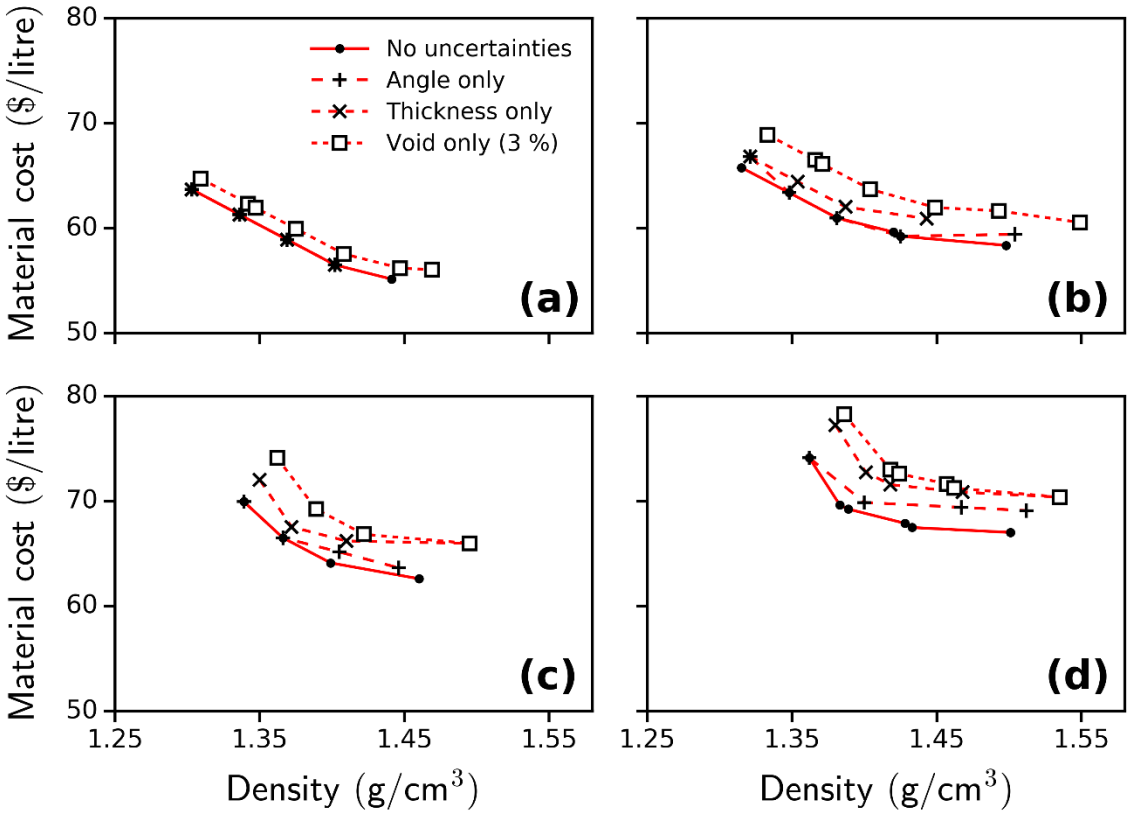


**Figure 8-6: The effect of different sources of uncertainties on the Pareto optimal fronts for multi-directional T700S carbon/S-2 glass fibre-reinforced epoxy composites: (a) $S_0$ = 500 MPa, (b) $S_0$ = 600 MPa,(c) $S_0$ = 700 MPa and (d) $S_0$ = 800 MPa.**

It can be observed from Figure 8-6 that, in general, uncertainties in angle and thickness have relatively less effect on the Pareto optimal solutions with Pareto optimal fronts for the composites containing only voids being above the other

curves. Simply stated, the degrading effect of 3% void content is greater than that of a 10% variation in thickness or a 3º variation in fibre orientation angle. Therefore, from the point of view of manufacturing, control of void content appears to be more effective than improving either the tolerance of thickness or fibre angle of laminas (for typical manufacturing tolerances).

It can be seen from Figure 8-6(a) that the optimal hybrid composites with a minimum required strength of 500 MPa are insensitive to uncertainties in thickness and angle. However, by increasing the minimum required strength it can be seen from Figures 6(b), 8-6(c) and 8-6(d) that uncertainties in lamina thickness play a more significant effect when compared to uncertainties in fibre orientation angle. It can also be noted that, upon increasing the minimum required strength, the distances between the curves increase which indicates that the effect of all sources of uncertainties become more important for high strength composites.

Further investigations were conducted to determine the effect of different uncertainty sources and their combinations. For optimization problems in which weight is the main design concern, minimising density is the main optimisation objective. In this case, the density of the lightest optimal composites is presented in Table 8-3. On the other hand, in some situations minimising cost is the main optimisation objective and for this case the cost of the cheapest optimal composites is shown in Table 8-4. In order to address each case more conveniently, ID codes were assigned to each case as shown in the first column of Table 8-3 and 8-4. In this column, “U” indicates uncertainty and “A”, “T” and “V” indicate the existence of uncertainties in fibre orientation angle, lamina thickness and the presence of 3% matrix voids, respectively. For example, UA and UAT represent cases with uncertainties in angle only and uncertainties in angle and thickness without voids, respectively, whereas UVAT represents the case with all source of uncertainties, *i.e.*, fibre angle and thickness when voids are present. In addition, NU denotes the “ideal” situation without any sources of uncertainty. For additional clarity, the second, third and fourth columns of Table 8-3 and 8-4 indicate the value of that particular uncertainty. It should be noted that, for the minimum required

strength of 800 MPa, when all sources of uncertainties were incorporated no solution could be found.

In order to measure the contribution of uncertainty sources on the optimal results, a Pareto ANOVA method was used. Pareto ANOVA, which is a simplified analysis of the variance (ANOVA) method, is a quick and simple technique to evaluate the results of a parametric design without establishing an ANOVA table [43, 44]. Figure 8-7 shows the results of the Pareto ANOVA analysis corresponding to the data in Table 8-3 for the lightest optimal designs and Table 8-4 for the cheapest optimal designs. The horizontal axis indicates the source of uncertainty and interaction between different sources while the vertical axis is the percentage of contribution. For example, "V" indicates the contribution of 3% void content on the performance of the optimal results (which is relatively high for all designs) whereas "V×T" denotes the contribution of the interaction between 3% void content and variation in thickness (which is relatively low). Since no solution could be found for composites with a minimum required strength of 800 MPa when all sources of uncertainties were present, *i.e.*, UVAT, the Pareto ANOVA analysis was only applied to minimum required strengths of 500 MPa, 600 MPa and 700 MPa.

**Table 8-3: Density of the lightest optimal composites subject to minimum required strengths of 500 MPa to 800 MPa.**

| ID | Void content (%) | Thickness variation (±%) | Misalignment angle (±º) | Density (g/cm$^3$) | | | |
|---|---|---|---|---|---|---|---|
| | | | | $S_0$ = 500 MPa | $S_0$ = 600 MPa | $S_0$ = 700 MPa | $S_0$ = 800 MPa |
| **NU** | 0 | 0 | 0 | 1.303 | 1.315 | 1.339 | 1.362 |
| **UA** | 0 | 0 | 3 | 1.303 | 1.321 | 1.339 | 1.362 |
| **UT** | 0 | 10 | 0 | 1.303 | 1.321 | 1.350 | 1.380 |
| **UAT** | 0 | 10 | 3 | 1.303 | 1.327 | 1.356 | 1.392 |
| **UV** | 3 | 0 | 0 | 1.309 | 1.333 | 1.362 | 1.386 |
| **UVA** | 3 | 0 | 3 | 1.321 | 1.339 | 1.368 | 1.404 |
| **UVT** | 3 | 10 | 0 | 1.315 | 1.344 | 1.380 | 1.427 |
| **UVAT** | 3 | 10 | 3 | 1.333 | 1.350 | 1.386 | - |

**Table 8-4: Cost of the cheapest optimal composites subject to minimum required strengths of 500 MPa to 800 MPa.**

| ID | Void content (%) | Thickness variation (±%) | Misalignment angle (±º) | Cost ($/litre) | | | |
|---|---|---|---|---|---|---|---|
| | | | | $S_0$ = 500 MPa | $S_0$ = 600 MPa | $S_0$ = 700 MPa | $S_0$ = 800 MPa |
| **NU** | 0 | 0 | 0 | 55.16 | 58.37 | 62.61 | 67.02 |
| **UA** | 0 | 0 | 3 | 56.05 | 59.42 | 63.65 | 69.10 |
| **UT** | 0 | 10 | 0 | 56.69 | 60.92 | 65.98 | 70.39 |
| **UAT** | 0 | 10 | 3 | 56.51 | 60.92 | 66.84 | 71.90 |
| **UV** | 3 | 0 | 0 | 56.05 | 60.55 | 65.98 | 70.39 |
| **UVA** | 3 | 0 | 3 | 57.33 | 61.59 | 65.98 | 71.43 |
| **UVT** | 3 | 10 | 0 | 57.51 | 62.94 | 69.57 | 75.84 |
| **UVAT** | 3 | 10 | 3 | 58.62 | 64.29 | 70.39 | - |

The results of Pareto ANOVA in Figure 8-7 show that, for the lightest optimal design, void-induced uncertainties ($V_v$ = 3%) have the largest effect. Following voids, uncertainties due to a 10% variation in lamina thickness exhibit the second largest effect with uncertainties due to a 3º variation in fibre orientation angle being the least effective uncertainty source. In contrast to this, for the cheapest optimal design, void-induced uncertainties ($V_v$ = 3%) and uncertainties due to a 10% variation in lamina thickness have comparable effects, with uncertainties due to a 3º variation in fibre orientation angle being the least effective uncertainty source. Thus, when light composites are of most concern, controlling the void content is more effective rather than controlling fibre angle orientation and lamina thickness. In contrast to this, when cheap composites are required, the importance of controlling both thickness and void content are more effective when compared to fibre angle orientation.

Figure 8-7 also shows that the effect of thickness variation increased with minimum required strength. This is because the variation in fibre volume fraction caused by the thickness variation is proportional to the fibre volume fraction, as indicated in Table 8-2. Since higher strength composites have laminas with a higher fibre volume fraction, the effect of thickness variation increases for higher strength

composites. On the other hand, the effect of fibre misalignment angle decreases with increasing minimum required strength.

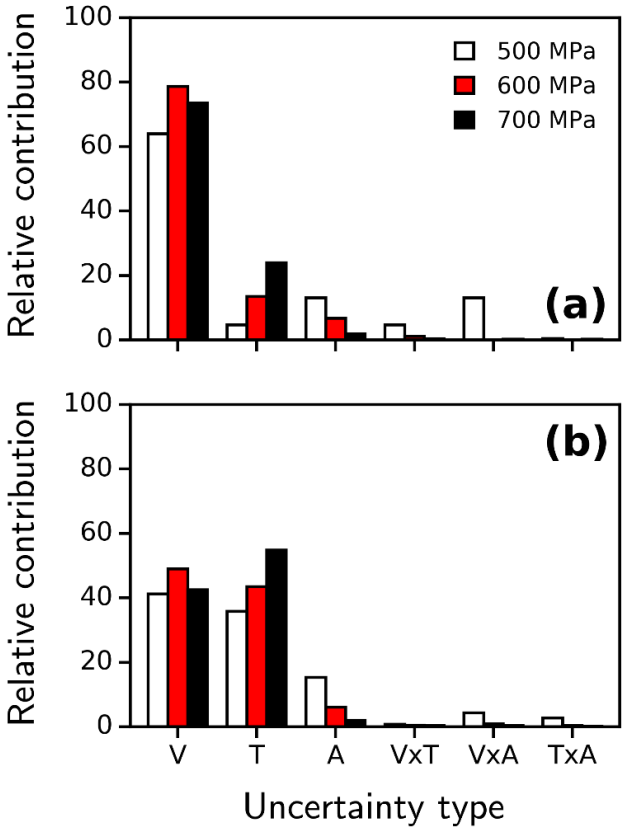


**Figure 8-7: Influence of uncertainty type on relative contribution: (a) lightest optimal composite - influence on density and (b) cheapest optimal composite - influence on cost.**

Detailed information concerning the optimal solutions for different combinations of uncertainty sources with 3% void content are presented in Tables 8-5 to 8-8.

From the optimal stacking configurations in Table 8-5 to 8-8 it is noted that, in general, laminas at the compressive (left) side possess higher volume fractions compared to laminas at the tensile side and that they are more affected by uncertainties, whereas laminas at the tensile (right) side are almost insensitive to uncertainties. This result is in agreement with experimental research [42] which reported the failure mode of carbon/glass fibre hybrid composites under bending load to be micro-buckling of fibres at the compressive side with the laminas at the compressive side being critical laminas, *i.e.*, first failed lamina (FPF). Since the two laminas at the outermost compressive side play an important role in the strength of

such composites, the first lamina is oriented at 0º to support the compressive load in the *x* direction with the second lamina being oriented at 90º to support the compressive load in the *y* direction. Similarly, the two outermost laminas at the tensile side carry most of the tensile load in bending and they were perpendicular to each other so that the composite could carry maximum load in both directions. Such a configuration allows the composite to possess the maximum possible flexural strength in both directions (and not only in one direction). The two laminas close to the mid-plane are the least load carrying elements and their orientation, fibre type and volume fraction may be used to adjust the cost, density and strength of the composite. Thus, for predicting the optimal and robust design of hybrid composites under bending load when uncertainties are incorporated, it is recommended that the fibre volume fraction of the outermost two laminas at the compressive side be increased by approximately 5% to 15% in order to overcome the degrading effect of uncertainties whilst the two outermost laminas at the tensile side can remain unchanged. In addition, the fibre type of the second, third and fourth laminas can be changed from carbon to a higher volume fraction of glass fibre in order to reduce the material cost although at the expense of higher composite density.

**Table 8-5: Optimal solutions achieved for a minimum required strength of 500 MPa*.**

| | ID | Stacking Configuration, $\theta^{\text{Vf \%}}_{\text{fibre type}}$ (compressive side at left) | Density (g/cm³) | Cost ($/litre) | $S_{Fxx}$ (MPa) | $S_{Fyy}$ (MPa) | FPF** |
|---|---|---|---|---|---|---|---|
| No Uncertainties | NU 1 | $0_c^{30\%}$ / $90_c^{30\%}$ / $+45_c^{30\%}$ / $0_c^{30\%}$ / $0_c^{30\%}$ / $90_c^{30\%}$ | 1.303 | 63.70 | 510 | 574 | 1-X |
| | NU 2 | $0_c^{30\%}$ / $90_g^{30\%}$ / $+45_c^{30\%}$ / $-45_c^{30\%}$ / $0_c^{30\%}$ / $90_c^{30\%}$ | 1.336 | 61.30 | 521 | 519 | 2-Y |
| | NU 3 | $0_c^{30\%}$ / $90_c^{30\%}$ / $+45_g^{30\%}$ / $+45_g^{30\%}$ / $0_c^{30\%}$ / $90_c^{30\%}$ | 1.369 | 58.91 | 523 | 570 | 1-X |
| | NU 4 | $0_c^{30\%}$ / $0_g^{30\%}$ / $-45_g^{30\%}$ / $90_g^{30\%}$ / $0_c^{30\%}$ / $90_c^{30\%}$ | 1.402 | 56.51 | 574 | 584 | 1-X |
| | NU 5 | $0_g^{30\%}$ / $90_g^{30\%}$ / $-45_g^{30\%}$ / $0_g^{30\%}$ / $90_c^{35\%}$ / $0_c^{30\%}$ | 1.441 | 55.16 | 520 | 510 | 1-Y |
| Void-Induced Uncertainties | UV 1 | $0_c^{35\%}$ / $0_c^{30\%}$ / $-45_c^{30\%}$ / $+45_c^{30\%}$ / $0_c^{30\%}$ / $90_c^{30\%}$ | 1.309 | 64.74 | 583 | 560 | 4-Y |
| | UV 2 | $0_c^{35\%}$ / $0_c^{30\%}$ / $-45_c^{30\%}$ / $+45_g^{30\%}$ / $0_c^{30\%}$ / $90_c^{30\%}$ | 1.342 | 62.35 | 582 | 540 | 1-Y |
| | UV 3 | $0_g^{35\%}$ / $0_c^{30\%}$ / $-45_c^{30\%}$ / $+45_c^{30\%}$ / $0_c^{30\%}$ / $90_c^{30\%}$ | 1.347 | 61.95 | 539 | 505 | 1-Y |
| | UV 4 | $0_c^{35\%}$ / $0_c^{30\%}$ / $-45_g^{30\%}$ / $+45_g^{30\%}$ / $0_c^{30\%}$ / $90_c^{30\%}$ | 1.375 | 59.95 | 582 | 504 | 1-Y |
| | UV 5 | $0_c^{35\%}$ / $0_g^{30\%}$ / $-45_g^{30\%}$ / $+45_g^{30\%}$ / $0_c^{30\%}$ / $90_c^{30\%}$ | 1.408 | 57.56 | 523 | 521 | 1-Y |
| | UV 6 | $0_c^{40\%}$ / $-45_g^{30\%}$ / $+45_g^{30\%}$ / $90_g^{30\%}$ / $0_c^{30\%}$ / $90_g^{30\%}$ | 1.447 | 56.20 | 544 | 513 | 1-X |
| | UV 7 | $0_g^{40\%}$ / $0_g^{30\%}$ / $90_g^{35\%}$ / $90_g^{30\%}$ / $0_c^{30\%}$ / $90_c^{30\%}$ | 1.469 | 56.05 | 523 | 526 | 3-Y |
| Void + Uncertainties in Angle | UVA 1 | $0_c^{40\%}$ / $90_c^{35\%}$ / $90_c^{30\%}$ / $+45_c^{30\%}$ / $0_c^{30\%}$ / $90_c^{30\%}$ | 1.321 | 66.83 | 536 | 591 | 1-X |
| | UVA 2 | $0_c^{40\%}$ / $90_c^{35\%}$ / $90_c^{30\%}$ / $0_g^{30\%}$ / $0_c^{30\%}$ / $90_c^{30\%}$ | 1.354 | 64.43 | 537 | 585 | 1-X |
| | UVA 3 | $0_c^{40\%}$ / $90_g^{35\%}$ / $90_c^{30\%}$ / $0_c^{30\%}$ / $0_c^{30\%}$ / $90_c^{30\%}$ | 1.359 | 64.03 | 539 | 602 | 1-X |
| | UVA 4 | $0_c^{40\%}$ / $90_c^{35\%}$ / $90_g^{30\%}$ / $0_g^{30\%}$ / $0_c^{30\%}$ / $90_c^{30\%}$ | 1.387 | 62.04 | 530 | 546 | 1-X |
| | UVA 5 | $0_c^{40\%}$ / $90_g^{35\%}$ / $90_c^{30\%}$ / $0_g^{30\%}$ / $0_c^{30\%}$ / $90_c^{30\%}$ | 1.392 | 61.64 | 538 | 604 | 1-X |
| | UVA 6 | $0_c^{40\%}$ / $90_g^{35\%}$ / $90_g^{30\%}$ / $0_g^{30\%}$ / $0_c^{30\%}$ / $90_c^{30\%}$ | 1.425 | 59.24 | 538 | 534 | 2-Y |
| | UVA 7 | $0_g^{50\%}$ / $90_g^{35\%}$ / $90_g^{30\%}$ / $0_g^{30\%}$ / $0_c^{30\%}$ / $90_c^{30\%}$ | 1.492 | 57.33 | 505 | 582 | 1-X |
| Void + Uncertainties in Thickness | UVT 1 | $0_c^{35\%}$ / $0_c^{30\%}$ / $-45_c^{30\%}$ / $+45_c^{35\%}$ / $0_c^{30\%}$ / $90_c^{30\%}$ | 1.315 | 65.78 | 519 | 507 | 3-Y |
| | UVT 2 | $0_c^{35\%}$ / $0_c^{30\%}$ / $-45_g^{35\%}$ / $+45_c^{30\%}$ / $0_c^{30\%}$ / $90_c^{30\%}$ | 1.353 | 62.99 | 519 | 511 | 4-Y |
| | UVT 3 | $0_c^{35\%}$ / $0_c^{30\%}$ / $-45_g^{35\%}$ / $+45_g^{35\%}$ / $0_c^{30\%}$ / $90_c^{30\%}$ | 1.398 | 61.24 | 518 | 514 | 1-Y |
| | UVT 4 | $0_c^{40\%}$ / $+45_c^{30\%}$ / $-45_g^{35\%}$ / $90_g^{35\%}$ / $0_c^{30\%}$ / $90_g^{30\%}$ | 1.437 | 59.88 | 501 | 504 | 1-X |
| | UVT 5 | $0_c^{45\%}$ / $+45_g^{35\%}$ / $-45_g^{35\%}$ / $90_g^{35\%}$ / $0_c^{30\%}$ / $90_g^{30\%}$ | 1.487 | 59.17 | 545 | 503 | 3-Y |
| | UVT 6 | $0_c^{40\%}$ / $+45_g^{45\%}$ / $-45_g^{35\%}$ / $-45_g^{30\%}$ / $0_c^{30\%}$ / $90_g^{30\%}$ | 1.493 | 58.77 | 504 | 506 | 1-X |
| | UVT 7 | $0_g^{55\%}$ / $90_g^{40\%}$ / $0_g^{30\%}$ / $90_g^{30\%}$ / $0_c^{30\%}$ / $90_c^{30\%}$ | 1.515 | 58.62 | 517 | 526 | 1-X |
| | UVT 8 | $0_g^{55\%}$ / $90_g^{40\%}$ / $+45_g^{30\%}$ / $+45_g^{30\%}$ / $0_c^{30\%}$ / $90_c^{30\%}$ | 1.515 | 58.62 | 504 | 526 | 1-X |
| | UVT 9 | $0_g^{55\%}$ / $90_g^{45\%}$ / $0_g^{30\%}$ / $-45_g^{30\%}$ / $0_c^{35\%}$ / $90_g^{30\%}$ | 1.565 | 57.91 | 512 | 502 | 2-Y |
| | UVT 10 | $0_g^{60\%}$ / $90_g^{40\%}$ / $90_g^{35\%}$ / $0_g^{30\%}$ / $0_c^{30\%}$ / $90_g^{30\%}$ | 1.571 | 57.51 | 504 | 522 | 6-X |
| Void + Uncertainties in Angle and Thickness | UVAT 1 | $0_c^{45\%}$ / $90_c^{40\%}$ / $90_c^{30\%}$ / $+45_c^{30\%}$ / $0_c^{30\%}$ / $90_c^{30\%}$ | 1.333 | 68.91 | 538 | 586 | 1-X |
| | UVAT 2 | $0_c^{45\%}$ / $90_c^{40\%}$ / $0_c^{30\%}$ / $-45_g^{30\%}$ / $0_c^{30\%}$ / $90_c^{30\%}$ | 1.366 | 66.51 | 527 | 520 | 2-Y |
| | UVAT 3 | $0_c^{45\%}$ / $90_g^{40\%}$ / $90_c^{30\%}$ / $0_c^{30\%}$ / $0_c^{30\%}$ / $90_c^{30\%}$ | 1.377 | 65.72 | 526 | 503 | 3-Y |
| | UVAT 4 | $0_c^{45\%}$ / $90_c^{40\%}$ / $90_g^{30\%}$ / $90_g^{30\%}$ / $0_c^{30\%}$ / $90_c^{30\%}$ | 1.399 | 64.12 | 539 | 536 | 2-Y |
| | UVAT 5 | $0_c^{45\%}$ / $90_g^{40\%}$ / $90_c^{30\%}$ / $90_g^{30\%}$ / $0_c^{30\%}$ / $90_c^{30\%}$ | 1.410 | 63.32 | 541 | 500 | 3-Y |
| | UVAT 6 | $0_c^{45\%}$ / $90_g^{40\%}$ / $90_g^{35\%}$ / $90_g^{30\%}$ / $0_c^{30\%}$ / $90_c^{30\%}$ | 1.454 | 61.57 | 540 | 549 | 1-X |
| | UVAT 7 | $0_g^{55\%}$ / $90_g^{40\%}$ / $90_c^{30\%}$ / $90_g^{30\%}$ / $0_c^{30\%}$ / $90_c^{30\%}$ | 1.482 | 61.01 | 501 | 544 | 1-X |
| | UVAT 8 | $0_g^{55\%}$ / $90_g^{40\%}$ / $0_g^{30\%}$ / $-45_g^{30\%}$ / $0_c^{30\%}$ / $90_c^{30\%}$ | 1.515 | 58.62 | 505 | 509 | 1-X |

*** Void content: Vv = 3%.**

**** First ply failure (Ply No. - Failure Direction); X:[0] and Y:[90]**

**Table 8-6: Optimal solutions achieved for a minimum required strength of 600 MPa*.**

| | ID | Stacking Configuration, $\theta^{\text{Vf \%}}_{\text{fibre type}}$ (compressive side at left) | Density (g/cm³) | Cost ($/litre) | $S_{Fxx}$ (MPa) | $S_{Fyy}$ (MPa) | FPF** |
|---|---|---|---|---|---|---|---|
| No Uncertainties | NU 1 | $0_c^{40\%}$ / $90_c^{30\%}$ / $90_c^{30\%}$ / $90_c^{30\%}$/ $0_c^{30\%}$ / $90_c^{30\%}$ | 1.315 | 65.78 | 614 | 669 | 1-X |
| | NU 2 | $0_c^{40\%}$ / $90_c^{30\%}$ / $90_c^{30\%}$ /+$45_c^{30\%}$/ $0_c^{30\%}$ / $90_c^{30\%}$ | 1.315 | 65.78 | 612 | 682 | 1-X |
| | NU 3 | $0_c^{40\%}$ / $90_g^{30\%}$ / $90_c^{30\%}$ / $90_c^{30\%}$/ $0_c^{30\%}$ / $90_c^{30\%}$ | 1.348 | 63.39 | 615 | 641 | 1-X |
| | NU 4 | $0_c^{40\%}$ / $90_c^{30\%}$ / $90_c^{30\%}$ / $0_g^{30\%}$/ $0_c^{30\%}$ / $90_c^{30\%}$ | 1.348 | 63.39 | 605 | 682 | 1-X |
| | NU 5 | $0_c^{40\%}$ / $90_g^{30\%}$ / $90_c^{30\%}$ / $0_g^{30\%}$/ $0_c^{30\%}$ / $90_c^{30\%}$ | 1.381 | 60.99 | 607 | 733 | 1-X |
| | NU 6 | $0_c^{40\%}$ / $90_g^{30\%}$ / $90_c^{30\%}$ / $90_g^{30\%}$/ $0_c^{30\%}$ / $90_c^{30\%}$ | 1.381 | 60.99 | 615 | 636 | 1-X |
| | NU 7 | $0_c^{40\%}$ / $90_g^{35\%}$ / $90_g^{30\%}$ / $0_g^{30\%}$/ $0_c^{30\%}$ / $90_c^{30\%}$ | 1.425 | 59.24 | 608 | 616 | 1-X |
| | NU 8 | $0_c^{40\%}$ / $90_g^{35\%}$ / $90_g^{30\%}$ / $90_g^{30\%}$/ $0_c^{30\%}$ / $90_c^{30\%}$ | 1.425 | 59.24 | 616 | 627 | 1-X |
| Void-Induced Uncertainties | UV 1 | $0_c^{50\%}$ / $90_c^{35\%}$ / $90_c^{30\%}$ / $0_c^{30\%}$ / $0_c^{30\%}$ / $90_c^{30\%}$ | 1.333 | 68.91 | 610 | 612 | 1-X |
| | UV 2 | $0_c^{50\%}$ / $90_c^{35\%}$ / $90_c^{30\%}$ / $0_g^{30\%}$ / $0_c^{30\%}$ / $90_c^{30\%}$ | 1.366 | 66.51 | 611 | 619 | 2-Y |
| | UV 3 | $0_c^{50\%}$ / $90_g^{35\%}$ / $90_c^{30\%}$ / $0_c^{30\%}$ / $0_c^{30\%}$ / $90_c^{30\%}$ | 1.371 | 66.11 | 612 | 627 | 1-X |
| | UV 4 | $0_c^{50\%}$ / $90_g^{35\%}$ / $90_c^{30\%}$ / $90_g^{30\%}$/ $0_c^{30\%}$ / $90_c^{30\%}$ | 1.404 | 63.72 | 628 | 628 | 3-Y |
| | UV 5 | $0_c^{50\%}$ / $90_g^{40\%}$ / $90_g^{30\%}$ / $0_g^{30\%}$ / $0_c^{30\%}$ / $90_c^{30\%}$ | 1.449 | 61.97 | 603 | 621 | 2-Y |
| | UV 6 | $0_g^{65\%}$ / $90_g^{35\%}$ / $90_c^{30\%}$ / $0_g^{30\%}$ / $0_c^{30\%}$ / $90_c^{30\%}$ | 1.493 | 61.66 | 617 | 652 | 6-X |
| | UV 7 | $0_g^{65\%}$ / $90_g^{45\%}$ / $90_g^{30\%}$ / $0_g^{30\%}$ / $0_c^{30\%}$ / $90_c^{30\%}$ | 1.549 | 60.55 | 617 | 619 | 6-X |
| Void + Uncertainties in Angle | UVA 1 | $0_c^{50\%}$ / $90_c^{40\%}$ / $90_c^{30\%}$ / $90_c^{30\%}$ / $0_c^{30\%}$ / $90_c^{30\%}$ | 1.339 | 69.95 | 624 | 621 | 2-Y |
| | UVA 2 | $0_c^{50\%}$ / $90_g^{35\%}$ / $90_c^{30\%}$ / $90_c^{30\%}$ / $0_c^{30\%}$ / $90_c^{30\%}$ | 1.371 | 66.11 | 625 | 615 | 3-Y |
| | UVA 3 | $0_c^{50\%}$ / $90_c^{40\%}$ / $90_g^{30\%}$ / $0_g^{30\%}$ / $0_c^{30\%}$ / $90_c^{30\%}$ | 1.405 | 65.16 | 616 | 601 | 2-Y |
| | UVA 4 | $0_c^{50\%}$ / $90_g^{40\%}$ / $90_g^{30\%}$ / $90_c^{30\%}$ / $0_c^{30\%}$ / $90_c^{30\%}$ | 1.416 | 64.36 | 625 | 609 | 2-Y |
| | UVA 5 | $0_c^{50\%}$ / $90_g^{40\%}$ / $90_g^{30\%}$ / $90_g^{30\%}$ / $0_c^{30\%}$ / $90_c^{30\%}$ | 1.449 | 61.97 | 625 | 601 | 2-Y |
| | UVA 6 | $0_g^{65\%}$ / $90_g^{45\%}$ / $90_g^{30\%}$ / $90_g^{30\%}$ / $0_c^{35\%}$ / $90_c^{30\%}$ | 1.555 | 61.59 | 609 | 604 | 1-Y |
| Void + Uncertainties in Thickness | UVT 1 | $0_c^{55\%}$ / $90_c^{40\%}$ / $90_c^{30\%}$ / $0_c^{30\%}$ / $0_c^{30\%}$ / $90_c^{30\%}$ | 1.344 | 70.99 | 604 | 605 | 1-X |
| | UVT 2 | $0_c^{55\%}$ / $90_c^{40\%}$ / $90_c^{30\%}$ / +$45_g^{30\%}$ / $0_c^{30\%}$ / $90_c^{30\%}$ | 1.377 | 68.60 | 604 | 617 | 2-Y |
| | UVT 3 | $0_c^{55\%}$ / $90_c^{45\%}$ / $90_g^{30\%}$ / +$45_g^{30\%}$ / $0_c^{30\%}$ / $90_c^{30\%}$ | 1.416 | 67.24 | 603 | 618 | 2-Y |
| | UVT 4 | $0_c^{55\%}$ / $90_g^{35\%}$ / $90_c^{40\%}$ / $90_g^{30\%}$ / $0_c^{30\%}$ / $90_c^{30\%}$ | 1.422 | 66.84 | 602 | 619 | 2-Y |
| | UVT 5 | $0_c^{55\%}$ / $90_g^{40\%}$ / $90_c^{35\%}$ / $90_g^{30\%}$ / $0_c^{30\%}$ / $90_c^{30\%}$ | 1.427 | 66.45 | 620 | 675 | 1-X |
| | UVT 6 | $0_c^{55\%}$ / $90_g^{45\%}$ / $90_g^{35\%}$ / $90_g^{30\%}$ / $0_c^{30\%}$ / $90_c^{30\%}$ | 1.477 | 64.29 | 612 | 620 | 2-Y |
| | UVT 7 | $0_g^{70\%}$ / $90_g^{40\%}$ / $90_c^{30\%}$ / $0_g^{30\%}$ / $0_c^{30\%}$ / $90_c^{30\%}$ | 1.516 | 62.94 | 601 | 611 | 6-X |
| Void + Uncertainties in Angle and Thickness | UVAT 1 | $0_c^{55\%}$ / $90_c^{40\%}$ / $90_c^{35\%}$ / -$45_c^{30\%}$ / $0_c^{30\%}$ / $90_c^{30\%}$ | 1.350 | 72.03 | 609 | 601 | 2-Y |
| | UVAT 2 | $0_c^{55\%}$ / $90_c^{45\%}$ / $90_c^{30\%}$ / -$45_g^{30\%}$ / $0_c^{30\%}$ / $90_c^{30\%}$ | 1.383 | 69.64 | 612 | 626 | 1-X |
| | UVAT 3 | $0_c^{55\%}$ / $90_g^{40\%}$ / $90_c^{35\%}$ / -$45_c^{30\%}$ / $0_c^{30\%}$ / $90_c^{30\%}$ | 1.394 | 68.84 | 610 | 657 | 1-X |
| | UVAT 4 | $0_c^{55\%}$ / $90_g^{40\%}$ / $90_c^{35\%}$ / -$45_g^{30\%}$ / $0_c^{30\%}$ / $90_c^{30\%}$ | 1.427 | 66.45 | 612 | 662 | 1-X |
| | UVAT 5 | $0_c^{55\%}$ / $90_g^{45\%}$ / $90_g^{35\%}$ / $90_g^{30\%}$ / $0_c^{30\%}$ / $90_c^{30\%}$ | 1.477 | 64.29 | 614 | 602 | 2-Y |

*** Void content: Vv = 3%.**

**** First ply failure (Ply No. - Failure Direction); X:[0] and Y:[90]**

**Table 8-7: Optimal solutions achieved for a minimum required strength of 700 MPa*.**

| | ID | Stacking Configuration, $\theta^{\text{Vf \%}}_{\text{fibre type}}$ (compressive side at left) | Density (g/cm³) | Cost ($/litre) | $S_{Fxx}$ (MPa) | $S_{Fyy}$ (MPa) | FPF** |
|---|---|---|---|---|---|---|---|
| No Uncertainties | **NU 1** | $0_c^{50\%} / 90_c^{30\%} / 90_c^{35\%} / \; 0_c^{30\%} / 0_c^{35\%} / 90_c^{30\%}$ | 1.339 | 69.95 | 704 | 706 | 1-X |
| | **NU 2** | $0_c^{55\%} / 90_c^{35\%} / 90_c^{30\%} / \; 0_c^{30\%} / 0_c^{30\%} / 90_c^{30\%}$ | 1.339 | 69.95 | 744 | 721 | 2-Y |
| | **NU 3** | $0_c^{55\%} / 90_g^{30\%} / 90_c^{30\%} / \; 0_c^{30\%} / 0_c^{30\%} / 90_c^{30\%}$ | 1.366 | 66.51 | 744 | 755 | 1-X |
| | **NU 4** | $0_c^{55\%} / 90_g^{30\%} / 90_c^{30\%} / \; 0_g^{30\%} / 0_c^{30\%} / 90_c^{30\%}$ | 1.399 | 64.12 | 715 | 755 | 6-X |
| | **NU 5** | $0_c^{50\%} / 90_g^{45\%} / 90_g^{30\%} / \; 0_g^{30\%} / 0_c^{30\%} / 90_c^{30\%}$ | 1.460 | 62.61 | 701 | 709 | 6-X |
| Void-Induced Uncertainties | **UV 1** | $0_c^{60\%} / 90_c^{45\%} / 90_c^{35\%} / \; 0_c^{30\%} / 0_c^{30\%} / 90_c^{30\%}$ | 1.362 | 74.12 | 702 | 704 | 1-X |
| | **UV 2** | $0_c^{60\%} / 90_g^{35\%} / 90_c^{35\%} / \; 0_c^{30\%} / 0_c^{30\%} / 90_c^{30\%}$ | 1.389 | 69.24 | 702 | 715 | 1-X |
| | **UV 3** | $0_c^{60\%} / 90_g^{35\%} / 90_c^{35\%} / \; 0_g^{30\%} / 0_c^{30\%} / 90_c^{30\%}$ | 1.422 | 66.84 | 710 | 715 | 1-X |
| | **UV 4** | $0_c^{60\%} / 90_g^{55\%} / 90_g^{30\%} / \; 0_g^{30\%} / 0_c^{30\%} / 90_c^{30\%}$ | 1.495 | 65.98 | 714 | 717 | 1-X |
| Void + Uncertainties in Angle | **UVA 1** | $0_c^{60\%} / 90_c^{50\%} / 90_c^{30\%} / -45_c^{30\%} / 0_c^{35\%} / 90_c^{30\%}$ | 1.368 | 75.16 | 713 | 712 | 2-Y |
| | **UVA 2** | $0_c^{60\%} / 90_c^{55\%} / 90_c^{30\%} / \; 0_g^{30\%} / 0_c^{30\%} / 90_c^{30\%}$ | 1.401 | 72.76 | 707 | 742 | 6-X |
| | **UVA 3** | $0_c^{60\%} / 90_c^{50\%} / 90_c^{30\%} / -45_g^{30\%} / 0_c^{35\%} / 90_c^{30\%}$ | 1.401 | 72.76 | 717 | 711 | 2-Y |
| | **UVA 4** | $0_c^{60\%} / 90_g^{45\%} / 90_c^{30\%} / \; 0_c^{30\%} / 0_c^{30\%} / 90_c^{30\%}$ | 1.406 | 69.48 | 700 | 714 | 1-X |
| | **UVA 5** | $0_c^{60\%} / 90_g^{45\%} / 90_c^{30\%} / \; 0_g^{30\%} / 0_c^{30\%} / 90_c^{30\%}$ | 1.439 | 67.09 | 707 | 713 | 1-X |
| | **UVA 6** | $0_c^{60\%} / 90_g^{55\%} / 90_g^{30\%} / \; 0_g^{30\%} / 0_c^{30\%} / 90_c^{30\%}$ | 1.495 | 65.98 | 708 | 708 | 2-Y |
| Void + Uncertainties in Thickness | **UVT 1** | $0_c^{70\%} / 90_c^{55\%} / 90_c^{30\%} / \; 0_c^{30\%} / 0_c^{30\%} / 90_c^{30\%}$ | 1.380 | 77.24 | 730 | 709 | 2-Y |
| | **UVT 2** | $0_c^{70\%} / 90_g^{40\%} / 90_c^{35\%} / \; 0_c^{30\%} / 0_c^{30\%} / 90_c^{30\%}$ | 1.412 | 71.97 | 730 | 704 | 3-Y |
| | **UVT 3** | $0_c^{70\%} / 90_g^{40\%} / 90_c^{35\%} / \; 0_g^{30\%} / 0_c^{30\%} / 90_c^{30\%}$ | 1.445 | 69.57 | 736 | 704 | 3-Y |
| Void + Uncertainties in Angle and Thickness | **UVAT 1** | $0_c^{70\%} / 90_c^{60\%} / 90_c^{30\%} / \; 0_c^{30\%} / 0_c^{30\%} / 90_c^{30\%}$ | 1.386 | 78.28 | 726 | 722 | 2-Y |
| | **UVAT 2** | $0_c^{70\%} / 90_c^{60\%} / 90_g^{30\%} / \; 0_c^{30\%} / 0_c^{30\%} / 90_c^{30\%}$ | 1.419 | 75.89 | 726 | 704 | 2-Y |
| | **UVAT 3** | $0_c^{70\%} / 90_g^{45\%} / 90_c^{35\%} / \; 0_c^{30\%} / 0_c^{30\%} / 90_c^{30\%}$ | 1.424 | 72.61 | 726 | 734 | 1-X |
| | **UVAT 4** | $0_c^{70\%} / 90_g^{45\%} / 90_c^{35\%} / \; 0_g^{30\%} / 0_c^{35\%} / 90_c^{30\%}$ | 1.462 | 71.25 | 749 | 734 | 2-Y |
| | **UVAT 5** | $0_c^{70\%} / 90_g^{60\%} / 90_g^{35\%} / \; 0_g^{30\%} / 0_c^{30\%} / 90_c^{30\%}$ | 1.535 | 70.39 | 751 | 706 | 2-Y |

*** Void content: Vv = 3%.**

**** First ply failure (Ply No. - Failure Direction); X:[0] and Y:[90]**

**Table 8-8: Optimal solutions achieved for a minimum required strength of 800 MPa*.**

| | ID | Stacking Configuration, $\theta^{Vf\,\%}_{\text{fibre type}}$ (compressive side at left) | Density (g/cm³) | Cost ($/litre) | $S_{Fxx}$ (MPa) | $S_{Fyy}$ (MPa) | FPF** |
|---|---|---|---|---|---|---|---|
| No Uncertainties | NU 1 | $0_c^{60\%}$ / $90_c^{50\%}$ / $90_c^{30\%}$ / $0_c^{30\%}$ / $0_c^{30\%}$ / $90_c^{30\%}$ | 1.362 | 74.12 | 801 | 824 | 1-X |
| | NU 2 | $0_c^{65\%}$ / $90_g^{35\%}$ / $90_c^{30\%}$ / $0_c^{30\%}$ / $0_c^{30\%}$ / $90_c^{30\%}$ | 1.389 | 69.24 | 844 | 800 | 2-Y |
| | NU 3 | $0_c^{70\%}$ / $90_g^{35\%}$ / $90_c^{30\%}$ / $0_g^{30\%}$ / $0_c^{35\%}$ / $90_c^{30\%}$ | 1.434 | 68.93 | 821 | 811 | 2-Y |
| | NU 4 | $0_c^{65\%}$ / $90_g^{40\%}$ / $90_c^{30\%}$ / $0_g^{30\%}$ / $0_c^{35\%}$ / $90_c^{30\%}$ | 1.439 | 68.53 | 810 | 832 | 6-X |
| | NU 5 | $0_c^{65\%}$ / $90_g^{55\%}$ / $90_g^{30\%}$ / $0_g^{30\%}$ / $0_c^{35\%}$ / $90_c^{30\%}$ | 1.506 | 68.06 | 810 | 829 | 6-X |
| Void-Induced Uncertainties | UV 1 | $0_c^{70\%}$ / $90_c^{60\%}$ / $90_c^{30\%}$ / $0_c^{30\%}$ / $0_c^{30\%}$ / $90_c^{30\%}$ | 1.386 | 78.28 | 810 | 808 | 2-Y |
| | UV 2 | $0_c^{70\%}$ / $90_c^{55\%}$ / $90_c^{30\%}$ / $0_c^{30\%}$ / $0_c^{30\%}$ / $90_c^{35\%}$ | 1.386 | 78.28 | 811 | 800 | 2-Y |
| | UV 3 | $0_c^{70\%}$ / $90_g^{40\%}$ / $90_c^{40\%}$ / $0_c^{30\%}$ / $0_c^{30\%}$ / $90_c^{30\%}$ | 1.418 | 73.01 | 809 | 818 | 1-X |
| | UV 4 | $0_c^{70\%}$ / $90_g^{45\%}$ / $90_c^{35\%}$ / $0_c^{30\%}$ / $0_c^{30\%}$ / $90_c^{30\%}$ | 1.424 | 72.61 | 810 | 821 | 1-X |
| | UV 5 | $0_c^{70\%}$ / $90_g^{40\%}$ / $90_c^{40\%}$ / $0_g^{30\%}$ / $0_c^{35\%}$ / $90_c^{30\%}$ | 1.457 | 71.65 | 834 | 818 | 2-Y |
| | UV 6 | $0_c^{70\%}$ / $90_g^{45\%}$ / $90_c^{35\%}$ / $0_g^{30\%}$ / $0_c^{35\%}$ / $90_c^{30\%}$ | 1.462 | 71.25 | 835 | 821 | 2-Y |
| | UV 7 | $0_c^{70\%}$ / $90_g^{65\%}$ / $90_g^{30\%}$ / $0_g^{30\%}$ / $0_c^{35\%}$ / $90_c^{30\%}$ | 1.535 | 70.39 | 841 | 814 | 2-Y |
| Void + Uncertainties in | UVA 1 | $0_c^{70\%}$ / $90_c^{65\%}$ / $90_c^{30\%}$ / $90_c^{30\%}$ / $0_c^{40\%}$ / $90_c^{30\%}$ | 1.404 | 81.41 | 802 | 804 | 6-X |
| | UVA 2 | $0_c^{65\%}$ / $90_c^{65\%}$ / $90_c^{30\%}$ / $45_c^{30\%}$ / $0_c^{45\%}$ / $90_c^{30\%}$ | 1.404 | 81.41 | 807 | 829 | 1-X |
| | UVA 3 | $0_c^{70\%}$ / $90_c^{65\%}$ / $90_c^{30\%}$ / $0_g^{30\%}$ / $0_c^{40\%}$ / $90_c^{30\%}$ | 1.437 | 79.01 | 805 | 819 | 6-X |
| | UVA 4 | $0_c^{65\%}$ / $90_g^{50\%}$ / $90_c^{35\%}$ / $45_c^{30\%}$ / $0_c^{45\%}$ / $90_c^{30\%}$ | 1.447 | 75.33 | 809 | 817 | 1-X |
| | UVA 5 | $0_c^{70\%}$ / $90_g^{50\%}$ / $90_c^{35\%}$ / $0_g^{30\%}$ / $0_c^{40\%}$ / $90_c^{30\%}$ | 1.480 | 72.94 | 846 | 826 | 2-Y |
| | UVA 6 | $0_c^{70\%}$ / $90_g^{65\%}$ / $90_g^{30\%}$ / $0_g^{30\%}$ / $0_c^{40\%}$ / $90_c^{30\%}$ | 1.541 | 71.43 | 851 | 803 | 2-Y |
| Void + Uncertainties in Thickness | UVT 1 | $0_c^{70\%}$ / $90_c^{70\%}$ / $90_c^{30\%}$ / $45_c^{30\%}$ / $0_c^{55\%}$ / $90_c^{30\%}$ | 1.427 | 85.58 | 805 | 806 | 1-X |
| | UVT 2 | $0_c^{70\%}$ / $90_c^{70\%}$ / $90_c^{30\%}$ / $-45_g^{30\%}$ / $0_c^{55\%}$ / $90_c^{30\%}$ | 1.460 | 83.18 | 806 | 807 | 1-X |
| | UVT 3 | $0_c^{70\%}$ / $90_g^{45\%}$ / $90_c^{45\%}$ / $90_c^{30\%}$ / $0_c^{55\%}$ / $90_c^{35\%}$ | 1.471 | 80.94 | 807 | 811 | 1-X |
| | UVT 4 | $0_c^{70\%}$ / $90_g^{55\%}$ / $90_c^{35\%}$ / $90_c^{30\%}$ / $0_c^{50\%}$ / $90_c^{35\%}$ | 1.476 | 79.10 | 800 | 800 | 3-Y |
| | UVT 5 | $0_c^{70\%}$ / $90_g^{60\%}$ / $90_c^{35\%}$ / $90_c^{30\%}$ / $0_c^{50\%}$ / $90_c^{30\%}$ | 1.481 | 78.70 | 801 | 812 | 1-X |
| | UVT 6 | $0_c^{70\%}$ / $90_g^{45\%}$ / $90_c^{45\%}$ / $90_g^{30\%}$ / $0_c^{55\%}$ / $90_c^{35\%}$ | 1.504 | 78.55 | 807 | 818 | 1-X |
| | UVT 7 | $0_c^{70\%}$ / $90_g^{55\%}$ / $90_c^{35\%}$ / $90_g^{30\%}$ / $0_c^{50\%}$ / $90_c^{35\%}$ | 1.509 | 76.71 | 800 | 807 | 1-X |
| | UVT 8 | $0_c^{70\%}$ / $90_g^{60\%}$ / $90_c^{35\%}$ / $90_g^{30\%}$ / $0_c^{50\%}$ / $90_c^{30\%}$ | 1.514 | 76.31 | 801 | 818 | 1-X |
| | UVT 9 | $0_c^{70\%}$ / $90_g^{70\%}$ / $90_g^{35\%}$ / $90_g^{30\%}$ / $0_c^{50\%}$ / $90_c^{35\%}$ | 1.582 | 75.84 | 805 | 800 | 2-Y |

*** Void content: Vv = 3%.**

**** First ply failure (Ply No. - Failure Direction); X:[0] and Y:[90]**

## 8.4. Conclusions

The problem of multi-objective robust optimization for multi-directional carbon/glass fibre-reinforced epoxy composites has been investigated in this chapter with manufacture related uncertainties in lamina thickness and fibre orientation angle, together with the presence of matrix voids, being considered.

Material cost and density were considered as conflicting objectives with the minimum required flexural strength being chosen as a constraint. Multi-objective optimization was combined with an anti-optimization method to determine the Pareto optimal and robust results. GA has been utilised as an anti-optimizer to find the worst case of each solution variable when uncertainties were incorporated and NSGA-II has been employed to find optimal and robust stacking configurations.

The effect of three uncertainty sources, namely: (i) uncertainties due to variation in lamina thickness, (ii) uncertainties due to variation in fibre angle orientation and (iii) uncertainties due to the presence of matrix voids, were investigated with the contribution of uncertainty sources on the optimal results being measured by the ANOVA method. It was concluded that, for the hybrid composites investigated in this study, the level of void content played an important role in the performance of the composite. Void contents up to 2% did not affect the cost and weight of the optimal solutions. This was attributed to the lamina strength generally not being affected by void contents less than 2%. When the void content exceeded 2%, the degrading effect on the composite performance became more critical in such a way that the degrading effect of 3% void content was higher than either ±10% variation in lamina thickness or ±3º variation in fibre orientation angle. Among the uncertainty sources investigated in this study, the fibre orientation angle exhibited a relatively small effect on the optimal cost and weight. Therefore, improvements of the manufacturing process to achieve tighter tolerances and a reduction of void content would be more critical for the case of high strength hybrid composites.

It should be noted that the specimen studied in this research was a rectangular beam with a large span-to-depth ratio, so that the inter-laminar shear and out of plane stress were considered to be negligible. However, the present approach would be unsuitable for complex geometries and more accurate methods, such as finite element analysis, would need to be coupled with the presented optimisation algorithm. In addition, this study was limited to six laminas based on first ply failure. The number of laminas could also be used as a design variable with progressive failure of the laminas being considered instead of first ply failure to increase the accuracy and applicability of the problem.

## 8.5. References


[1] Mallick PK. Fiber-Reinforced Composites: Materials, Manufacturing, and Design. 3rd edition. London: CRC press; 1993.

[2] Liebig WV, Viets C, Schulte K, Fiedler B. Influence of voids on the compressive failure behaviour of fibre-reinforced composites. Composites Science and Technology, 2015;117:225-233.

[3] Hagstrand P-O, Bonjour F, Månson J-AE. The influence of void content on the structural flexural performance of unidirectional glass fibre reinforced polypropylene composites. Composites Part A: Applied Science and Manufacturing, 2005;36(5):705-714.

[4] Huang H, Talreja R. Effects of void geometry on elastic properties of unidirectional fiber reinforced composites. Composite Science and Technology, 2005;65:1964-1981.

[5] Wisnom MR. The effect of fibre misalignment on the compressive strength of unidirectional carbon fibre/epoxy. Composites, 1990;21(5):403-407.

[6] Ruiz E, Achim V, Soukane S, Breard J. Optimization of injection flow rate to minimize micro/macro-voids formation in resin transfer molded composites. Composites Science and Technology, 2006;66:475-486.

[7] Lukaszewicz DH-JA, Potter KD. The internal structure and conformation of prepreg with respect to reliable automated processing. Composites Part A: Applied Science and Manufacturing, 2011;42(3):283-292.

[8] Perner M, Algermissen S, Keimer R, Monner HP. Avoiding defects in manufacturing processes: A review for automated CFRP production. Robotics and Computer-Integrated Manufacturing, 2016;38:82-92.

[9] Ghiorse SR. Effect of void content on the mechanical properties of carbon/epoxy laminates. S.A.M.P.E. quarterly, 1993;24 (2):54-59.

[10] Liu L, Zhang B-M, Wang D-F, Wu Z-J. Effects of cure cycles on void content and mechanical properties of composite laminates. Composite Structures, 2006;73(3):303-309.

[11] Dong C. Effects of process-induced voids on the properties of fibre reinforced composites. Journal of Materials Science & Technology, 2016;32(7):597-604.

[12] de Almeida SFM. Effect of void content on the strength of composite laminates. Composite Structures, 1994;28(2):139-148.

[13] Guo Z-S, Liu L, Zhang B-M, Du S. Critical void content for thermoset composite laminates. Journal of Composite Materials, 2009;43(17):1775-1790.

[14] Chamis CC. Probabilistic simulation of multi-scale composite behaviour. Theoretical and Applied Fracture Mechanics, 2004;41(1–3):51-61.

[15] Shaw A, Sriramula S, Gosling PD, Chryssanthopoulos MK. A critical reliability evaluation of fibre reinforced composite materials based on probabilistic micro and macro-mechanical analysis. Composites Part B: Engineering, 2010;41(6):446-453.

[16] Taguchi G. Performance analysis design. International Journal of Production Research, 1978;16(6):521-530.

[17] Cheng S, Zhou J, Li M. A new hybrid algorithm for multi-objective robust optimization with interval uncertainty. Journal of Mechanical Design, 2015;137: 021401-021401.

[18] Kalantari M, Dong C, Davies IJ. Numerical investigation of the hybridisation mechanism in fibre reinforced hybrid composites subjected to flexural load. Composites Part B: Engineering, 2016;102:100-111.

[19] Marom G, Fischer S, Tuler FR, Wagner HD. Hybrid effects in composites: conditions for positive or negative effects versus rule-of-mixtures behaviour. Journal of Materials Science 1978;13(7):1419-1426.

[20] Ghiasi H, Pasini D, Lessard L. Optimum stacking sequence design of composite materials part i: constant stiffness design. Composite Structures, 2009;90:1-11.

[21] Cai H, Aref AJ. On the design and optimization of hybrid carbon fiber reinforced polymer-steel cable system for cable-stayed bridges. Composites Part B: Engineering, 2015;68:146-152.

[22] Ghasemi H, Kerfriden P, Bordas SP, Muthu J, Zi G, Rabczuk T. Probabilistic multiconstraints optimization of cooling channels in ceramic matrix composites. Composites Part B: Engineering, 2015;81:107-119.

[23] Kim D-H, Choi D-H, Kim H-S. Design optimization of a carbon fiber reinforced composite automotive lower arm. Composites Part B: Engineering, 2014;58:400-407.

[24] Kočí V, Kočí J, Čáchová M, Vejmelková E, Černý R. Multi-parameter optimization of lime composite design using a modified downhill simplex method. Composites Part B: Engineering, 2016;93:184-189.

[25] Kursa M, Kowalczyk-Gajewska K, Petryk H. Multi-objective optimization of thermo-mechanical properties of metal–ceramic composites. Composites Part B: Engineering, 2014;60:586-596.

[26] Lopez RH, Luersen MA, Cursi ES. Optimization of laminated composites considering different failure criteria. Composites Part B: Engineering, 2009; 40(8):731-740.

[27] Rouhi M, Ghayoor H, Hoa SV, Hojjati M. Multi-objective design optimization of variable stiffness composite cylinders. Composites Part B: Engineering, 2015;69:249-255.

[28] Deb K. Multi-Objective Optimization Using Evolutionary Algorithms: John Wiley & Sons, 2001.

[29] Zitzler E, Laumanns M, Thiele L. SPEA2: Improving the strength Pareto evolutionary algorithm. Tech Rep 103, Computer Engineering and Networks Laboratory (TIK). Swiss Federal Institute of Technology (ETH), Zurich, Switzerland, 2001.

[30] Knowles J, Corne D. The Pareto archived evolution strategy: a new baseline algorithm for multi-objective optimisation. In: Proceedings of the 1999 congress on evolutionary computation. IEEE Press, Piscataway, 2002;99-105.

[31] Deb K, Pratap A, Agarwal S, Meyarivan T. A fast and elitist multi-objective genetic algorithm: NSGA-II. IEEE Transactions on Evolutionary Computation 2002;6(2):182-197.

[32] Dong C, Kalantari M, Davies IJ. Robustness for unidirectional carbon/glass fibre reinforced hybrid epoxy composites under flexural loading. Composite Structures, 2015;128:354-362.

[33] Kalantari M, Dong C, Davies IJ. Multi-objective analysis for optimal and robust design of unidirectional glass/carbon fibre reinforced hybrid epoxy composites under flexural loading. Composites Part B: Engineering, 2016;84:130-139.

[34] Kalantari M, Dong C, Davies IJ. Multi-objective robust optimization of unidirectional carbon/glass fibre reinforced hybrid composites under flexural loading. Composite Structures, 2016;138:264-275.

[35] Elishakoff I, Ohsaki M. Optimization and anti-optimization of structures under uncertainty. 3rd edition. London: Imperial College Press; 2010.

[36] Kerner EH. The elastic and thermos-elastic properties of composite media. Proceedings of the Physical Society, London, Section B, 1956;69(8):808-813.

[37] Hashin Z, Rosen BW. The elastic moduli of fiber-reinforced materials. Journal of Applied Mechanics, 31 (1964):223-232.

[38] Panda B, Garg A, Jian Z, Heidarzadeh A, Gao L. Characterization of the tensile properties of friction stir welded aluminum alloy joints based on axial force, traverse speed, and rotational speed. Frontiers of Mechanical Engineering, 2016;11 (3):289-298.

[39] Garg A, Sarma S, Panda BN, Zhang J, Gao L. Study of effect of nanofluid concentration on response characteristics of machining process for cleaner production. Journal of Cleaner Production, 2016;135:476-489.

[40] Kalantari M, Nami MR, Kadivar MH. Optimization of composite sandwich panel against impact using genetic algorithm. International Journal of Impact Engineering, 2010:37(6):599-604.

[41] Badalló, P, Trias D, Marín L, Mayugo JA. A comparative study of genetic algorithms for the multi-objective optimization of composite stringers under compression loads. Composites Part B: Engineering, 2013;47:130-136.

[42] Dong C, Ranaweera-Jayawardena HA, Davies IJ. Flexural properties of hybrid composites reinforced by S-2 glass and T700S carbon fibres. Composites Part B: Engineering, 2012;43(2):573-581.

[43] Rafai NH, Islam MN. An investigation into dimensional accuracy and surface finish achievable in dry turning. Machining Science and Technology, 2009;13:571-589.

[44] Islam MN, Boswell B. An investigation of surface finish in dry turning. pp. 895-900 in Proceedings of the World Congress on Engineering 2011 (WCE 2011), Volume 1, July 6-8th 2011, London, U.K. 2011.

# 9

# Conclusions and Future Work

The main results and achievements of the work presented in this thesis can be summarized as follows;

- The sensitivity of laminated hybrid composites under flexural load to manufacture related uncertainties in the design variables was understood and a method to assess the robustness of such materials was proposed.
- An efficient method was introduced for analysing hybrid composite materials comprised of high elongation and low elongation fibres when uncertainties were included and which can be simply utilized by designers without solving cumbersome numerical or analytical computations.
- The reasons behind the emergence of a hybrid effect in laminated hybrid composite containing low elongation and high elongation fibres (and specifically in carbon and glass fibre-reinforced epoxy hybrid laminates) were addressed.
- Methods were proposed for solving the problem of minimizing the weight and cost of unidirectional and multidirectional laminated hybrid composites when a minimum strength is required and uncertainties in design parameters and material properties are incorporated.
- High performance optimization algorithms were developed for solving the problem of robust optimization of hybrid composites at a higher rate when compared to other commonly used algorithms.

- The effects of manufacture related uncertainties on the Pareto optimal solution of weight and cost minimization of carbon and glass fibre-reinforced epoxy hybrid laminated plates were studied in detail with several options and recommendations for improving manufacturing processes being presented.

Chapters 1 and 2 of this thesis gave a comprehensive introduction and background concerning the flexural behaviour of hybrid composites and associated optimization problems.

The robustness and sensitivity of unidirectional S-2 glass and T700S carbon reinforced epoxy hybrid composites under flexural loading was studied in Chapter 3 and the hybrid effect was fitted using a regression model. A robustness index was introduced to evaluate the robustness of hybrid composites with guidelines being presented for the design of robust hybrid composites by introducing the concept of robust strength.

In Chapter 4, the classical lamination theory and finite element analysis were used to estimate the flexural stress and modulus of hybrid composites comprised of low elongation and high elongation fibres, *i.e.*, carbon and glass fibres. The results for flexural strength based on commonly used failure theories were compared and it was found that the most suitable failure theory for the hybrid composites investigated in this study was maximum strain theory. By comparing the stress distribution within hybrid composite with different stacking configurations and their apparent flexural strength and modulus, the reasons behind the emergence of a hybrid effect in the flexural strength of unidirectional and multidirectional hybrid composites were investigated. It was found that there are several conflicting factors which contributed to the presence of a hybrid effect. Based on these factors, four general rules were obtained for improving the flexural strength of such laminated hybrid composites. In general, it was concluded that a positive hybrid effect can be achieved for both unidirectional and multidirectional hybrid composites only if the proper stacking configuration is used.

A multi-objective analysis of unidirectional hybrid S-2 glass and T700S carbon fibre-reinforced epoxy composites with respect to the flexural properties was presented

in Chapter 5. Classical lamination theory was employed and four objectives, namely, maximizing the flexural strength and robustness and minimizing the weight and cost were considered with a robust index being used to evaluate the robustness of the hybrid composites. The weighted sum method was employed to convert the multi-objective optimization problem to a single-objective with the weighting factors being determined based on an analytical hierarchy process for different scenarios.

In Chapter 6, the multi-objective robust optimization of T700S carbon/E glass fibre-reinforced epoxy hybrid composites with respect to minimum weight and cost and subject to a prescribed flexural strength was investigated through the aid of a new modified hybrid evolutionary algorithm based on NSGA-II that was enhanced through the incorporation of a fractional factorial design based on a local search. It was shown that the proposed modified hybrid algorithm possessed superior performance compared to the original NSGA-II, with the convergence rate and diversity of the solution points being significantly better. Pareto optimal fronts for different levels of minimum flexural strength with and without considering uncertainties were obtained and different example scenarios were studied to illustrate the applicability of the results. It was indicated that, in general, uncertainties increase the weight and cost of the hybrid composites, however through appropriate hybridization of CFRP composites, not only the strength but also the weight and cost can be optimized.

Multi-directional hybrid composites have been investigated in Chapter 7. The objectives, constraint and uncertain variables were considered to be the same as that considered in previous chapters with the worst case for the flexural strength being determined through an anti-optimization method using a GA optimizer. The results of the optimization problem indicated that manufacturing uncertainties increase the material cost and density and that high strength composites are more sensitive to uncertainties. Sensitivity analysis also showed that the hybrid composites investigated in this study were more sensitive to variations in thickness when compared to variations in fibre orientation angle.

The effect of three sources of uncertainties, namely, matrix voids, fibre misalignment and thickness variation on the flexural performance of hybrid composites were studied in Chapter 8 with the contribution of uncertainty sources on the optimal

results being measured by the ANOVA method. It was concluded that, for the hybrid composites investigated in this study, the level of void content played an important role in the performance of the composite. Results indicated that when the void content exceeded 2%, the degrading effect on the composite performance became more critical compared to ±10% variation in lamina thickness and ±3º variation in fibre orientation angle.

A limitation of this study is that the specimen was a rectangular beam with large span-to-depth ratio subject to flexural load, so that the inter-laminar shear and out of plane stresses were considered to be negligible. However, for more complex geometries, instead of CLT, more accurate methods for estimating the critical stress within the specimen such as first order shear deformation theory (FSDT) or higher order theories or FEM could be coupled with the presented optimisation algorithms. By employing more accurate methods for determining the load capacity, the response of the specimen under other load types, such as tensile, compression and torsion could be determined more accurately and the results could be used for sensitivity analysis and optimization with the aid of similar methods. However, most of the other theories such as FSDT require significant additional computational power and thus makes the optimization problem even more time consuming.

The same methodology can be used for other loading configurations and more complex geometries subject to taking into account inter-laminar shear and out of plane stresses for more complex geometries. More accurate results can be achieved by developing and performing FEM.

In addition, this study was limited to six laminas based on first ply failure (FPF). The number of laminas could be used as a design variable with progressive failure of the laminas being considered instead of first ply failure to increase the accuracy and applicability of the problem. Since only uncertainties in lamina thickness, fibre angle orientation and presence of voids were investigated, a further study could assess the effect of other defects and uncertainties, such as fibre waviness or undulation, uncertainty in bonding between fibre and matrix and matrix cracking as well as variation in the geometry of the specimen or applied load and boundary conditions.

Since the presence of voids were found to be a critical factor in uncertainty, the geometry of the voids and their location should also be more precisely studied, especially from the microscopic point of view and resulting initiation of local failure modes.

The objective functions of the optimization problems were chosen to be cost and weight of the material. Material cost was used as the cost index regardless of manufacturing cost, however, it is known that manufacture costs are affected by the composite fibre type and their stacking sequence, thus the inclusion of more accurate cost models which incorporate manufacturing parameters will improve the accuracy of optimized problems.

The scope of this study is also limited to carbon and glass fibres, hence, the performance of the other fibre types through hybridisation would be a fruitful area for further work where experimental data is available. It is noteworthy that in case of using other fibre types, applying the appropriate failure theory would be the key factor.

Since there is limited experimental data available in the field of optimization of multi-directional hybrid composites, the findings in the present study suggest optimal stacking configuration for such materials, therefore, further experimental investigation into the hybrid effect for multi-directional carbon/glass hybrid composites is strongly recommended for not only static loads but also dynamic loads.

p r d d d pr

## Statement of Contribution

To Whom It May Concern,

I, **Mehdi Kalantari**, contributed (developed model and generated some of the results) to the paper entitled

- Robustness for unidirectional carbon/glass fibre reinforced hybrid epoxy composites under flexural loading, Composite Structures, Volume 128, 15 September 2015, Pages 354-362, ISSN 0263-8223, http://dx.doi.org/10.1016/j.compstruct.2015.03.059

Kalantari

*Signature*

I, as an Author/Co-Author, endorse that this level of contribution by the candidate indicated above is

appropriate.

**Dr Chensong Dong**

*Signature*

**Dr Ian J. Davies**

Ian Davies

*Signature*

## Statement of Contribution

To Whom It May Concern,

I, **Mehdi Kalantari**, contributed substantially (as the main author) to the papers entitled:

- Multi-objective analysis for optimal and robust design of unidirectional glass/carbon fibre reinforced hybrid epoxy composites under flexural loading, Composites Part B: Engineering, Volume 84, January 2016, Pages 130-139, http://dx.doi.org/10.1016/j.compositesb.2015.08.050
- Multi-objective robust optimisation of unidirectional carbon/glass fibre reinforced hybrid composites under flexural loading, Composite Structures, Volume 138, 15 March 2016, Pages 264-275, http://dx.doi.org/10.1016/j.compstruct.2015.11.034
- Numerical investigation of the hybridisation mechanism in fibre reinforced hybrid composites subjected to flexural load, Composites Part B: Engineering, Volume 102, 1 October 2016, Pages 100-111, http://dx.doi.org/10.1016/j.compositesb.2016.07.012
- Effect of matrix voids, fibre misalignment and thickness variation on multi-objective robust optimization of carbon/glass fibre-reinforced hybrid composites under flexural loading, Composites Part B: Engineering, Volume 123, 15 August 2017, Pages 136-147, http://dx.doi.org/10.1016/j.compositesb.2017.05.022
- Multi-objective robust optimization of multi-directional carbon/glass fibre-reinforced hybrid composites with manufacture related uncertainties under flexural loading. Composite Structures, Volume 182, 15 December 2017, Pages 132-142, http://dx.doi.org/10.1016/j.compstruct.2017.09.019

*Signature*

I, as a Co-Author, endorse that this level of contribution by the candidate indicated above is appropriate.

**Dr Chensong Dong**

*Signature*

**Dr Ian J. Davies**

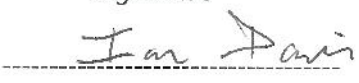

*Signature*

# Copyright Permission



**ELSEVIER LICENSE**
**TERMS AND CONDITIONS**

Jun 11, 2017

This Agreement between Mehdi Kalantari ("You") and Elsevier ("Elsevier") consists of your license details and the terms and conditions provided by Elsevier and Copyright Clearance Center.

| | |
|---|---|
| License Number | 4112320944657 |
| License date | May 19, 2017 |
| Licensed Content Publisher | Elsevier |
| Licensed Content Publication | Composite Structures |
| Licensed Content Title | Robustness for unidirectional carbon/glass fibre reinforced hybrid epoxy composites under flexural loading |
| Licensed Content Author | Chensong Dong,Mehdi Kalantari,Ian J. Davies |
| Licensed Content Date | Sep 15, 2015 |
| Licensed Content Volume | 128 |
| Licensed Content Issue | n/a |
| Licensed Content Pages | 9 |
| Start Page | 354 |
| End Page | 362 |
| Type of Use | reuse in a thesis/dissertation |
| Intended publisher of new work | other |
| Portion | full article |
| Format | both print and electronic |
| Are you the author of this Elsevier article? | Yes |
| Will you be translating? | No |
| Order reference number | 103 |
| Title of your thesis/dissertation | Optimum and Robust Design of Fibre-Reinforced Composites with Manufacture Related Uncertainties |
| Expected completion date | Jun 2017 |
| Estimated size (number of pages) | 150 |
| Elsevier VAT number | GB 494 6272 12 |
| Requestor Location | Mehdi Kalantari<br>Victoria Park, WA 6100<br>Australia<br>Attn: Mehdi Kalantari |
| Total | 0.00 AUD |
| Terms and Conditions | |

## INTRODUCTION

1. The publisher for this copyrighted material is Elsevier. By clicking "accept" in connection with completing this licensing transaction, you agree that the following terms and conditions apply to this transaction (along with the Billing and Payment terms and conditions

**ELSEVIER LICENSE**
**TERMS AND CONDITIONS**

Jun 11, 2017

This Agreement between Mehdi Kalantari ("You") and Elsevier ("Elsevier") consists of your license details and the terms and conditions provided by Elsevier and Copyright Clearance Center.

| | |
|---|---|
| License Number | 4112320467383 |
| License date | May 19, 2017 |
| Licensed Content Publisher | Elsevier |
| Licensed Content Publication | Composites Part B: Engineering |
| Licensed Content Title | Numerical investigation of the hybridisation mechanism in fibre reinforced hybrid composites subjected to flexural load |
| Licensed Content Author | Mehdi Kalantari,Chensong Dong,Ian J. Davies |
| Licensed Content Date | Oct 1, 2016 |
| Licensed Content Volume | 102 |
| Licensed Content Issue | n/a |
| Licensed Content Pages | 12 |
| Start Page | 100 |
| End Page | 111 |
| Type of Use | reuse in a thesis/dissertation |
| Portion | full article |
| Format | both print and electronic |
| Are you the author of this Elsevier article? | Yes |
| Will you be translating? | No |
| Order reference number | 104 |
| Title of your thesis/dissertation | Optimum and Robust Design of Fibre-Reinforced Composites with Manufacture Related Uncertainties |
| Expected completion date | Jun 2017 |
| Estimated size (number of pages) | 150 |
| Elsevier VAT number | GB 494 6272 12 |
| Requestor Location | Mehdi Kalantari<br><br>Victoria Park, WA 6100<br>Australia<br>Attn: Mehdi Kalantari |
| Total | 0.00 AUD |
| Terms and Conditions | |

## INTRODUCTION

1. The publisher for this copyrighted material is Elsevier. By clicking "accept" in connection with completing this licensing transaction, you agree that the following terms and conditions apply to this transaction (along with the Billing and Payment terms and conditions established by Copyright Clearance Center, Inc. ("CCC"), at the time that you opened your Rightslink account and that are available at any time at http://myaccount.copyright.com).

**ELSEVIER LICENSE**
**TERMS AND CONDITIONS**

Jun 11, 2017

This Agreement between Mehdi Kalantari ("You") and Elsevier ("Elsevier") consists of your license details and the terms and conditions provided by Elsevier and Copyright Clearance Center.

| | |
|---|---|
| License Number | 4112320746608 |
| License date | May 19, 2017 |
| Licensed Content Publisher | Elsevier |
| Licensed Content Publication | Composites Part B: Engineering |
| Licensed Content Title | Multi-objective analysis for optimal and robust design of unidirectional glass/carbon fibre reinforced hybrid epoxy composites under flexural loading |
| Licensed Content Author | Mehdi Kalantari,Chensong Dong,Ian J. Davies |
| Licensed Content Date | Jan 1, 2016 |
| Licensed Content Volume | 84 |
| Licensed Content Issue | n/a |
| Licensed Content Pages | 10 |
| Start Page | 130 |
| End Page | 139 |
| Type of Use | reuse in a thesis/dissertation |
| Intended publisher of new work | other |
| Portion | full article |
| Format | both print and electronic |
| Are you the author of this Elsevier article? | Yes |
| Will you be translating? | No |
| Order reference number | 105 |
| Title of your thesis/dissertation | Optimum and Robust Design of Fibre-Reinforced Composites with Manufacture Related Uncertainties |
| Expected completion date | Jun 2017 |
| Estimated size (number of pages) | 150 |
| Elsevier VAT number | GB 494 6272 12 |
| Requestor Location | Mehdi Kalantari<br><br>Victoria Park, WA 6100<br>Australia<br>Attn: Mehdi Kalantari |
| Total | 0.00 AUD |
| Terms and Conditions | |

## INTRODUCTION

1. The publisher for this copyrighted material is Elsevier. By clicking "accept" in connection with completing this licensing transaction, you agree that the following terms and conditions

**ELSEVIER LICENSE**
**TERMS AND CONDITIONS**

Jun 11, 2017

This Agreement between Mehdi Kalantari ("You") and Elsevier ("Elsevier") consists of your license details and the terms and conditions provided by Elsevier and Copyright Clearance Center.

| | |
|---|---|
| License Number | 4112321214196 |
| License date | May 19, 2017 |
| Licensed Content Publisher | Elsevier |
| Licensed Content Publication | Composite Structures |
| Licensed Content Title | Multi-objective robust optimisation of unidirectional carbon/glass fibre reinforced hybrid composites under flexural loading |
| Licensed Content Author | Mehdi Kalantari,Chensong Dong,Ian J. Davies |
| Licensed Content Date | Mar 15, 2016 |
| Licensed Content Volume | 138 |
| Licensed Content Issue | n/a |
| Licensed Content Pages | 12 |
| Start Page | 264 |
| End Page | 275 |
| Type of Use | reuse in a thesis/dissertation |
| Intended publisher of new work | other |
| Portion | full article |
| Format | both print and electronic |
| Are you the author of this Elsevier article? | Yes |
| Will you be translating? | No |
| Order reference number | 106 |
| Title of your thesis/dissertation | Optimum and Robust Design of Fibre-Reinforced Composites with Manufacture Related Uncertainties |
| Expected completion date | Jun 2017 |
| Estimated size (number of pages) | 150 |
| Elsevier VAT number | GB 494 6272 12 |
| Requestor Location | Mehdi Kalantari<br><br>Victoria Park, WA 6100<br>Australia<br>Attn: Mehdi Kalantari |
| Total | 0.00 AUD |
| Terms and Conditions | |

## INTRODUCTION

1. The publisher for this copyrighted material is Elsevier. By clicking "accept" in connection with completing this licensing transaction, you agree that the following terms and conditions apply to this transaction (along with the Billing and Payment terms and conditions

**ELSEVIER LICENSE**
**TERMS AND CONDITIONS**

Jun 11, 2017

This Agreement between Mehdi Kalantari ("You") and Elsevier ("Elsevier") consists of your license details and the terms and conditions provided by Elsevier and Copyright Clearance Center.

| | |
|---|---|
| License Number | 4112321364930 |
| License date | May 19, 2017 |
| Licensed Content Publisher | Elsevier |
| Licensed Content Publication | Composites Part B: Engineering |
| Licensed Content Title | Effect of matrix voids, fibre misalignment and thickness variation on multi-objective robust optimization of carbon/glass fibre-reinforced hybrid composites under flexural loading |
| Licensed Content Author | Mehdi Kalantari,Chensong Dong,Ian J. Davies |
| Licensed Content Date | Aug 15, 2017 |
| Licensed Content Volume | 123 |
| Licensed Content Issue | n/a |
| Licensed Content Pages | 12 |
| Start Page | 136 |
| End Page | 147 |
| Type of Use | reuse in a thesis/dissertation |
| Intended publisher of new work | other |
| Portion | full article |
| Format | both print and electronic |
| Are you the author of this Elsevier article? | Yes |
| Will you be translating? | No |
| Order reference number | 108 |
| Title of your thesis/dissertation | Optimum and Robust Design of Fibre-Reinforced Composites with Manufacture Related Uncertainties |
| Expected completion date | Jun 2017 |
| Estimated size (number of pages) | 150 |
| Elsevier VAT number | GB 494 6272 12 |
| Requestor Location | Mehdi Kalantari<br><br>Victoria Park, WA 6100<br>Australia<br>Attn: Mehdi Kalantari |
| Total | 0.00 AUD |
| Terms and Conditions | |

## INTRODUCTION

1. The publisher for this copyrighted material is Elsevier. By clicking "accept" in connection with completing this licensing transaction, you agree that the following terms and conditions

established by Copyright Clearance Center, Inc. ("CCC"), at the time that you opened your Rightslink account and that are available at any time at http://myaccount.copyright.com).

**GENERAL TERMS**

2. Elsevier hereby grants you permission to reproduce the aforementioned material subject to the terms and conditions indicated.

3. Acknowledgement: If any part of the material to be used (for example, figures) has appeared in our publication with credit or acknowledgement to another source, permission must also be sought from that source. If such permission is not obtained then that material may not be included in your publication/copies. Suitable acknowledgement to the source must be made, either as a footnote or in a reference list at the end of your publication, as follows:

"Reprinted from Publication title, Vol /edition number, Author(s), Title of article / title of chapter, Pages No., Copyright (Year), with permission from Elsevier [OR APPLICABLE SOCIETY COPYRIGHT OWNER]." Also Lancet special credit - "Reprinted from The Lancet, Vol. number, Author(s), Title of article, Pages No., Copyright (Year), with permission from Elsevier."

4. Reproduction of this material is confined to the purpose and/or media for which permission is hereby given.

5. Altering/Modifying Material: Not Permitted. However figures and illustrations may be altered/adapted minimally to serve your work. Any other abbreviations, additions, deletions and/or any other alterations shall be made only with prior written authorization of Elsevier Ltd. (Please contact Elsevier at permissions@elsevier.com). No modifications can be made to any Lancet figures/tables and they must be reproduced in full.

6. If the permission fee for the requested use of our material is waived in this instance, please be advised that your future requests for Elsevier materials may attract a fee.

7. Reservation of Rights: Publisher reserves all rights not specifically granted in the combination of (i) the license details provided by you and accepted in the course of this licensing transaction, (ii) these terms and conditions and (iii) CCC's Billing and Payment terms and conditions.

8. License Contingent Upon Payment: While you may exercise the rights licensed immediately upon issuance of the license at the end of the licensing process for the transaction, provided that you have disclosed complete and accurate details of your proposed use, no license is finally effective unless and until full payment is received from you (either by publisher or by CCC) as provided in CCC's Billing and Payment terms and conditions. If full payment is not received on a timely basis, then any license preliminarily granted shall be deemed automatically revoked and shall be void as if never granted. Further, in the event that you breach any of these terms and conditions or any of CCC's Billing and Payment terms and conditions, the license is automatically revoked and shall be void as if never granted. Use of materials as described in a revoked license, as well as any use of the materials beyond the scope of an unrevoked license, may constitute copyright infringement and publisher reserves the right to take any and all action to protect its copyright in the materials.

9. Warranties: Publisher makes no representations or warranties with respect to the licensed material.

10. Indemnity: You hereby indemnify and agree to hold harmless publisher and CCC, and their respective officers, directors, employees and agents, from and against any and all claims arising out of your use of the licensed material other than as specifically authorized pursuant to this license.

11. No Transfer of License: This license is personal to you and may not be sublicensed, assigned, or transferred by you to any other person without publisher's written permission.

12. No Amendment Except in Writing: This license may not be amended except in a writing signed by both parties (or, in the case of publisher, by CCC on publisher's behalf).

13. Objection to Contrary Terms: Publisher hereby objects to any terms contained in any purchase order, acknowledgment, check endorsement or other writing prepared by you, which terms are inconsistent with these terms and conditions or CCC's Billing and Payment terms and conditions. These terms and conditions, together with CCC's Billing and Payment terms and conditions (which are incorporated herein), comprise the entire agreement between you and publisher (and CCC) concerning this licensing transaction. In the event of

any conflict between your obligations established by these terms and conditions and those established by CCC's Billing and Payment terms and conditions, these terms and conditions shall control.
14. Revocation: Elsevier or Copyright Clearance Center may deny the permissions described in this License at their sole discretion, for any reason or no reason, with a full refund payable to you. Notice of such denial will be made using the contact information provided by you. Failure to receive such notice will not alter or invalidate the denial. In no event will Elsevier or Copyright Clearance Center be responsible or liable for any costs, expenses or damage incurred by you as a result of a denial of your permission request, other than a refund of the amount(s) paid by you to Elsevier and/or Copyright Clearance Center for denied permissions.

**LIMITED LICENSE**

The following terms and conditions apply only to specific license types:
15. **Translation**: This permission is granted for non-exclusive world **English** rights only unless your license was granted for translation rights. If you licensed translation rights you may only translate this content into the languages you requested. A professional translator must perform all translations and reproduce the content word for word preserving the integrity of the article.
16. **Posting licensed content on any Website**: The following terms and conditions apply as follows: Licensing material from an Elsevier journal: All content posted to the web site must maintain the copyright information line on the bottom of each image; A hyper-text must be included to the Homepage of the journal from which you are licensing at http://www.sciencedirect.com/science/journal/xxxxx or the Elsevier homepage for books at http://www.elsevier.com; Central Storage: This license does not include permission for a scanned version of the material to be stored in a central repository such as that provided by Heron/XanEdu.
Licensing material from an Elsevier book: A hyper-text link must be included to the Elsevier homepage at http://www.elsevier.com . All content posted to the web site must maintain the copyright information line on the bottom of each image.

**Posting licensed content on Electronic reserve**: In addition to the above the following clauses are applicable: The web site must be password-protected and made available only to bona fide students registered on a relevant course. This permission is granted for 1 year only. You may obtain a new license for future website posting.
17. **For journal authors:** the following clauses are applicable in addition to the above:
**Preprints:**
A preprint is an author's own write-up of research results and analysis, it has not been peer-reviewed, nor has it had any other value added to it by a publisher (such as formatting, copyright, technical enhancement etc.).
Authors can share their preprints anywhere at any time. Preprints should not be added to or enhanced in any way in order to appear more like, or to substitute for, the final versions of articles however authors can update their preprints on arXiv or RePEc with their Accepted Author Manuscript (see below).
If accepted for publication, we encourage authors to link from the preprint to their formal publication via its DOI. Millions of researchers have access to the formal publications on ScienceDirect, and so links will help users to find, access, cite and use the best available version. Please note that Cell Press, The Lancet and some society-owned have different preprint policies. Information on these policies is available on the journal homepage.
**Accepted Author Manuscripts:** An accepted author manuscript is the manuscript of an article that has been accepted for publication and which typically includes author-incorporated changes suggested during submission, peer review and editor-author communications.
Authors can share their accepted author manuscript:

- immediately
    - via their non-commercial person homepage or blog
    - by updating a preprint in arXiv or RePEc with the accepted manuscript

- via their research institute or institutional repository for internal institutional uses or as part of an invitation-only research collaboration work-group
- directly by providing copies to their students or to research collaborators for their personal use
- for private scholarly sharing as part of an invitation-only work group on commercial sites with which Elsevier has an agreement

- After the embargo period
  - via non-commercial hosting platforms such as their institutional repository
  - via commercial sites with which Elsevier has an agreement

In all cases accepted manuscripts should:

- link to the formal publication via its DOI
- bear a CC-BY-NC-ND license - this is easy to do
- if aggregated with other manuscripts, for example in a repository or other site, be shared in alignment with our hosting policy not be added to or enhanced in any way to appear more like, or to substitute for, the published journal article.

**Published journal article (JPA):** A published journal article (PJA) is the definitive final record of published research that appears or will appear in the journal and embodies all value-adding publishing activities including peer review co-ordination, copy-editing, formatting, (if relevant) pagination and online enrichment.
Policies for sharing publishing journal articles differ for subscription and gold open access articles:
**Subscription Articles:** If you are an author, please share a link to your article rather than the full-text. Millions of researchers have access to the formal publications on ScienceDirect, and so links will help your users to find, access, cite, and use the best available version.
Theses and dissertations which contain embedded PJAs as part of the formal submission can be posted publicly by the awarding institution with DOI links back to the formal publications on ScienceDirect.
If you are affiliated with a library that subscribes to ScienceDirect you have additional private sharing rights for others' research accessed under that agreement. This includes use for classroom teaching and internal training at the institution (including use in course packs and courseware programs), and inclusion of the article for grant funding purposes.
**Gold Open Access Articles:** May be shared according to the author-selected end-user license and should contain a CrossMark logo, the end user license, and a DOI link to the formal publication on ScienceDirect.
Please refer to Elsevier's posting policy for further information.
18. **For book authors** the following clauses are applicable in addition to the above:
Authors are permitted to place a brief summary of their work online only. You are not allowed to download and post the published electronic version of your chapter, nor may you scan the printed edition to create an electronic version. **Posting to a repository:** Authors are permitted to post a summary of their chapter only in their institution's repository.
19. **Thesis/Dissertation**: If your license is for use in a thesis/dissertation your thesis may be submitted to your institution in either print or electronic form. Should your thesis be published commercially, please reapply for permission. These requirements include permission for the Library and Archives of Canada to supply single copies, on demand, of the complete thesis and include permission for Proquest/UMI to supply single copies, on demand, of the complete thesis. Should your thesis be published commercially, please reapply for permission. Theses and dissertations which contain embedded PJAs as part of the formal submission can be posted publicly by the awarding institution with DOI links back to the formal publications on ScienceDirect.

**Elsevier Open Access Terms and Conditions**
You can publish open access with Elsevier in hundreds of open access journals or in nearly 2000 established subscription journals that support open access publishing. Permitted third party re-use of these open access articles is defined by the author's choice of Creative Commons user license. See our open access license policy for more information.

**Terms & Conditions applicable to all Open Access articles published with Elsevier:**
Any reuse of the article must not represent the author as endorsing the adaptation of the article nor should the article be modified in such a way as to damage the author's honour or reputation. If any changes have been made, such changes must be clearly indicated.
The author(s) must be appropriately credited and we ask that you include the end user license and a DOI link to the formal publication on ScienceDirect.
If any part of the material to be used (for example, figures) has appeared in our publication with credit or acknowledgement to another source it is the responsibility of the user to ensure their reuse complies with the terms and conditions determined by the rights holder.
**Additional Terms & Conditions applicable to each Creative Commons user license:**
**CC BY:** The CC-BY license allows users to copy, to create extracts, abstracts and new works from the Article, to alter and revise the Article and to make commercial use of the Article (including reuse and/or resale of the Article by commercial entities), provided the user gives appropriate credit (with a link to the formal publication through the relevant DOI), provides a link to the license, indicates if changes were made and the licensor is not represented as endorsing the use made of the work. The full details of the license are available at http://creativecommons.org/licenses/by/4.0.
**CC BY NC SA:** The CC BY-NC-SA license allows users to copy, to create extracts, abstracts and new works from the Article, to alter and revise the Article, provided this is not done for commercial purposes, and that the user gives appropriate credit (with a link to the formal publication through the relevant DOI), provides a link to the license, indicates if changes were made and the licensor is not represented as endorsing the use made of the work. Further, any new works must be made available on the same conditions. The full details of the license are available at http://creativecommons.org/licenses/by-nc-sa/4.0.
**CC BY NC ND:** The CC BY-NC-ND license allows users to copy and distribute the Article, provided this is not done for commercial purposes and further does not permit distribution of the Article if it is changed or edited in any way, and provided the user gives appropriate credit (with a link to the formal publication through the relevant DOI), provides a link to the license, and that the licensor is not represented as endorsing the use made of the work. The full details of the license are available at http://creativecommons.org/licenses/by-nc-nd/4.0.
Any commercial reuse of Open Access articles published with a CC BY NC SA or CC BY NC ND license requires permission from Elsevier and will be subject to a fee.
Commercial reuse includes:

- Associating advertising with the full text of the Article
- Charging fees for document delivery or access
- Article aggregation
- Systematic distribution via e-mail lists or share buttons

Posting or linking by commercial companies for use by customers of those companies.

20. **Other Conditions**:

v1.9

**Questions? customercare@copyright.com or +1-855-239-3415 (toll free in the US) or +1-978-646-2777.**

## Bibliography


Abachizadeh M, Tahani M. An ant colony optimization approach to multi-objective optimal design of symmetric hybrid laminates for maximum fundamental frequency and minimum cost. Structural and Multidisciplinary Optimization. 2009;37:367-376.

Adali S, Lene F, Duvaut G, Chiaruttini V. Optimization of laminated composites subject to uncertain buckling loads. Composite Structures. 2003;62:261-269.

Adali S, Verijenko VE. Optimum stacking sequence design of symmetric hybrid laminates undergoing free vibrations. Composite Structures 2001;54(2-3):131-138.

Adali S, Walker M, Verijenko VE. Multi-objective optimization of laminated plates for maximum pre buckling, buckling and post buckling strengths using continuous and discrete ply angles. Composite Structures 1996;35(1):117-130.

Allen JK, Seepersad C, Choi H, Mistree F. Robust design for multiscale and multidisciplinary applications. Journal of Mechanical Design. 2006;128:832-843.

Almeida F.S, Awruch A.M. Design optimization of composite laminated structures using genetic algorithms and finite element analysis. Composite Structures 2009;88(3):443-454.

ANSYS Mechanical APDL Element Reference. Release 15. November 2013.

Antonio CAC. A hierarchical genetic algorithm with age structure for multimodal optimal design of hybrid composites. Structural and Multidisciplinary Optimization 2006;31(4):280-294.

António CC, Hoffbauer LN. An approach for reliability-based robust design optimisation of angle-ply composites. Composite Structures 2009;90(1):53-59.

António CC, Hoffbauer LN. From local to global importance measures of uncertainty propagation in composite structures. Composite Structures. 2008;85(3):213-225.

António CC. A hierarchical genetic algorithm with age structure for multimodal optimal design of hybrid composites. Structural and Multidisciplinary Optimization. 2006;31:280-294.

Ary Subagia IDG, Kim Y, Tijing LD, Kim CS, Shon HK. Effect of stacking sequence on the flexural properties of hybrid composites reinforced with carbon and basalt fibers. Composites Part B: Engineering. 2014;58:251-258.

Aveston J, Kelly A. Tensile First Cracking Strain and Strength of Hybrid Composites and Laminates. Philosophical Transactions of the Royal Society of London. Series A, Mathematical and Physical Sciences. 1980;294:519-534.

Aveston J, Sillwood JM, Synergistic fibre strengthening in hybrid composites. Journal of Materials Science. 1976;11:1877-1883.

Awad ZK, Aravinthan T, Zhuge Y, Gonzalez F. A review of optimization techniques used in the design of fibre composite structures for civil engineering applications. Materials & Design. 2012;33: 534-544.

Aymerich F, Serra M. Optimization of laminate stacking sequence for maximum buckling load using the ant colony optimization (ACO) metaheuristic. Composites Part A: Applied Science and Manufacturing. 2008;39:262-272.

Badalló, P, Trias D, Marín L, Mayugo JA. A comparative study of genetic algorithms for the multi-objective optimization of composite stringers under compression loads. Composites Part B: Engineering, 2013;47:130-136.

Banerjee S, Sankar BV. Mechanical properties of hybrid composites using finite element method based micromechanics. Composites Part B: Engineering. 2014;58:318-327.

Basseur M, Burke EK. Indicator-based multi-objective local search. 2007 IEEE Congress on Evolutionary Computation. 2007;3100-3107.

Bechikh S, Belgasmi N, Ben Said L, Ghédira K. PHC-NSGA-II: a novel multi-objective memetic algorithm for continuous optimization. In: Proceedings of 20th IEEE International Conference on Tools with Artificial Intelligence. 2008;1:180-189.

Bendsøe MP, Olhoff N, Taylor JE. A variational formulation for multicriteria structural optimization. Journal of Structural Mechanics. 1983;11:523-544.

Beyer H-G, Sendhoff B. Robust optimization–a comprehensive survey. Computer methods in applied mechanics and engineering 2007;196(33-34):3190-31218.

Bruyneel M, Fleury C. Composite structures optimization using sequential convex programming. Advances in Engineering Software. 2002;33:697-711.

Bullock RE. Strength ratios of composite materials in flexure and in tension. Journal of Composite Materials. 1974;8:200-206.

Bunsell A, Harris B. Hybrid carbon and glass fibre composites. Composites, 1974;5:157-164.

Cai H, Aref AJ. On the design and optimization of hybrid carbon fiber reinforced polymer-steel cable system for cable-stayed bridges. Composites Part B: Engineering, 2015;68:146-152.

Callahan KJ, Weeks GE. Optimum design of composite laminates using genetic algorithms. Composites Engineering. 1992;2:149-160.

Chamis CC, Abumeri GH. Probabilistic dynamic buckling of composite shell structures. Composites Part A: Applied Science and Manufacturing. 2005;36(10):1368-1380.

Chamis CC, Shiao MC. IPACS – integrated probabilistic assessment of composite structures: Code development and application. Third NASA Advanced Composite Technology Conference 1992;987-999.

Chamis CC, Shiao MC. IPACS (Integrated Probabilistic Assessment of Composite Structures): Code development and applications.

Chamis CC. Probabilistic simulation of multi-scale composite behavior. Theoretical and applied fracture mechanics. 2004;41(1):51-61.

Cheng S, Zhou J, Li M. A new hybrid algorithm for multi-objective robust optimization with interval uncertainty. Journal of Mechanical Design, 2015;137: 021401-021401.

Chiachio M, Chiachio J, Rus G. Reliability in composites–A selective review and survey of current development. Composites Part B: Engineering. 2012;43(3):902-913.

Chou TW. Microstructural design of fiber composites. Cambridge University Press; 2005.

Conceição António CA. A hierarchical genetic algorithm with age structure for multimodal optimal design of hybrid composites. Structural and Multidisciplinary Optimization. 2006;31(4):280-94.

Curtin WA. Dimensionality and size effects on the strength of fiber-reinforced composites. Composites Science and Technology. 2000;60:543-551.

Czyżżak P, Jaszkiewicz A. Pareto simulated annealing—a metaheuristic technique for multiple-objective combinatorial optimization. Journal of Multi-Criteria Decision Analysis. 1998;7(1):34-47.

Davidon WC. Variable metric method for minimization. SIAM Journal on Optimization. 1991;1:1-17.

Davies IJ, Hamada H. Flexural properties of a hybrid polymer matrix composite containing carbon and silicon carbide fibres. Advanced Composite Materials. 2001;10:77-96.

de Almeida SFM. Effect of void content on the strength of composite laminates. Composite Structures, 1994;28(2):139-148.

De Melo W. Stability and optimization of several functions. Topology. 1976;15:1-12.

Deb K, Pratap A, Agarwal S, Meyarivan T. A fast and elitist multi-objective genetic algorithm: NSGA-II. IEEE Transactions on Evolutionary Computation 2002;6(2):182-197.

Deb K. "Multi-objective optimisation using evolutionary algorithms: an introduction." In: Wang L, Amos HC. Ng, Deb K, editors. Multi-objective evolutionary optimisation for product design and manufacturing. London: Springer, 2011. p. 3-34.

Deb K. Multi-objective optimization using evolutionary algorithms: John Wiley & Sons; 2001.

Defaria AR. Buckling optimization and anti-optimization of composite plates - uncertain loading combination. International Journal for Numerical Methods in Engineering 2002;53(3):719-732.

Di Sciuva M, Lomario D. A comparison between Monte Carlo and FORMs in calculating the reliability of a composite structure. Composite Structures. 2003;59(1):155-162.

Dickson RF, Fernando G, Adam T, Reiter H, Harris B. Fatigue behaviour of hybrid composites. Journal of materials science. 1989;24:227-233.

Dong C, Davies IJ. Flexural and tensile moduli of unidirectional hybrid epoxy composites reinforced by S-2 glass and T700S carbon fibres. Materials & Design (1980-2015). 2014;54:893-899.

Dong C, Davies IJ. Flexural and tensile strengths of unidirectional hybrid epoxy composites reinforced by S-2 glass and T700S carbon fibres. Materials & Design (1980-2015). 2014;54:955-966.

Dong C, Davies IJ. Flexural and tensile strengths of unidirectional hybrid epoxy composites reinforced by S-2 glass and T700S carbon fibres. Materials & Design. 2014;54:955-966.

Dong C, Davies IJ. Flexural properties of E glass and TR50S carbon fiber reinforced epoxy hybrid composites. Journal of materials engineering and performance. 2013;22(1):41-49.

Dong C, Davies IJ. Flexural properties of glass and carbon fiber reinforced epoxy hybrid composites. Proceedings of the Institution of Mechanical Engineers, Part L: Journal of Materials: Design and Applications. 2013;227(4):308-317.

Dong C, Davies IJ. Flexural strength of bidirectional hybrid epoxy composites reinforced by E glass and T700S carbon fibres. Composites Part B: Engineering. 2015;72:65-71.

Dong C, Davies IJ. Optimal design for the flexural behaviour of glass and carbon fibre reinforced polymer hybrid composites. Materials & Design. 2012;37:450-457.

Dong C, Duong J, Davies IJ. Flexural properties of S-2 glass and TR30S carbon fiber-reinforced epoxy hybrid composites. Polymer Composites. 2012;33(5):773-781.

Dong C, Duong J, Davies IJ. Flexural properties of S-2 glass and TR30S carbon fiber-reinforced epoxy hybrid composites. Polymer Composites. 2012;33(5):773-781.

Dong C, Kalantari M, Davies IJ. Robustness for unidirectional carbon/glass fibre reinforced hybrid epoxy composites under flexural loading. Composite Structures 2015;128:354-362.

Dong C, Ranaweera-Jayawardena HA, Davies IJ. Flexural properties of hybrid composites reinforced by S-2 glass and T700S carbon fibres. Composites Part B: Engineering. 2012;43(2):573-581.

Dong C, Sudarisman, Davies IJ. Flexural properties of E glass and TR50S carbon fiber reinforced epoxy hybrid composites. Journal of Materials Engineering and Performance. 2013;22:41-49.

Dong C. Effects of process-induced voids on the properties of fibre reinforced composites. Journal of Materials Science & Technology, 2016;32(7):597-604.

Dong C, Davies IJ. Effect of stacking sequence on the flexural properties of carbon and glass fibre-reinforced hybrid composites. Advanced Composites and Hybrid Materials. 2018;1-1-11.

Dorigo M, Birattari M, Stutzle T. Ant colony optimization. IEEE Computational Intelligence Magazine. 2006;1(4):28-39.

Dutra TA, Almeida SFM. Composite plate stiffness multicriteria optimization using lamination parameters. Composite Structures. 2015;133:166-177.

Elishakoff I, Ohsaki M. Optimization and anti-optimization of structures under uncertainty. 3rd edition. London: Imperial College Press; 2010.

Elishakoff IE, Haftka RT, Fang J. Structural design under bounded uncertainty - optimization with anti-optimization. Computers and Structures 1994;53(5):1401-1405.

Elishakoff IE, Kriegesmann B, Rolfes R, Huhne C, Kling A. Optimization and antioptimization of buckling load for composite cylindrical shells under uncertainties. AIAA Journal, 2012;50(7):1513-1524.

Elishakoff IE, Li YW, Starners JH. Deterministic method to predict the effect of unknown-but-bounded elastic moduli on the buckling of composite structures. Computer Methods in Applied Mechanics and Engineering 1994;111(1-2):155-167.

Erdal O, Sonmez FO. Optimum design of composite laminates for maximum buckling load capacity using simulated annealing. Composite Structures. 2005;71:45-52.

Federation. 1972;149-152.

Fernando G, Dickson RF, Adam T, Reiter H, Harris B. Fatigue behaviour of hybrid composites. Journal of materials science. 1988;23:3732-3743.

Fertig RS, Jensen EM. Effect of fiber volume fraction variation across multiple length scales on composite stress variation: the possibility of stochastic multiscale analysis. In55th AIAA/ASMe/ASCE/AHS/SC Structures, Structural Dynamics, and Materials Conference 2014 (p. 1169).

Frey HC, Patil SR. Identification and review of sensitivity analysis methods. Risk Analysis. 2002;22:553-578.

Fu SY, Lauke B, Mäder E, Yue CY, Hu X. Tensile properties of short-glass-fiber-and short-carbon-fiber-reinforced polypropylene composites. Composites Part A: Applied Science and Manufacturing. 2000;31:1117-1125.

Fukuda H, Chou TW. Stress Concentrations in a Hybrid Composite Sheet. Journal of Applied Mechanics. 1983;50:845-848.

Garg A, Sarma S, Panda BN, Zhang J, Gao L. Study of effect of nanofluid concentration on response characteristics of machining process for cleaner production. Journal of Cleaner Production, 2016;135:476-489.

Ghasemi H, Kerfriden P, Bordas SP, Muthu J, Zi G, Rabczuk T. Probabilistic multiconstraints optimization of cooling channels in ceramic matrix composites. Composites Part B: Engineering, 2015;81:107-119.

Ghiasi H, Fayazbakhsh K, Pasini D, Lessard L. Optimum stacking sequence design of composite materials Part II: Variable stiffness design. Composite Structures. 2010;93:1-13.

Ghiasi H, Pasini D, Lessard L. Optimum stacking sequence design of composite materials Part I: Constant stiffness design. Composite Structures. 2009;90:1-11.

Ghiasi H., Pasini D, Lessard L. A non-dominated sorting hybrid algorithm for multi-objective optimization of engineering problems. Engineering Optimization 2011;43(1):39-59.

Ghiorse SR. Effect of void content on the mechanical properties of carbon/epoxy laminates. S.A.M.P.E. quarterly, 1993;24 (2):54-59.

Giancaspro JW, Papakonstantinou CG, Balaguru PN. Flexural response of inorganic hybrid composites with E-Glass and Carbon fibers. Journal of Engineering Materials and Technology. 2010;132:021005-1-8.

Giancaspro JW, Papakonstantinou CG, Balaguru PN. Flexural response of inorganic hybrid composites with E-Glass and Carbon fibers. Journal of Engineering Materials and Technology 2010;132(2):0210051-02100518.

Guo Z-S, Liu L, Zhang B-M, Du S. Critical void content for thermoset composite laminates. Journal of Composite Materials, 2009;43(17):1775-1790.

Gurit. Guid to composites, www.gurit.com, Accessed: 5 June 2014

Gurit. Guide to composites, www.gurit.com, Accessed: 7 April 2015.

Hagstrand P-O, Bonjour F, Månson J-AE. The influence of void content on the structural flexural performance of unidirectional glass fibre reinforced polypropylene composites. Composites Part A: Applied Science and Manufacturing, 2005;36(5):705-714.

Han L, Neumann M. Effect of dimensionality on the Nelder–Mead simplex method. Optimization Methods and Software. 2006;21:1-16.

Harlow DG. Statistical Properties of Hybrid Composites. I. Recursion Analysis. Proceedings of the Royal Society of London. A. Mathematical and Physical Sciences. 1983;389:67-100.

Harris B, Bunsell AR. Impact properties of glass fibre/carbon fibre hybrid composites. Composites. 1975;6:197-201.

Hashin Z, Rosen BW. The elastic moduli of fiber-reinforced materials. Journal of Applied Mechanics. 1964;31:223-232.

Hashin Z. Analysis of composite materials—a survey. Journal of Applied Mechanics. 1983;50(3):481-505.

Hashin, Z. Analysis of composite materials - a survey. Journal of Applied Mechanics. 1983;50(3):481-505.

Hayashi T. On the improvement of mechanical properties of composites by hybrid composition. 8th Int. Reinforced Plastics Conf. Brighton, UK: British Plastics Federation. 1972;149-152.

Hedgepeth JM, Van Dyke P. Local Stress Concentrations in Imperfect Filamentary Composite Materials. Journal of Composite Materials. 1967;1:294-309.

Helton JC, Johnson JD, Sallaberry CJ, Storlie CB. Survey of sampling-based methods for uncertainty and sensitivity analysis. Reliability Engineering & System Safety. 2006;91:1175-1209.

Hemmatian H, Fereidoon A, Assareh E. Optimization of hybrid laminated composites using the multi-objective gravitational search algorithm (MOGSA). Engineering Optimization. 2014;46:1169-1182.

Hemmatian H, Fereidoon A, Sadollah A, Bahreininejad A. Optimization of laminate stacking sequence for minimizing weight and cost using elitist ant system optimization. Advances in engineering Software. 2013;57:8-18.

Hinton MJ, Kaddour AS, Soden PD. A comparison of the predictive capabilities of current failure theories for composite laminates, judged against experimental evidence. Composites Science and Technology. 2002;62(12-13):1725-1797.

Hu X, Huang Z, Wang Z. Hybridization of the multi-objective evolutionary algorithms and the gradient-based algorithms. In: Proceedings of the IEEE Congress on Evolutionary Computation (CEC 2003), 8–12 December, Canberra, Australia. New York: IEEE Press. 2003:870–877.

Huang B, Du X. Analytical robustness assessment for robust design. Structural and Multidisciplinary Optimization. 2007;34:123-37.

Huang H, Talreja R. Effects of void geometry on elastic properties of unidirectional fiber reinforced composites. Composite Science and Technology, 2005;65:1964-1981.

Hubert P, Poursartip A. Aspects of the compaction of composite angle laminates: an experimental investigation. Journal of Composite Materials. 2001;35(1):2-6.

Isa MT, Ahmed AS, Aderemi BO, Taib RM, Mohammed-Dabo IA. Effect of fiber type and combinations on the mechanical, physical and thermal stability properties of polyester hybrid composites. Composites Part B: Engineering. 2013;52:217-223.

Islam MN, Boswell B. An investigation of surface finish in dry turning. pp. 895-900 in Proceedings of the World Congress on Engineering 2011 (WCE 2011), Volume 1, July 6-8th 2011, London, U.K. 2011.

Jaeggi DM, Parks GT, Kipouros T, Clarkson PJ. The development of a multi-objective Tabu Search algorithm for continuous optimisation problems. European Journal of Operational Research. 2008;185(3):1192-1212.

Jang BZ, Chen LC, Wang CZ, Lin HT, Zee RH. Impact resistance and energy absorption mechanisms in hybrid composites. Composites science and technology. 1989;34:305-335.

Jarukumjorn K, Suppakarn N. Effect of glass fiber hybridization on properties of sisal fiber–polypropylene composites. Composites Part B: Engineering. 2009;40:623-627.

Jones RM. Mechanics of composite materials. 2nd Edition. Philadelphia: Taylor & Francis; 1998.

Kalantari M, Dong C, Davies IJ. Multi-objective analysis for optimal and robust design of unidirectional glass/carbon fibre reinforced hybrid epoxy composites under flexural loading. Composites Part B: Engineering. 2016;84:130-139.

Kalantari M, Dong C, Davies IJ. Multi-objective robust optimization of unidirectional carbon/glass fibre reinforced hybrid composites under flexural loading. Composite Structures 2016;138:264-275.

Kalantari M, Dong C, Davies IJ. Numerical investigation of the hybridisation mechanism in fibre reinforced hybrid composites subjected to flexural load. Composites Part B: Engineering, 2016;102:100-111.

Kalantari M, Nami MR, Kadivar MH. Optimization of composite sandwich panel against impact using genetic algorithm. International Journal of Impact Engineering. 2010;37:599-604.

Karahan M, Lomov SV, Bogdanovich AE, Mungalov D, Verpoest I. Internal geometry evaluation of non-crimp 3D orthogonal woven carbon fabric composite. Composites Part A: Applied Science and Manufacturing. 2010;41(9):1301-1311.

Karlsson M. The development of a technical cost model for composites. Stockholm, Sweden: KTH Royal Institute of Technology; 2013.

Kathiravan R, Ganguli R. Strength design of composite beam using gradient and particle swarm optimization. Composite Structures. 2007;81:471-479.

Kaufmann M, Zenkert D, Wennhage P. Integrated cost/weight optimization of aircraft structures. Structural and Multidisciplinary Optimization. 2010;41:325-334.

Kere P, Lyly M, Koski J. Using multicriterion optimization for strength design of composite laminates. Composite Structures. 2003;62:329-333.

Kerner EH. The elastic and thermos-elastic properties of composite media. Proceedings of the Physical Society, London, Section B, 1956;69(8):808-813.

Kim C, Lee DY. Design optimization of a curved actuator with piezoelectric fibers. International Journal of Modern Physics B. 2003;17:1971-1975.

Kim D-H, Choi D-H, Kim H-S. Design optimization of a carbon fiber reinforced composite automotive lower arm. Composites Part B: Engineering, 2014;58:400-407.

Kim HS, Hong SI, Kim SJ. On the rule of mixtures for predicting the mechanical properties of composites with homogeneously distributed soft and hard particles. Journal of Materials Processing Technology. 2001;112:109-113.

Knowles J, Corne D. The pareto archived evolution strategy: A new baseline algorithm for pareto multiobjective optimisation. in Evolutionary Computation, 1999. CEC 99. Proceedings of the 1999 Congress on. 1999. IEEE.

Knowles J, Corne D. The Pareto archived evolution strategy: a new baseline algorithm for multi-objective optimisation. In: Proceedings of the 1999 congress on evolutionary computation. IEEE Press, Piscataway, 2002;99-105.

Kočí V, Kočí J, Čáchová M, Vejmelková E, Černý R. Multi-parameter optimization of lime composite design using a modified downhill simplex method. Composites Part B: Engineering, 2016;93:184-189.

Kogiso N, Watson LT, Gürdal Z, Haftka RT. Genetic algorithms with local improvement for composite laminate design. Structural and Multidisciplinary Optimization. 1994;7:207-218.

Kretsis G. A review of the tensile, compressive, flexural and shear properties of hybrid fibre-reinforced plastics. Composites. 1987;18:13-23.

Kursa M, Kowalczyk-Gajewska K, Petryk H. Multi-objective optimization of thermo-mechanical properties of metal–ceramic composites. Composites Part B: Engineering, 2014;60:586-596.

Lakshmi K, Rama Mohan Rao A. Multi-objective optimal design of laminated composite skirt using hybrid NSGA. Meccanica 2013;48(6):1431-1450.

Lanzi L, Giavotto V. Post-buckling optimization of composite stiffened panels: Computations and experiments. Composite Structures 2006;73(2):208-220.

Latalski J. Ply thickness tolerances in stacking sequence optimization of multilayered laminate plates. Journal of theoretical and applied mechanics 2013;51(4):1039-1052.

Le Riche R, Haftka RT. Optimization of laminate stacking sequence for buckling load maximization by genetic algorithm. AIAA journal 1993;31(5):951-956.

Lee D, Morillo C, Oller S, Bugeda G, Oñate E. Robust design optimisation of advance hybrid (fiber–metal) composite structures. Composite Structures. 2013;99:181-192.

Lee MC, Mikulik Z, Kelly DW, Thomson RS, Degenhardt R. Robust design–a concept for imperfection insensitive composite structures. Composite Structures. 2010;92:1469-1477.

Lekou D.J, Philippidis T.P. Mechanical property variability in FRP laminates and its effect on failure prediction. Composites Part B: Engineering. 2008;39:1247-1256.

Le-Manh T, Lee J. Stacking sequence optimization for maximum strengths of laminated composite plates using genetic algorithm and isogeometric analysis. Composite Structures. 2014;116:357-363.

Liao Y-S, Chiou C-Y. Robust optimum designs of fiber-reinforced composites using constraints with sensitivity. Journal of Composite Materials 2006;40(22):2067-2080.

Liebig WV, Viets C, Schulte K, Fiedler B. Influence of voids on the compressive failure behaviour of fibre-reinforced composites. Composites Science and Technology, 2015;117:225-233.

Lin CC, YJ Lee. Stacking sequence optimization of laminated composite structures using genetic algorithm with local improvement. Composite structures. 2004;63:339-345.

Liu L, Zhang B-M, Wang D-F, Wu Z-J. Effects of cure cycles on void content and mechanical properties of composite laminates. Composite Structures, 2006;73(3):303-309.

Lo KH, Chim ESM. Compressive strength of unidirectional composites. Journal of Reinforced Plastics and Composites. 1992;11:838-896.

Lombardi M, Haftka, RT. Anti-optimization technique for structural design under load uncertainties. Computer Methods in Applied Mechanics and Engineering 1998;157(1-2):19-31.

Lopez RH, Luersen MA, Cursi ES. Optimization of laminated composites considering different failure criteria. Composites Part B: Engineering, 2009; 40(8):731-740.

Lukaszewicz DH-JA, Potter KD. The internal structure and conformation of prepreg with respect to reliable automated processing. Composites Part A: Applied Science and Manufacturing, 2011;42(3):283-292.

Lund E, Stegmann J. On structural optimization of composite shell structures using a discrete constitutive parametrization. Wind Energy. 2005;8:109-124.

Madeira JFA, Araújo AL, Mota Soares CM, Mota Soares CA, Ferreira AJM. Multiobjective design of viscoelastic laminated composite sandwich panels. Composites Part B: Engineering 2015;77:391-401.

Mallick PK. Fiber-Reinforced Composites: Materials, Manufacturing, and Design. 3rd edition. London: CRC press; 1993.

Manan A, Cooper J. Design of composite wings including uncertainties: a probabilistic approach. Journal of Aircraft. 2009;46:601-607.

Manders PW, Bader MG. The strength of hybrid glass/carbon fibre composites - Part 1 Failure strain enhancement and failure mode. Journal of Materials Science. 1981;16:2233-2245.

Marom G, Fischer S, Tuler FR, Wagner HD. Hybrid effects in composites: conditions for positive or negative effects versus rule-of-mixtures behaviour. Journal of Materials Science. 1978;13(7):1419-1426.

Miki M, Murotsu Y, Tanaka T, Shao S. Reliability-based optimization of fibrous laminated composites. Reliability Engineering & System Safety. 1997;56:285-290.

Miwa M, Horiba N. Effects of fibre length on tensile strength of carbon/glass fibre hybrid composites. Journal of materials science. 1994;29(4):973-977.

Moh J, Hwu C. Optimization for buckling of composite sandwich plates. AIAA journal. 1997;35:863-868.

Montgomery D.C. Design and analysis of experiments. New York: John Wiley & Sons, 2008.

Murphy T, Tsui K-L, Allen J. A review of robust design methods for multiple responses. Research Engineering Design. 2005;15:201-215.

Nocedal J, Wright SJ. Sequential quadratic programming. 2006: Springer.

Oh JH, Kim YG, Lee DG. Optimum bolted joints for hybrid composite materials. Composite Structures 1997;38(1-4):329-341.

Onal L, Adanur S. Effect of Stacking Sequence on the Mechanical Properties of Glass–Carbon Hybrid Composites before and after Impact. Journal of Industrial Textiles. 2002;31:255-271.

Panda B, Garg A, Jian Z, Heidarzadeh A, Gao L. Characterization of the tensile properties of friction stir welded aluminum alloy joints based on axial force, traverse speed, and rotational speed. Frontiers of Mechanical Engineering, 2016;11 (3):289-298.

Pandya KS, Veerraju C, Naik NK. Hybrid composites made of carbon and glass woven fabrics under quasi-static loading. Materials & Design. 2011;32(7):4094-4099.

Park R, Jang J. Impact behavior of aramid fiber/glass fiber hybrid composite: Evaluation of four-layer hybrid composites. Journal of materials science. 2001;36:2359-2367.

Peijs A, De Kok J. Hybrid composites based on polyethylene and carbon fibres. Part 6: Tensile and fatigue behaviour. Composites. 1993;24:19-32.

Peijs AA, Catsman P, Govaert LE, Lemstra PJ. Hybrid composites based on polyethylene and carbon fibres Part 2: influence of composition and adhesion level of polyethylene fibres on mechanical properties. Composites. 1990;21:513-521.

Perner M, Algermissen S, Keimer R, Monner HP. Avoiding defects in manufacturing processes: A review for automated CFRP production. Robotics and Computer-Integrated Manufacturing, 2016;38:82-92.

Personal communication between one of the authors (MK) and J. N. Reddy (Texas A&M University), June 18th 2015.

Phillips L. The hybrid effect—does it exist? Composites. 1976;7:7-8.

Phillips LN. The hybrid effect — does it exist? Composites. 1976;7:7-8.

Phillips MG. Author's reply. Composites. 1982;13:18-20.

Phillips MG. Composition parameters for hybrid composite materials. Composites. 1981;12:113-116.

Qiu Y, Schwartz P. Micromechanical behavior of Kevlar-149/S-glass hybrid seven-fiber microcomposites. II: Stochastic modeling of stress-rupture of hybrid composites. Composites Science and Technology. 1993;47:303-315.

Radebe IS, Adali S. Minimum cost design of hybrid cross-ply cylinders with uncertain material properties subject to external pressure. Ocean Engineering 2014;88:310-317.

Rafai NH, Islam MN. An investigation into dimensional accuracy and surface finish achievable in dry turning. Machining Science and Technology, 2009;13:571-589.

Rahimi-Vahed AR, Rabbani M, Tavakkoli-Moghaddam R, Torabi SA, Jolai F. A multi-objective scatter search for a mixed-model assembly line sequencing problem. Advanced Engineering Informatics. 2007;21(1):85-99.

Rahul, Sandeep G, Chakraborty D, Dutta A. Multi-objective optimization of hybrid laminates subjected to transverse impact. Composite Structures 2006;73(3)360-369.

Rao S. Engineering Optimization: Theory and Practice: New Age International; 1996.

Ray SF, Eric MJ. Effect of fiber volume fraction variation across multiple length scales on composite stress variation: the possibility of stochastic multiscale analysis. 55th AIAA/ASMe/ASCE/AHS/SC Structures, Structural Dynamics, and Materials Conference: American Institute of Aeronautics and Astronautics. 2014.

Reddy CV, Babu PR, Ramnarayanan R, Das D. Mechanical Characterization Of Unidirectional Carbon And Glass/Epoxy Reinforced Composites For High Strength Applications. Proceedings of Materials Today 2017.

Reddy JN, Pandey AK. A first-ply failure analysis of composite laminates. Computers and Structures. 1987;25:371-393.

Reddy JN. Mechanics of laminated composite plates and shells: theory and analysis. London: CRC press; 2004.

Ren P, Zhang Z, Xie L, Ren F, Jin Y, Di Y, Fang C. Hybrid effect on mechanical properties of M40-T300 carbon fiber reinforced Bisphenol A Dicyanate ester composites. Polymer Composites. 2010;31:2129-2137.

Reyes-Sierra M, Coello CC. Multi-objective particle swarm optimizers: A survey of the state-of-the-art. International journal of computational intelligence research. 2006;2(3):287-308.

Romeijn HE, Zabinsky ZB, Graesser DL, Neogi S. New reflection generator for simulated annealing in mixed-integer/continuous global optimization. Journal of Optimization Theory and Applications. 1999;101:403-427.

Rouhi M, Ghayoor H, Hoa SV, Hojjati M. Multi-objective design optimization of variable stiffness composite cylinders, Composites Part B: Engineering. 2015;69:249-255.

Ruiz E, Achim V, Soukane S, Breard J. Optimization of injection flow rate to minimize micro/macro-voids formation in resin transfer molded composites. Composites Science and Technology, 2006;66:475-486.

Saaty TL. Axiomatic foundation of the analytic hierarchy process. Management Science. 1986;32:841-855.

Saaty TL. How to make a decision: The analytic hierarchy process. European Journal of Operational Research. 1990;48:9-26.

Sandeep G, Chakraborty D, Dutta A. Multi-objective optimization of hybrid laminates subjected to transverse impact. Composite Structures. 2006;73:360-369.

Saravanos D, Chamis C. An integrated methodology for optimizing the passive damping of composite structures. Polymer composites. 1990;11:328-336.

Saunders RA, Lekakou C, Bader MG. Compression in the processing of polymer composites 1. A mechanical and microstructural study for different glass fabrics and resins. Composites Science and Technology. 1999;59(7):983-993.

Sayer M, Bektaş NB, Sayman O. An experimental investigation on the impact behavior of hybrid composite plates. Composite Structures. 2010;92:1256-1262.

Sen P, Yang JB. Multiple criteria decision support in engineering design. Springer, London, 1998.

Sevkat E, Liaw B, Delale F, Raju BB. Drop-weight impact of plain-woven hybrid glass–graphite/toughened epoxy composites. Composites Part A: Applied Science and Manufacturing. 2009;40:1090-1110.

Sfiso Radebe I, Adali S. Minimum cost design of hybrid cross-ply cylinders with uncertain material properties subject to external pressure. Ocean Engineering. 2014;88:310-317.

Shaw A, Sriramula S, Gosling PD, Chryssanthopoulos MK. A critical reliability evaluation of fibre reinforced composite materials based on probabilistic micro and macro-mechanical analysis. Composites Part B: Engineering. 2010;41(6):446-453.

Shaw A, Sriramula S, Gosling PD, Chryssanthopoulos MK. A critical reliability evaluation of fibre reinforced composite materials based on probabilistic micro and macro-mechanical analysis. Composites Part B: Engineering 2010;41(6):446-453.

Shiao MC, Chamis CC. Probabilistic evaluation of fuselage-type composite structures. Probabilistic engineering mechanics. 1999;14(1):179-187.

Smale S. Global Analysis and Economics I: Pareto Optimum and a Generalization of Morse Theory. In: Peixoto MM, editor. Dynamical Systems: Academic Press. 1973;531-544.

Soden PD, Hinton MJ, Kaddour AS. A comparison of the predictive capabilities of current failure theories for composite laminates. Composites Science and Technology. 1998;58(7):1225-1254.

Song JH. Pairing effect and tensile properties of laminated high-performance hybrid composites prepared using carbon/glass and carbon/aramid fibers. Composites Part B: Engineering. 2015;79:61-66.

Sonmez FO. Optimum design of composite structures: A literature survey (1969-2009). Journal of Reinforced Plastics and Composites. 2016;36:3-39.

Spurgeon WA. Thickness and reinforcement fiber content control in composites by vacuum-assisted resin transfer molding fabrication processes. DTIC Document: Army Research Lab Aberdeen Proving Ground MD. 2005.

Sriramula S, Chryssanthopoulos MK. Quantification of uncertainty modelling in stochastic analysis of FRP composites. Composites Part A: Applied Science and Manufacturing. 2009;40(11):1673-1684.

Stevanovic MM, Stecenko TB. Mechanical behaviour of carbon and glass hybrid fibre reinforced polyester composites. Journal of Materials Science. 1992;27:941-946.

Subagia I.D.G, Kim Y, Tijing LD, Kim CS, Shon HK. Effect of stacking sequence on the flexural propertiesof hybrid composites reinforced with carbon and balast fibres. Composites Part B: Engineering. 2014;58:251-258.

Sudarisman, Davies IJ. The effect of processing parameters on the flexural properties of unidirectional carbon fibre-reinforced polymer (CFRP) composites. Materials Science and Engineering A. 2008;498:65-68.

Summerscales J, Short D. Carbon fibre and glass fibre hybrid reinforced plastics. Composites 1978;9(3):157-166.

Sun CT, Quinn BJ, Tao J, Oplinger DW. Comparative evaluation of failure analysis methods for composite laminates. Report No: DOT/FAA/AR-95/109, U.S. Department of Transportation. Washington; 1996.

Suresh S, Sujit P, Rao A. Particle swarm optimization approach for multi-objective composite box-beam design. Composite Structures. 2007;81:598-605.

Svanberg K. The method of moving asymptotes—a new method for structural optimization. International journal for numerical methods in engineering. 1987;24:359-373.

Swolfs Y, Gorbatikh L, Verpoest I. Fibre hybridisation in polymer composites: A review. Composites Part A: Applied Science and Manufacturing. 2014;67:181-200.

Swolfs Y, Gorbatikh L, Verpoest I. Stress concentrations in hybrid unidirectional fibre-reinforced composites with random fibre packings. Composites Science and Technology. 2013;85:10-16.

Swolfs, Y., L. Gorbatikh, and I. Verpoest, Fibre hybridisation in polymer composites: A review. Composites Part A: Applied Science and Manufacturing, 2014. 67: p. 181-200.

Taguchi G. Performance analysis design. International Journal of Production Research, 1978;16(6):521-530.

Taketa I, Ustarroz J, Gorbatikh L, Lomov SV, Verpoest I. Interply hybrid composites with carbon fiber reinforced polypropylene and self-reinforced polypropylene. Composites Part A: Applied Science and Manufacturing. 2010;41:927-932.

Taketa I. Analysis of Failure Mechanisms and Hybrid Effects in Carbon Fibre Reinforced Thermoplastic Composites (Analyse van faalmechanismen en hybride effecten in koolstofvezelversterkte thermoplastische composieten). 2011.

Tekalur SA, Shivakumar K, Shukla A. Mechanical behavior and damage evolution in E-glass vinyl ester and carbon composites subjected to static and blast loads. Composites Part B: Engineering. 2008;39:57-65.

Todoroki A, Tanaka M, Shimamura Y. Measurement of orthotropic electric conductance of CFRP laminates and analysis of the effect on delamination monitoring with an electric resistance change method. Composites Science and Technology. 2002;62(5):619-628.

Topal U, Uzman U. Maximization of buckling load of laminated composite plates with central circular holes using MFD method. Structural and Multidisciplinary Optimization. 2008;35:131-139.

Tsai SW, Wu EM. A general theory of strength for anisotropic materials. Journal of Composite Materials. 1971;5:58-80.

Tsau LR, Chang YH, Tsao FL. The design of optimal stacking sequence for laminated FRP plates with inplane loading. Computers & structures. 1995;55:565-580.

Tserpes K.I, Koumpias A.S. A numerical methodology for optimizing the geometry of composite structural parts with regard to strength. Composites Part B: Engineering. 2015;68:176-184.

Velea MN, Wennhage P, Zenkert D. Multi-objective optimization of vehicle bodies made of FRP sandwich structures. Composite Structures, 2014;111:75-84.

Venkataraman S, Haftka RT. Optimization of composite panels-a review. in Proceedings-American Society For Composites. 1999.

Visweswaraiah SB, Ghiasi H, Pasini D, Lessard L. Multi-objective optimization of a composite rotor blade cross-section. Composite Structures. 2013;96:75-81.

Vosoughi AR, Nikoo MR. Maximum fundamental frequency and thermal buckling temperature of laminated composite plates by a new hybrid multi-objective optimization technique. Thin-Walled Structures. 2015;95:408-415.

Vučina D, Lozina Z, Vlak F. NPV-based decision support in multi-objective design using evolutionary algorithms. Engineering Applications of Artificial Intelligence 2010;23(1):48-60.

Waddoups ME, McCullers LA, Olsen FO, Ashton JE. Structural synthesis of anisotropic plates. in AIAA/ASME 11th Struct., Struct. Dyn. and Math Conf., Denver, Colorado. 1970.

Walker M, Hamilton R. A methodology for optimally designing fibre-reinforced laminated structures with design variable tolerances for maximum buckling strength. Thin-Walled Structures 2005;43(1):161-174.

Walker M, Hamilton R. A technique for optimally designing fibre-reinforced laminated plates with manufacturing uncertainties for maximum buckling strength. Engineering Optimization. 2005;37:135-144.

Walker M, Reiss T, Adali S. A procedure to select the best material combinations and optimally design hybrid composite plates for minimum weight and cost. Engineering Optimization 1997;29(1-4):65-83.

Walker M, Reiss T, Adali S. Multi-objective design of laminated cylindrical shells for maximum torsional and axial buckling loads. Computers & Structures 1997;62(2):237-242.

Walker M, Smith R. A technique for the multiobjective optimization of laminated composite structures using genetic algorithms and finite element analysis. Composite Structures 2003;62(1):123-128.

Wang CM, Lim GT, Reddy JN, Lee KH. Relationships between bending solutions of Reissner and Mindlin plate theories. Engineering Structures. 2001;23(7):838-849.

Wikipedia. Composite laminates. 2016 [cited 2017]; Available from: https://en.wikipedia.org/wiki/Composite_laminates.

Wisnom MR, Khan B, Hallett SR. Size effects in unnotched tensile strength of unidirectional and quasi-isotropic carbon/epoxy composites. Composite Structures. 2008;84:21-28.

Wisnom MR. The effect of fibre misalignment on the compressive strength of unidirectional carbon fibre/epoxy. Composites, 1990;21(5):403-407.

Wu Z, Wang X, Iwashita K, Sasaki T, Hamaguchi Y. Tensile fatigue behaviour of FRP and hybrid FRP sheets. Composites Part B: Engineering. 2010;41:396-402.

Xing JI, Hsiao GC, Chou TW. A Dynamic Explanation of The Hybrid Effect. Journal of Composite Materials. 1981;15:443-461.

You YJ, Park YH, Kim HY, Park JS. Hybrid effect on tensile properties of FRP rods with various material compositions. Composite Structures. 2007;80:117-122.

Zeng QD, Fan FQ, Zhang YY. A random critical-core theory of microdamage in interply hybrid composites: I—First failure and hybrid effect. Composites Science and Technology. 1993;49:341-348.

Zhang J, Chaisombat K, He S, Wang CH. Hybrid composite laminates reinforced with glass/carbon woven fabrics for lightweight load bearing structures. Materials & Design. 2012;36:75-80.

Zhang X-M, Ding H. Design optimization for dynamic response of vibration mechanical system with uncertain parameters using convex model. Journal of Sound and Vibration 2008;318(1-2):406-415.

Zhang Y, Li Y, Ma H, Yu T. Tensile and interfacial properties of unidirectional flax/glass fiber reinforced hybrid composites. Composites Science and Technology. 2013;88:172-177.

Zitzler E, Laumanns M, Thiele L. SPEA2: Improving the strength Pareto evolutionary algorithm. 2001, Tik-report.

Zitzler E, Laumanns M, Thiele L. SPEA2: Improving the strength Pareto evolutionary algorithm. Tech Rep 103, Computer Engineering and Networks Laboratory (TIK). Swiss Federal Institute of Technology (ETH), Zurich, Switzerland, 2001.

Zweben C. Tensile strength of hybrid composites. in 18th Structural Dynamics and Materials Conference. 1977.

Zweben C. Tensile strength of hybrid composites. Journal of Materials Science. 1977;12:1325-1337.

*Every reasonable effort has been made to acknowledge the owners of copyright material. I would be pleased to hear from any copyright owner who has been omitted or incorrectly acknowledged.*